



EFFECT OF ROUND ORIFICE ASPECT RATIOS ON NON- NEWTONIAN FLUID DISCHARGE FROM TANKS

by

TSEPANG MABASIA MOHAJANE

**Thesis submitted in fulfilment of the requirements for the degree
Master of Engineering: Civil Engineering**

**in the Faculty of Engineering and Built Environment
at the Cape Peninsula University of Technology**

Supervisor: Prof Rainer Haldenwang

Co-supervisor: Mrs Morakane Khahledi

Bellville Campus

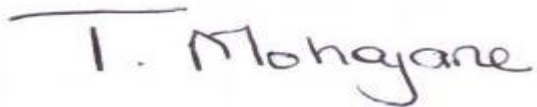
Date submitted: February 2020

CPUT copyright information

This thesis may not be published either in part (in scholarly, scientific or technical journals), or as a whole (as a monograph), unless permission has been obtained from the University.

Declaration

I, Tsepang Mabasia Mohajane, declare that this research thesis is my own unaided work. It is submitted for the MEng Degree at Cape Peninsula University of Technology, Cape Town. It has not been submitted before for any degree or examination at any other university.

A handwritten signature in black ink that reads "T. Mohajane". The signature is written in a cursive style with a horizontal line above the first letter 'T'.

(Signature)

Signed in Cape Town this 10th day of Febraury 2020.

Abstract

Flow rate measurement of Newtonian and non-Newtonian liquids out of tanks and reservoirs has been conducted broadly dating as far back as the 16th century. However, as far as can be ascertained, the outflow of non-Newtonian liquids from the bottom of a tank has only been reported in a few papers. Non-Newtonian liquids behave differently from water; they have complex rheological characteristics. It is therefore difficult to determine the flow rate of these liquids when they are discharged from the bottom of a tank. The aim of this work is to establish the impact of round orifice aspect ratios (L/d) on the gravitational discharge of non-Newtonian liquids from a tank, as a function of liquid properties.

Tests were carried out in the Flow Process and Rheology Centre laboratory of the Cape Peninsula University of Technology. A rectangular tank with clear Perspex walls (0.4, 0.4 and 0.6) m was used for conducting the tests. Four circular orifices – 20 mm in diameter with lengths of 1, 20, 60 and 100 mm and L/d ratios 0.05 (sharp-crested), 1, 3 and 5, respectively – were each fitted in the bottom centre of the tank, flush with the inside surface. The change in liquid weight was measured by a load cell. For calibration purposes, water was used. Various concentrations of glycerine solutions were used as Newtonian liquids, and aqueous solutions of carboxymethylcellulose (CMC) and water-based suspensions of kaolin and bentonite were used as non-Newtonian liquids. The rheology of the tested liquids was established using a Paar-Physica MCR 300 rotational rheometer. Flow rate measurements were conducted for each liquid and concentration. From these, the coefficient of discharge (C_d) values and appropriate Reynolds number was calculated.

Data analysis was presented in the form of C_d against the Reynolds number. The existing literature shows that in the turbulent region, Newtonian and non-Newtonian liquids have an average C_d value of 0.62 and 0.67, respectively, irrespective of the L/d ratio used. Calibration results of the current study showed that in the turbulent flow there was a non-consistent increase in C_d values as the L/d ratio increased. For Newtonian liquids the C_d was nearly constant with average C_d values of 0.60, 0.59, 0.80 and 0.78 for L/d ratios of 0.05, 1, 3 and 5, respectively. For Newtonian liquids, a single composite power-law function was used to relate the C_d versus Re relationship for each L/d ratio. The correlations estimated the C_d values to within ± 3 % error margins.

This thesis adds new coefficient of discharge and Reynolds number data from laminar to turbulent region for an L/d ratio of 5 to the literature. It also adds other kinds of non-Newtonian liquids. Findings from this research will benefit the food processing and engineering industries where high concentrations of non-Newtonian liquids are stored and transported from one tank to the other.

Dedication

To my family – for their neverending support and encouragement by prayer.

“Pray to God, but keep rowing to shore” **Russian Proverb**

*“The Lord hath appeared of old unto me, saying,
Yea, I have loved thee with an everlasting love:
therefore with lovingkindness have I drawn thee”.*

Jeremiah 31:3

Acknowledgements

I wish to thank:

- Prof Rainer Haldenwang for his excellent supervision, support, prayers and patience throughout this journey
- Mrs Morakane Khahledi for her tremendous supervision, mentorship, positivity, unfailing persistence and being my source of strength throughout this journey
- Prof Fester for constructive input and wisdom
- Prof Chabbra for his great input and advice
- Mr Andrew Sutherland for his assistance in some of the numerical derivations
- Mr Naziem George for his fantastic assistance with rheology
- Mr Richard du Toit for his superb laboratory supervision
- Mr Kwezi Xashimba for his exceptional laboratory assistance
- Mr Siya Makaluza and Miss Pamela Matshaya for assistance with all the admin work
- Ms Nontuthuzelo Mralaza for always keeping the lab clean
- Dr Angés Akim Aminou Moussavou for his support and valuable input
- My parents for their support, love and prayers
- My friends and colleagues – Mr L Mohobane, Mr M Melamu, Miss M Montsi, Miss M Loke and Mr B Seithleko – as we held each other's hands and soldiered together

Conferences

The listed conferences showcase the author's input to the body of literature available on the gravitational flow of Newtonian and non-Newtonian liquids out of tanks:

- 1) Mohajane, T.M., Khahledi. M., Haldenwang. R., Fester & Chhabra. R.P. 2019. Effect of Round Orifice Aspect Ratio on Non-Newtonian Fluid Discharge From Tanks. *19th International Conference on Transportation and sedimentation of Solid particles*. 24-27 September, Cape Town, South Africa, pp.129-136 (Oral).
- 2) Mohajane, T.M., Khahledi. M., Haldenwang. R., Fester & Chhabra. R.P. 2019. *Flow Rate Measurement of Non-Newtonian Fluids using Orifices of Varying Aspect Ratios Fitted at The Bottom of A Tank*. Cape Peninsula University of Technology annual postgraduate conference. 7 November 2019, Cape Town, South Africa, (Poster).

Table of Contents

	Page
Declaration	i
Abstract	ii
Dedication	iii
Acknowledgements	iv
Conferences	v
Table of Contents	vi
List of Figures	ix
List of Tables	xi
Nomenclature.....	xiii
Terms and concepts	xv
Chapter 1 INTRODUCTION	1
1.1 Background and motivation	1
1.2 Research problem.....	1
1.3 Research question	2
1.4 Aims and objectives.....	2
1.5 Context of the research	2
1.6 Significance	3
1.7 Delineation	3
1.8 Assumptions	3
1.9 Methodology	3
1.10 Organisation of the thesis.....	3
1.10.1 Literature review – Chapter 2	3
1.10.2 Research methodology – Chapter 3.....	3
1.10.3 Results and analysis – Chapter 4.....	4
1.10.4 Model prediction – Chapter 5	4
1.10.5 Contrast of current outcomes with outcomes from literature – Chapter 6	4
1.10.6 Conclusion and recommendations – Chapter 7	4
Chapter 2 LITERATURE REVIEW AND THEORY	5
2.1 Introduction	5
2.2 Orifices.....	5
2.2.1 Classification of orifices.....	6
2.2.2 Orifice geometries.....	7
2.2.3 Application of orifice plates	7
2.2.4 Design and installation.....	7
2.2.5 Pros and cons of orifice plates	8
2.2.6 Flow through an orifice fitted at the bottom of a tank.....	9
2.2.7 Coefficient of discharge	9
2.3 Rheology	11
2.3.1 Rheometer	11
2.4 Liquid characterisation	12
2.4.1 Newtonian liquids	13
2.4.2 Non-Newtonian liquids	14

2.4.3	Yield stress	16
2.5	Reynolds number.....	16
2.5.1	Metzner and Reed Reynolds number	17
2.5.2	Slatter and Lazarus Reynolds number.....	17
2.6	Flow rate measurements: previous research	18
2.6.1	Newtonian and non-Newtonian liquids flow rate measurement from tanks	18
2.6.2	Newtonian liquids flow rate measurement in pipes.....	28
2.6.3	Non-Newtonian liquids flow rate measurement in pipes.....	32
2.7	Conclusion and summary of literature review	36
Chapter 3	RESEARCH METHODOLOGY.....	42
3.1	Introduction.....	42
3.2	Description of the experimental rig.....	42
3.3	Experimental matrix	43
3.4	Instrumentation.....	44
3.4.1	Orifice plates	44
3.4.2	Mixing tank.....	46
3.4.3	Orifice locating plate and backing ring	46
3.4.4	Camera and tripod	47
3.4.5	Computer	47
3.4.6	Load cell	48
3.4.7	Data acquisition system	48
3.4.8	Measuring tape	49
3.4.9	Top pan balance.....	49
3.5	Material tested	49
3.5.1	Preparation of slurries	50
3.5.2	Water	50
3.5.3	Glycerine	50
3.5.4	Carboxymethylcellulose (CMC).....	50
3.5.5	Kaolin.....	51
3.5.6	Bentonite.....	51
3.6	Calibration	51
3.6.1	Calibration of the load cell.....	51
3.6.2	Calibration of orifices	53
3.7	Flow rate measurements.....	55
3.7.1	Load cell method.....	55
3.7.2	Camera method	56
3.8	Experimental errors.....	57
3.8.1	Systematic errors	57
3.8.2	Random errors	58
3.8.3	Parallax error.....	58
3.8.4	Errors of computable variables	58
3.9	Rheometry	59
3.9.1	Rheological characterisation of flow curves	60
3.9.2	Measurements of relative density.....	62
3.9.3	Slurry temperature.....	63

3.10	Conclusion	63
Chapter 4	RESULTS AND ANALYSIS	64
4.1	Introduction	64
4.2	Rheological characterisation and relative density results of Newtonian and non-Newtonian liquids used	64
4.2.1	Glycerine	65
4.2.2	CMC.....	66
4.2.3	Bentonite.....	67
4.2.4	Kaolin.....	68
4.3	Presentation of C_d versus Re plots for each L/d ratio.....	69
4.3.1	Discharge coefficients for L/d ratios of 0.05, 1, 3 and 5	69
4.1	Relationship between C_d and Re versus L/d ratios.....	76
4.2	Conclusion	78
Chapter 5	MODEL PREDICTION FOR C_d	79
5.1	Introduction	79
5.1.1	Single composite equation.....	79
5.2	Conclusion	85
Chapter 6	COMPARISON OF CURRENT RESULTS WITH LITERATURE	86
6.1	Introduction	86
6.2	Calibration	86
6.3	C_d - Re relationship	86
6.3.1	Newtonian liquids	86
6.3.2	Non-Newtonian liquids	91
6.4	Conclusion	96
Chapter 7	CONCLUSION AND RECOMMENDATIONS.....	99
7.1	Introduction	99
7.2	Summary.....	99
7.3	Recommendations.....	101
References	102	
Appendices	108	
Appendix A.	Calibration certificate	108
Appendix B.	Load cell specifications.....	110
Appendix C.	Data acquisition voltage input range	111
Appendix D.	NI USB 6001.....	112
Appendix E.	Signal Description	112
Appendix F.	Orifice calibration results	113
Appendix G.	Compatibility between load cell and camera.....	117
Appendix H.	Rheometer measuring system data sheet	119
Appendix I.	Flow rate measurements using aspect ratio of 0.05.....	120
Appendix J.	Flow rate measurements using aspect ratio of 1	133
Appendix K.	Flow rate measurements using aspect ratio of 3	146
Appendix L.	Flow rate measurements using aspect ratio of 5.....	159

List of Figures

	Page
Body	
Figure 2.1 Representation of an orifice meter (Tuğçe, 2010)	5
Figure 2.2 a) Cavitated flow b) separated flow followed by attachment and c) separated flow (Hall, 1963)	6
Figure 2.3 Discharge of water from a tank through an orifice and the orifice cross-sectional detail (Spencer, 2013)	9
Figure 2.4 Rheometer: cylinder, cone and plate and plate and plate measuring system (Haldenwang, 2003)	12
Figure 2.5 Schematic representation of a unidirectional shearing flow (Chhabra & Richardson, 2008)	13
Figure 2.6 Rheograms of various Newtonian liquids (Liu, 2003).....	13
Figure 2.7 Various non-Newtonian liquids flow curve (Paterson & Cooke, 1999).....	15
Figure 2.8 Lea's 1938 data and Medaugh and Johnson's (1940) data, redrawn by Brater and King (1982)	19
Figure 2.9 Coefficient of discharge against Reynolds number (Medaugh & Johnson, 1940)	20
Figure 2.10 Relationship of head loss coefficient and C_d plotted against the Re for an L/d of 3, d= 4 mm	21
Figure 2.11 Laminar flow for L/d=0 (Kiljański, 1993).....	22
Figure 2.12 Laminar flow for L/d=0.5 (Kiljański, 1993).....	22
Figure 2.13 Laminar flow for L/d=1 (Kiljański, 1993).....	23
Figure 2.14 C_d vs Re (Kiljański, 1993).....	24
Figure 2.15 C_d values against Reynolds number for Newtonian liquids (Dziubiński & Marcinkowski, 2006)	25
Figure 2.16 C_d vs Re_{MR} (Dziubiński & Marcinkowski, 2006).....	26
Figure 2.17 Çobanoğlu's (2008) experimental results	27
Figure 2.18 C_d versus Re for Newtonian and non-Newtonian liquids for various researchers.....	28
Figure 2.19 Johansen's (1930) experimental results for various beta ratios	29
Figure 2.20 Lichtarowicz et al.'s (1965) experimental results for various aspect ratios.....	30
Figure 2.21 Variation of discharge coefficient for a 0.3 mm diameter orifice at different aspect ratios (Ramamurthi & Nandakumar, 1999).....	31
Figure 2.22 Variation of discharge coefficient for a 2 mm diameter orifice at different aspect ratios ...	31
Figure 2.23 C_d against Re (Chowdhury, 2010)	33
Figure 2.24 C_d against Re for $\beta = 0.2$ (Ntamba Ntamba, 2011)	34
Figure 2.25 C_d against Re for $\beta = 0.57$ (Ntamba Ntamba, 2011)	35
Figure 3.1 Experimental test rig (current study)	43
Figure 3.2 Side views of orifices of varying lengths	44
Figure 3.3 Section detail of a 1 mm thick orifice.....	44
Figure 3.4 Section detail of a 20 mm orifice.....	45
Figure 3.5 Section detail of a 60 mm orifice.....	45
Figure 3.6 Section detail of a 100 mm orifice.....	46
Figure 3.7 Schematic diagram of orifice locating plate.....	46

Figure 3.8 Orifice backing ring.....	47
Figure 3.9 Schematic diagram depicting the placement of the camera and tripod	47
Figure 3.10 Amplifier device.....	48
Figure 3.11 Data acquisition.....	49
Figure 3.12 Connection of the data acquisition system to the computer	49
Figure 3.13 Calibration results of a 250 kg load cell.....	52
Figure 3.14 100 kg load cell calibration.....	53
Figure 3.15 Comparison between a 250 kg load cell and a 100 kg load cell.....	54
Figure 3.16 Orifice calibration results for aspect ratios of 0.05, 1, 3 and 5	55
Figure 3.17 Compatibility between load cell and camera for L/d of 1.....	57
Figure 3.18 Paar-Physica MCR-300 rotational rheometer	60
Figure 3.19 Concentric cylinder geometry CC27	60
Figure 3.20 Rheogram for 100% glycerine	60
Figure 3.21 Rheogram for kaolin 20.4% v/v	61
Figure 3.22 Rheogram for bentonite 7.3% w/w.....	61
Figure 3.23 Rheogram for CMC 6.6% w/w	62
Figure 4.1 Flow curves for 65, 93, 96 and 100% glycerine	66
Figure 4.2 Pseudo shear flow curves for 6.6, 5.2, 7.6 and 2.4% CMC solutions	67
Figure 4.3 Bentonite 3.8, 7.2 and 7.3% w/w pseudo shear graphs.....	68
Figure 4.4 Pseudo shear diagram for 13.1 and 20.4% kaolin suspensions	69
Figure 4.5 Coefficient of discharge versus Reynolds number for L/d ratio of 0.05	70
Figure 4.6 Coefficient of discharge versus Reynolds number for L/d ratio of 1.....	71
Figure 4.7 Coefficient of discharge versus Reynolds number for L/d ratio of 3.....	72
Figure 4.8 Coefficient of discharge versus Reynolds number for L/d ratio of 5.....	73
Figure 4.9 Coefficient of discharge versus Reynolds number of Newtonian liquids for L/d ratios of 0.05, 1, 3 and 5.....	74
Figure 4.10 Coefficient of discharge versus Reynolds number of non-Newtonian liquids for L/d ratios of 0.05, 1, 3 and 5.....	75
Figure 4.11 Coefficient of discharge versus Reynolds number of Newtonian and non-Newtonian liquids for L/d ratios of 0.05, 1, 3 and 5.....	76
Figure 4.12 Effect of L/d ratio on the laminar region for Newtonian and non-Newtonian liquids	77
Figure 4.13 Effect of L/d t on the turbulent region for Newtonian and non-Newtonian liquids.....	78
Figure 5.1 Logistic dose response curve for L/d ratio of 0.05	80
Figure 5.2 Logistic dose response curve for L/d ratio of 1	81
Figure 5.3 Logistic dose response curve for L/d ratio of 3	81
Figure 5.4 Logistic dose response curve for L/d ratio of 5	82
Figure 5.5 Comparison between the actual and predicted flow rates through L/d ratio of 0.05.....	83
Figure 5.6 Comparison between the actual and predicted flow rates through L/d ratio of 1.....	83
Figure 5.7 Comparison between the actual and predicted flow rates through L/d ratio of 3.....	84
Figure 5.8 Comparison between the actual and predicted flow rates through L/d ratio of 5.....	84
Figure 6.1 C_d versus the Re graphs for Newtonian liquids for Lea, 1938; Medaugh & Johnson, 1940; and the current study.....	87
Figure 6.2 C_d versus the Re graphs for Newtonian liquids for an orifice with L/d ratio of 1	88

Figure 6.3 Comparison of C_d versus the Re graphs for Newtonian liquids for an orifice with L/d ratio of 3 between Dziubiński & Marcinkowski (2006); Fox & Stark (1989); and the current study.....	89
Figure 6.4 Comparison of C_d versus the Re graphs for Newtonian liquids for an orifice with L/d ratio of 3 between Çobanoğlu (2008) and the current study.....	90
Figure 6.5 Effect of the L/d ratio in the turbulent region for Newtonian liquids as per the current study and that of Dziubiński and Marcinkowski (2006).....	91
Figure 6.6 Comparison of C_d versus the Re graphs for non-Newtonian liquids for an orifice with L/d ratio of 0 between Dziubiński and Marcinkowski (2006) and the current study.....	92
Figure 6.7 Comparison of C_d versus the Re graphs for non-Newtonian liquids for an orifice with L/d ratio of 1 between Dziubiński and Marcinkowski (2006) and the current study.....	93
Figure 6.8 Comparison of C_d versus the Re graphs for non-Newtonian liquids for an orifice with L/d ratio of 3 between Dziubiński and Marcinkowski (2006) and the current study.....	94
Figure 6.9 Comparison of C_d versus the Re graphs for non-Newtonian liquids between Dziubiński and Marcinkowski (2006) and the current study.....	95
Figure 6.10 Effect of the L/d ratio in the turbulent region of non-Newtonian liquids as per the current study and that of Dziubiński and Marcinkowski (2006).....	96

List of Tables

	Page
Body	
Table 2.1 Orifices and their nominal coefficients (Dally et al., 1993)	6
Table 2.2 Allowable tolerance for orifice diameters (de Almeida Medeiros et al., 2006)	8
Table 2.3 Peak and asymptotic values of Re and C_d for different L/d ratios (Çobanoğlu, 2008)	27
Table 2.4 Different orifice sizes (Chowdhury, 2010).....	32
Table 2.5 Different orifice dimensions (Ntamba Ntamba, 2011).....	35
Table 2.6 Summary of literature review.....	38
Table 3.1 Experimental matrix	43
Table 3.2 Combined errors.....	59
Table 4.1 Rheological parameters of the liquids used in this study.....	65
Table 4.2 Flow regions for an L/d ratio of 0.05	69
Table 4.3 Flow regions for an L/d ratio of 1	69
Table 4.4 Flow regions for an L/d ratio of 3	71
Table 4.5 Flow regions for an L/d ratio of 5	72
Table 5.1 Optimised composite equation factor values	80
Table 6.1 Summary of the effect of aspect ratio on flow regions.....	97

Symbols

Notation	Meaning	Units
A_1^*	Constant in Equation 5.2	(-)
A_1	Constant in Equation 2.23	(-)
A_2	Constant in Equation 2.23	(-)
A_2^*	Constant in Equation 5.3	(-)
A_3	Constant in Equation 2.23	(-)
A_0	Orifice area	m^2
b	Constant in Equation 2.21	(-)
c	Constant in Equation 2.21	(-)
c^*	Constant in Equation 5.1	(-)
$B' B$	Constants in Equation 2.22 and 2.20 respectively, depended on L/d ratio	(-)
C_d	Coefficient of discharge	(-)
C_{davg}	Average coefficient of discharge	(-)
$C_{d peak}$	Highest value of coefficient of discharge	(-)
$C_{d(predicted)}$	Predicted C_d in Equation 5.9	(-)
C_v	Coefficient of velocity	(-)
C_c	Coefficient of contraction	(-)
d	Orifice diameter	(mm)
d^*	Constants in Equation 5.1	(-)
D	Tank diameter	(mm)
D_{shear}	Shear diameter	
Eu	Euler number	(-)
F	Force	(N)
f_1	Constant in Equation 5.2	(-)
f_2	Constant in Equation 5.3	(-)
g	Acceleration due to gravity	(m/s^2)
H	Liquid height	(m)
h_1	Liquid height in the tank measured from the orifice	(m)
h_2	Reference height at the orifice (m)	(m)
k	Fluid consistency coefficient	($Pa \cdot s^n$)
L	Orifice length	(m)

n	Flow behaviour index	(-)
N	Number of C_d values	(-)
P_a	Atmospheric pressure	(N/m ²)
P_1	Pressure in tank	(N/m ²)
P_2	Pressure in orifice	(N/m ²)
Q_1	Liquid flow rate in a tank Equation 2.9	(m ³ /s)
Q_2	Liquid flow rate in the orifice Equation 2.9	(m ³ /s)
Q_{actual}	Actual flow rate in Equation 5.9	(m ³ /s)
$Q_{\text{predicted}}$	Predicted flow rate	(m ³ /s)
$Q_{\text{theoretical}}$	Theoretical flow rate in Equation 2.1	(m ³ /s)
r	radius at a point in the pipe	m
R	radius of the pipe	m
R^2	Coefficient of determination	(-)
Re	Newtonian Reynolds number Equation 2.16	(-)
Re_{MR}	Metzner and Reed Reynolds number Equation 2.17	(-)
Re_2	Slatter and Lazarus (1993) Reynolds number Equation 2.18	(-)
Re_3	Slatter and Lazarus (1996) Reynolds number Equation 2.19	(-)
Re_{peak}	Maximum value of Re	(-)
S	Estimate of standard deviation Equation 3.3	(-)
V_{ann}	Annulus velocity	(m/s)
V_1	Liquid velocity in the orifice Equation 2.2	(m/s)
V_2	Liquid velocity in the tank Equation 2.2	(m/s)
t^*	Constants in Equation 5.1	(-)

Nomenclature

Greek letters

Notation	Meaning	Units
\emptyset	Coefficient of discharge	(-)
ΔX	Computed result absolute error	(-)
ρ	Density	(kg m ⁻³)
Δn	Independent absolute errors	(-)
n	Independent variables involved	(-)
$\dot{\gamma}$	Shear rate	(s ⁻¹)

τ	Shear stress	(Pa)
Σ	Summation	(-)
σ	Surface tension	(N/m)
X	Computed result	(-)
μ	Viscosity	(Pa.s)
τ_w	Wall shear stress	(Pa)
τ_y	Yield stress	(Pa)

Subscripts

2	Second point of measurement
3	Third point of measurement
B	Bingham
HB	Herschel-Bulkley
M-R	Metzner-Reed
ann	of the annulus
plug	of the plug
shear	over the sheared zone

Terms and concepts

Term	Explanation
Aspect ratio	Relationship of the orifice length to the orifice diameter symbolised as L/d
Cavitation	The formation and collapse of air cavities in liquids
Coefficient of discharge	Relationship of the actual flow discharge to the theoretical flow discharge
CMC	Carboxymethylcellulose
CPUT	Cape Peninsula University of Technology
DAQ	Data acquisition
DIO	Digital input/output
Euler number	The pressure loss coefficient expressed as a function of orifice plate bulk mean velocity
Flow curve	Correlation between shear stress and shear rate for a liquid
Flow rate	Volume of liquid which passes per unit time
FPRC	Flow Process and Rheology Centre
Head	Height
ISO	International Organisation for Standardisation
Jet	Fast stream of liquid forced out of a small opening
Laminar flow	Flow of liquids where particles of the liquid move smoothly in parallel layers
Newtonian liquid	A liquid whose flow curve has a linear relationship between shear stress and shear rate
Non-Newtonian liquid	A liquid whose flow curve does not follow Newton's law of viscosity there is a non-linear relationship between shear stress and shear rate
Orifice	Ring-like device used to quantify the discharge of liquids
Reynolds Number	Relationship of internal to viscid forces
Rheology	The study of deformation and flow of liquids
Transition	Region between laminar and turbulent flow
Turbulent flow	Flow region whereby fluid particles move in irregular paths because inertial forces are more dominant than viscous forces.
Viscosity	Resistance of liquids to flow
Yield stress	Stress at which a liquid starts to deform plastically

Chapter 1 INTRODUCTION

An orifice, the least expensive and generally used hydraulic structure for estimating the discharge of fluids in pipes and out of tanks and reservoirs, it is used in various industrial applications like water pipe systems and drainage works (Tuğçe, 2010). Despite the fact that the flow of Newtonian liquids from tanks is broadly reviewed, the gravitational flowrate measurements of non-Newtonian liquids from tanks have not been broadly investigated. This could be due to the problematic rheological features of non-Newtonian liquids, which makes it difficult to quantify them during transportation. Data is only available for non-Newtonian power-law liquids (carboxymethylcellulose) with Reynolds numbers spanning from 0.01 to 1000 and width to height ratios ranging from 0 to 3. Therefore, there is a need to conduct further studies using other types of non-Newtonian liquids and different L/d ratios .

1.1 Background and motivation

In the industrial world, specialists are often needed to observe or regulate the flow of different fluids through channels, pipes and out of tanks and reservoirs. These fluids extend from highly viscous liquids to light gasses (Tuğçe, 2010). In recent years, the consistency and accuracy of the flow rate measurements have been critically prioritised as compared to when the data was used primarily for accounting purposes (Crabtree, 2009). A number of authors (Lea, 1938; Medaugh & Johnson, 1940; Lienhard & Lienhard, 1984; Fox & Stark, 1989; Çobanoğlu, 2008) have conducted extensive research on the gravitational flow measurement of water (Newtonian liquids from tanks using circular orifices, where turbulent conditions were generally observed. The coefficient of discharge was mainly stable with an average C_d value of 0.61 for an L/d ratio of 0.

Few studies, however, have investigated the influence of the L/d ratio on the gravitational flow measurement of non-Newtonian liquids from the bottom of tanks through orifices of varying L/d ratios (Dziubiński & Marcinkowski, 2006). Dziubiński & Marcinkowski (2006) have determined the correlation of the C_d and the Reynolds number (Re) for Newtonian liquids (water, solutions of starch syrup in water and ethylene glycol) and between C_d and the Metzner and Reed (1955) Reynolds number Re_{MR} for non-Newtonian liquid (Carboxymethylcellulose). Using circular sharp-crested orifices of diameter 5, 8, 12.5 and 17 mm with L/d ratios of 0, 0.50, 0.75, 1 and 3, they established that in the turbulent region, Newtonian and non-Newtonian liquids have an average C_d value of 0.62 and 0.67, respectively, irrespective of the L/d ratio used. Kiljański (1993) conducted research on the gravitational discharge of highly viscous Newtonian liquids using circular orifices with various L/d ratios, however, his data only concerned the laminar region. Therefore, gravitational flow measurement of non-Newtonian liquids through orifices of varying aspect ratios from tanks is an area that requires more inspection.

1.2 Research problem

Products such as mayonnaise and tomato sauce are manufactured, stored and transported from one stage to the other and sold as non-Newtonian liquids (White *et al.*, 2008). Maintaining the motion of non-Newtonian liquids through the entire volume of an open tank discharging through an open lower exit is problematic. This is caused by air entering from the top as a long slug which decreases the velocity in the tank, leaving a liquid film on the sidewalls of the tank (Ali *et al.*, 2016). Furthermore, non-Newtonian

liquids exhibit funnel flow patterns that create immobility areas at the downstream wall where recirculation vortices develop, thereby forming dead zones (Sakri *et al.*, 2017). This results in liquid quantities that are not discharged. The stagnant material creates pressure build-up which can result in cracks on the outside walls. When changing to a new batch or maintaining a tank, water is usually used to push down the remaining material and the film on the walls of the tank. The water initially pushes out a focal centre of the liquid; then the liquid that is clinging on the walls is progressively cleared by the force caused by the water (Mickaily & Middleman, 1993; Palabiyik *et al.*, 2014; Fan *et al.*, 2015). Despite flushing being quick and viable, it results in material wastage and the formation of enormous quantities of polluted water, which must be purified (Ali *et al.*, 2016). With rising environmental awareness and the scarcity and expense of water, numerous industries are faced with the challenge of properly measuring and regulating non-Newtonian liquids from their storage reservoirs at sensible prices (Haldenwang *et al.*, 2010).

In applications where the flow is controlled, orifice plates are used as obstruction devices to control fluid movement or decrease the downstream pressure. They are also used in agricultural irrigation schemes (Spencer, 2013). Even so, limited research has been conducted on the gravitational flow rate estimation of non-Newtonian liquids from the base of tanks (Dziubinski & Marcinkowski, 2006). In turbulent flow of Newtonian liquids Dziubinski & Marcinkowski (2006) found the average C_d value to be 0.62 for all the different L/d ratios, while that of non-Newtonian liquids was found to be 0.67. Fox and Stark (1989) and Çobanoğlu (2008), conducting gravitational experiments with water using orifices of varying L/d ratios, found the C_d values to vary with change in the L/d ratio. Therefore, it is essential to carry out this research using other kinds of non-Newtonian liquids through circular orifices of varying L/d ratios.

1.3 Research question

The research question to be investigated is as follows: What impact does the L/d ratio of round orifices have on the C_d values of Newtonian and non-Newtonian liquid flow out of tanks?

1.4 Aims and objectives

This research aims to establish the impact of round orifice L/d ratios on the gravitational flow of Newtonian and non-Newtonian liquids from the base of a tank as a component of liquid characteristics. This was achieved by the following objectives:

- calibrating each orifice aspect ratio using water and various concentrations of glycerine solutions;
- determining the flow rates through circular orifice plates of varying aspect ratios using various concentrations of CMC solutions, and bentonite and kaolin suspensions;
- establishing a relationship between the C_d values and Reynolds number for Newtonian and non-Newtonian liquids for each L/d ratio.

1.5 Context of the research

This research falls within the discipline of civil engineering (water engineering).

1.6 Significance

This study contributes in the chemical, food processing and civil engineering industries where non-Newtonian liquids are manufactured, stored, transported from one stage to the other. It adds experimental data of the coefficient of discharge (C_d) and Reynolds number (Re) for aspect ratios of 0, 1, 3 and 5 using aqueous solutions of carboxymethylcellulose (CMC), bentonite and kaolin suspensions.

1.7 Delineation

In this study, flow rate measurements of Newtonian and non-Newtonian liquids were conducted using circular orifices with L/d ratios of 0, 1, 3 and 5. No other measuring device was used. Only liquids representing Newtonian, power-law, Bingham plastic and Herschel-Bulkley were tested.

1.8 Assumptions

A 100 and a 250 kg 'S' type multipurpose revere universal load cells model 9363 made of stainless steel were used to obtain the mass of the liquid discharged by measuring the change in voltage over time as the liquids were discharged from the tank. It was assumed that the changes in the temperature had no effect on the voltage interpretation of the load cell. The liquids used during the study were assumed to be homogenous and non-reactive with the tank material as well as orifice material.

1.9 Methodology

The experimental investigation for this research was conducted in the slurry lab at the Flow Process and Rheology Centre (FPRC) at the Cape Peninsula University of Technology (CPUT) in Cape Town, South Africa. Different concentrations of Newtonian (glycerine) and non-Newtonian (CMC) bentonite and kaolin liquids were used for this research. The rheological characteristics of the liquids were determined using a Paar-Physica MCR 300 rheometer. The test rig consisted of a rectangular tank fitted with one orifice at a time at the centre of the tank base flush with the inside surface of the tank. Four circular orifices, 20 mm in diameter with lengths of 1, 20, 60 and 100 mm with L/d ratios of 0.05, 1, 3 and 5 respectively, were used for determining the flow rate of the liquids as they were discharged from the tank. The rheological characteristics obtained were used to calculate the Slatter and Lazarus Reynolds number. The C_d values versus the Reynolds number were plotted for each L/d ratio.

1.10 Organisation of the thesis

1.10.1 Literature review – Chapter 2

Literature pertaining to flow rate measurement of Newtonian and non-Newtonian liquids using orifices has been extensively discussed in this chapter. This chapter also includes research on rheological characterisation of the liquids, used to calculate the Reynolds number (Re).

1.10.2 Research methodology – Chapter 3

The details of each component of the equipment that was used to carry out relative density, flow rate and rheology tests are described in this chapter. The calibration procedures for load cell and orifices with the

results obtained are also outlined. Testing procedures for flow rate measurement using four circular orifices of different aspect ratios is explained. The rheological measurements were done by a Paar-Physica MCR 300 rotational rheometer are explained.

1.10.3 Results and analysis – Chapter 4

The outcomes attained from the measurements are shown. The rheology and flow rate measurement results for each orifice and each concentration are discussed.

1.10.4 Model prediction – Chapter 5

This chapter explains the prediction of single composite equations for circular orifices of varying L/d ratios for Newtonian liquids. The predicted error margins are compared to the measured values of the flow rates and presented.

1.10.5 Contrast of current outcomes with outcomes from literature – Chapter 6

In this chapter, the outcomes attained with reference to the available literature are discussed. Emphasis is on the impact of the orifice aspect ratio on the C_d values and the effect of rheological parameters on the different definitions of Reynolds number used.

1.10.6 Conclusion and recommendations – Chapter 7

This chapter reviews the findings from this study, describing how research aim and objectives have been answered. The final remarks are discussed and suggestions for future examinations are made.

Chapter 2 LITERATURE REVIEW AND THEORY

2.1 Introduction

This chapter analyses the theories and applicable research work on both non-Newtonian and Newtonian liquids flow using circular orifices of varying L/d ratios. The significance, use and explanation of the orifice plate are given. The methodology applied for the determination of the coefficient of discharge (C_d) and Reynolds number using circular orifices is demonstrated. However, the major focus is on non-Newtonian and Newtonian liquids and the fundamentals of rheology.

2.2 Orifices

An *orifice meter* or plate is a ring, as shown in Figure 2.1. The ring hole may be of any shape (circular, square, triangular or rectangular). It can either be fixed on the side or base of a reservoir or tank or fitted in a pipe with considerable length. An orifice plate causes a variation in the energy in the form of a reduction in static pressure and increases the velocity via the orifice (ISO 5167-1, 2003). In this research an aspect ratio is defined as the relationship of the orifice length to the orifice diameter and it is symbolised by L/d .

The characteristics impacting flow rate measurement are as follows:

- orifice length (L) to orifice bore diameter (d);
- orifice bore diameter (d) to tank diameter (D); and
- orifice edge geometry.

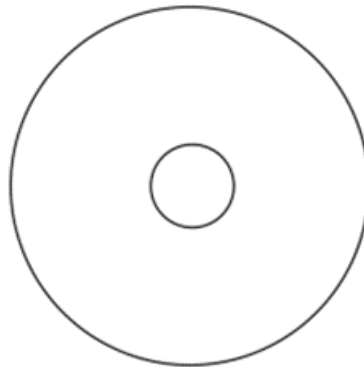


Figure 2.1 Representation of an orifice meter (Tuğçe, 2010)

Orifices with longer sides, such as a pipe 2-3 times the diameter in length or an opening in a thick wall, are called *orifice tubes*; they are classified such that sides of 2-3 times the diameters are referred to as short tubes and those longer than 2-3 are long tubes (Brater & King, 1982; Dally *et al.*, 1993). L/d ratio is another important feature influencing orifice readings (Tuğçe 2010). Davis (1952) categorised tube orifices based on their geometry and length, ranging from 0.1 to 4.27 m. The entrance of the tube was changed from sharp-edged to the four-sided elliptical entrance. Davis (1952) presented the C_d spanning from 0.62 to 0.96 for numerous matrices of lengths and geometries. Dally *et al.* (1993) reported C_d values for free and submerged jets, as shown in Table 2.1. Short tube orifices were found to have an average C_d value of 0.8 with the value limited to an L/d ratio of 2.5. Brater and King (1982) stated that for short tube orifices the exiting jet firsts contracts and then expands, filling the tube. The C_d varies from 0.78 to 0.83 with an average C_d value of 0.82.

Table 2.1 Orifices and their nominal coefficients (Dally *et al.*, 1993)

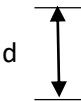


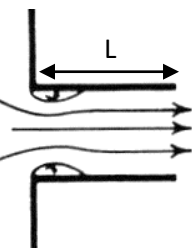

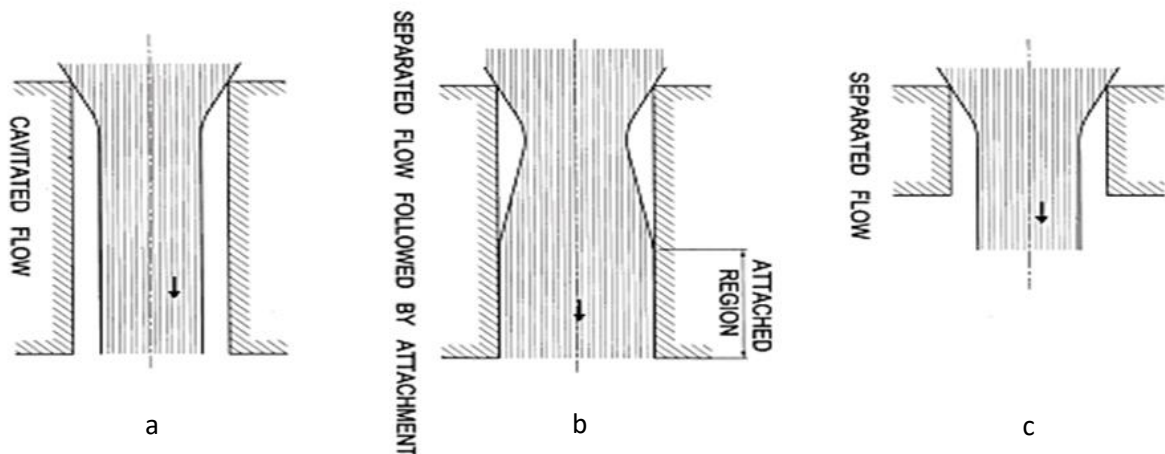
	Sharp-edged	Rounded	Short tube	Borda
				
C_d	0.61	0.98	0.80	0.51
C_c	0.62	1.00	1.00	0.52
C_v	0.98	0.98	0.80	0.98

Figure 2.2 shows that the flow through an orifice tube may be cavitated, separated followed by attachment or separated flow depending on the orifice length and other factors such as surface roughness. Cavitation is the formation and collapse of air bubbles in the liquid. It has been found to cause discharge instabilities, thereby resulting in low C_d values (Hall, 1963). In a round tube orifice with a square edge entry, the flow isolates from the sides at the inlet edge and a recirculation bubble forms, affecting the value of C_d (Hall, 1963). The bubble reattachment region is defined by $1.09d$ below the orifice entry-edge (Hall, 1963). The discharge instabilities can be eluded by using chamfered or round orifice entry edge (Hall, 1963). As the liquid travels only a short distance before exiting the orifice, chances of the turbulent region developing are minimal (Ramamurthi & Nandakumar, 1999).

**Figure 2.2 a) Cavitated flow b) separated flow followed by attachment and c) separated flow (Hall, 1963)**

2.2.1 Classification of orifices

According to Upandhyay (2012), orifices are classified based on size, shape, discharge conditions and shape of the upstream edge.

Short and long orifices

- For a short orifice, the ratio between the orifice plate length and the orifice plate diameter is less than 0.75, ($L/d < 0.75$) (ESDU, 2007).
- When the ratio between the orifice plate length and orifice plate diameter is more than 1, ($L/d > 1$), it is called a long orifice, the characteristic flow regime is fully reattached at the orifice wall (ESDU, 2007).

2.2.2 Orifice geometries

There are numerous geometrically different types of orifices. The following parameters define the orifice plate geometry:

- relationship between the length of the orifice and its diameter (L/d);
- diameter of the orifice (d);
- orifice length (L);
- orifice material;
- entrance edge profile such as square-edged, knife-edged and rounded with edge radius; and
- exit edge profile such as square back cut and square-edged.

2.2.3 Application of orifice plates

For many years orifice plates have been used and accepted as devices for bulk flow measurement in numerous sectors (Morrison *et al.*, 1990). Besides flow metering applications, orifice plates can be used in a variety of ways (Nally, 2010):

- to create incorrect head for centrifugal pump to operate close to the pump best efficiency point (or BEP);
- to increase line pressure;
- to reduce the flow in the line;
- to dissipate energy in flood conduits; and
- to dissipate energy in slurry flow application.

2.2.4 Design and installation

Orifice plates are designed and manufactured to meet certain requirements so as to guarantee precise and comprehensive dimensions in accordance with the standards defined by International Standard Organisation (ISO) 5167 (1991). Table 2.2 shows the allowable tolerance for different orifice diameters.

Table 2.2 Allowable tolerance for orifice diameters (de Almeida Medeiros *et al.*, 2006)

Orifice diameter	Maximum deviation
$d \leq 12$	± 0.1
$12 < d \leq 16$	± 0.08
$16 < d \leq 20$	± 0.07
$20 < d \leq 25$	± 0.06
$d > 25$	± 0.05

When an orifice's length is equal to or less than 2 mm, it is categorised as a sharp-edged orifice. If the length is greater than 2 mm, it should be chamfered at an angle larger than 45° from the parallel side (de Almeida Medeiros *et al.*, 2006).

- The side in direct contact with the flow ought to be aligned: It is aligned when it has a slope under 1%. It should be free of imperfections like unevenness and rough edges. It should be manufactured such that the upstream surface corresponds to the downstream surface (Delmée, 2003).
- The plate is fabricated in accordance with standard specifications (Delmée, 2003).
- The inlet edge must not display flaws as this will influence the coefficient of discharge. Instead, it must be sharp; this happens when the edge radius is smaller than $0.0004d$ (Martins, 1998).
- The quality of the downstream edges inside the region of exit of the flow is less strict than for those of the upstream; in this case, small defects are acceptable (Martins, 1998).

2.2.5 Pros and cons of orifice plates

Orifice plates have been acknowledged for a many years as instruments for mass flow estimation in numerous productions (Morrison *et al.*, 1990). Significant benefits of using orifice flow meters, as indicated by Abou El-Azem Aly *et al.* (2010), include the following:

- simple construction;
- inexpensive;
- no moving parts;
- large range of sizes and opening ratio; and
- well understood and proven.

However, they also have disadvantages:

- They are subject to corrosion, which will ultimately bring about inaccuracies of 2-3% when determining the flow rate.
- Precision is influenced by viscosity variations and temperature.

2.2.6 Flow through an orifice fitted at the bottom of a tank

The theoretical approach of the discharge in tanks started with Torricelli (1643) when he developed the kinetics of water jets dependent on Galileo's movement of projectiles, which brought about the equation, $V_2 = \sqrt{2gH}$. This equation permits the calculation of the velocity (V_2) of a liquid stream under gravity (g), exiting from a little opening in the wall of a vessel, to which the distance to the free water surface is (h) (de Nevers, 1991; Wilkes, 1999; Bird *et al.*, 2002; Bistafa, 2018). This does away with the friction loss in the tank and the vena contracta. The narrowing of the liquid jet happens some distance after the orifice and is likewise reliant on turbulent flow. These influences are catered for by the C_d , normally taken as 0.61 for Reynolds numbers more than 10,000, yet occasionally ranging from 0.60-0.64 (Wilkes, 1999; Bos, 1989). Bernoulli and continuity equations are frequently used when flow occurs through a tank with an orifice placed either at the side or at the bottom of a tank. The head is estimated from the liquid surface to the end of the exit pipe; it incorporates pipe length when the pipe is placed vertically because the head increases with increasing pipe length (Wilkes, 1999).

Figure 2.3 shows the gravitational discharge of water from a tank freely into the atmosphere through a fully flooded sharp-edged orifice plate fitted at the bottom of a tank. Water travels towards the opening at a moderately low speed, goes through the zone of increased flow (at the orifice) and exits from the opening as a contracted jet downstream of the opening where H is the overall head above the orifice entry, P_a is the atmospheric pressure, D is the diameter of the tank, d is the diameter of the orifice, h_1 is the liquid height measured from the orifice to the surface of the water and h_2 is the reference height. Water particles converge from all directions as it approaches the opening.

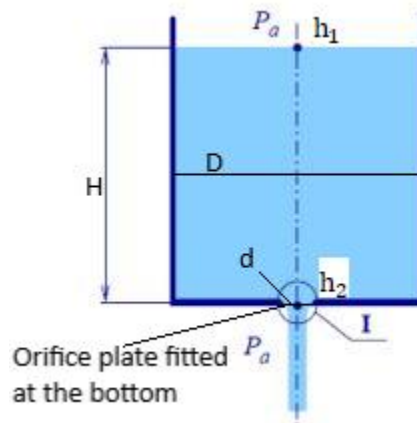


Figure 2.3 Discharge of water from a tank through an orifice and the orifice cross-sectional detail (Spencer, 2013)

2.2.7 Coefficient of discharge

Knowledge of the coefficient of discharge (C_d) is an important aspect when designing an orifice meter, but this can only be achieved when the flow properties are known (Sahin & Ceyhan, 1996). In liquid systems, the C_d is a unitless number normally described by the correlation between the actual flow rate, Q_{actual} to the largest theoretical volume flow rate, $Q_{\text{theoretical}}$ as shown in Equation 2.1 (ESDU, 2007). It is reliant on the characteristics of the orifice and on the Reynolds number defined by the flow regime (Borutzky *et al.*, 2002).

$$C_d = \frac{Q_{\text{actual}}}{Q_{\text{theoretical}}} \quad \text{Equation (2.1)}$$

The basic principle behind the flow through an orifice is ruled by the laws of conservation of mass, energy and momentum. For water flowing gravitationally out of an open tank through an orifice that discharges freely into the atmosphere, the conservation of energy is applicable when using a number of assumptions to the Bernoulli equation:

$$P_1 + \rho gh_1 + \frac{1}{2} \rho V_1^2 = P_2 + \rho gh_2 + \frac{1}{2} \rho V_2^2 \quad \text{Equation (2.2)}$$

Where

$$P_1 = P_2 = P_a$$

For an orifice that discharges freely into the atmosphere, h_1 is the liquid height measured from the orifice to the liquid surface, and h_2 is considered as 0 because it is the reference height; therefore the water level in the tank is denoted by 'H' as shown in Figure 2.3. V_1 , the velocity in the tank, is practically 0 as compared to the velocity V_2 through the orifice,

$$V_1 \ll V_2$$

$$\therefore V_1 = 0.$$

$$0 + \rho gH + \frac{1}{2} \rho(0) = 0 + \rho g(0) + \frac{1}{2} \rho V_2^2 \quad \text{Equation (2.3)}$$

Equation 2.3 simplifies to

$$gh = \frac{1}{2} \rho V_2^2 \quad \text{Equation (2.4)}$$

Equation, 2.4 simplifies to

$$V_2 = \sqrt{2gH} \quad \text{Equation (2.5)}$$

The energy loss may be taken care of by applying a coefficient of velocity to the theoretical velocity C_v as follows:

$$V_2 = C_v \sqrt{2gH} \quad \text{Equation (2.6)}$$

The discharge through an orifice is obtained from the outcome of the velocity and the area at the vena contracta. The area at the vena contracta a_2 is smaller than the area of the orifice A_2 ; the relation between the two is named the *coefficient of contraction* C_c . The product of C_c and C_v is called the *coefficient of discharge* C_d .

$$C_d = C_c C_v \quad \text{Equation (2.7)}$$

The flow through the orifice may therefore be written as

$$Q_2 = C_d A_0 \sqrt{2gH} \quad \text{Equation (2.8)}$$

From the conservation of mass, the flow in the tank (Q_1) is proportional to the flow through the orifice (Q_2), where the former is the actual flow and the latter the theoretical flow.

$$Q_1 = Q_2 \quad \text{Equation (2.9)}$$

The coefficient of discharge is written as shown in Equation 2.10:

$$C_d = \frac{Q_1}{A_0 \sqrt{2gH}} \quad \text{Equation (2.10)}$$

2.3 Rheology

Bingham (1916) explained the term *rheology* as the investigation of distortion and flow of matter. The term was first acknowledged in 1929 with the establishment of the American Society of Rheology (Barnes *et al.*, 1989). It was propelled by a statement by Heraclitus: "πανταρει" deciphered as "everything flows". In reality, everything flows, depending on how much power is applied, in what bearing, and to what extent. The objective of rheology is to give measurable limits that characterise how a material will disfigure as an element of power, time and spatial direction. Rheometry, then, is the examination of the progression of complex liquids in both simple and complex stream geometries. According to Tanner (2002), rheology is explained as the investigation of the deformation of matter.

2.3.1 Rheometer

Rheological models are meaningful when the shear stress and shear rate data can be accurately defined. This is made possible by the use of different physical instruments available such as the rotational or oscillation rheometer used for this purpose: the former is more suitable for liquid-like material, and the latter for viscous to solid materials. A rheometer is an instrument used to quantify the manner by which a liquid, suspension or slurry flows because of the imposed forces. It is utilised for those liquids which cannot be characterised by a single value of consistency and consequently require more limits set and estimated (Chhabra & Richardson, 1999). There are two types of rheometers: rotational rheometers and extensional rheometers. When the shear stress and shear rate data are determined, rheological models become more meaningful.

A rheometer, uses different attachments depending on the type of liquid measured, it uses the technique of either pre-setting the shear stress so the shear rate is measured or pre-setting the shear rate so the shear stress is measured. In rotational motion, the rotational speed and the torque or the force applied to the rotation must be considered, as this makes possible the control of the flow of the liquid as the

speed of the bob rotation can be fixed (Chhabra & Richardson, 1999). The expected result will be the torque required by the liquid depending on its viscosity in order to cause the shearing. Shear stress can be derived from torque and shear rate from rotational speed. Software incorporated within the rheometer renders conversion computation easy. A shear rheometer has different geometries such as plate-plate, cone and plate and cup and bob; several measuring systems are shown in Figure 2.4.

Rotational cylinder

A rotational cylinder is a one-plate measuring system whereby the cylinder is spun such that the shear rate is quantifiable. The current rotational cylinder devices turn at 600, 300, 200, 100, 6 and 3 RPM to determine the shear stress of liquids (Chhabra & Richardson, 1999).

Cone and plate

Here, a liquid is positioned on a flat plate and a short, shallow cone is placed on top. The cone is typically at a one-degree slant. The plate is revolved and the force exerted on the cone is measured. Oscillating types of this rheometer can quantify added values such as elasticity (Chhabra & Richardson, 1999).

Plate-plate

The attachment consists of two parallel plates with a minute distance between them (Chhabra & Richardson, 1999).

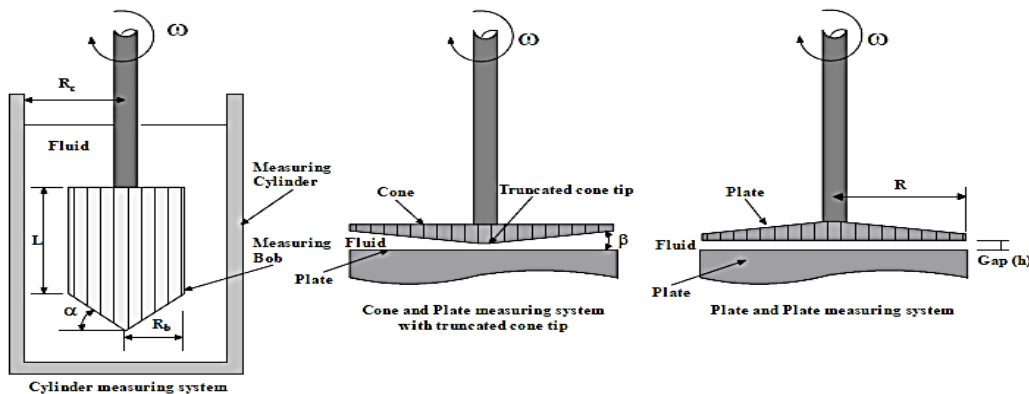


Figure 2.4 Rheometer: cylinder, cone and plate and plate and plate measuring system (Haldenwang, 2003)

2.4 Liquid characterisation

A liquid is generally a material which shows very little opposition to distortion and conforms to the shape of a container enclosing it. A force is required to move a solid resting on a horizontal plane (Woodford, 2018). Chhabra and Richardson (2008) describe a liquid as a material capable of flowing and deforming constantly under the action of shearing stress. According to Coulson and Richardson (2008), liquids are normally characterised as Newtonian or non-Newtonian.

2.4.1 Newtonian liquids

Newtonian liquids follow Newton's law of viscosity, which states that the correlation amongst shear rate and shear stress is proportional and passes through the origin; that is, the viscosity of the liquid remains constant with applied shear stress. As the shear rate changes, the viscosity of Newtonian liquid stays steady (Tanner, 2002; Brookfield Engineering Labs Inc., 2010). When a thin layer of liquid is placed in the middle of two horizontal plates (Figure 2.5) by a distance ' d_y ' apart, and a force ' F ' is applied to the top plate when the bottom plate is fixed, this force is stabilised by the opposite internal friction forces in the liquid (Chhabra & Richardson, 2008).

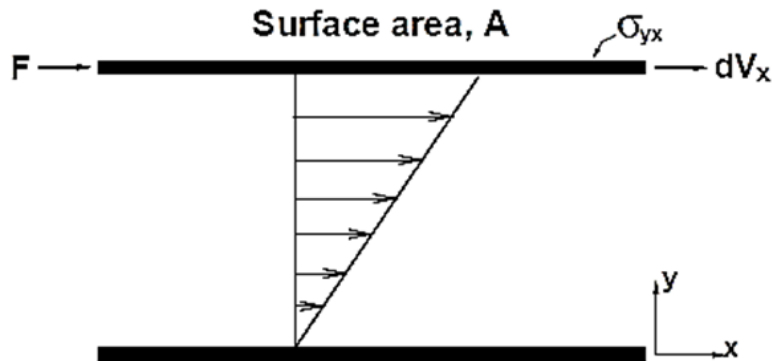


Figure 2.5 Schematic representation of a unidirectional shearing flow (Chhabra & Richardson, 2008)

For Newtonian liquids with low values of Re , the correlation between the total stresses is equal to the product of the viscosity and the shear rate of the liquid. The shear force is equal to the force exerted on the liquid per unit area, and the shear rate is the change in the velocity with respect to the force applied normal to the x -axis. The relationship is mathematically expressed as follows:

$$\frac{F}{A} = \tau_{yx} = \mu \left[-\frac{dv_x}{dy} \right] = \mu \dot{\gamma}_{yx} \quad \text{Equation (2.11)}$$

The subscript of τ specifies the direction normal to the shear force, while the subscript $\dot{\gamma}$ reflects the bearing of the liquid flow (Chhabra & Richardson, 2008). Sir Isaac Newton was the first to define this relationship in 1687 (Barr, 1931). The coefficient of dynamic viscosity, called the constant of proportionality, is denoted by μ . Figure 2.6 shows that the higher the viscosity of the liquid the steeper the gradient; as the liquid viscosity increases, the liquid's ability to flow reduces (Liu, 2003). Thus, viscosity symbolises the gradient of the straight line in any rheogram of a Newtonian liquid.

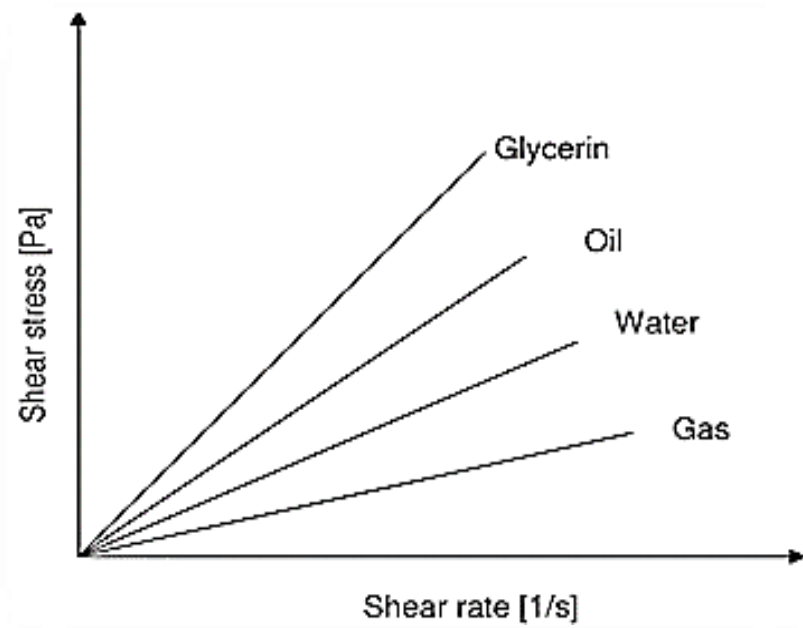


Figure 2.6 Rheograms of various Newtonian fluids (Liu, 2003)

Viscosity

Viscosity is the determination of the internal forces that must be surpassed before flow initiates. Water has a lower viscosity, the lower the viscosity, the easier the flow of the liquid. Viscosity, defining a liquid's interior resistance to flow, may be thought of as a measure of liquid friction (Bird, 2002). The correlation among share stress and shear rate is used to categorise several kinds of liquids.

The shear stress τ is related to the shear rate $\dot{\gamma}$ by Equation 2.12:

$$\tau = \mu(\dot{\gamma}) \quad \text{Equation (2.12)}$$

This specific correlation, originally proposed by Newton, has been found to define precisely the characteristics of numerous other liquids. For each liquid, there is an exact value for the factor μ at a given temperature. Such liquids are referred to as Newtonian liquids (Chhabra & Richardson, 2008).

2.4.2 Non-Newtonian liquids

Non-Newtonian liquids do not follow Newton's law of viscosity; viscosity can change when under force to either more liquid or more solid, they are described by rheological parameters. The amount of force required to move them is determined by factors such as shape, density and size (Brookfield Engineering Labs Inc., 2010). Chhabra and Richardson (2008) characterised the non-Newtonian liquids as liquids with a non-linear flow curve between the shear stress versus shear rate they have yield stress or consistency that is reliant on distortion (or a mix of the two). Non-Newtonian liquids are ordinarily grouped into three categories: time-independent, time-dependent; and visco-elastic liquids. Only time-independent and time-dependent will be elaborated on see Figure 2.7.

Figure 2.7 provides various models of both time-dependent and time-independent liquids. In this research, only time-independent liquids are considered.

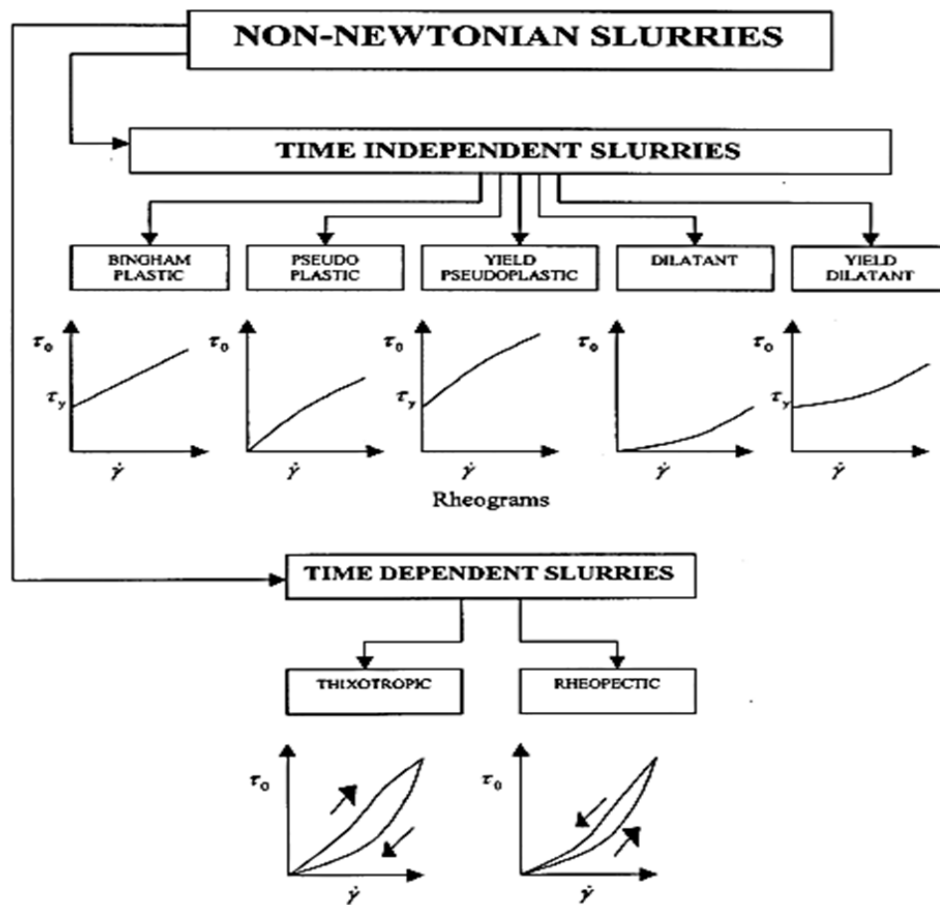


Figure 2.7 Various non-Newtonian liquids flow curve (Paterson & Cooke, 1999)

Time independent non-Newtonian liquids

Time-independent non-Newtonian liquids are reliant on temperature as well as on the shear rate. The shear rate at a particular point is resolved uniquely by the estimation of shear stress at that particular point. These liquids might be subdivided further into three kinds: shear-thinning or pseudoplastic, viscoplastic; and shear thickening or dilatants. Only shear-thinning or pseudoplastic and viscoplastic are discussed.

Shear-thinning or pseudoplastic model

Chhabra and Richardson (2008) stated that the apparent viscosity of pseudoplastic or shear-thinning liquids reduces as the shear rate increases. The power-law or Ostwald de Waele model is used to model shear-thinning liquids. The flow curve estimates the correlation between shear stress and shear rate for a shear thinning liquid over a restricted scope of shear rate (or stress) for this phase of the flow curve. Equation 2.13 is appropriate.

$$\tau = k(\dot{\gamma})^n \quad \text{Equation (2.13)}$$

Whereby:

$n < 1$, the liquid exhibits shear-thinning behaviour;
 $n > 1$, the liquids exhibits shear-thickening behaviour; and
 $n = 1$, the liquid shows Newtonian behaviour.

k and n are material parameters (constant under given conditions), usually determined experimentally. They are known as fluid consistency coefficient and the flow behaviour index respectively. For shear-thinning liquids, the index may have a value somewhere in the range of 0 and 1. The lesser the value of n , the bigger the gradation of shear thinning. For a shear thickening liquid, the index n will be larger than 1 (Chhabra & Richardson, 2008).

Viscoplastic fluid behaviour

This type of fluid behaviour, categorised by the presence of yield stress, must be surpassed to initiate flow (Chhabra & Richardson, 2008). The flow curve does not pass through the origin. There is a continuous discussion over the very presence of a 'true' yield stress (Hartnett & Hu, 1989).

a) Bingham plastic model

A Bingham plastic fluid is categorised by steady plastic viscosity and a yield stress. The plastic viscosity is the gradient of the shear stress versus the shear rate curve (Chhabra & Richardson, 2008). The Bingham plastic model is described by Equation 2.14:

$$\tau = \tau_y + \mu_p \dot{\gamma} \quad \text{Equation (2.14)}$$

b) Yield: pseudoplastic/Herschel–Bulkley model

This model retains yield stress and a non-linear flow curve on linear coordinates. The yield pseudoplastic fluids can be described by Equation 2.15 (Chhabra & Richardson, 1999):

$$\tau = \tau_y + k \dot{\gamma}^n \quad \text{Equation (2.15)}$$

2.4.3 Yield stress

Yield stress, as explained by Beaupré *et al.* (2004), is the quantity of shear vital for the liquid to flow. In other words, the yield stress is the amount of shear to be overcome by the liquid for the flow to start. Flocculation and colloidal forces are predominant: the resulting link between particles due to their interaction is weak to a point where a small amount of shear applied to the material is enough to break the link in question so the flow can start. The required shear stress to break this link between particles is referred to as yield stress (Kazemian *et al.*, 2012).

2.5 Reynolds number

Reynolds number is a unitless value that defines the relationship of inertial to viscous forces. It is used to describe the flow regime of a liquid. In 1883, Osborne Reynolds found for liquids that undergo laminar flow have Reynolds numbers smaller than 2320 for and those that undergo turbulent region have Reynolds numbers that exceed 4000. According to Upadhyay (2012), liquids that undergo transition region

have a Reynolds number between 2320 and 4000. For Newtonian liquids, the viscosity is constant so the Reynolds number is well-defined, classifying the flow pattern (calculated by Equation 2.16).

$$\text{Re} = \frac{\rho d V_2}{\mu} \quad \text{Equation (2.16)}$$

2.5.1 Metzner and Reed Reynolds number

Equation 2.17 is only valid for liquids with constant viscosity. The highly viscous liquids investigated in the present study are non-Newtonian liquids with more complex rheology as compared to Newtonian liquids. For the identification of different flow regimes, Metzner and Reed, in 1955, introduced a generalised Reynolds number Re_{MR} useable for power-law liquids. This number, resulted from the Darcy friction factor, is given by:

$$\text{Re}_{\text{MR}} = \frac{V_2^{2-n} d^n \rho}{k((3n + 1)/4n)^n 8^{n-1}} \quad \text{Equation (2.17)}$$

2.5.2 Slatter and Lazarus Reynolds number

The Metzner and Reed Reynolds number has a limitation that does not cater for the yield stress. Slatter and Lazarus (1993) proposed a Reynolds number for Herschel-Bulkley and Bingham model liquids, stated as Re_2 comparable to that of Clapp Reynolds number as stated by Torrance (1963), but now incorporating the yield stress Equation 2.18.

$$\text{Re}_2 = \frac{8\rho V_2^2}{\tau_y + k \left[\frac{8V_2}{d} \right]^n} \quad \text{Equation (2.18)}$$

Slatter (1994) formulated a new pipe Reynolds number which proved to be more reliable for non-Newtonian fluids pipe flow and which focused only on the flow of the sheared fluid in the annulus where the radius of the plug given by:

$$r_{\text{plug}} = \frac{\tau_y}{\tau_0} R \quad \text{Equation (2.19)}$$

The area of the annulus is:

$$A_{\text{ann}} = \pi(R^2 - r_{\text{plug}}^2) \quad \text{Equation (2.20)}$$

The sheared diameter, D_{shear} , represents the zone in which the shearing of the material actually takes place and is defined by:

$$D_{\text{shear}} = D - D_{\text{plug}} \quad \text{Equation (2.21)}$$

Where

$$D_{\text{plug}} = 2r_{\text{plug}} \quad \text{Equation (2.22)}$$

The unsheared core is treated as a solid body in the centre of the pipe, the flow represented by the core is subtracted as it is no longer treated as part of the fluid flow. The corrected mean velocity in the annulus V_{ann} is then obtained from:

$$V_{\text{ann}} = \frac{Q_{\text{ann}}}{A_{\text{ann}}} \quad \text{where } Q_{\text{ann}} = Q - Q_{\text{plug}} \quad \text{and } u_{\text{plug}} A_{\text{plug}} \quad \text{Equation (2.23)}$$

The new Reynolds number Re_3 is given by

$$Re_3 = \frac{8\rho V_{\text{ann}}^2}{\tau_y + K \left[\frac{8V_{\text{ann}}}{D_{\text{shear}}} \right]^n} \quad \text{Equation (2.24)}$$

2.6 Flow rate measurements: previous research

Flow estimation is the measurement of mass liquid or gas flow that goes through a specific measuring device per unit time. Precise estimation of the flow rate of liquids and gases is a basic necessity for maintaining the nature of mechanical procedures. Due to lack of research done on gravitational discharge of non-Newtonian fluids from tanks, orifices placed in horizontal pipes were also considered.

2.6.1 Newtonian and non-Newtonian liquids flow rate measurement from tanks

According to Tuğçe (2010), the pioneer in determining the coefficients of discharge for a broad variety of Reynolds numbers out of a tank through an orifice was Lea (1938), his orifice was fitted at the side. Lea carried out more than 100 tests with water, glycerine solutions and a number of oils. He graphically represented the relationship of C_d versus Re for Newtonian liquids, as shown in Figure 2.8. Laminar flow occurred where Reynolds numbers were less than 12 and in this region C_d , increased linearly with an increase in Re . Fully turbulent flow occurred for Reynolds numbers greater than 10000 where C_d was constant with an average value of 0.61.

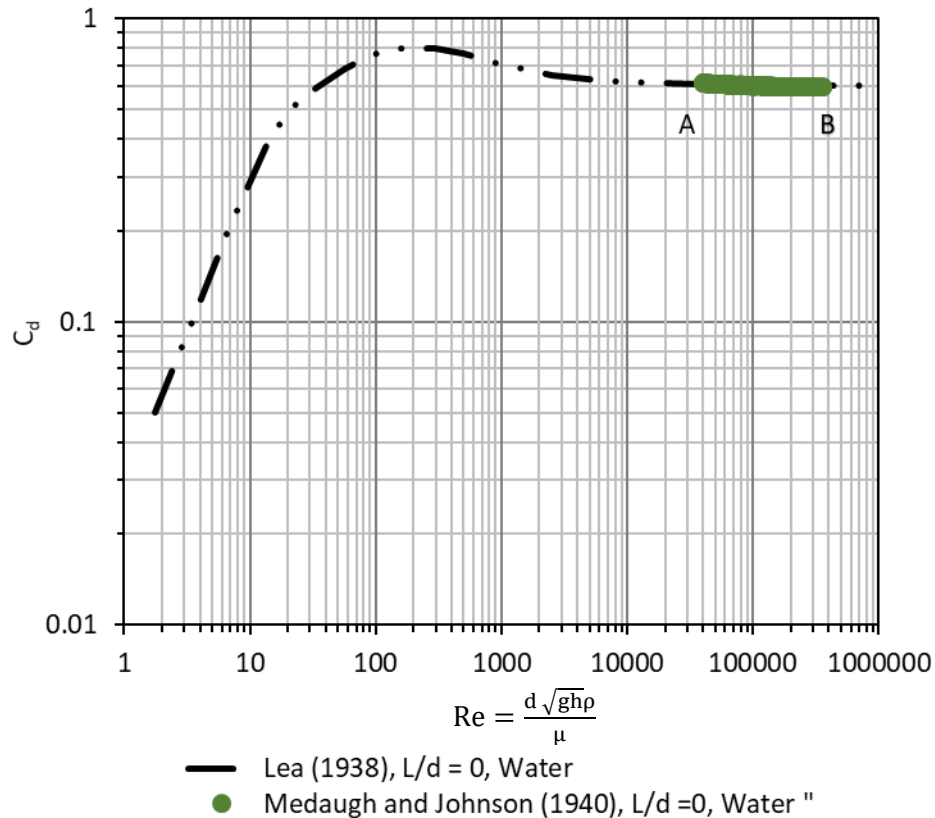


Figure 2.8 Lea's 1938 data and Medaugh and Johnson's (1940) data, redrawn by Brater and King (1982)

In 1940, Medaugh and Johnson constructed a test facility measured flow rate and pressure drop through brass orifices using water. The water temperature was maintained at 16.94°C with pressure drops ranging from 2.41 to 358.5 kPa. Orifice diameters of 6.35, 12.7, 19.05, 25.4 and 50.8 mm were fabricated from a 6.35 mm thick brass sheet yielding aspect ratios of 0, 0.5, 0.33, 0.25 and 0.13, respectively. The plates were mounted, one at a time, on the side of a vertical tank 0.9 m in diameter and 4.1 m high. The head was kept constant when conducting the experiments. It was perceived that as the flow rate through the opening magnified, the coefficient of discharge reduced; similarly, as the diameter enlarged, the coefficient of discharge decreased for the same pressure drop. As the flow rate increased there was a reduction in the coefficient of discharge. It was also established that with enlargement in orifice diameter the coefficient of discharge decreased. Figure 2.9 shows plots of C_d against Re for Newtonian liquids whereby for L/d ratio of 0 the C_d was in the range of 0.615-0.6 and for L/d ratios of 0.5, 0.33, 0.25 and 0.13, the C_d range was between 0.615-0.595. This could be due to the cavitated flow which caused a reduction in the coefficient of discharge, as suggested by Ramamurthi and Nandakumar (1999). Medaugh and Johnson (1940) proposed that if the flow rate was sufficiently increased, the coefficient of discharge would ultimately reduce to a value of 0.588. The range of Reynolds number covered by Medaugh and Johnson (1940) is shown in Figure 2.8, denoted by the green line AB.

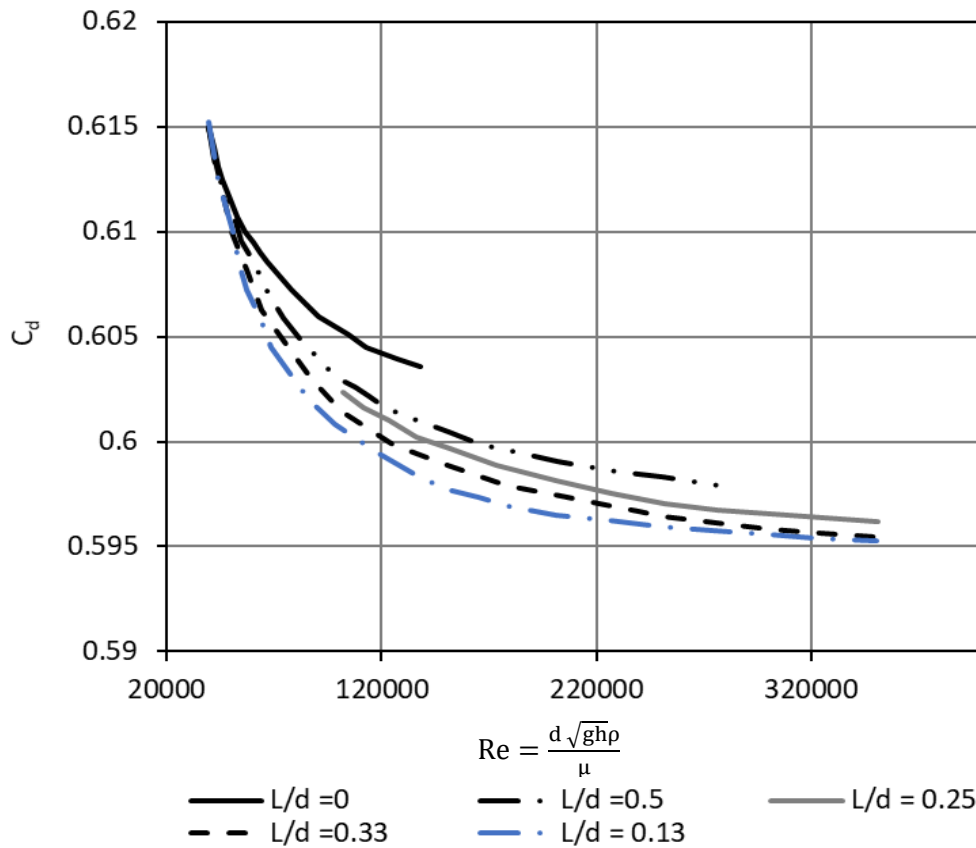


Figure 2.9 Coefficient of discharge against Reynolds number (Medaugh & Johnson, 1940)

Lienhard and Lienhard (1984) measured C_c and C_v independently for sharp-edged orifice placed at the side of a tank. The experiments were conducted using water for a 1 inch (25.4 mm) orifice, reporting an average C_d value of 0.61 and C_v of 0.99.

Fox and Stark (1989) conducted gravitational flow experiments using tap water through short-tube orifices normally used for fuel injection. One orifice at a time was fixed at the bottom of a 220 mm long feed-up pipe made from a 1.1 mm (i.d.) infusion tube. The outcomes were graphically demonstrated whereby C_d was plotted against the Newtonian Re . Displayed in Figure 2.10 are the outcomes of a 4 mm diameter orifice with an L/d ratio of 3. Figure 2.10 shows that in the laminar region (Re under 2000) the C_d becomes bigger as the Re increases and in the turbulent region where Re is more than 3000, the C_d assumes a steady C_d estimation of 0.8.

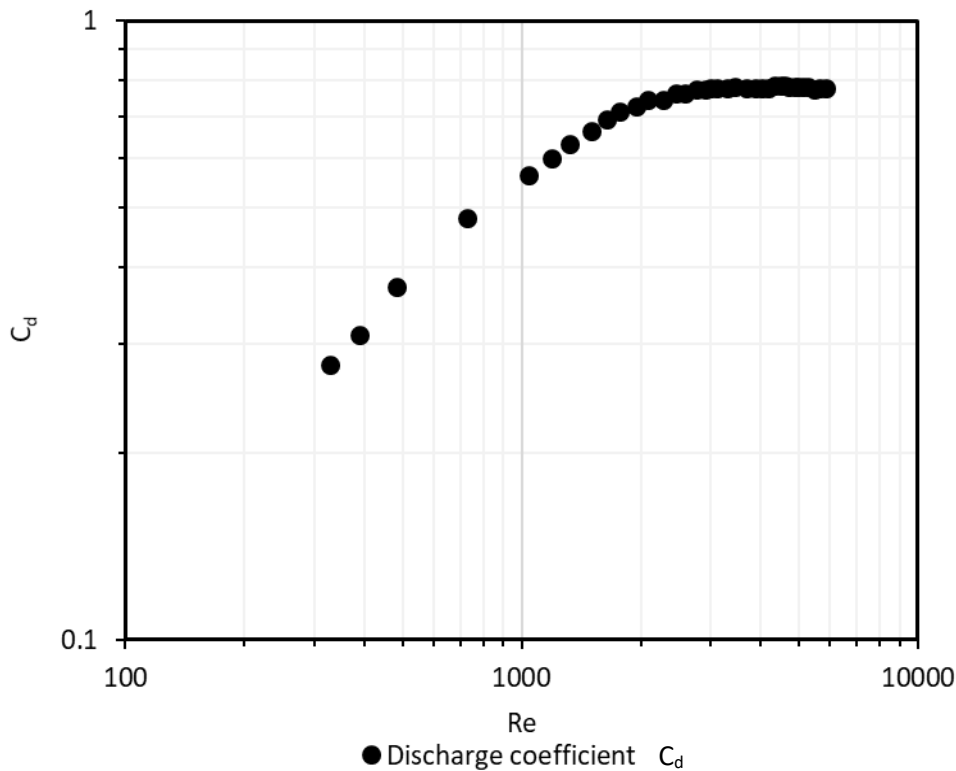


Figure 2.10 C_d plotted against the Re for an L/d of 3, $d=4$ mm (Fox & Stark, 1989)

Kiljański (1993) conducted a number of tests to establish the C_d values using highly viscous Newtonian liquids, data evaluation was based on the correlation of the C_d and Newtonian Re . The experiments were performed using a vertical Perspex cylindrical tube 38 mm in diameter, the bottom part of the tank was made out of brass. When conducting the experiments, one orifice at the time was fitted at the side of the tank. The orifices used had diameters of 2, 3 and 5 mm all of L/d ratio of 0.5. Also two orifices of diameter 3 mm which had L/d ratios of 1 and 0 were used. The head of the liquid was kept constant when conducting the experiments. For Reynolds numbers less than 10, he proposed that the coefficient discharge is directly proportional to the square root of the Reynolds number (Equation 2.25).

$$C_d = B\sqrt{Re}, \quad \text{Equation (2.25)}$$

Where B is an experimentally determined constant based on the aspect ratio. Figures 2.11 to 2.13 show the individual equations for each L/d ratio. It is evident from the graphs that B decreases as L/d ratio increases.

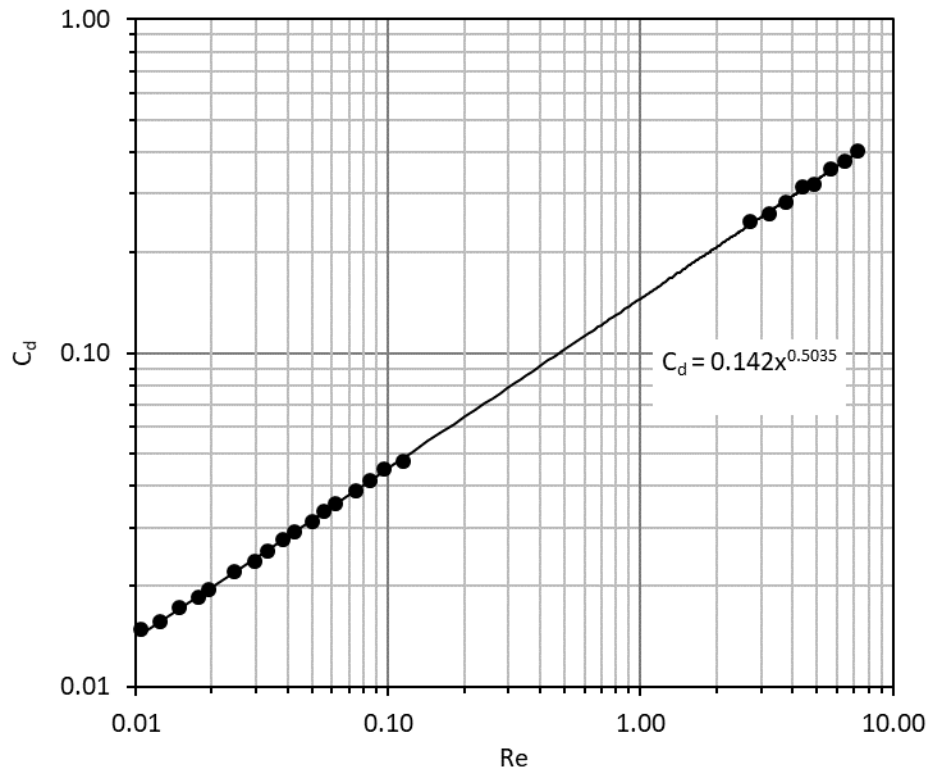


Figure 2.11 Laminar flow for $L/d=0$ (Kiljański, 1993)

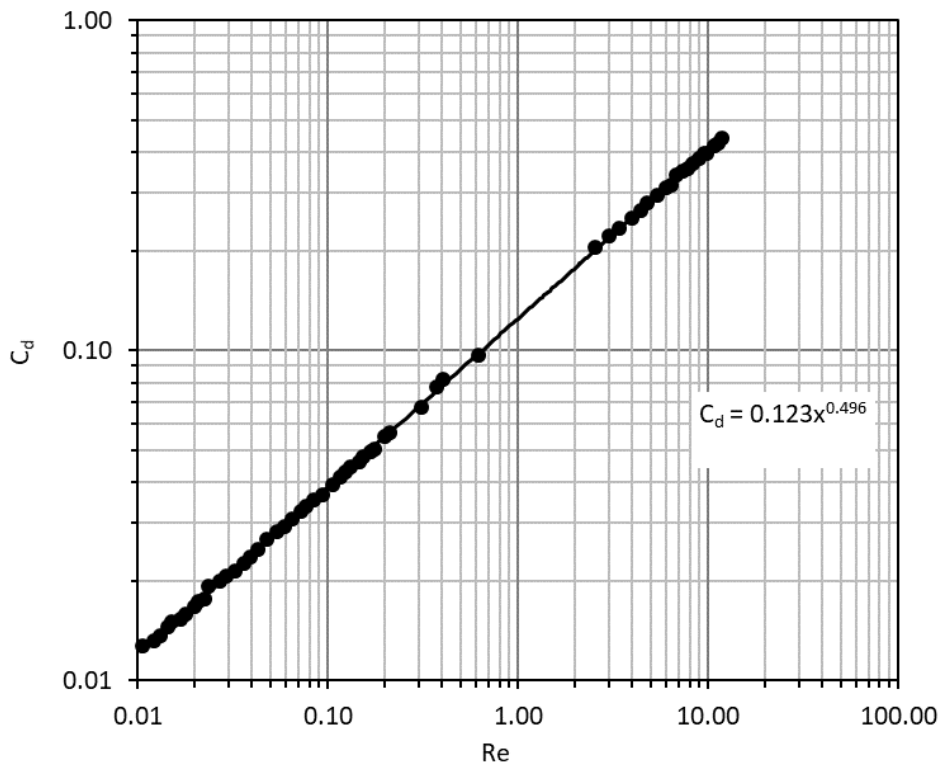


Figure 2.12 Laminar flow for $L/d=0.5$ (Kiljański, 1993)

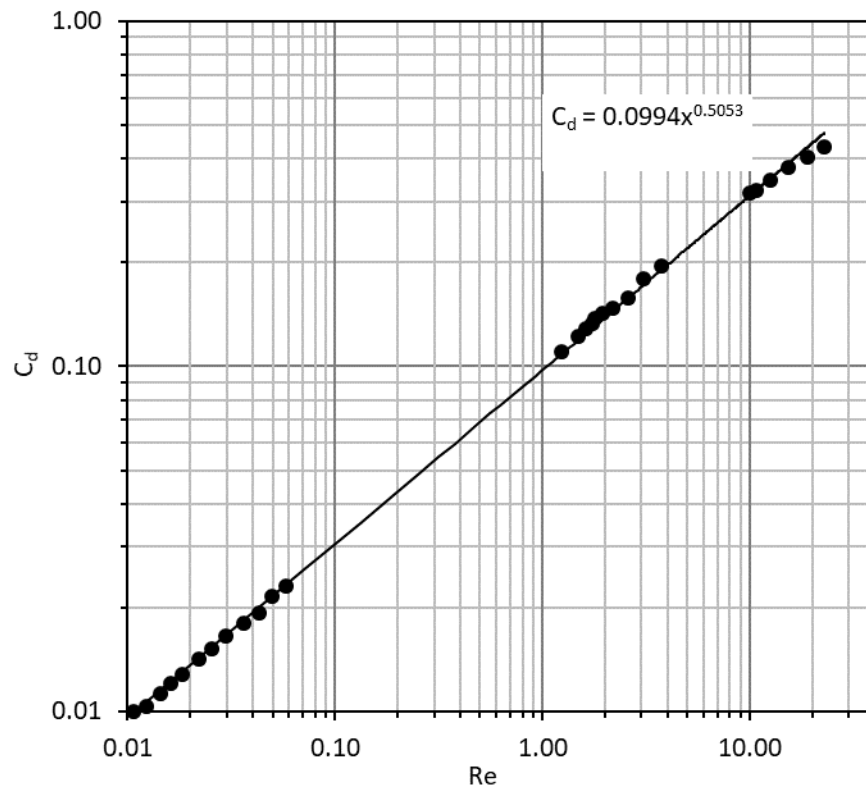


Figure 2.13 Laminar flow for $L/d=1$ (Kiljański, 1993)

Four liquids (ethylene glycol, potato syrup and two glycerol solutions), all Newtonian liquids, were tested using orifices of varying L/d ratios over a flow range of $0.01 < Re < 500$. Tests were carried out from an upright Perspex tube of 38 mm in diameter, with a base made of brass. Three orifices with aspect ratios of 0.5 and diameters of 2, 3, and 5 mm were used, along with two additional 3 mm diameter orifices with aspect ratios of 0 (sharp-edged), 0.5 and 1.0. In Figure 2.14, showing plots of C_d versus Reynolds number, it is evident that for $Re < 10$, each aspect ratio has its own flow trend and when Re is greater than 10, the flow curves produced by the different aspect ratios begin to converge and become one curve near $Re=300$. The researchers suggest that this occurs because of the dominant effects of kinetic energy in this region. They stated that for $Re > 300$, the aspect ratio no longer affects the discharge coefficient.

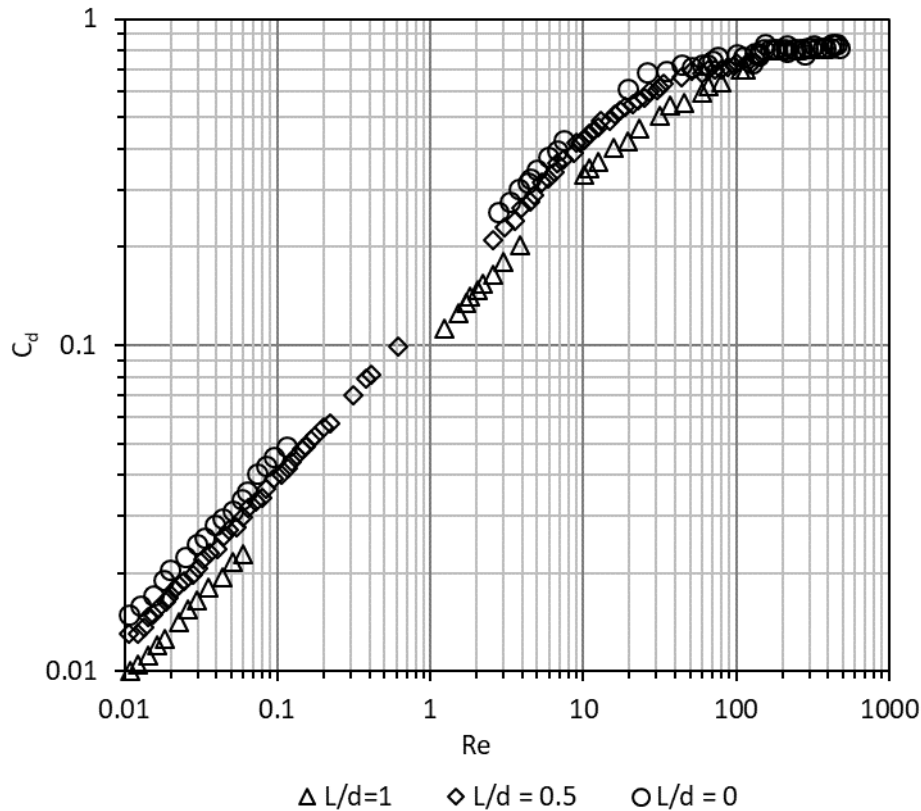


Figure 2.14 C_d vs Re (Kiljański, 1993)

Dziubiński & Marcinkowski (2006) conducted flow rate measurement experiments using water, ethylene glycol, water solutions of starch syrup (all Newtonian) and CMC solution (non-Newtonian). Circular orifices of varying aspect ratios were fitted one at a time at the bottom of a 0.2 m diameter tank. The orifices had diameters of 5, 8, 12.5 and 17 mm with aspect ratios of 0, 0.35, 0.5, 0.75, 1 and 3. The discharge coefficients for Newtonian liquids were calculated as a product of the Newtonian Reynolds number. Figure 2.15 shows the correlation amid the C_d and Re for Newtonian liquids. In the turbulent region where $Re > 100$, an average C_d value of 0.62 was established for all the aspect ratios. In the laminar flow region where the $Re < 10$, the C_d values increased linearly as the Reynolds number increased from 0.001 to 10. Each L/d ratio was found to have its own flow trend (a similar outcome to that of Kiljański [1993]) with the most viscous liquids yielding low C_d values. The experimental points in this region were estimated by the graphs that are described by the power-law equation:

$$\phi = bRe^c \quad \text{Equation (2.26)}$$

The constants b and c were determined to be dependent on the orifice geometry whereby the values of coefficient c were found to be close to 0.5. Thus the coefficient of discharge becomes,

$$\phi = B' \sqrt{Re} \quad \text{Equation (2.27)}$$

Coefficient B' , a constant, depends on the ratio of orifice length to diameter L/d . As a result, B' was approximated by

$$B' = A_1 + A_2 \left(\frac{L}{d}\right)^{A_3} \tag{Equation (2.28)}$$

The coefficients A_1 , A_2 , and A_3 , also constants, were obtained by correlating experimental data. The coefficient of discharge correlation equation for Newtonian liquids when Re is less than 10 was established as:

$$\phi = \left[0.186 - 0.0756 \left(\frac{L}{d}\right)^{0.333} \right] \sqrt{Re} \tag{Equation (2.29)}$$

The proposed equation is valid for: $0.005 \text{ m} < d < 0.017 \text{ m}$; $0 < L/d < 3$; $0.273 \text{ Pa s} < \eta < 26.2 \text{ Pa s}$; $0.00226 < Re < 10$.

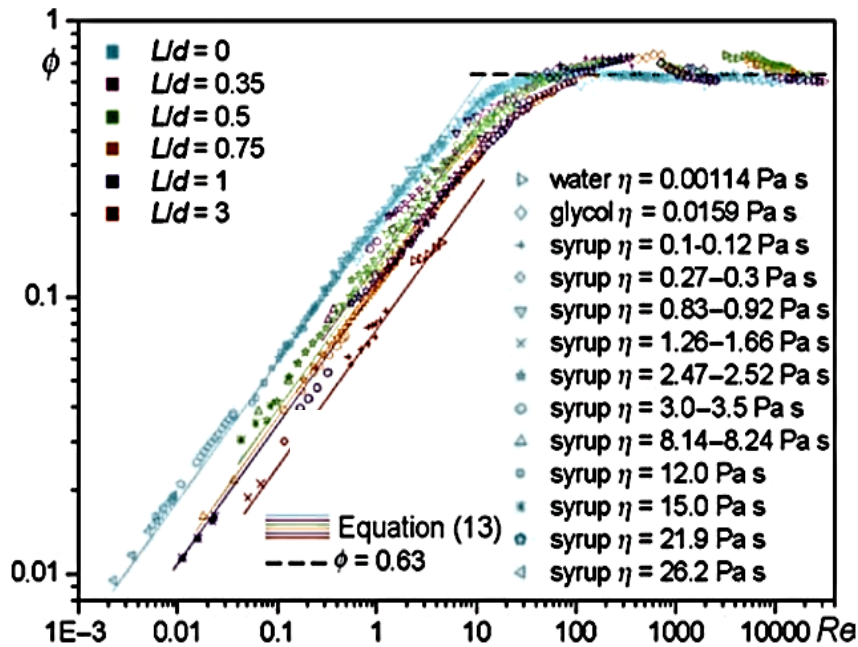


Figure 2.3 C_d values against Reynolds number for Newtonian liquids (Dziubiński & Marcinkowski, 2006)

Figure 2.16 displays the correlation amongst C_d and Re for non-Newtonian liquids. The discharge coefficient for non-Newtonian liquids was calculated as a product of the generalised Metzner and Reed Reynolds number Re_{MR} . Where the Re was less than 100, the C_d increased as the Reynolds number increased and became constant at $Re_{MR} > 100$. The average coefficient of discharge of 0.67 was obtained for all aspect ratios. Similar to Newtonian liquids, each L/d ratio was found to have its own flow trend. The coefficient of discharge correlation equation for non-Newtonian liquids when Re is less than 100 was established as:

$$\phi = \left[0.101 - 0.0164 \left(\frac{L}{d}\right)^{0.48} \right] \sqrt{Re_{MR}^{0.426}} \tag{Equation (2.30)}$$

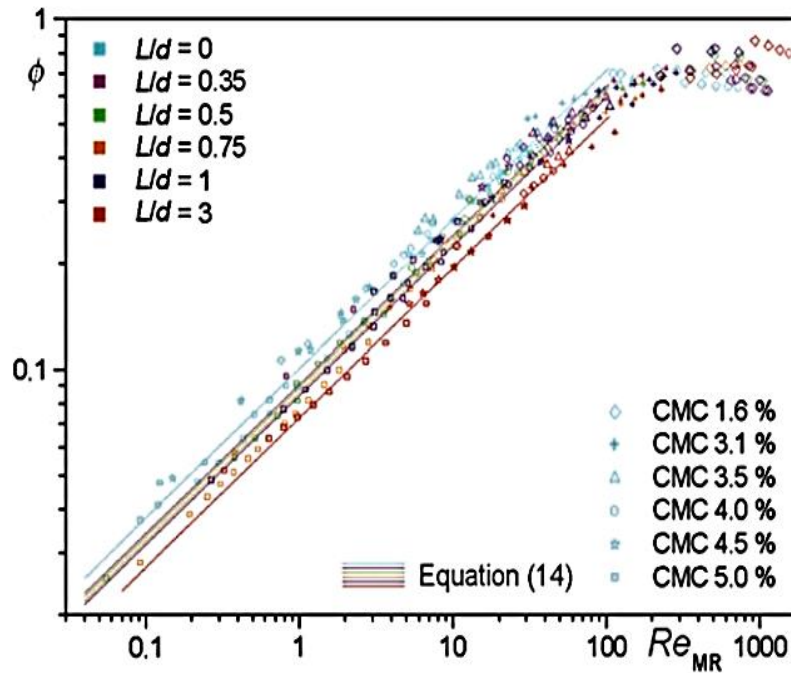


Figure 2.4 C_d vs Re_{MR} (Dziubiński & Marcinkowski, 2006)

Çobanoğlu (2008) conducted flow rate measurement experiments using water to establish the influence of the orifice L/d ratios on the C_d values in relation to the Re . The orifice diameters were 6 and 10.35 mm and L/d ratios were 8 and 5. A rectangular tank with clear Perspex walls (0.37, 0.47 and 0.4) m with a hole machined at the side of the tank was used for all experiments. The Re values ranged from 2000 to 20000 and the head of the liquid was kept constant during the experiments. Based on the results obtained in this study, it is evident that only the turbulent flow regime was obtained (Figure 2.17). The results showed that the C_d values of an L/d ratio of 8 were higher than those of an L/d ratio of 5. Figure 2.17 shows a graphical representation of Çobanoğlu's (2008) results: he found that for an L/d ratio of 5, the C_d values ranged from 0.75 to 0.83 with an average C_d of 0.79; and for an L/d ratio of 8, the C_d values ranged from 0.77 to 0.85 with an average of 0.83. It was concluded that the C_d values increased as the L/d ratio increased.

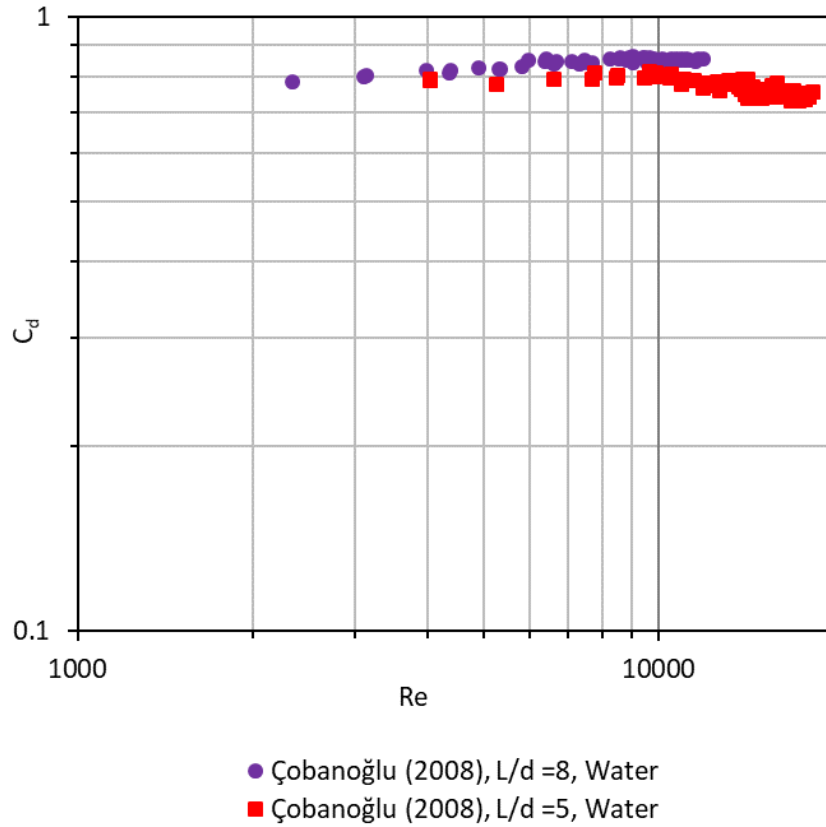


Figure 2.5 Çobanoğlu's (2008) experimental results

Table 2.3 shows peak and asymptotic values of Re and C_d for different L/d ratios. The peak C_d values increased as the L/d ratio increased. Moreover, the peak Reynolds number increased with an increase in L/d ratio.

Table 2.3 Peak and asymptotic values of Re and C_d for different L/d ratios (Çobanoğlu, 2008)

L/d	Re_{peak}	C_{dpeak}	Re_{asym}
0.35	363	0.77	1640
0.5-0.75	2482	0.78	19700
5	9640	0.83	-
8	11700	0.86	-

Swamee and Swamee (2010) proposed a discharge equation for a circular sharp crested orifice meter placed on the side of a large tank using Lea's 1938 experimental data to smoothen the transition zone.

$$C_d = 0.611 \left[87 \left(\frac{v}{d\sqrt{gh}} \right)^{1.43} - \left(1 + \frac{4.5v}{d\sqrt{gh}} \right)^{-1.26} \right]^{-0.7} \quad \text{Equation (2.31)}$$

The analysis, based on the relationship between the Reynolds number, orifice diameter and the coefficient of discharge, revealed that for $Re > 10\,000$, the coefficient of discharge attained a relative

constant C_d value of 0.61 and for low Reynolds numbers, the C_d value increased as the Reynolds number increased.

Figure 2.18 shows a graphical representation of the results from researchers who conducted their studies from tanks. As seen from the graph, in the laminar flow, each L/d ratio has its own flow trend. For Newtonian liquids, an agreement is seen in turbulent flow for an aspect ratio of 0.

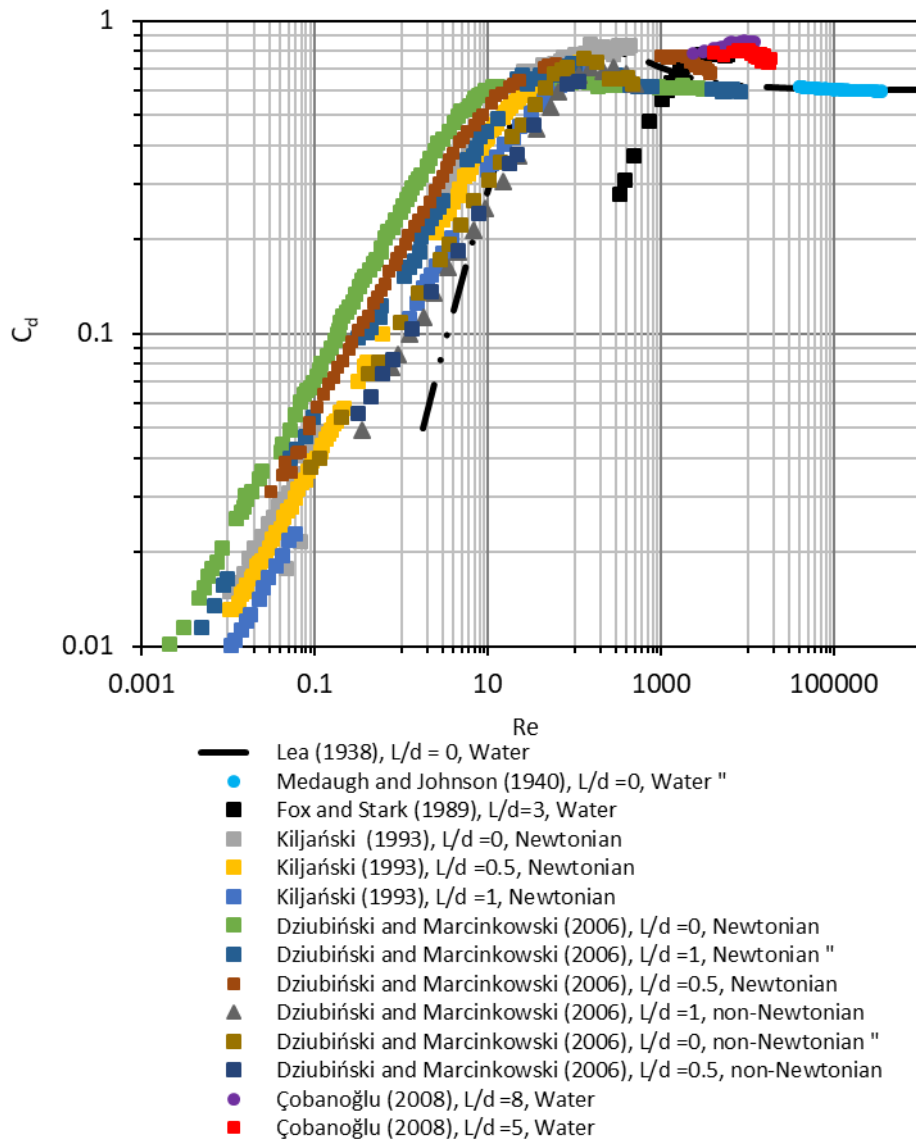


Figure 2.6 C_d versus Re for Newtonian and non-Newtonian liquids for various researchers

2.6.2 Newtonian liquids flow rate measurement in pipes

Johansen (1930) conducted an experimental study of flow rate measurement of water, castor oil and mineral lubricating oil, keeping the temperature of these liquids at $\pm 18^\circ\text{C}$. Coefficients of discharge for orifices with five different diameter ratios ($\beta = 0.090, 0.209, 0.401, 0.595$ and 0.794) over a range of Reynolds numbers from 0 to 25000 were determined. Figure 2.19 shows C_d versus Re curves for all diameter ratios. The coefficient of discharge was found to have a steep linear slope from $0 \leq Re \leq 1000$. As the Reynolds number increases beyond 1000, the graph forms a hump with increasing speed to reach

a maximum C_d value (at $2000 < Re < 3000$). Past the maximum point ($Re > 3000$), the C_d was found to drop with declining speed and ultimately reach a constant value of $C_d = 0.615$. Johansen (1930) also notes that as the diameter ratio increases, the Reynolds number at which these flow transitions occur is higher; thus, the flow remains laminar at higher Reynolds numbers for increased diameter ratios.

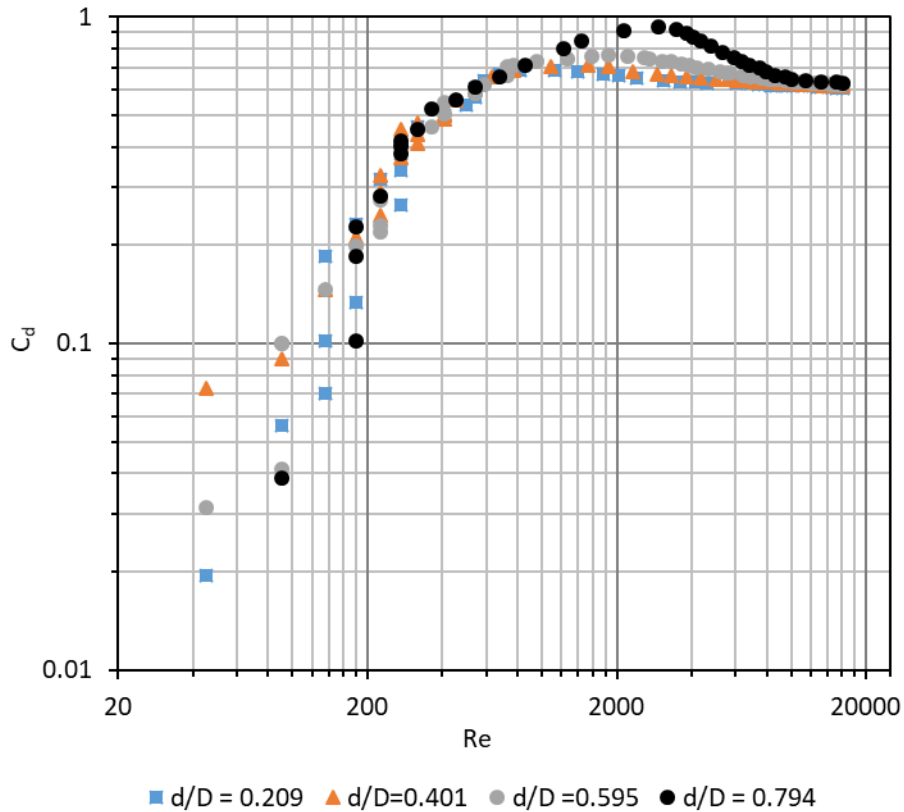


Figure 2.7 Johansen's (1930) experimental results for various beta ratios

Lichtarowicz *et al.* (1965) presented experimental results investigated by James (1961), Sanderson (1962) and Morgan (1963), who all examined the effect of L/d on the C_d of circular square-edged orifices fitted in horizontal pipes. The researchers used Newtonian liquids (water, glycerine solutions and a variety of oils) with Re ranging from 1 to 50000; the L/d ratios ranged from 0.5 to 10. Their results (Figure 2.20) showed that as the aspect ratio increased from 0.5 to approximately 1, the C_d value increased from 0.61 to 0.78, while in the range of aspect ratios from 1 to 2, the increase is non-linear and achieves a maximum value of 0.81. Further increases in aspect ratio result in a gradual linear decrease in the C_d value to a value of 0.74 at an aspect ratio of 10.

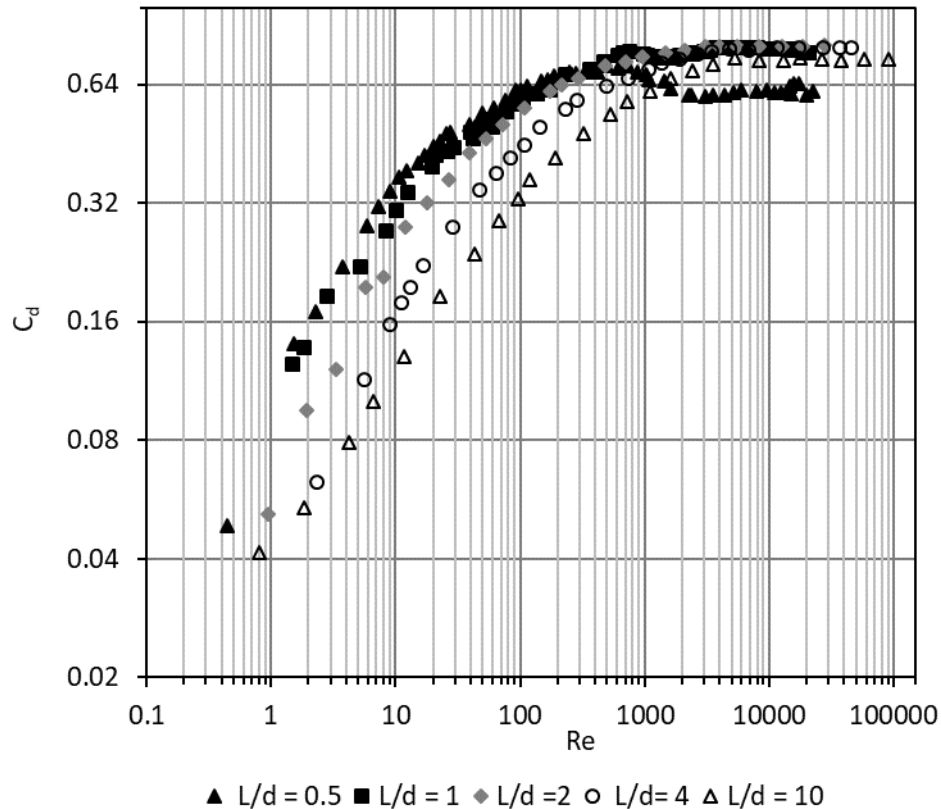


Figure 2.8 Lichtarowicz *et al.*'s (1965) experimental results for various aspect ratios

Ramamurthi and Nandakumar (1999), carrying out flow rate measurement research using deionised water, used circular shaped-edged orifices of diameters of 0.3, 0.5, 1 and 2 mm. They had the length of diameter ratios ranging from 1 to 50. The test set-up consisted of a tank with water, a nitrogen gas tank for initiating water flow and a feed line with flow control valves for providing water at pressures in the range of 0.05 and 1.5 MPa to the opening. The orifices discharged into the ambient atmosphere. The coefficient of discharge was determined using Equation 2.27:

$$Q = C_d A_0 \sqrt{\frac{\Delta P}{\rho}} \quad \text{Equation (2.32)}$$

A digital pressure gauge was used for recording pressure prior to the orifice. The discharge rate through the orifice over a certain period of time was determined by collecting water in a bucket and weighing it with a scale. Data evaluation was based on the correlation of the coefficient of discharge and Reynolds number for each orifice diameter and L/d . Figures 2.21 and 2.22 show the attained discharge coefficients versus the Reynolds numbers.

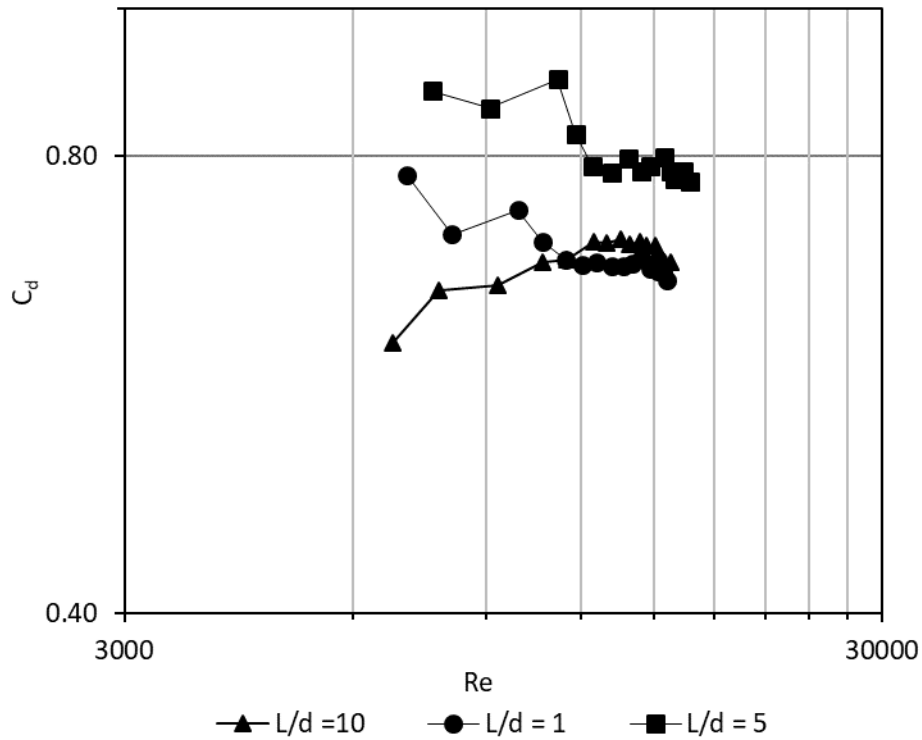


Figure 2.21 Variation of discharge coefficient for a 0.3 mm diameter orifice at different aspect ratios (Ramamurthi & Nandakumar, 1999)

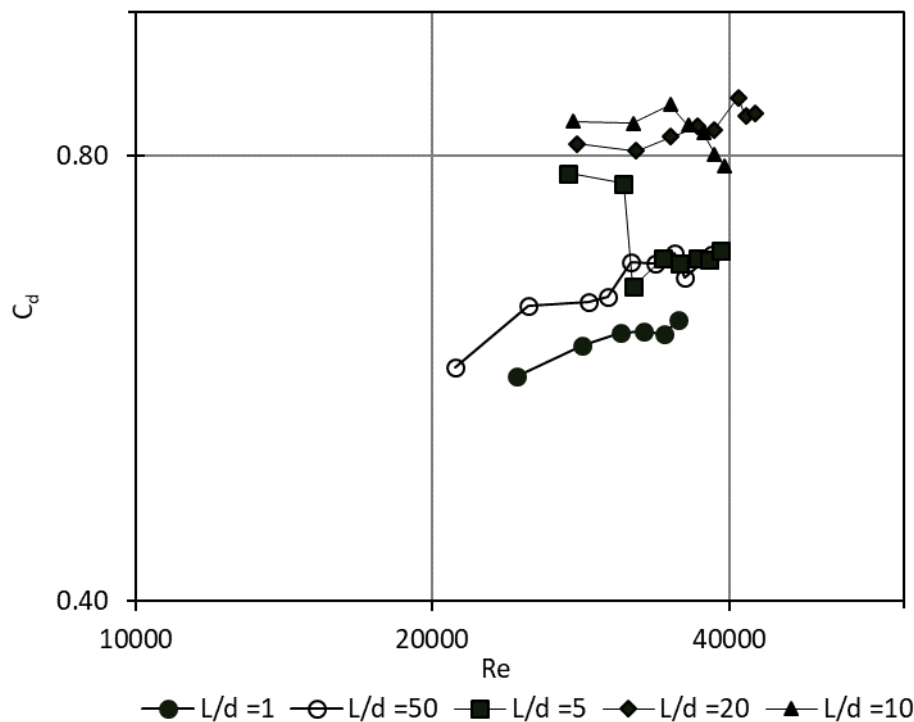


Figure 2.22 Variation of discharge coefficient for a 2 mm diameter orifice at different aspect ratios (Ramamurthi & Nandakumar, 1999)

For an aspect ratio of 1, it was found that the discharge via the opening was detached from the boundaries of the orifice; this is supported by the small values of coefficient of discharge attained for L/d ratios of 0.3 and 2 mm. For an L/d of 5 the C_d at first increased as the Re increased and attained the highest value and then afterward decreased to values comparable to detached flow values. At the point when the Reynolds

number has increased past the values at which detachment occurs, the C_d values remain fairly steady. At the point where the L/d increased to 10, it is seen that the C_d does not decrease as suddenly when contrasted to L/d of 5. The Reynolds number, at which the flow separates, increases to higher values. When the L/d is enlarged to 20 and 50 there is no evidence of detached. The C_d increases as the Re increases.

Bohra (2004) studied the pressure drop and discharge of Newtonian liquids (water and variety of oils) with low values of Re using small circular orifices of varying aspect ratios. Pressure drops were measured for each orifice over a broad range of flow rates ($2.86 \times 10^{-7} < Q < 3.33 \times 10^{-4} \text{ m}^3/\text{s}$). The liquids tested exhibited non-Newtonian properties at the lower temperatures. It was found that in the laminar region, as the L/d increased, the Euler number also increased and was highly dependent on the Reynolds number. In the turbulent region, the Euler number was not dependent on the Reynolds number and attained constant values dependent on the L/d ratio and the beta ratio.

Tunay *et al.* (2004) used the CFD method to simulate a study on flow rate measurement of water and variety of oils. The beta ratio used was of 0.6 and the orifice length to diameter ratios varied from 0.08 to 1. The Reynolds number was from 0 to 20000. The C_d values were found to be more sensitive to Reynolds number in the range of smallest values of L/d . Higher C_d values, however, were attained for longer orifices in the turbulent region.

2.6.3 Non-Newtonian liquids flow rate measurement in pipes

Salas-Valerio and Steffe (1990) conducted a study on flow rate measurements using power law liquids (modified waxy maize food starch solutions at concentrations of 5, 7.5 and 10%) through horizontal pipes. Circular orifices of diameters 3.18, 4.76 and 7.84 mm were used to conduct the study. Rheological parameters were determined by a hake Rv-12 concentric cylinder viscometer. The coefficient of discharge was steady at high velocities but dropped as the density increased. Data analysis was presented graphically where the C_d was plotted against the Re . The C_d , in the range of 0-0.7, was dependent on density, orifice diameter and liquid velocity. The C_d values increased with increasing Reynolds number and assumed steady values at high Reynolds number with an average value of 0.6. They found that C_d decreases as the viscosity increases.

Chowdhury (2010) conducted a study in pipes to establish pressure loss and C_d for non-Newtonian liquids (CMC and kaolin) using long square-edged orifices of varying β ratios, as presented in Table 2.4.

Table 2.4 Different orifice sizes (Chowdhury, 2010)

Orifice bore diameter, d , (mm)	β ratio d/D	Orifice bore thickness, t , (mm)	L/d ratio	C_d
16.56	0.36	66.21	4	-
23.00	0.50	115.00	5	0.79
32.00	0.70	161.00	5	0.83

A tube viscometer with diameters of 25 and 46 mm was used to define the rheological parameters of the test liquids. Data evaluation was based on the correlation of the C_d and Re for each beta ratio. Figure 2.23 shows that the laminar region was observed when $Re_{MR} < 100$, as in this region each β had its own flow trend. Also, the C_d values increased with an increase in Re values. For a given Reynolds number, as the beta ratio increased, the C_d values decreased. The turbulent flow region was observed when $Re_{MR} > 1000$. In this region, the C_d values were constant at separate average C_d values of 0.79 and 0.83 for the β ratios of 0.5 and 0.7, respectively. As a result of the effect of the diameter ratio, the C_d values increased with an increase in the beta ratio, shifting toward a higher Reynolds number for bigger beta ratios.

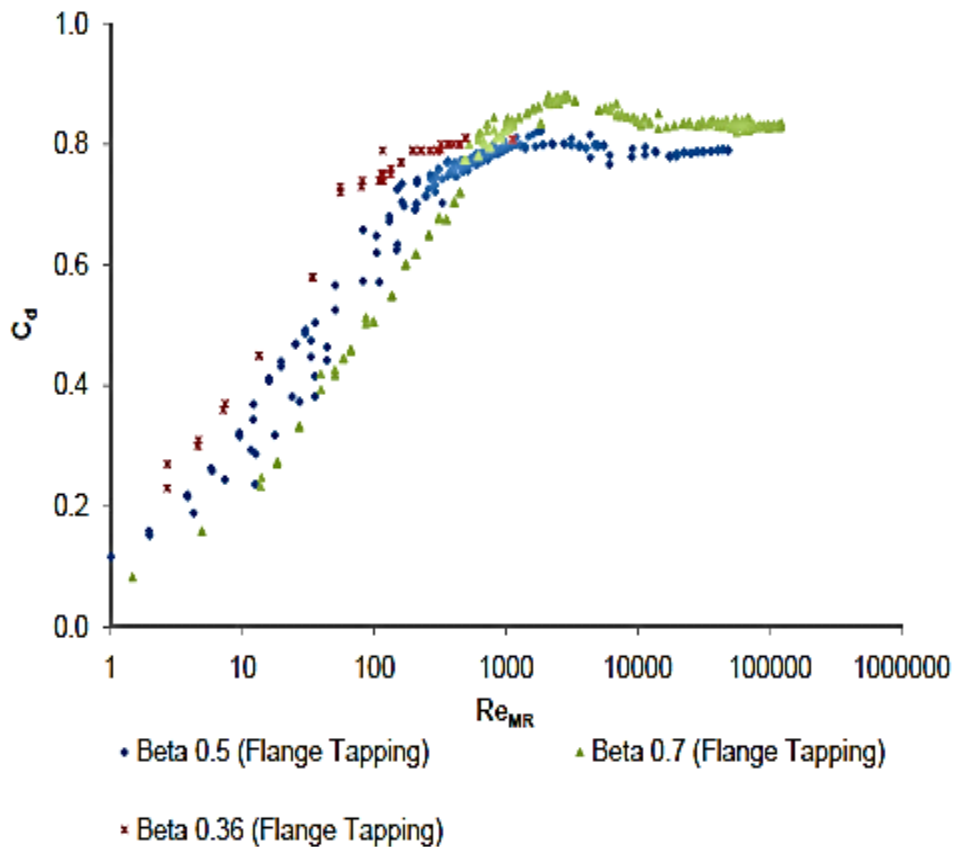


Figure 2.23 C_d against Re (Chowdhury, 2010)

Ntamba Ntamba (2011) conducted a pressure loss study using short square-edged orifices fitted in horizontal pipes. The test materials were kaolin suspensions, bentonite suspensions and CMC solutions. His focus was on short square-edged orifices of diameter sizes 9.2, 13.8, 26.2 and 32.2 mm, each with beta ratios of 0.2, 0.30, 0.57 and 0.7, respectively. Figures 2.25 and 2.26 show outcomes attained for β of 0.2 and 0.57. Figure 2.24 shows that the turbulent flow occurred when $Re_3 > 100$ and the discharge coefficient approached steady average C_d values of 0.71. The transition zone was observed when $10 \leq Re_3 \leq 100$ where data was scattered, reaching a peak of 0.83. The laminar flow region was observed when $Re_3 < 10$ and the C_d value were found to increase as the Reynolds number increased. For a beta ratio of $\beta = 0.3$, the laminar flow regime occurred at $Re_3 < 10$, where the C_d values increased with an increase in Reynolds numbers. The discharge coefficients reached a peak in the transition zone where $10 < Re_3 < 250$. In turbulent flow for $Re_3 > 250$, the discharge coefficient became nearly constant with an average C_d value of 0.67.

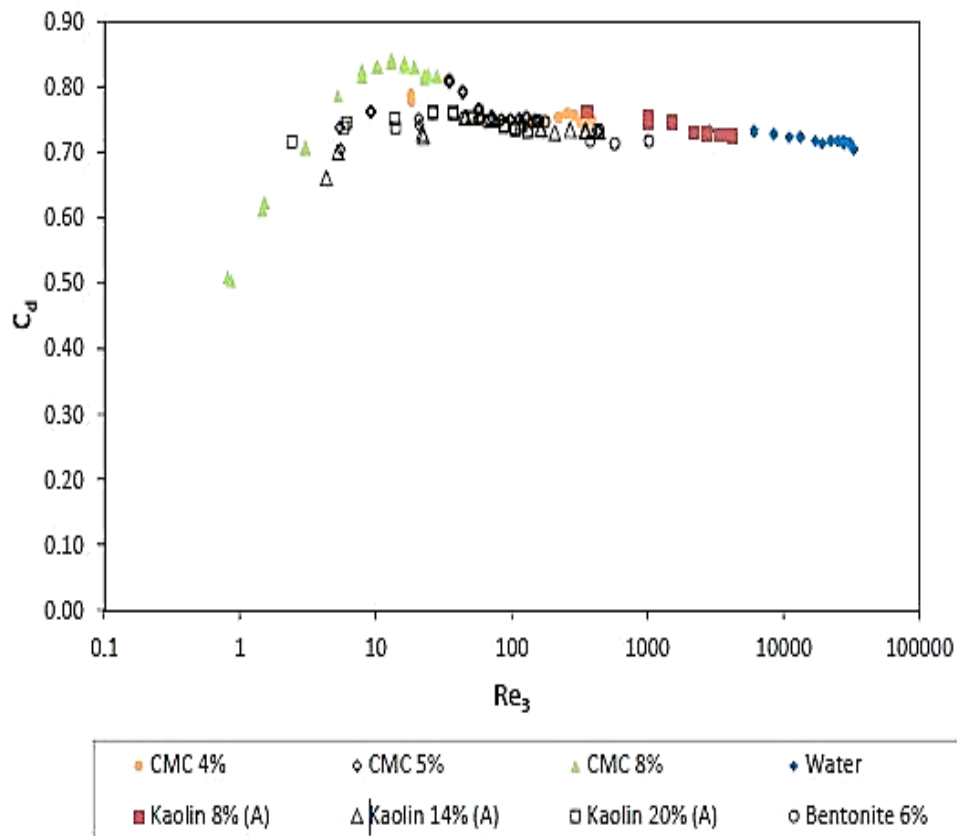


Figure 2.24 C_d against Re for $\beta = 0.2$ (Ntamba Ntamba, 2011)

Figure 2.25, presenting results for a beta ratio of 0.57, shows that the laminar flow regime was observed when $Re_3 < 100$ after which the discharge coefficient increased with the Reynolds numbers until it reached a peak. The transition zone occurred over a range of Reynolds numbers from 400 to 1 000. In turbulent flow where $Re_3 > 1 000$, the discharge coefficients were independent of the Reynolds numbers and assumed a constant average C_d value of 0.63. The transition zone occurred at Reynolds numbers between 1000 and 10 000, where the discharge coefficient reached its peak value. Above the transition, the discharge coefficient becomes constant with an average value of 0.64. The results showed that the C_d values increased with an increase in L/d ratio and shifted towards a higher Reynolds number for bigger L/d ratios (Table 2.5).

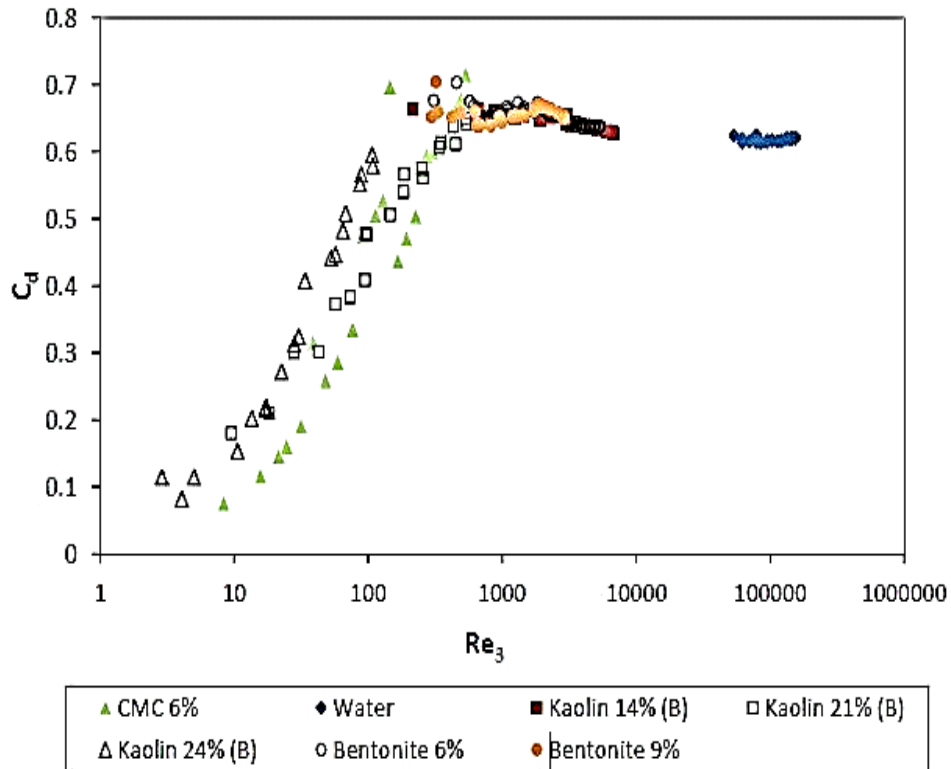


Figure 2.25 C_d against Re for $\beta = 0.57$ (Ntamba Ntamba, 2011)

Table 2.5 shows the different orifice dimensions used by Ntamba Ntamba (2011) when conducting his study. The results reveal that as the orifice diameter increased the L/d ratios were decreasing. The C_d values show a non-linear increase as the L/d ratio and orifices diameter increased.

Table 2.5 Different orifice dimensions (Ntamba Ntamba, 2011)

Orifice bore diameter, d , (mm)	β ratio d/D	Orifice bore thickness, t , (mm)	L/d ratio	C_d
9.2	0.2	6	0.65	0.71
13.8	0.3	6	0.43	0.67
26.2	0.57	6	0.23	0.63
32.2	0.7	6	0.19	0.64

Rituraj and Vacca (2018) claimed that the coefficient of discharge is reliant on the orifice geometry and liquids properties. They further stated that the C_d caters for frictional loss. Fester *et al.* (2008) carried out experimental work on energy losses of viscous liquids in sudden pipe constrictions. A union was used to create the sudden constriction. Test materials represented Newtonian, pseudoplastic and yield pseudoplastic behaviour. The analysis of the study was based on the correlation amongst the loss coefficient, Reynolds number and diameter ratio. In the laminar flow region, the loss coefficient was reliant on the Reynolds number, decreasing as the Re increased. The turbulent region was observed for Reynolds numbers bigger than 10000; it is in this region that the loss coefficient attained a relatively constant number.

Chemical and polymer manufacturing industries use orifices for measuring and regulating non-Newtonian liquids. In 2018, Rituraj and Vacca conducted research focusing on the correlation for sharp orifices at lesser diameter ratios using circular sharp orifices of diameters 3.18, 1.59 and 0.79 mm. Each orifice was fitted into a horizontal pipe with a diameter of 19.05 mm. Three different shear thinning liquids – referred to as A, B and C – were used as test materials. It was observed that the viscosity of liquid C changed as the shear rate changed, that is, the viscosity decreased as the shear rate increased. The decrease in viscosity led to an increase in the Reynolds number. The evaluation of the study was based on the relationship between Euler number, Reynolds number and diameter ratio. For small Reynolds numbers, it was established that an increase in aspect ratio causes an increase in the Euler number. It was also observed that at low Reynolds numbers, the Euler number was strongly influenced by Reynolds the number but towards the turbulent flow region, the dependence reduced, and the Euler number assumed became relatively constant. These results agreed to Borah's (2004) study on flow and pressure drop of highly viscous liquids in small aperture circular square-edged orifices. Comparable studies which related the non-dimensional pressure drop to the orifice geometry and Reynolds number have shown that at low flow rates, C_d is considered to be a function of the aspect ratio, the diameter ratio and the orifice Reynolds number. At high Reynolds numbers, the C_d becomes independent of the Reynolds number, primarily dependent on diameter ratio (Steffe & Salas-Valerio, 1990; Mincks, 2002; Borutzky, 2002).

2.7 Conclusion and summary of literature review

Work to date shows that the standard Newtonian liquid C_d value for sharp-crested orifices is approximately 0.61 from tanks and in pipe flow (Lea, 1938; Lienhard & Lienhard, 1984; Swamnee, 2010). Research has been done on non-Newtonian liquid flow through orifices by researchers such as Salas-Valerio and Steffe (1990), Chowdhury (2010) and Ntamba Ntamba (2011) in pipes. Dziubiński and Marcinkowski (2006) reported on the correlation between C_d and Re for Newtonian and power law non-Newtonian liquids. There was no significant difference in the effect of the aspect ratio in the turbulent flow region: for Newtonian and non-Newtonian liquids, they found an average C_d value of 0.62 and 0.67, respectively. The effect of aspect ratio was clearly seen in the laminar flow where each aspect ratio had its own flow trend. For Newtonian liquids, conducting tests in the range of 0.001 to 10000 and for non-Newtonian liquids in the range 0.01 to 1000 (power-law liquids only), they established a coefficient of discharge correlation equation for Newtonian and non-Newtonian liquids respectively from tanks through small cylindrical orifices that are valid for $0.005 \text{ m} < d < 0.017 \text{ m}$; $0 < L/d < 3$; $0.273 \text{ Pa s} < \eta < 26.2 \text{ Pa s}$; $0.00226 < Re < 10$ and $0.005 \text{ m} < d < 0.017 \text{ m}$; $0 < L/d < 3$; $1.45 \text{ Pa s}^n < k < 15.1 \text{ Pa s}^n$; $0.457 \text{ Pa s} < n < 0.606 \text{ Pa s}$; $0.0495 < Re < 100$.

Kiljański (1993) conducted gravitational flow measurements of viscous Newtonian liquids from the side of a tank. Using five circular orifices of varying aspect ratios ranging from 0 to 1, his results agreed with those of Dziubiński and Marcinkowski (2006) in that each aspect ratio was found to have its own flow trend. Unlike Dziubiński and Marcinkowski (2006), however, Kiljański (1993) did not have data for the turbulent flow region. According to Dziubiński and Marcinkowski (2006), their correlation equation for an L/d of 0.5 agreed with Kiljański's (1993) data. Furthermore, neither Dziubiński and Marcinkowski (2006) nor Kiljański (1993) generated a model which would allow the separate flow trends to form one flow trend for each L/d .

The L/d ratios used by Kiljański (1993) and Dziubiński and Marcinkowski (2006) ranged from 0 to 1 and from 0 to 3 respectively (all short tube orifices except for 3). Although Çobanoğlu's (2008) study was conducted using long orifices and focused on turbulent flow, he only used water and had a narrow range of Reynolds numbers. Furthermore, Çobanoğlu's (2008) orifices were placed on the side of the tank. From the literature, it is evident that extensive research on the flow rate measurement of Newtonian liquids has been given to the aspect ratio of 0 and it is clear, that the flow phenomenon through this orifice ($L/d = 0$) is well understood. The same cannot be said, though, about the other aspect ratios, especially those of 1 and 3.

Ramamurthi and Nandakumar (1999) conducted studies on flow rate measurements of water using various aspect ratios in the range of 1- 50. They found the aspect ratios to have a considerable effect on the coefficient of discharge depending on the length of the orifice which determined if the flow was cavitating, separated or separated flow followed by attachment. They concluded that for smaller aspect ratios, a cavitating flow is observed thus yielding lower C_d values because the length of the orifice is not long enough to allow a completely developed flow. For longer aspect ratios that allowed complete flow to occur, the coefficient of discharge was determined as relatively constant and higher. However, the increase in the coefficient of discharge was not proportional to the increase in orifice length as the orifice diameter was another factor that contributed to the final value of the C_d values obtained. Their study was conducted in horizontal pipes.

In this study, the orifices investigated are all 20 mm in diameter, with lengths of 0, 20, 60 and 100 mm and aspect ratios of 0, 1, 3 and 5, respectively. This study aims at better understanding the orifice flow characteristics over a broad range of Reynolds numbers. Thus far, there is limited literature pertaining to the discharge of non-Newtonian liquids from the bottom of tanks using orifices of varying aspect ratios. It is evident that additional experimental data is needed for a more comprehensive comparison. This research uses additional types of non-Newtonian liquids exhibiting different non-Newtonian liquid models. The models used to characterise non-Newtonian liquids for this study are Bingham plastic, pseudoplastic and yield-pseudoplastic or Herschel-Bulky. The Reynolds numbers used for this study are calculated from Slatter and Lazarus Reynolds number Re_2 . In the studies of orifices, the C_d values are correlated to the Reynolds number (Lea, 1938; Dziubiński & Marcinkowski, 2006; Ntamba Ntamba, 2011). In order to obtain the Reynolds number for non-Newtonian liquids, rheological parameters of the liquids must be known

Table 2.6 displays the outline of previous work from 1930 to 2018.

Table 2.6 Summary of literature review

Authors and Placement of orifice	Orifice geometry	Re range	L\vd ratios	Orifice diameter (mm)	liquids & Temperature °C	Data Presentation Format & Findings
Newtonian liquids in tanks						
Lea (1938) <i>Side of tank</i>	Circular sharp crested orifice	1 to 1000000	0	-	Water, mixtures of water and glycerine and number of oils	Plots of C_d versus square root of Re for experiments. The coefficient of discharge for all ratios was found to be approximately 0.6
Medaugh and Johnson (1940) <i>Side of tank</i>	Circular Square-edged	30,000 to 350,000	0, 0.5, 0.33, 0.25 and 0.13	6.35, 12.7, 19.05, 25.4 and 50.8	Water at 16.94 °C	Plots of C_d versus head and plot of C_d vs Re. The coefficient of discharge for perfect contraction was found to be about 0.588
Lienhard and Lienhard (1984) <i>Site of tank</i>	Circular Sharp-Edged	-	0	-	Water	C_v Vs Head
Fox and stalk (1989) <i>Vertical pipe</i>	miniature short-tube orifices	0-11000	1-14	0.3, 0.5 and 4	Water	C_d Vs Re and K Vs Re
Kiljański (1993) <i>Side of tank</i>	Circular Sharp-Edged	10 to 500	0,0.5,1	2, 3 and 5	Ethylene, Glycol, Glycerol Solutions and Potato Syrup	C_d vs Re plots

Authors and Placement of orifice	Orifice geometry	Re range	L/d ratios	Orifice diameter (mm)	liquids & Temperature °C	Data Presentation Format & Findings
Dziubiński and Marcinkowski (2006) <i>Bottom of tank</i>	circular sharp-crested orifice	0.001 to 10000	0, 0.35, 0.5, 0.75, 1 & 3	5, 8, 12.5 and 17 mm	Water	In the turbulent flow, average C_d value was found to be 0.62
Çobanoğlu (2008) <i>Side of tank</i>	Circular orifices	2000-20000	5 and 8	6.35 and 10	Water	Plot of C_d vs generalized Re. C_d varied with aspect ratio. $L/d=5 = 0.78$ $L/d=8 = 0.80$
Swamee (2010) <i>Analysis of experimental data</i>	circular sharp-crested orifice	0.1 to 1000000			Analytical approach of experimental data	Discharge coefficient equation's has been developed for circular sharp crested orifice meter
Mohajane <i>et al.</i> (2019) <i>Bottom of tank</i>	Circular orifices	100 - 66000	0 and 5	20	Water and glycerine	C_d Vs Re $L/d = 0, C_d = 0.60$ $L/d = 5, C_d = 0.78$
Non-Newtonian liquids in tanks						
Dziubiński and Marcinkowski (2006) <i>Bottom of tank</i>	circular sharp-crested orifice	0.01 to 1000	0, 0.35, 0.5, 0.75, 1 & 3	5, 8, 12.5 and 17	CMC	In the turbulent flow, average C_d value was found to be 0.67
Authors and Placement of orifice	Orifice geometry	Re range	L/d ratios	Orifice diameter (mm)	liquids & Temperature °C	Data Presentation Format & Findings

Newtonian liquids in pipes						
Johansen (1930) <i>Horizontal Pipe</i>	Circular Sharp- edged with 45° slope	<1 to 25000	0	-	Water, castor oil and mineral lubricating oil at 18 °C	Plots of C_d versus square root of Re for experiments. The coefficient of discharge for all ratios was found to be approximately 0.615
Lichtarowicz <i>et al.</i> (1965) <i>Horizontal pipes</i>	Square- Edged	0.5 to 50,000	0.5-10	-	Water, water- glycerine mixture, oil	Plots of C_d vs Re for various aspect ratios
Ramamurthi and Nandakumar (1999) <i>End of horizontal pipe</i>	circular sharp- edged orifices	2000 to 100000	1-50	0.3 and 0.5	Demineralised water	C_d vs Re plots for different geometries determined that orifices with aspect ratios of less than 5 are most affected by separated flow
Bohra (2004) <i>Horizontal pipes</i>	circular sharp- edged orifices	1 to 10000	0.5, 1 and 3	1,2 and 3	Highly viscous oils	Euler numbers vs Reynolds numbers for various aspect ratios
Tunay (2004) <i>CFD simulation</i>	Circular square edged orifices.	0 to 200000	0-080 -1	-	Simulation	Plots of C_d vs Re for various aspect ratios.

Authors and Placement of orifice	Orifice geometry	Re range	L/d ratios	Orifice diameter (mm)	liquids & Temperature °C	Data Presentation Format & Findings
-------------------------------------	---------------------	----------	---------------	-----------------------------	-----------------------------	--

non-Newtonian liquids in pipes						
Salas-Valerio and Steffe (1990) <i>Horizontal pipes</i>	Hole in a pipe	0 to 2300	0	13.18, 4.76 & 7.84	5, 7.5 and 10 % corn starch solution	C_d Vs Generalised Reynolds number. C_d varies from 0 to 0.7 for power law liquids. C_d decreases as consistency coefficient increases
Fester <i>et al.</i> (2008) <i>Horizontal pipes</i>	Unions	1 to 1000000	-	-	CMC and Kaolin	Pressure loss coefficient K_{con} against Re_{MR}
Chowdhury (2010) <i>Horizontal pipes</i>	Circular long sharp square-edged	1 to 1000000	16.56, 23 and 32	4 and 5	Water, Kaolin, Bentonite and CMC at 20 °C and pH 9	Pressure loss coefficient K_{or} against Re_{MR} and coefficient of discharge against Re_{MR} . For $L/d = 5$ and $\beta = 0.5$ $C_d = 0.729$ For $L/d = 5$ and $\beta = 0.7$ $C_d = 0.813$
Ntamba Ntamba (2011) <i>Horizontal pipes</i>	Circular Short square-edged	1 to 1000000	9.2, 13.8, 26.2 & 32.2	0.65, 0.43, 0.23 & 0.19	Water, Bentonite and CMC at 20 °C and pH 9	pressure loss coefficient K_{or} vs Re_{MR} and Coefficient of discharge vs Re_{MR}
Rituraj and Vacca 2018 <i>Horizontal pipes</i>	sharp orifices	1 to 1000000	3.18, 1.59 and 0.79	-	shear thinning liquids referred to as A, B and C	Euler number Vs Reynolds number

Chapter 3 RESEARCH METHODOLOGY

3.1 Introduction

This chapter showcases the apparatus used and techniques applied to analyse the models explained in the literature. The experimental investigations for this study were conducted at the slurry lab of the Flow Process and Rheology Centre at the Cape Peninsula University of Technology in Cape Town, South Africa. The details of the test rig concerning how it was assembled and used to collect flow rate data are defined.

The rig was built for this project in order to:

- test various slurries using four circular orifices of the same diameter with varying aspect ratios over a wide range of flow rates to include laminar, transition and turbulent flow.

The design of the test rig was such that the tank was manually filled with slurries that were allowed to gravitationally flow out from the bottom of the tank through the orifice to establish the flow rates. The tests were conducted for percentage volume concentrations of kaolin suspensions, percentage mass concentrations of bentonite suspensions, CMC and glycerine solutions. For CMC and bentonite, the amount of powder to be used to prepare the slurry was calculated using percentage of weight/weight and for kaolin the amount of powder to be used to prepare the slurry was calculated using percentage of volume/volume. Water was used for calibration purposes. The rheology was conducted using A Paar-Physica MCR 300 rheometer with a cup and bob attachment.

The following aspects of the experimental work are presented in this chapter:

- description of the test rig;
- experimental layout;
- instrumentation;
- material tested;
- calibration;
- flow rate measurements;
- experimental errors; and
- rheometry.

3.2 Description of the experimental rig

The experimental rig, shown in Figure 3.1, consisted of a rectangular tank with clear Perspex walls (0.4, 0.4 and 0.6) m with a hole machined at the bottom. The tank material was chosen to avoid chemical reactions with the liquids. The height was selected to allow a fully developed flow prior to the orifice before the liquid vortexed. The tank was supported by a steel frame structure suspended on a load cell. CMC, bentonite and kaolin are in powder form therefore the slurries were prepared in a tank with a mixer five days prior to testing to permit a homogeneous mix of the liquids. During the 5-day period the prepared slurries were on a daily bases mixed in the morning and in the afternoon to prevent the formation of lumps. Just before testing the slurries were once again mixed to avoid slurry segregation. One orifice at a time was fixed at the bottom of the tank flush with the inside of the tank and an orifice backing ring was used to position the orifice. The orifice hole was closed with a universal stopper. The test

material was then manually poured into the tank to avoid air entrapment by the liquid. The load cell was connected to a data acquisition unit that was connected to a computer by a USB cable. Change in voltage over time was recorded by the load cell; data was processed by the data acquisition system and then transferred to the computer by USB. The calibration constants were used to convert the voltage to obtain the flow rate.

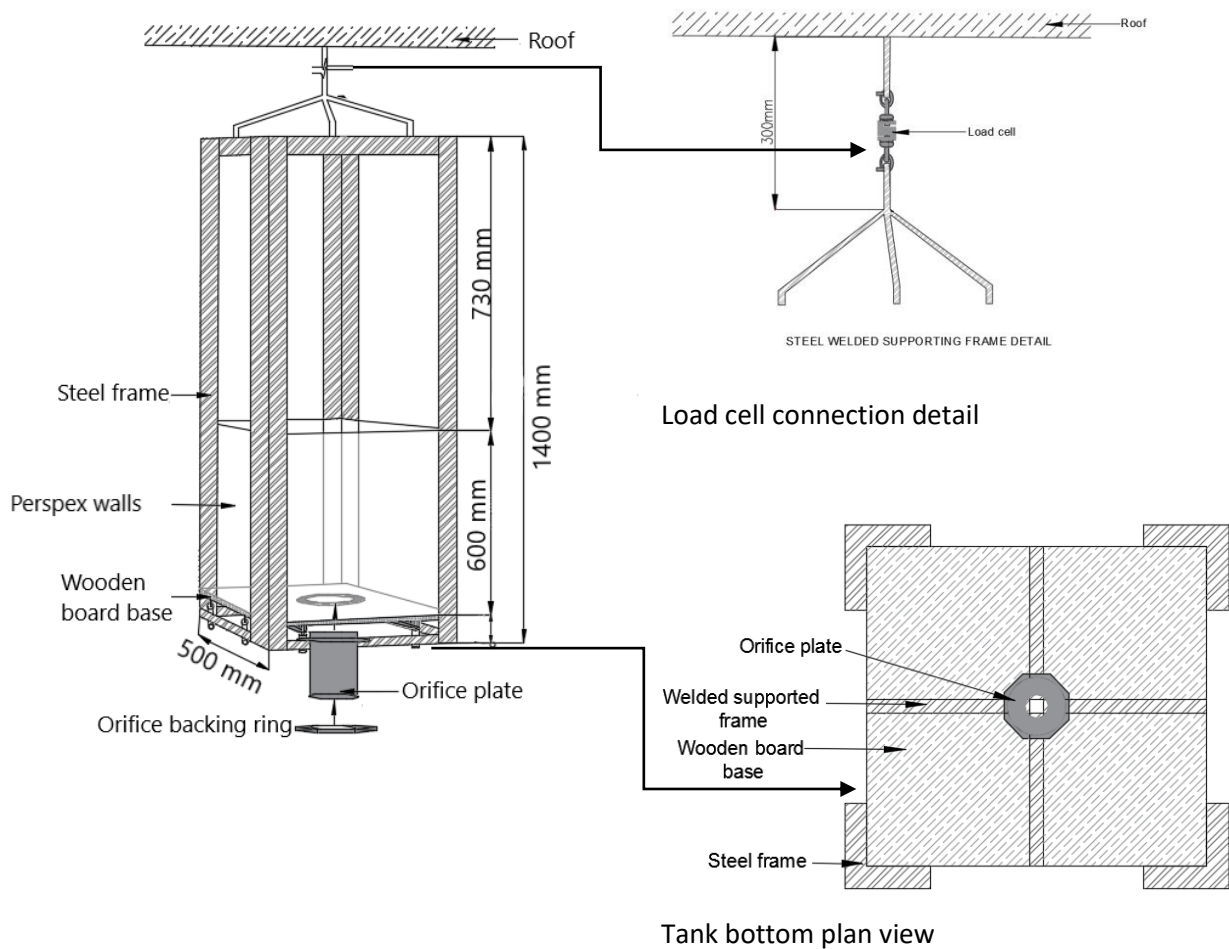


Figure 3.1 Experimental test rig (current study)

3.3 Experimental matrix

Table 3.1 shows the experimental matrix used in this project.

Table 3.1 Experimental matrix

Orifice shape	Orifice diameter (mm)	Orifice thickness (mm)	L/d ratio (-)	Materials to be used
Circular	20	1	0.05	Water, various concentrations of glycerine and CMC solution, bentonite and kaolin suspensions
		20	1	
		60	3	
		100	5	

3.4 Instrumentation

3.4.1 Orifice plates

Four circular orifices made of grey PVC were used to carry out the flow rate tests. They were all 20 mm in diameter but had varying thicknesses of 100, 60, 20 and 1 mm with aspect ratios of 5, 3, 1 and 0.05 (sharp-crested) respectively, as shown in Figure 3.2. Figures 3.3, 3.4, 3.5 and 3.6 display the cross-sectional details of the orifices used in this research.

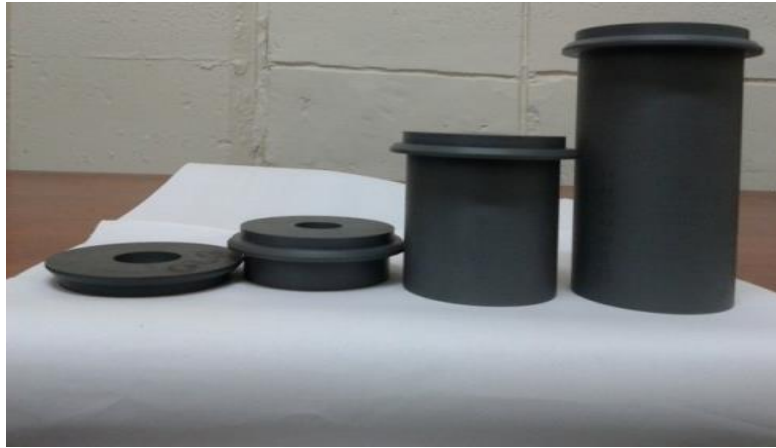


Figure 3.2 Side views of orifices of varying lengths

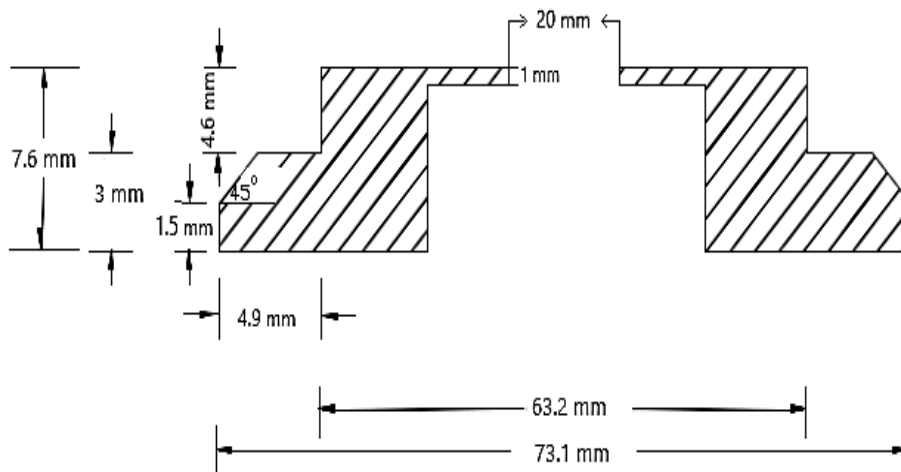


Figure 3.3 Section detail of a 1 mm thick orifice

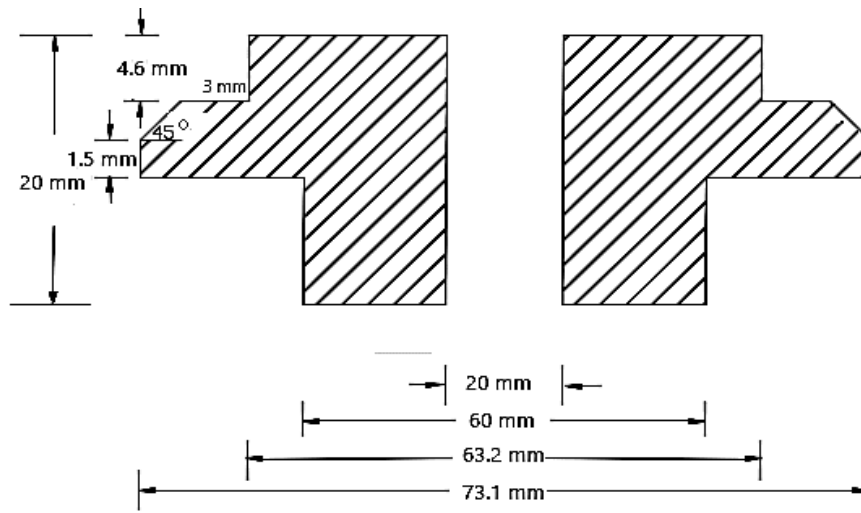


Figure 3.4 Section detail of a 20 mm orifice

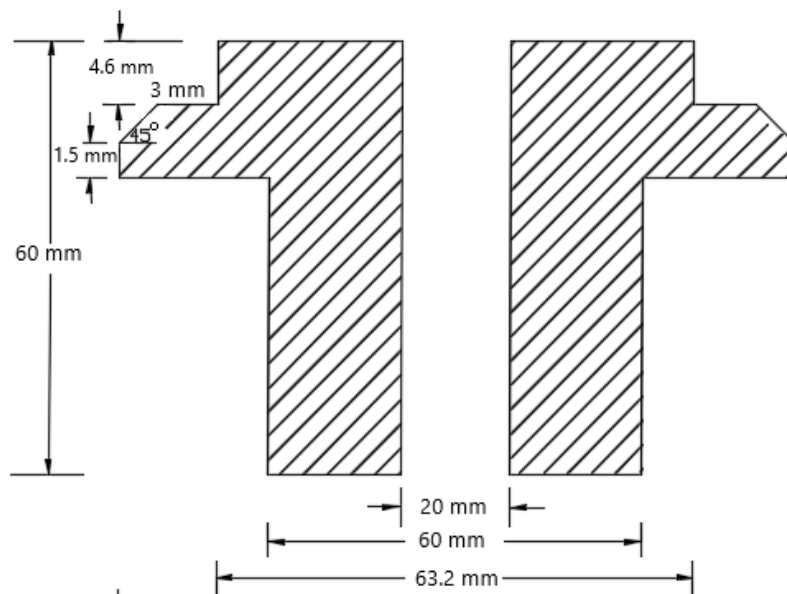


Figure 3.5 Section detail of a 60 mm orifice

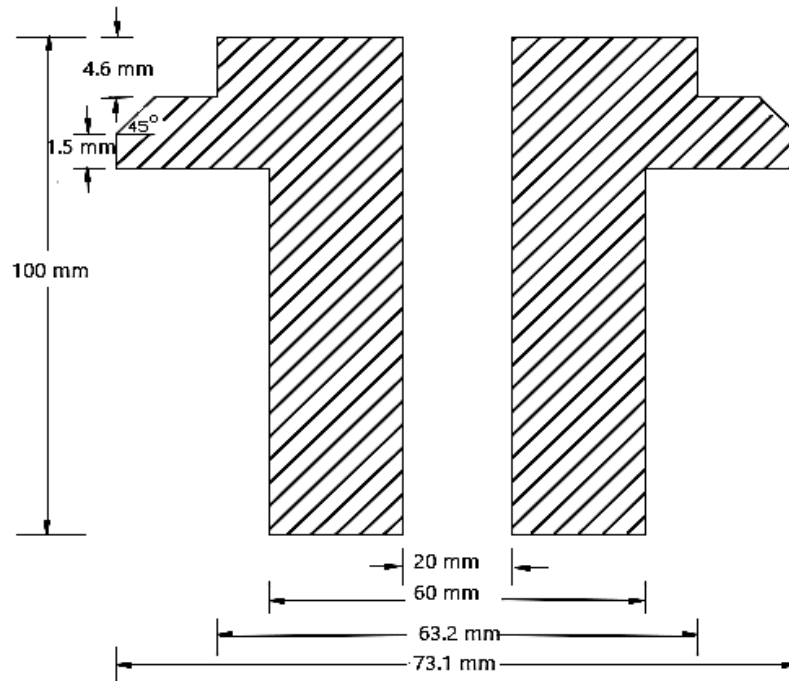


Figure 3.6 Section detail of a 100 mm orifice

3.4.2 Mixing tank

All the material concentrations to be tested were mixed and stored in the mixing tank. It was used for mixing tap water with CMC, bentonite and kaolin in powder form to produce hydrated slurry. Glycerine was also mixed with water to achieve desired concentrated solutions.

3.4.3 Orifice locating plate and backing ring

The orifice plate was positioned into the orifice locating plate Figure 3.7 (fixed at the base of the tank) to ensure that the base is completely sealed; the orifice backing ring (Figure 3.8) was used to hold the orifice plate in position and prevent it from falling due to pressure build-up caused by the liquid.



Figure 3.7 Schematic diagram of orifice locating plate



Figure 3.8 Orifice backing ring

3.4.4 Camera and tripod

Figure 3.9 depicts how the camera was mounted onto the tripod and placed 1.47 m away from the tank to allow the least possible parallax error while at the same time capturing the liquid discharge motion from the top to the bottom of the tank without moving the camera. The camera had a frame rate of 25 frames per second. The number of frames extracted for the liquid to flow from one height to the other was used to calculate the volumetric flow rate discharged through the orifice.

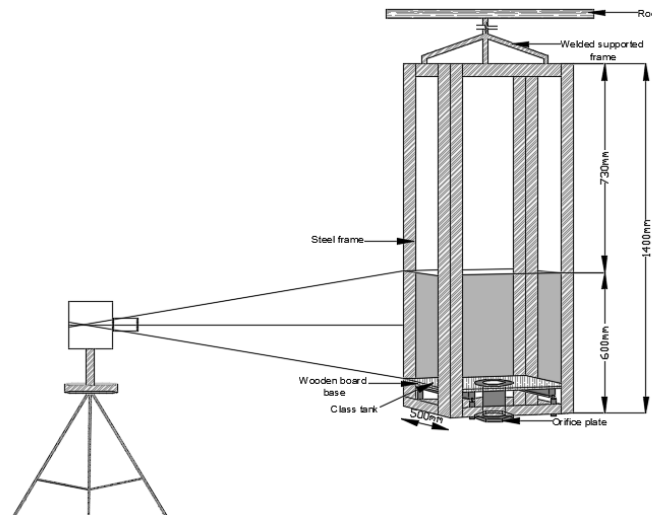


Figure 3.9 Schematic diagram depicting the placement of the camera and tripod

3.4.5 Computer

KMPlayer software was used to analyse all video clips copied to a computer by extracting frames from the videos which were used to determine the time taken by the liquid to flow from one point to the other and the amount of volume discharged per the calculated time. Using this information, the volumetric flow rate through the orifice was determined.

3.4.6 Load cell

Both 100 and 250 kg 'S' type multipurpose reverse universal load cells model 9363 made of stainless steel were used to obtain the mass of the tank and liquids. Their rated output was 3.0 m V/V with an error margin of ± 0.0075 m V/V. This function was to measure the change in mass of the liquid over time as it flowed out of the tank through the orifice. Appendix A contains the 100 and 250 kg load cell calibration certificates obtained from the supplier. Appendix B lists the specifications of the load cells.

3.4.7 Data acquisition system

Power supply

A power supply was used to power up the amplifier device.

Amplifier

An amplifier device (Figure 3.10) was used to amplify the voltage signal from the load cell to the data acquisition (DAQ). The load cell voltage output was 3 m V/V and the data acquisition intake voltage goes up to 10 V (Appendix C).



Figure 3.10 Amplifier device

Data acquisition (DAQ)

Data acquisition (DAQ) NI USB 6001 in Figure 3.11 is an eight-channel unit with a fixed voltage input range of ± 10 V. The amplified load cell signals from the amplifier were sampled and read by NI-DAQmx 9.9 software. The signals were transferred from NI USB 6001 to the computer by a universal serial bus cable (USB) (Appendix D) and transferred to the excel spreadsheet. Only one channel (where the red and blue cables are connected) was used to transfer the voltage (see Figure 3.11). Appendix E shows the cross-sections of the left and right screw terminator connector plugs.



Figure 3.11 Data acquisition

Figure 3.12 shows how the data acquisition system was connected to the computer.



Figure 3.12 Connection of the data acquisition system to the computer

3.4.8 Measuring tape

A measuring tape was used to determine the height of the liquid from one point to the other.

3.4.9 Top pan balance

Top pan balance was used for weighing the test material samples when conducting the relative density test.

3.5 Material tested

Water tests were conducted for the calibration of the orifices and to define the turbulent region for Newtonian liquids; for the laminar region of Newtonian liquids, glycerine solution tests were carried out

at different concentrations. liquids of varying concentrations of carboxymethylcellulose (CMC) solutions and kaolin and bentonite suspensions were selected and tested to represent a broad range of rheological parameters of non-Newtonian liquids similar to those used in industry. CMC represented pseudoplastic liquids, bentonite Bingham plastic liquids and kaolin Herschel–Bulkley liquids.

3.5.1 Preparation of slurries

The liquids were prepared in advance before the rheology and flow rate measurements could be carried out, as the material came in powder form. The slurry preparation method was as follows:

- Calculate the volume of the tank to be used when conducting the experiments.
- For kaolin, calculate the amount of powder based on percentage volume/volume as shown in 93.1:

$$\% \frac{v}{v} = \frac{\text{volume dry solids}}{\text{volume total mix}} \times 2.65 \times 100 \quad \text{Equation (3.1)}$$

For bentonite and CMC, calculate the amount of powder to be used using a percentage of weight/weight as shown in Equation 3.2:

$$\% \frac{w}{w} = \frac{\text{mass dry solids}}{\text{mass total mix}} \times 100 \quad \text{Equation (3.2)}$$

- Pour the required amount of water into the mixing tank.
- Switch on the electric mixer and run it on slow speed.
- Gently add the required powder to the water in the mixing tank.
- Leave the mixture for five days to thoroughly mix (making sure to stir the mix daily to avoid lump formation).

3.5.2 Water

Normal tap water was used to calibrate the orifices and load cell to determine the precision and authenticity of the methodology and equipment. Water was also used for making up other liquids and when conducting the relative density tests.

3.5.3 Glycerine

Glycerine is a highly viscous transparent, sweetened liquid used for flavouring food and in the production of make-ups and colognes. It was mixed with water to give the desired concentrations corresponding to the laminar to turbulent regions.

3.5.4 Carboxymethylcellulose (CMC)

As CMC comes in powder form, it was mixed with tap water in specified percentages and given at least five days' hydration prior to testing to allow for complete hydration. It was mixed on a daily basis during the hydration period to avoid the formation of lumps. CMC is used in industrial applications such as drilling

mud. It is also used in food processing industries as an emulsifier, stabiliser and thickener. It is an excellent food additive to improve product flavour and prolong storage time.

3.5.5 Kaolin

Kaolin is a dry white powder that was prepared in varying volumetric concentrations using tap water. The mixture was given three days to hydrate and was regularly mixed to avoid lumps. Kaolin is often used in paper industries as a paper coating to enhance the look of paper by altering parameters such as brightness, smoothness and gloss.

3.5.6 Bentonite

Bentonite slurries were made by mixing measured quantities of both the bentonite powder and tap water; the mixture was given five days to hydrate while undergoing constant mixing to avoid the development of lumps. Bentonite is used in civil engineering structures such as foundations, horizontal directional drilling (HDD) and pipe jacking.

3.6 Calibration

The precision of measuring equipment often shifts after a period of time. Calibration describes the precision and nature of estimations recorded utilising certain equipment comparing it to a known set of parameters. The apparatus used as a benchmark should be traceable to equipment calibrated in accordance with ISO. The calibration procedure is described in the subsequent section.

3.6.1 Calibration of the load cell

Before calibrating the load cell, the tank was properly cleaned to ensure that the force acting on the load cell was solely that of the tank and cage. The load cell was used to weigh the liquid that flows from the tank through the orifice. To calibrate the load cell, water was weighed in a container on a scale. With the orifice closed, water was manually poured into the tank and the voltage output recorded. For every increase of the load (water quantity) the increase in the voltage was recorded. The calibration procedure was as follows:

- Connect DAQ into the USB port of the computer.
- Switch on the computer and open the NI-DAQmx software.
- Select an appropriate channel on the NI-DAQmx (channel Dev/10) assigned to capture the voltage induced on the load cell.
- Select the frequency (e.g. 60 Hz) with which the load cell is required to transmit the signals.
- Measure the voltage induced by an empty tank on the load cell for about a minute.
- After a minute, re-initialize the programme and re-enter the channel and frequency through which the load cell is required to transmit the voltage.
- With the orifice hole closed, pour in 10 liters of water into the tank. When the system has stabilised, run the programme for about a minute to measure the voltage induced on the load cell by the tank plus the added water.
- Repeat the procedure a number of times, each time adding 10 liters of water until the tank is full.

- Plot the graph of voltage versus weight; determine the slope and the intercept of the linear relationship.

The linear relationship of the weight versus the voltage for the load cell calibration is given in Figure 3.13. A linear regression of the points revealed the relationship between the loads and the equivalent voltages. This information was then entered into the spreadsheet that was used to calculate the flow rate. The linear regression over the range tested gives an R^2 value of 0.99.

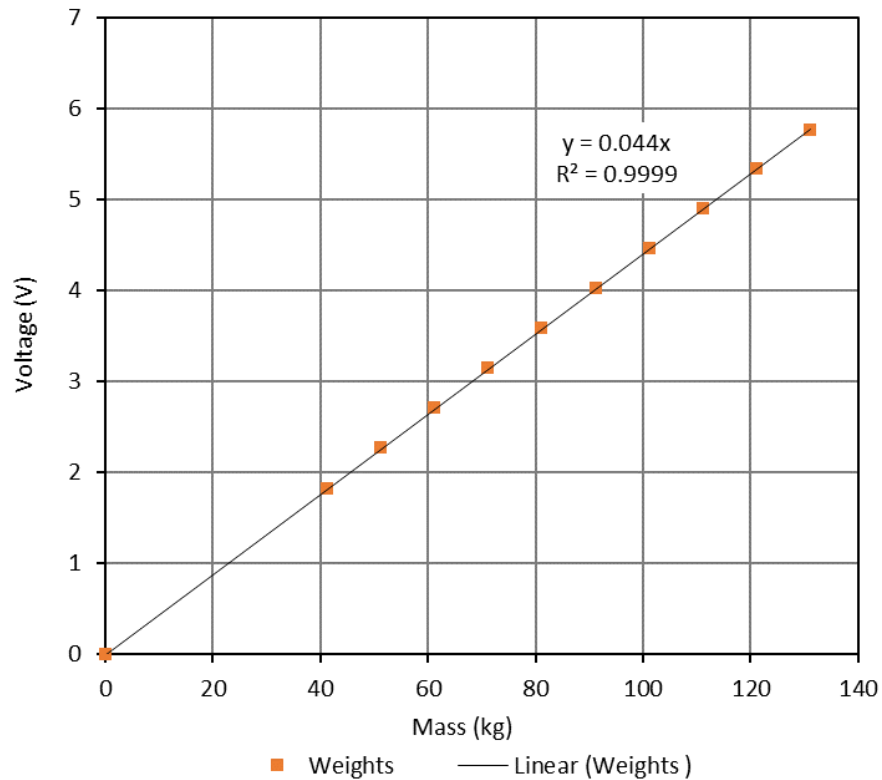


Figure 3.13 Calibration results of a 250 kg load cell

The 100 kg load cell was calibrated at five litre increments: the calibration results are shown in Figure 3.14. The 250 and 100 kg load cell, camera and tape were used during the calibration of the orifices to check the orifice accuracy.

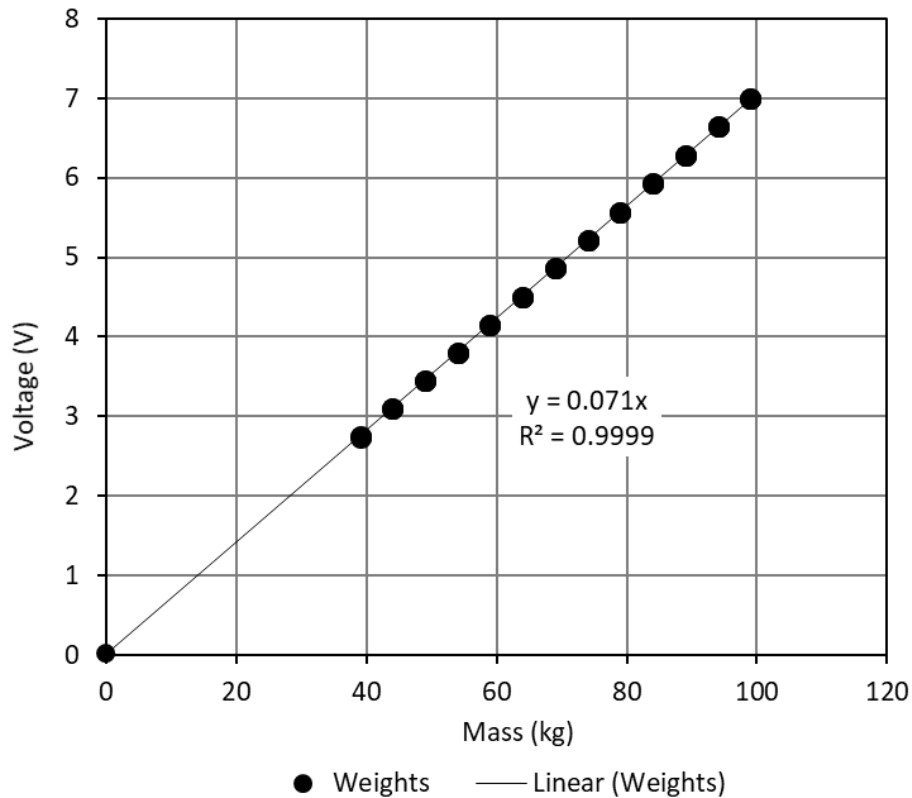


Figure 3.14 100 kg load cell calibration

3.6.2 Calibration of orifices

As explained by Tuğçe (2010), orifices have been used by a number of industries for measuring various kinds of liquids, but the most tested liquid and the one whose flow phenomenon is well understood and accepted as a standard measure for circular sharp crested orifices is water. The only way to determine if the orifices used in this study were constructed and manufactured correctly was to calibrate them. Data obtained was graphically presented and compared to data of Çobanoğlu (2008) and Dziubiński and Marcinkowski (2006). The procedure was as follows:

- Insert the orifice at the bottom of the tank so that it flushes with the inside surface of the tank.
- Plug the orifice hole with a universal stopper and manually fill the tank with water.
- Allow the tank to stabilise and then switch on the computer and load the DAU programme.
- Select an appropriate channel on the DAU (channel Dev/10) assigned to capture the voltage induced on the load cell.
- Select the frequency (e.g. 60 Hz) which the load cell uses to record the change in mass over time as the water flows out of the tank.
- Simultaneously pull the plug so that the water flows out of the tank through the orifice; run the programme to capture the data as the water is discharged out of the tank.
- Close the programme before the water vortexes.
- Repeat the same procedure for the different orifices.

Compatibility results of orifice calibration of L/d ratio of 0.05 using the 100 and 250 kg load cell are shown in Figure 3.15.

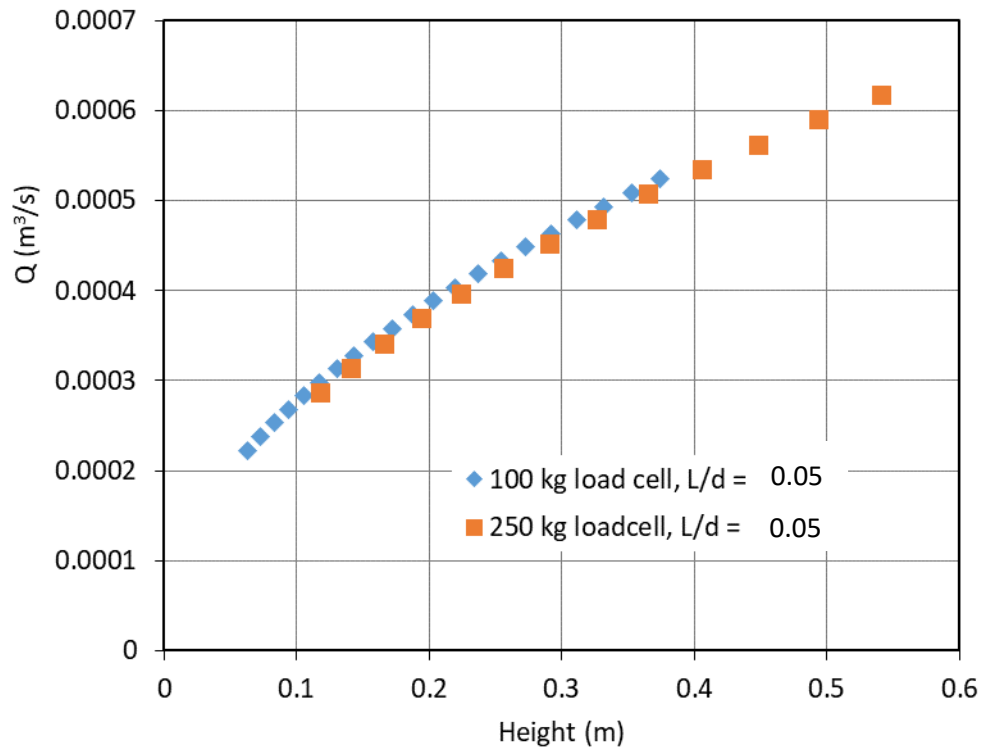


Figure 3.15 Comparison between a 250 kg load cell and a 100 kg load cell

The C_d values were calculated using Equation 2.11:

$$C_d = \frac{Q_1}{A_0 \sqrt{2gh}} \quad \text{Equation (2.11)}$$

Calibration results were conducted for each orifice length (1, 20, 60 and 100 with L/d ratios of 0.05, 1, 3 and 5 respectively). For each orifice L/d ratio the C_d values obtained were plotted against the Reynolds number and compared to the existing data to verify the validity of the calibration results, as shown in Figure 3.16. For an L/d ratio of 0.05, the C_d values were generally constant with an average C_d value of 0.60, and for an L/d ratio of 1, the C_d values ranged from 0.60 to 0.58 with an average C_d value of 0.59; the average C_d values are within $\pm 2\%$ and $\pm 5.5\%$ respectively of the error margins of the standard C_d value of 0.61 for circular sharp-crested orifices (Lea, 1938; Lienhard & Lienhard, 1984; Tuğçe, 2010). Dziubiński and Marcinkowski (2006) average C_d value of 0.62 falls within the $\pm 2\%$ of the standard C_d value of 0.61 for circular sharp crested orifices. For an L/d ratio of 5, the C_d values ranged from 0.79 to 0.77 with an average C_d of 0.78; and for an L/d ratio of 3 the C_d value was relatively constant with an average C_d value of 0.8. The values are within $\pm 2\%$ of Çobanoğlu's (2008) C_d value of 0.79. The average C_d value of L/d ratios of 3 is in agreement with Fox and Stark's (1989) average C_d value of 0.80. The calibration results show a non-constant increase in C_d values as the aspect ratio increases; the average C_d values were 0.60, 0.59, 0.80 and 0.78 with standard deviations of 0.002, 0.006, 0.001 and 0.004 for L/d ratios of 0.05, 1, 3 and 5 respectively. Dally *et al.* (1993) stated that tube orifices placed on the side of the tank have an average C_d value of 0.80 and Brater and King (1982) determined that the C_d value of short tube orifices varies from 0.78 to 0.83 with a mean C_d value of 0.82; these values are in line with the C_d values obtained for the current study for an L/d ratio of 3 and 5. The orifices used in Brater and King (1982) and Dally *et al.* (1993) were placed on the side of the tank. Appendix F shows water flow rate calibration calculations.

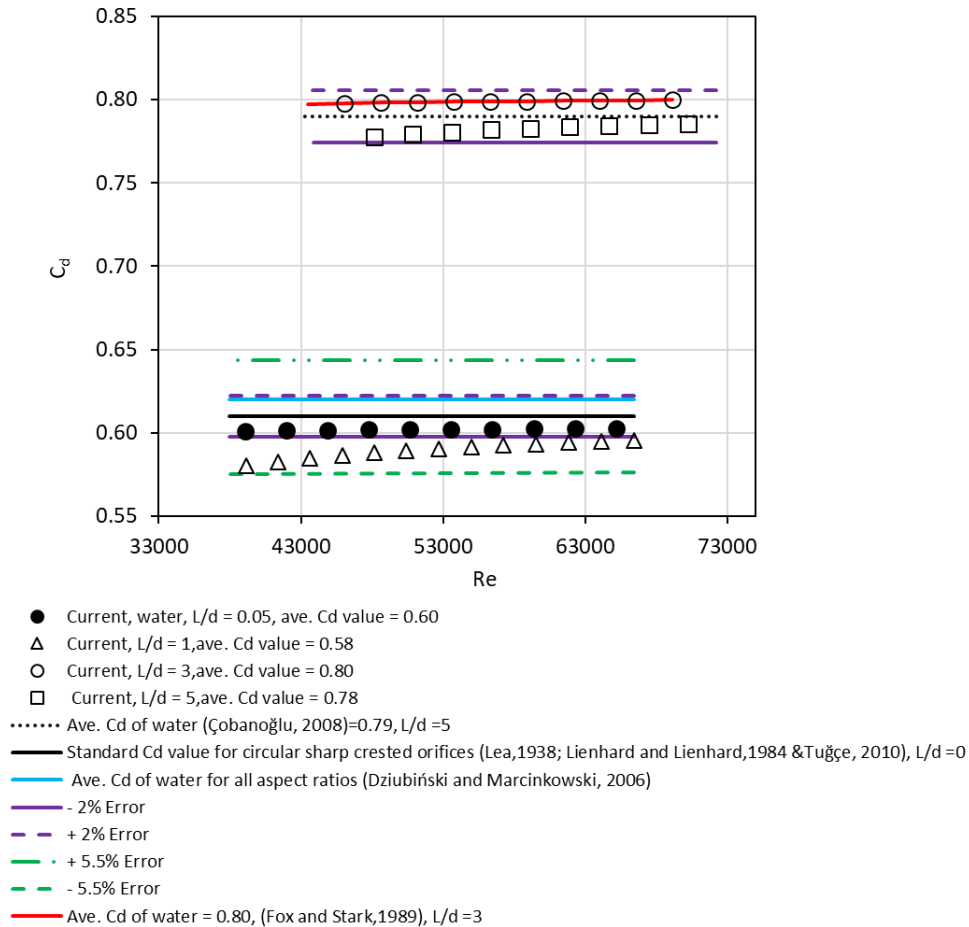


Figure 3.16 Orifice calibration results for aspect ratios of 0, 1, 3 and 5

3.7 Flow rate measurements

3.7.1 Load cell method

The equipment used included:

- orifice test rig;
- test material;
- load cell; and
- data acquisition unit (DAU).

The procedure was as follows:

- Close the orifice hole with a plug.
- Pour the liquid into the tank and allow it to stabilise.
- Connect the DAU to the computer and initialise the load cell programme.
- Select an appropriate channel on the DAU (e.g. channel Dev/10) assigned to capture the force induced on the load cell.
- Select the frequency (e.g. 60 Hz) at which the load cell is required to transmit the signals.

- When the liquid has settled, pull the plug from the orifice opening and begin the capturing programme simultaneously.
- As the liquid flows out of the tank, signals in the form of voltage are transmitted to the computer.
- The data on the computer was then used to calculate the flow rate and velocity of the liquids from the tank, and ultimately, the coefficient of discharge.
- This procedure was adhered to for each liquid and each concentration.

3.7.2 Camera method

The equipment used included:

- orifice test rig;
- water;
- camera and tripod; and
- computer with KMPlayer software.

The procedure was as follows:

- Assemble the test rig.
- Place measuring tape along the side of the tank.
- Plug the orifice hole.
- Fill the tank with liquid and allow it to stabilise.
- When the liquid has finally stabilised, start capturing the video.
- Extract the frames using the KMPlayer programme.
- Record the number of frames it takes for the liquid to reach each designated level in the tank as it flows out of the tank.
- Repeat the processes at least three times to obtain an average time and reduce the error percentage.
- With the volume of each section in the tank known, the flow rate can now be determined.

Figure 3.17 implies compatibility between the camera method and load cells method for an L/d of 1. Other compatibility graphs for aspect ratios of 0.05, 3 and 5 are shown in Appendix G.

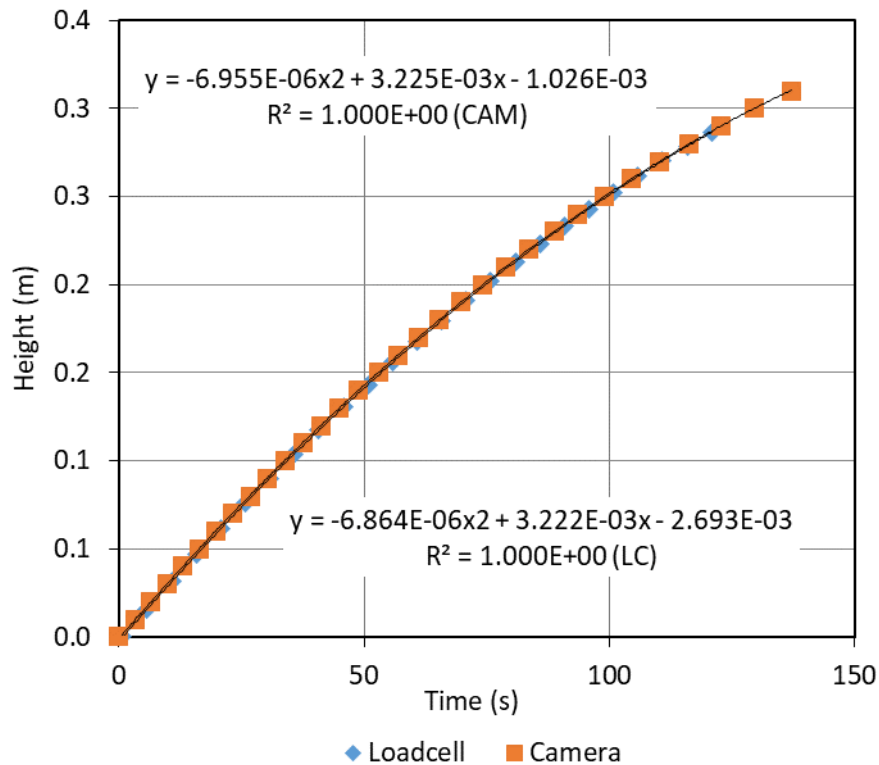


Figure 3.17 Compatibility between load cell and camera for L/d ratio of 1

3.8 Experimental errors

In every experimental study or research, errors are inevitable; it is therefore vital to be observant of their origin and keep them as minimal as possible. In as much as procedures and protocols are performed to reduce the errors, complete accuracy is not always attained. There are three types of errors: gross errors, systematic errors and random errors (Benziger & Aksay, 1999). Some quantities like Reynolds numbers and discharge coefficients are calculated from different variables such as discharge velocity with their subsequent errors. These measurements are all said to influence the value of the quantity differently.

3.8.1 Systematic errors

Systematic errors frequently occur as a result of constant faults which continue through the entire experimental study. These faults may be caused by several factors:

- instrumentation (calibration inconsistencies);
- human error (inability to be precise);
- natural factors (temperature, bacterial action, atmospheric pressure and moisture); and
- theoretical factors (simplification of the model system or approximations in the equations describing it).

In efforts to reduce the degrees of these errors, parameters such as temperature were recorded before, during and after each experiment. Experiments for the same quantity were repeated at least three times for repeatability.

3.8.2 Random errors

Random errors usually result from the experimenter's inability to take the same measurement in exactly the same way to get the exact same number (Benzinger & Aksay, 1999). This type of error is evaluated only by studying the discrepancies that occur among repeated measurements of the same quantity (Barry, 1991). Figure 3.17 depicts the height versus time graph of both the load cell and camera: as seen from the graph, the difference in measurement is $0.009 \times 10^{-6}x^2 + 0.003 \times 10^{-3}x - 1.667$. The water coefficient of discharge standard deviation was calculated from Equation 3.1. The standard deviations were found to be 0.002, 0.006, 0.001 and 0.004 for aspect ratios of 0.05, 1, 3 and 5 respectively.

$$S = \sqrt{\frac{\Sigma(C_d - C_{davg})^2}{N - 1}} \quad \text{Equation (3.3)}$$

3.8.3 Parallax error

The camera, mounted onto the tripod and placed 1.47 m away from the tank, recorded the water discharged from the tank through the orifice. The number of frames extracted for the liquid to flow from one point to the other was used to calculate the displacement height. For each water level drop, the height difference obtained was 0.01; therefore, the parallax error from the extracted camera frames per height was calculated by a trigonometric function tangent formula. Each height recorded was out by $\pm 0.39^\circ$.

$$\tan^{-1} = \left[\frac{\text{height difference}}{\text{distance from camera to tank}} \right]$$

$$\begin{aligned} \tan^{-1} &= \left[\frac{0.01}{1.47} \right] \\ &= 0.39^\circ \end{aligned}$$

Therefore, each measurement that was read by frames was out by $\pm 0.39^\circ$.

3.8.4 Errors of computable variables

Some errors result from the accumulation of additional errors from previously calculated variables; the resulting error is a combination of those individual variable errors (mean quadratic value of the independent errors). Errors are unavoidable when analogue signals from instruments such as a load cell are converted into a digital signal by the DAU. Quantities such as volume and flow rate are reliant on supplementary measurements such as mass and density with their substituent errors (Brinkworth, 1968). The highest predictable inaccuracy can be calculated from:

$$\left[\frac{\Delta X}{X} \right]^2 = \sum \left[\frac{\partial X}{\partial n} \right]^2 \left[\frac{n}{X} \right]^2 \left[\frac{\Delta n}{n} \right]^2 \quad \text{Equation (3.4)}$$

The volume of liquid in the tank was calculated from the density and the mass was calculated from the load cell calculations.

$$\text{volume} = \frac{\text{mass}}{\text{density}} \quad \therefore \quad v = \frac{m}{\rho}$$

The highest expected error is calculated from

$$\left[\frac{\Delta \text{vol}}{\text{vol}}\right]^2 = \left[\frac{1}{\rho} \frac{m}{\text{vol}} \frac{\Delta m}{m}\right]^2 + \left[\frac{m}{\rho^2} \frac{\rho}{\text{vol}} \frac{\Delta \rho}{\rho}\right]^2$$

Table 3.2 Combined errors

L/d	Combined errors for volume %
0	2.5
1	0.9
3	1.8
5	3.1

3.9 Rheometry

A rheometer is used in various ways to assess the rheological behaviour of the material under consideration. In order to use the rheometer efficiently, some parameters had to be established to accommodate the material under investigation. These measurement parameters include the gap, temperature, measuring time at each point, pre-shearing rate and duration of measurement. The slurries used in this study were liquid-like; hence, a rotational rheometer was used for slurry characterisation. After each slurry concentration was prepared for testing, rheological measurements were conducted by an MCR 300 Paar-Physica rheometer (Figure 3.18). The measuring geometry used in this study was a CC 27 (Figure 3.19) measuring system consisting of a smooth cylindrical cup and a sandblasted bob. The rough exteriors were to lessen the wall slip effect; the lower end of the bob was shaped as a truncated cone to reduce end effects. The measuring system datasheet of CC27, shown in Appendix H, has settings as follows:

- Shear rate range: 0.01 -1000 1/s for Newtonian and power law liquids.
- Shear rate range: 100 -1000 1/s for Herschel-Bulkley and Bingham plastic liquid. This was due to the orifice shear rate limitations and instability of the results attained below 100 1/s by the rheometer.
- The temperature was maintained in accordance with temperature of the slurry during flow rate testing.
- Gap: 1 mm.
- Data fitted with Herschel-Bulkley fitting for kaolin, Bingham plastic for bentonite suspensions, power-law fitting for CMC solutions and Newtonian fitting for glycerine.

For more reliable measurements, it is advisable to control the environment in which the experiments are conducted as a form of attaining a baseline. This was not possible, however, as the laboratory where flow tests were conducted was not climate controlled.

Data collected: density, viscosity, height, liquid flow rate, velocity, flow behaviour index, liquid consistency index and yield stress.

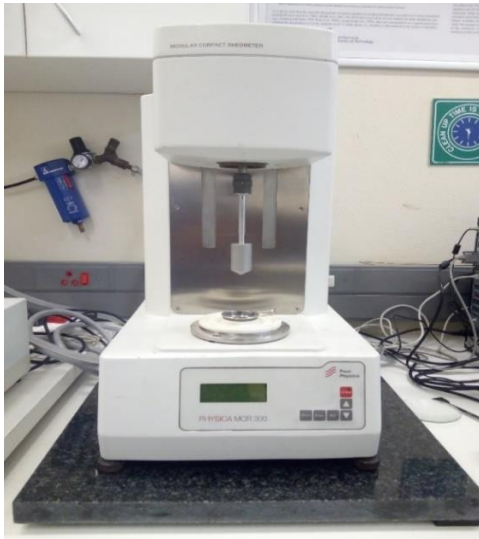


Figure 3.18 Paar-Physica MCR-300 rotational rheometer



Figure 3.19 Concentric cylinder geometry CC27

3.9.1 Rheological characterisation of flow curves

The prepared material was rheologically characterised using either the power-law, Herschel-Bulkley or Newtonian models. Figures 3.20, 3.21, 3.22 and 3.23 show graphical shear diagrams (shear stress against shear rate) for 100% glycerine solution, 20.4% kaolin suspension, 7.3% bentonite suspension and 6.6% CMC solution. Shear stresses and shear rates were used to calculate yield stress, fluid consistency coefficient and flow behaviour index. These parameters were used to calculate the appropriate Reynolds number of the liquids.

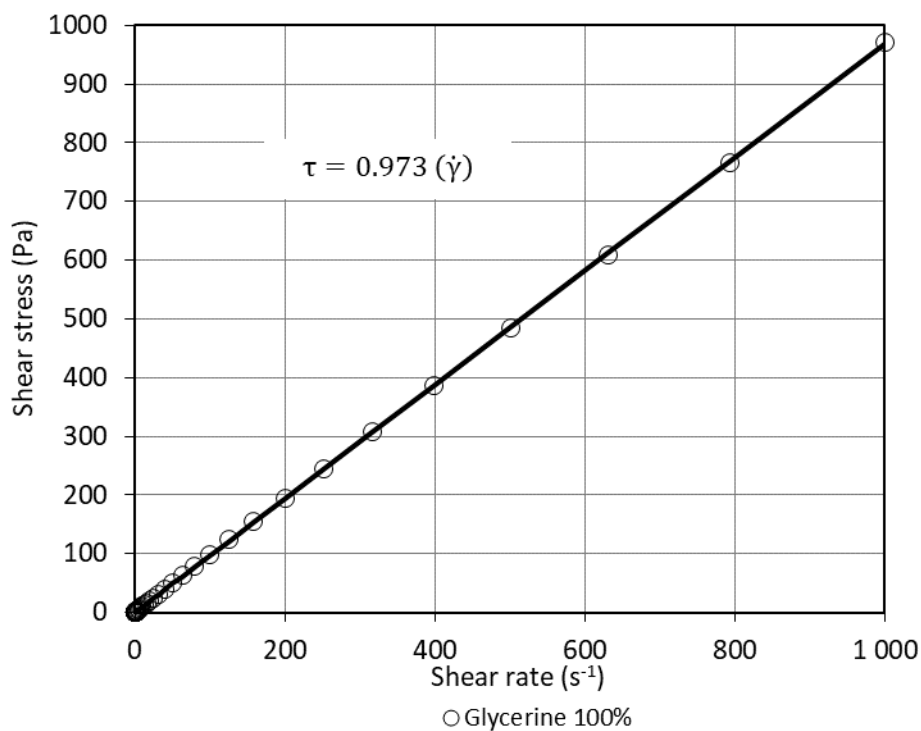


Figure 3.20 Rheogram for 100% glycerine

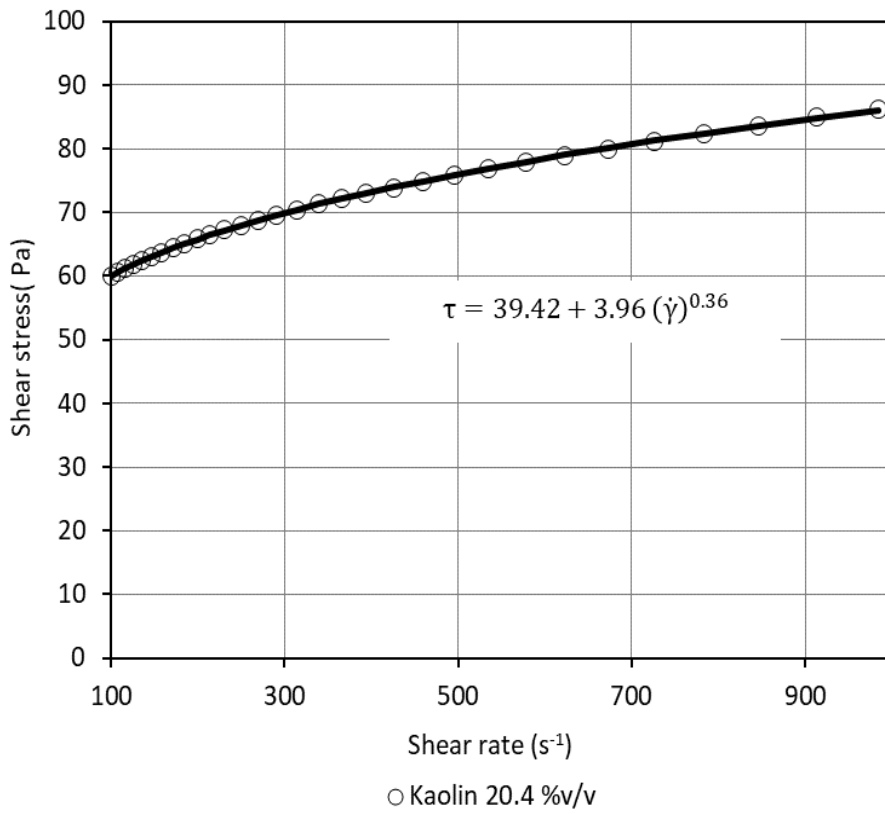


Figure 3.21 Rheogram for kaolin 20.4% v/v

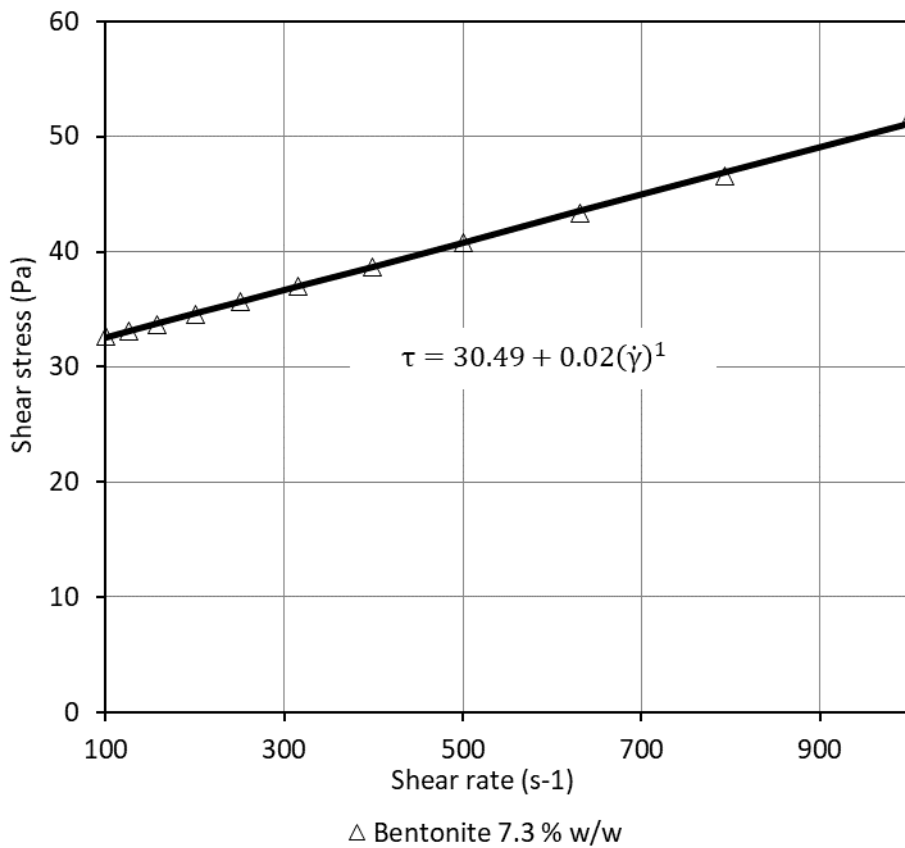


Figure 3.22 Rheogram for bentonite 7.3% w/w

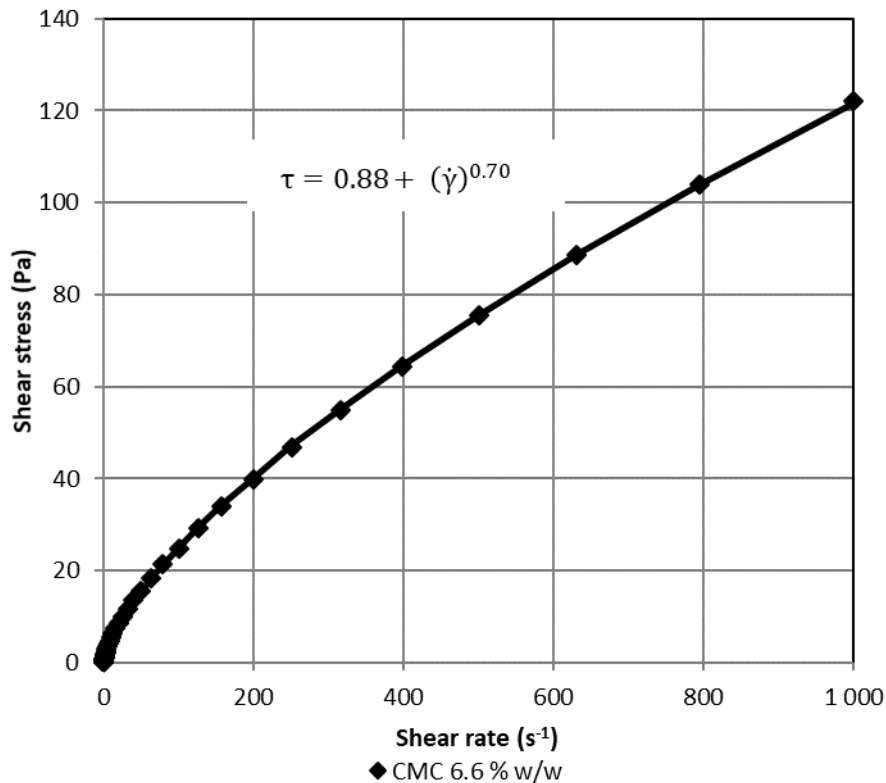


Figure 3.23 Rheogram for CMC 6.6% w/w

3.9.2 Measurements of relative density

The apparatus needed for the relative density determination included:

- top pan balance;
- volumetric flasks;
- water bottle;
- certain quantity of each concentration of slurry; and
- tap water.

To determine the relative densities of the various concentrations to be tested, the following procedure was followed:

- Clearly label three clean (empty) volumetric flasks (250 ml) with numbers 1, 2 and 3.
- Weigh each flask and record the masses as (M_1).
- Half fill the empty flasks with the test material.
- Weigh each half-filled flask and record the masses as (M_2).
- With the test material still in the flask, carefully fill each flask with water (ensuring that the material clinging to the walls of the flask is carried down with the water poured) until the meniscus coincide with the graduated mark.
- Weigh all three full flasks and record the masses as (M_3).
- Pour out the test material plus water in each flask and thoroughly clean the flasks.
- Fill each flask with water such that the meniscus coincides with the graduated mark.

- Weigh all the flasks and record the masses as (M_4).
- The temperature of the water and the slurry were also noted.

Weights recorded were:

M_1 Mass of bottle

M_2 Mass of bottle and test material

M_3 Mass of bottle + test material + water

M_4 Mass of bottle and water

After all masses (M_1 to M_4) have been recorded, the relative density (RD) of the mixture was calculated by Equation 3.5.

$$RD = \frac{\text{Mass of liquid}}{\text{Mass of equal volume of water}} = \frac{M_2 - M_1}{M_4 - M_1 - M_3 + M_2} \quad \text{Equation (3.5)}$$

3.9.3 Slurry temperature

A laboratory thermometer was used for recording the slurry and water temperatures when conducting the relative density tests as well as for measuring the temperature of the liquids before, during and after each run. Each reading was repeated three times for repeatability. Most of the tests were done during the winter and spring months. For each slurry concentration, flow rate measurements were conducted within a maximum period of six hours; the maximum and minimum temperatures when conducting tests were 16° and 25° respectively. The difference in temperature was due to the fact that the tests were conducted in different seasons. Temperature change is the key factor toward the change in rheology; as a result, characterisation was carried out before and after testing and no difference was noticed in terms of characterisation. The effect of temperature on the tests was therefore deemed negligible.

3.10 Conclusion

This chapter has introduced and discussed the facility, equipment and material as a suitable methodology for this study. The procedures which have been followed to obtain rheology parameters, C_d values and Reynolds numbers are also discussed. The methods used for the analysis of the results and the prediction of the predicted flow curve fittings are outlined including discussion on error analysis. The Flow Process Research Centre laboratory was used to conduct all the experiments. The testing equipment was the tank rig. A mixing tank was used as storage, with liquids poured manually into the tank. A Paar-Physica MCR 300 rheometer was used to measure the rheological properties of the liquids used to conduct the research. Materials tested comprised of various concentrations of CMC solution, kaolin and bentonite suspensions. The average C_d value for L/d ratio of 0.05 ($C_d = 0.60$) is within $\pm 2\%$ error of the standard C_d value for sharp-crested orifices ($C_d = 0.61$) and the average C_d value for L/d ratio of 1 ($C_d = 0.59$) is within $\pm 5.5\%$ error of the standard C_d value for sharp-crested orifices. For an L/d ratio of 3, an average C_d value of 0.80 was obtained, comparable to the average C_d value obtained by Stark and Fox (1989) of 0.80. Lastly, an L/d ratio of 5 had an average C_d value of 0.78 which is within $\pm 2\%$ error of Çobanoğlu's (2008) average C_d value of 0.79.

Chapter 4 RESULTS AND ANALYSIS

4.1 Introduction

The experimental results and analysis are explained in detail in this chapter. The aim of this work was to measure the flow rates of different Newtonian and non-Newtonian liquids from a tank through circular orifices of varying L/d ratios, as a function of liquid properties. The tests were carried out for water; different percentage volume concentrations of kaolin suspensions; percentage mass concentrations of bentonite suspensions; CMC and glycerine solutions. The results include density, rheology and flow rate measurement data. Water tests were carried out to calibrate the apparatus used. For each aspect ratio, the Reynolds number was calculated based on the corresponding velocity, flow rate and diameter of orifice. In this chapter, three flow regimes will be examined in separate sections, namely:

- laminar flow;
- transition from laminar to turbulent flow; and
- turbulent flow.

The work in this chapter is divided into two parts:

- 1) rheological characterisation and relative density results of Newtonian and non-Newtonian liquids; and
- 2) presentation of C_d versus Re plots for each L/d ratio.

4.2 Rheological characterisation and relative density results of Newtonian and non-Newtonian liquids used

A Paar-Physica MCR 300 rheometer was used to perform rheology tests. Rheological fitting parameters were obtained from the interpretation of data using power-law, Bingham plastic, Herschel-Bulkley and Newtonian models. Rheological characteristics of the liquids tested are presented in Table 4.1. For CMC, the fluid behaviour index decreased with the increase in concentration (the smaller the value of 'n' the greater the degree of shear thinning). Kaolin and bentonite yield stresses and the flow consistency index increased with increasing concentration of the liquids. The information in Table 4.1 has been used to calculate the Reynolds numbers. Most of the tests were done during the winter months (cold season) and spring months (hot season) hence the difference in the temperature readings.

Table 4.1 Rheological parameters of the liquids used in this study

Newtonian	Concentration (%)	Density (kg/m ³)	Shear rate (s ⁻¹)	Temperature (°C)	μ	-	-
Water	-	1000	-	18	0.001		
Glycerine	100	1258	370.61-930.75	20	0.973		
	96	1248	426.18-918.39	19	0.304		
	93	1242	445.72-715.64	18	0.130		
	65	1179	568.41-1106.87	18	0.019		
Non-Newtonian	Concentration (%)	Density (kg/m ³)	Shear rate range (Pa)		Rheological properties		
					τ_y (Pa)	k (Pa.s ⁿ)	n
CMC	2.4	1014	602.28-1452.19	25		0.01	1
	5.2	1029	589.58-1166.82	18	-	0.21	0.79
	6.6	1037	556.48-1124.17	18	-	0.88	0.70
	7.6	1043	461.32-1057.65	21	-	2.39	0.64
Kaolin	13.1	1217	560.23-1110.70	18	8.90	0.07	0.72
	20.4	1336	556.41-1106.43	16	39.42	3.96	0.36
Bentonite	3.8	1023	528.44-1068.66	18	1.01	0.01	1
	7.2	1044	548.90-1192.14	17	15.74	0.01	1
	7.3	1046	662.43-1470.89	21	30.49	0.02	1

4.2.1 Glycerine

Flow curve fittings of 65, 93, 96 and 100% glycerine solutions are presented in Figure 4.1. Newtonian viscosity (Equation 2.12) was used to characterise the different concentrations of glycerine.

$$\tau = \mu \dot{\gamma} \quad \text{Equation (2.12)}$$

Figure 4.1 shows graphs of shear stress and shear rate for the varying concentrations of glycerine. For each concentration, there is a linear increase in shear stress with increasing shear rate. The slope is defined by the viscosity of the liquid. For each concentration, the viscosity remains constant no matter the amount of force applied (meaning that the viscosity of the liquid does not change as the force applied increases); as the concentration of the liquid increases, the viscosity increases and the slope becomes steeper. For CMC and glycerine, the shear rate range was from 0.01-1000 s⁻¹.

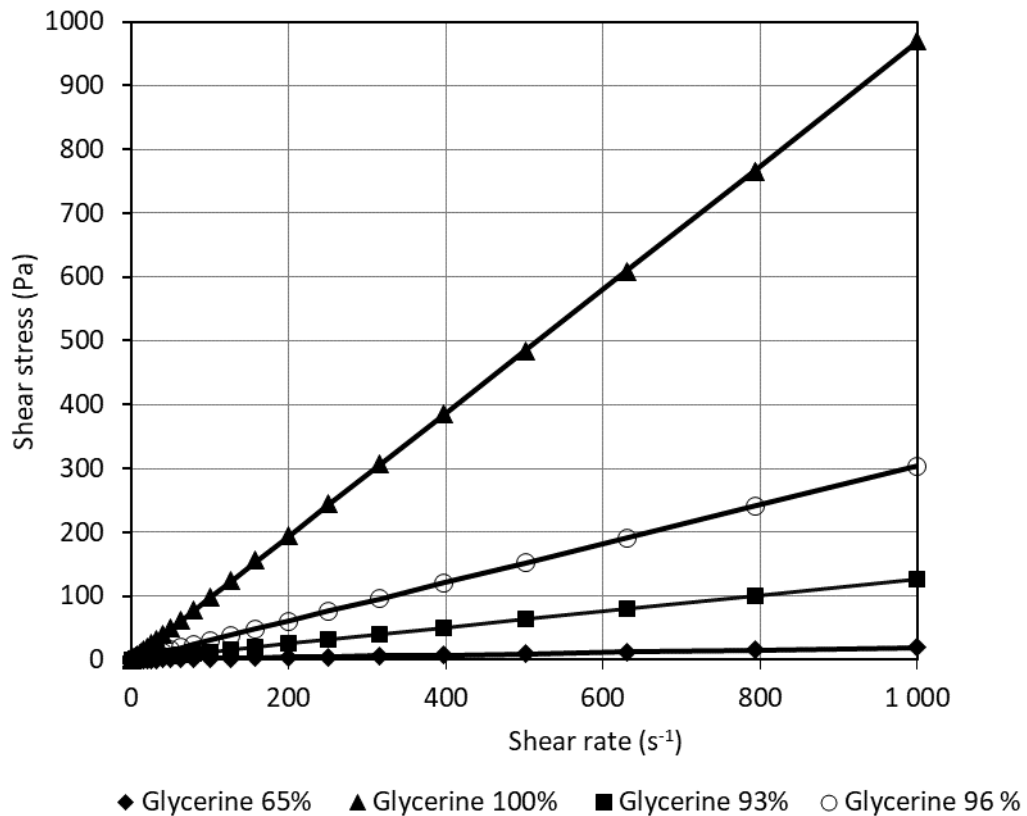


Figure 4.1 Flow curves for 65, 93, 96 and 100% glycerine

4.2.2 CMC

Four concentrations of CMC were separately prepared and tested. Figure 4.2 shows flow curves for 2.4, 5.2, 6.6 and 7.6 % CMC Solution. The concentrations were characterised using the power-law flow curve fitting Equation 2.13. The shear rate range was from 0.01-1000 s⁻¹.

$$\tau = k(\dot{\gamma})^n \quad \text{Equation (2.13)}$$

The flow curves show that the viscosity increases in a non-linear manner as the force applied increases; shear thinning behaviour is observed. For CMC, 2.4% a Newtonian behaviour is observed as seen from Table 4.1 ($n=1$).

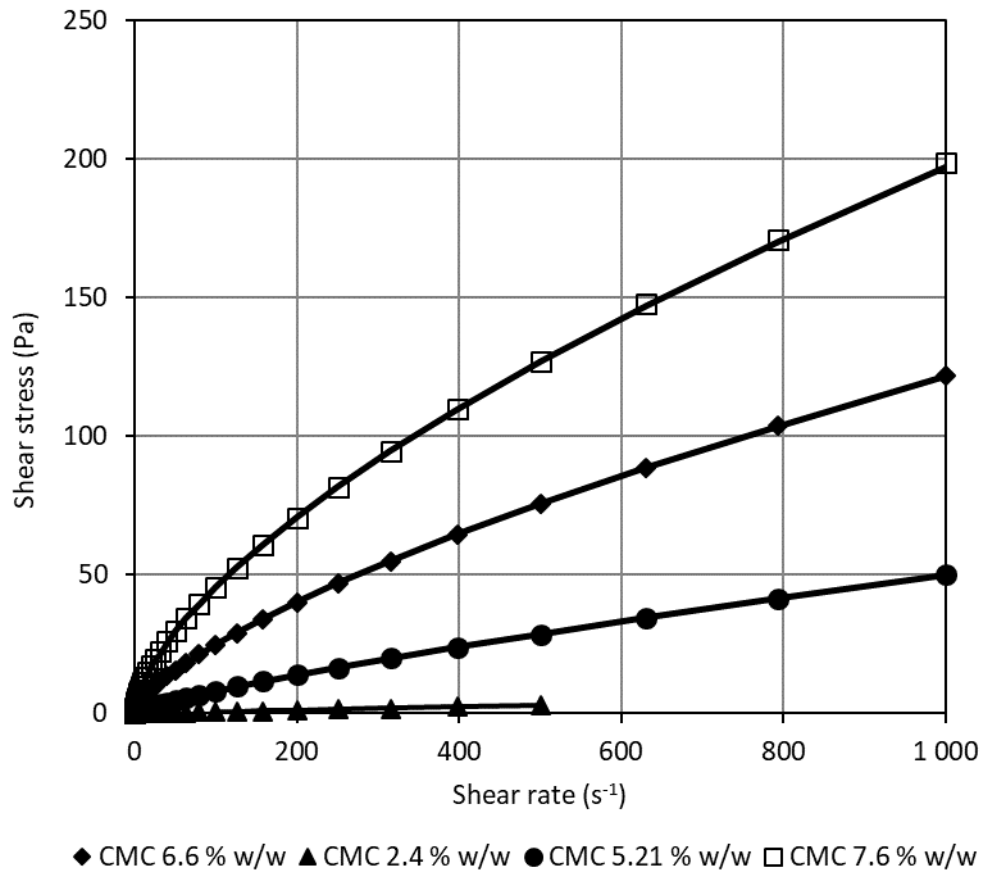


Figure 4.2 Pseudo shear flow curves for 6.6, 5.2, 7.6 and 2.4% CMC solutions

4.2.3 Bentonite

Figure 4.3 illustrates 3.8, 7.2 and 7.3% w/w bentonite suspension pseudo shear flow curves. Three concentrations of bentonite were separately prepared and tested. Bentonite was characterised by Bingham plastic model Equation 2.14: For bentonite and kaolin suspensions the shear rate range was from 100-1000 s⁻¹ because results lower than 100 s⁻¹ were not stable.

$$\tau = \tau_y + \mu_p \dot{\gamma} \quad \text{Equation (2.14)}$$

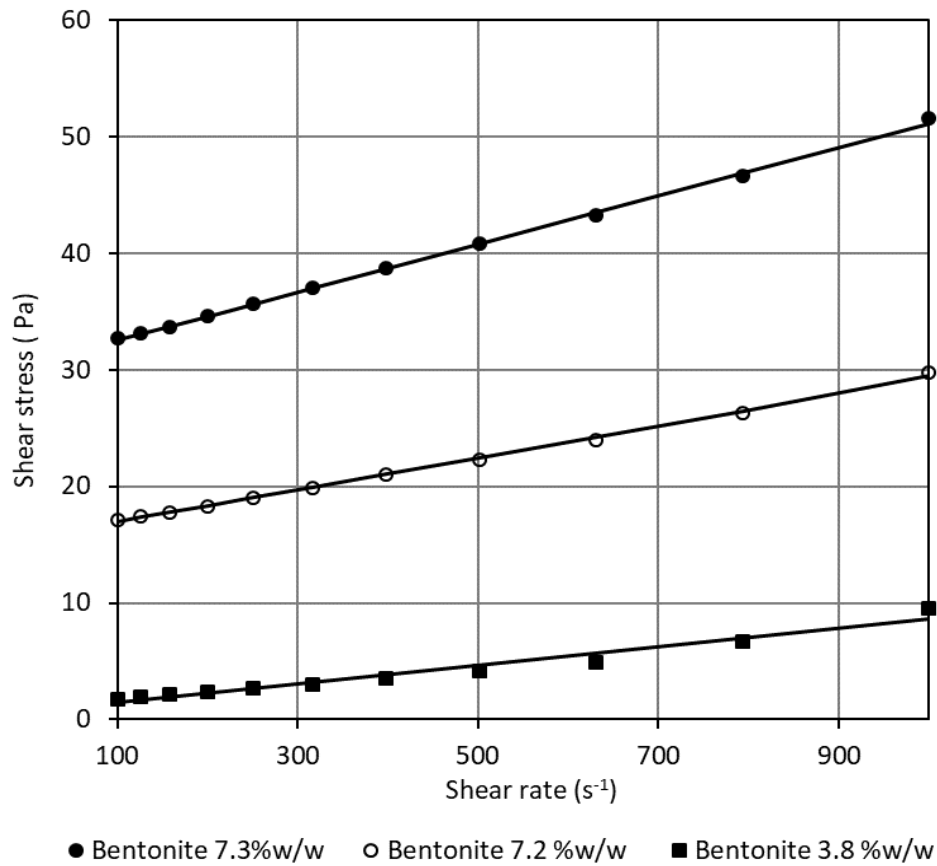


Figure 4.3 Bentonite 3.8, 7.2 and 7.3% w/w pseudo shear graphs

4.2.4 Kaolin

Two concentrations of kaolin were separately prepared and tested. Figure 4.4 shows flow curves for 13.1 and 20.4% kaolin suspensions, characterised using the Herschel-Bulkley fitting (Equation 2.14). The shear rate range was from 100-1000s⁻¹.

$$\tau = \tau_y + k\dot{\gamma}^n$$

Equation (2.14)

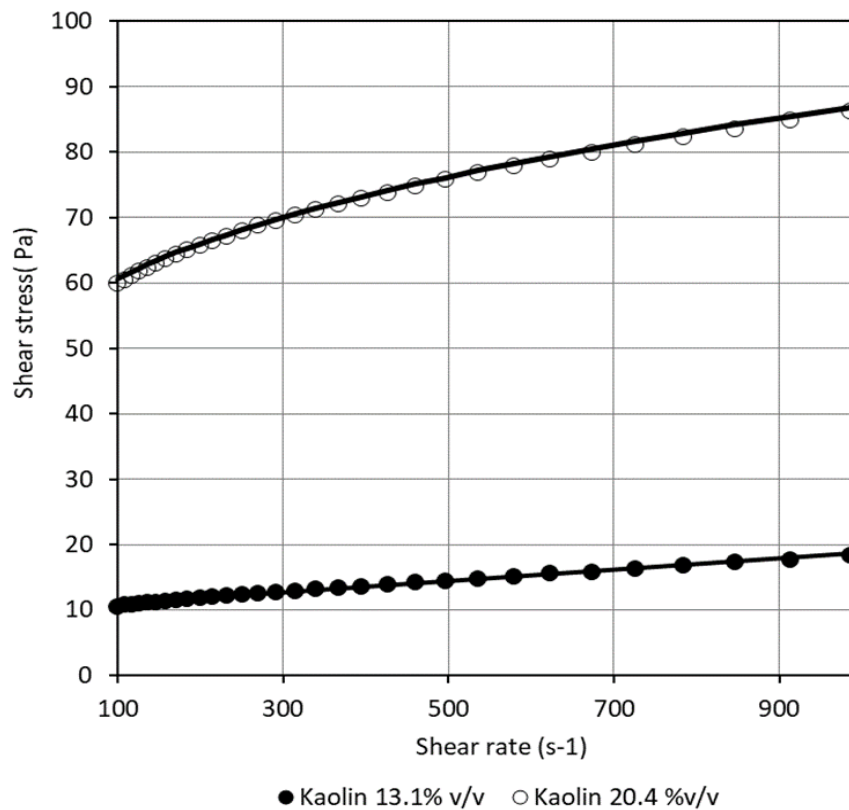


Figure 4.4 Pseudo shear diagram for 13.1 and 20.4% kaolin suspensions

4.3 Presentation of C_d versus Re plots for each L/d ratio

4.3.1 Discharge coefficients for L/d ratios of 0.05, 1, 3 and 5

Aspect ratio of 0.05

Figure 4.5 presents the C_d values against Re_2 for L/d ratio of 0.05 for all the liquids tested. In the laminar flow region, each liquid type has its own flow trend as indicated by Figure 4.5. The graph also shows that in the laminar flow region, the C_d values are dependent on Re_2 , increasing as the Re_2 increases, this behaviour is also valid for other L/d ratios. The turbulent flow region for glycerine is observed at $Re_2 > 24000$ with an average value of 0.60. For non-Newtonian liquids, turbulent flow is observed at $Re_2 > 7000$ for 2.4 % CMC, $Re_2 > 4200$ for 3.8 % bentonite and $Re_2 > 2300$ for 13.1 % kaolin, with an average C_d value of 0.62. The highest C_d value of 0.67 is obtained where $Re_2 = 620$ for 5.2 % CMC. Appendix I shows flow rate measurements using L/d ratio of 0.05.

Table 4.2 shows the different Re definitions for glycerine, CMC, bentonite and kaolin for L/d ratio of 0.05.

Table 4.2 Flow regions for an L/d ratio of 0.05

Flow region	Glycerine	CMC	Bentonite	Kaolin
Laminar	$20 < Re_2 < 100$	$80 < Re_2 < 200$	$500 < Re_2 < 1000$	$200 < Re_2 < 700$
Transition	$100 < Re_2 < 2000$	$200 < Re_2 < 2000$	$1000 < Re_2 < 2000$	$700 < Re_2 < 2000$
Turbulent	$24000 < Re$	$7000 < Re_2$	$4200 < Re_2$	$2300 < Re_2$

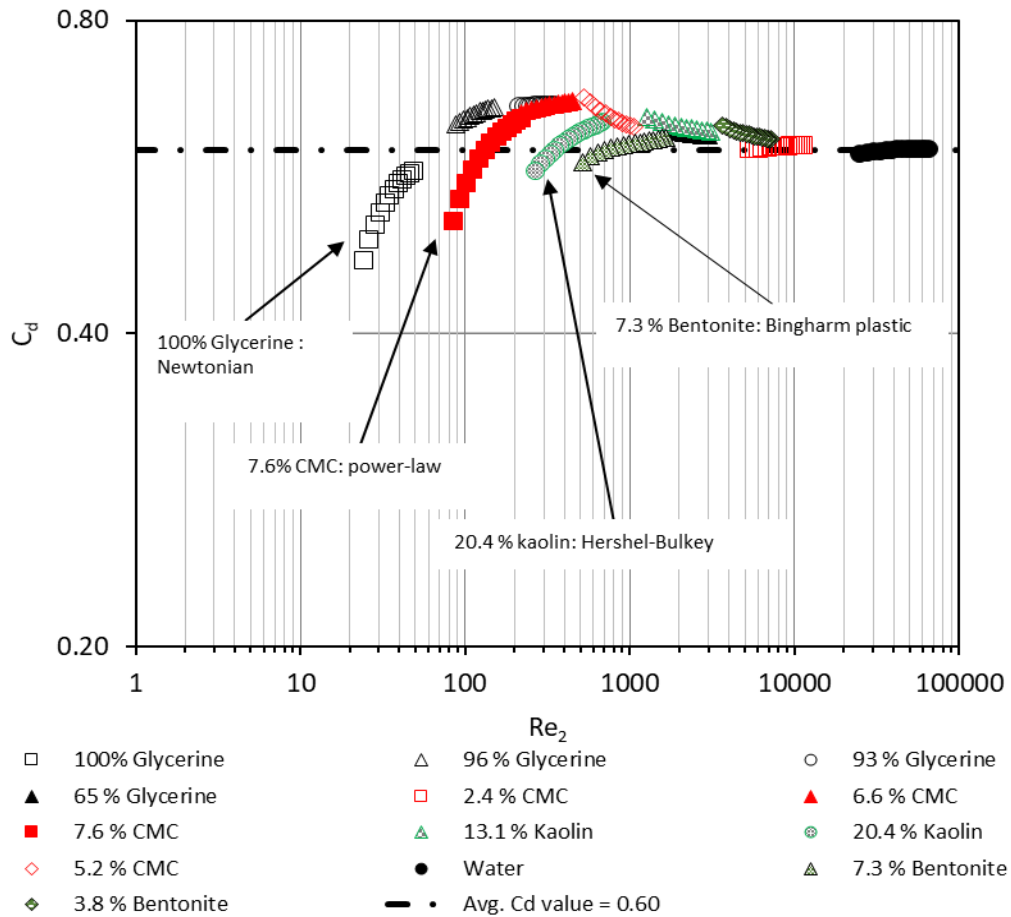


Figure 4.5 Coefficient of discharge versus Reynolds number for L/d ratio of 0.05

Aspect ratio of 1

Figure 4.6 presents the C_d against Re_2 for L/d ratio of 1 for all liquids tested. In the laminar flow region all the non-Newtonian liquids (kaolin, bentonite and CMC) combined forming one flow trend which is a different flow behaviour than that observed for an L/d ratio of 0.05 where each liquid type had its own flow trend. For glycerine, the laminar flow is defined by $30 < Re_2 < 200$ and for non-Newtonian liquids (Kaolin, Bentonite and CMC) the laminar flow is defined by $100 < Re_2 < 230$. In the turbulent region $Re_2 > 2000$ Newtonian and non-Newtonian liquids have combined and attained an average C_d value of 0.59. The highest C_d values were of 0.64 where $Re_2 = 434$ for 6.6 % CMC. Appendix J shows flow rate measurements using L/d ratio of 1.

Table 4.3 Flow regions for an L/d ratio of 1

Flow region	Glycerine	Kaolin, Bentonite & CMC
Laminar	$30 < Re_2 < 200$	$100 < Re_2 < 230$
Transition	$236 < Re_2 < 1000$	$301 < Re_2 < 1000$
Turbulent	$Re_2 > 2000$	$Re_2 > 2000$

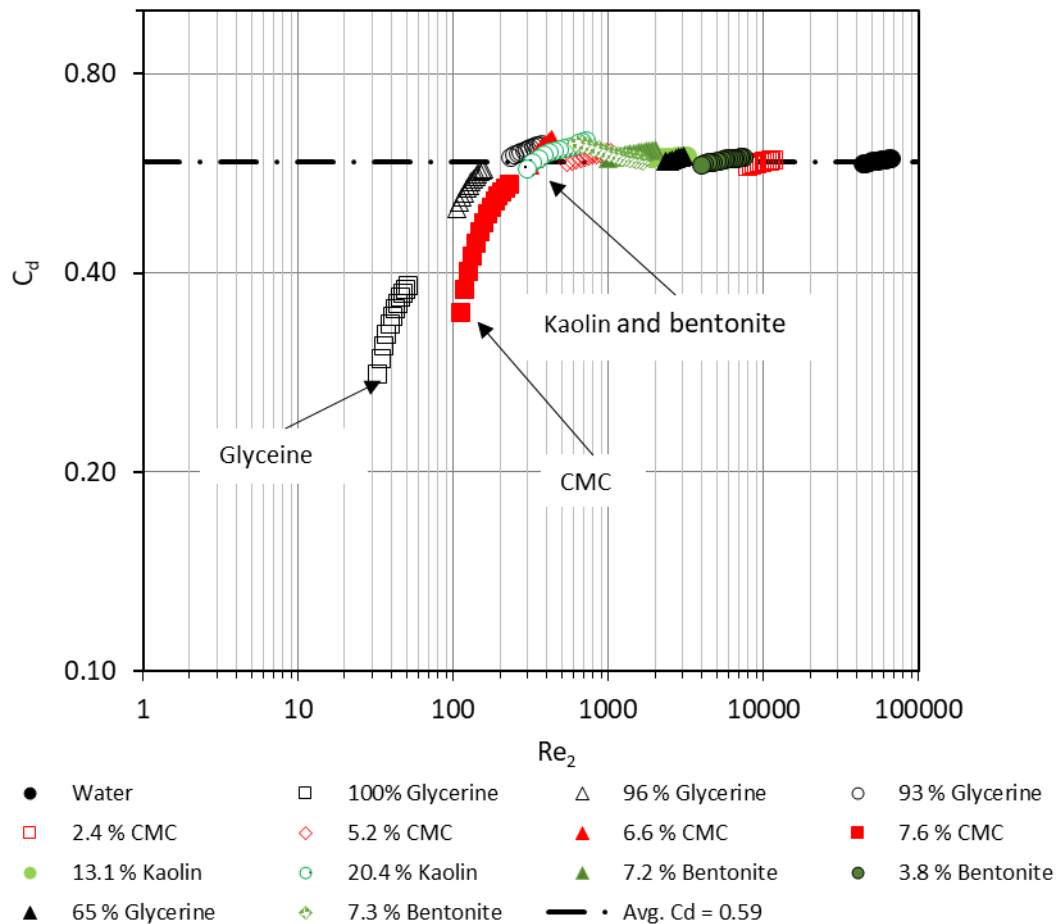


Figure 4.6 Coefficient of discharge versus Reynolds number for L/d of 1

Aspect ratio of 3

Figure 4.7 presents the C_d against Re_2 for an L/d ratio of 3. In the laminar flow region, non-Newtonian liquids (kaolin and CMC have combined to form one flow trend and bentonite is forming another) this behaviour is also observed for an L/d ratio of 5. For kaolin and CMC, the laminar region is defined by $130 < Re_2 < 510$, the laminar region of bentonite is defined by $732 < Re_2 < 1000$ and for glycerine the laminar region is defined by $38 < Re_2 < 120$ as shown in Table 4.4. The turbulent flow region for Newtonian liquids is observed at $Re_2 > 46000$ with an average value of 0.80. Non-Newtonian liquids have an average C_d value of 0.78 in the turbulent flow region. Appendix K provides flow rate measurements for an L/d ratio of 3.

Table 4.4 Flow regions for an L/d ratio of 3

Flow region	Glycerine	Bentonite	Kaolin & CMC
Laminar	$30 < Re_2 < 400$	$732 < Re_2 < 1000$	$130 < Re_2 < 510$
Transition	$2000 < Re_2 < 4000$	$1000 < Re_2 < 2000$	$700 < Re_2 < 1000$
Turbulent	$Re_2 > 46000$	$Re_2 > 3900$	$Re_2 > 6900$

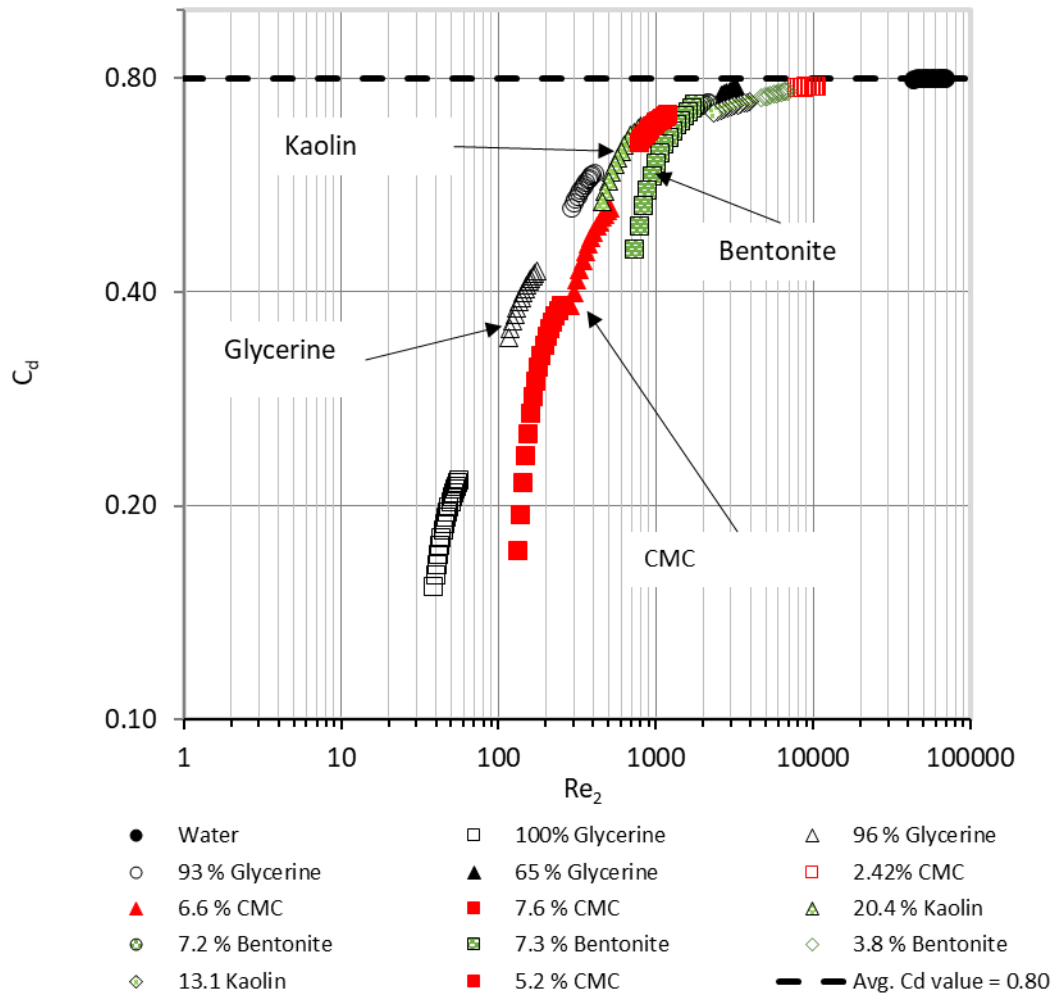


Figure 4.7 Coefficient of discharge versus Reynolds number L/d of 3

Aspect ratio of 5

Figure 4.8 shows C_d versus Re_2 for an L/d ratio of 5. For kaolin and CMC, the laminar region is defined by $167 < Re_2 < 930$, the laminar region of bentonite is defined by $820 < Re_2 < 1400$ and for glycerine, the laminar region is defined by $45 < Re_2 < 440$ as displayed in Table 4.5. The turbulent flow region for glycerine is observed at $Re_2 > 43000$ with an average value of 0.78. In the turbulent flow region, non-Newtonian liquids have an average C_d value of 0.74. Appendix L shows flow rate measurements for an L/d ratio of 5.

Table 4.5 Different definitions of laminar flow region for an L/d ratio of 5

Flow region	Glycerine	CMC & kaolin	Bentonite
Laminar	$45 < Re_2 < 440$	$167 < Re_2 < 930$	$820 < Re_2 < 1400$
Transition	$2000 < Re_2 < 4000$	$1000 < Re_2 < 4000$	$1000 < Re_2$
Turbulent	$Re_2 > 43000$	$Re_2 > 4000$	$Re_2 > 4000$

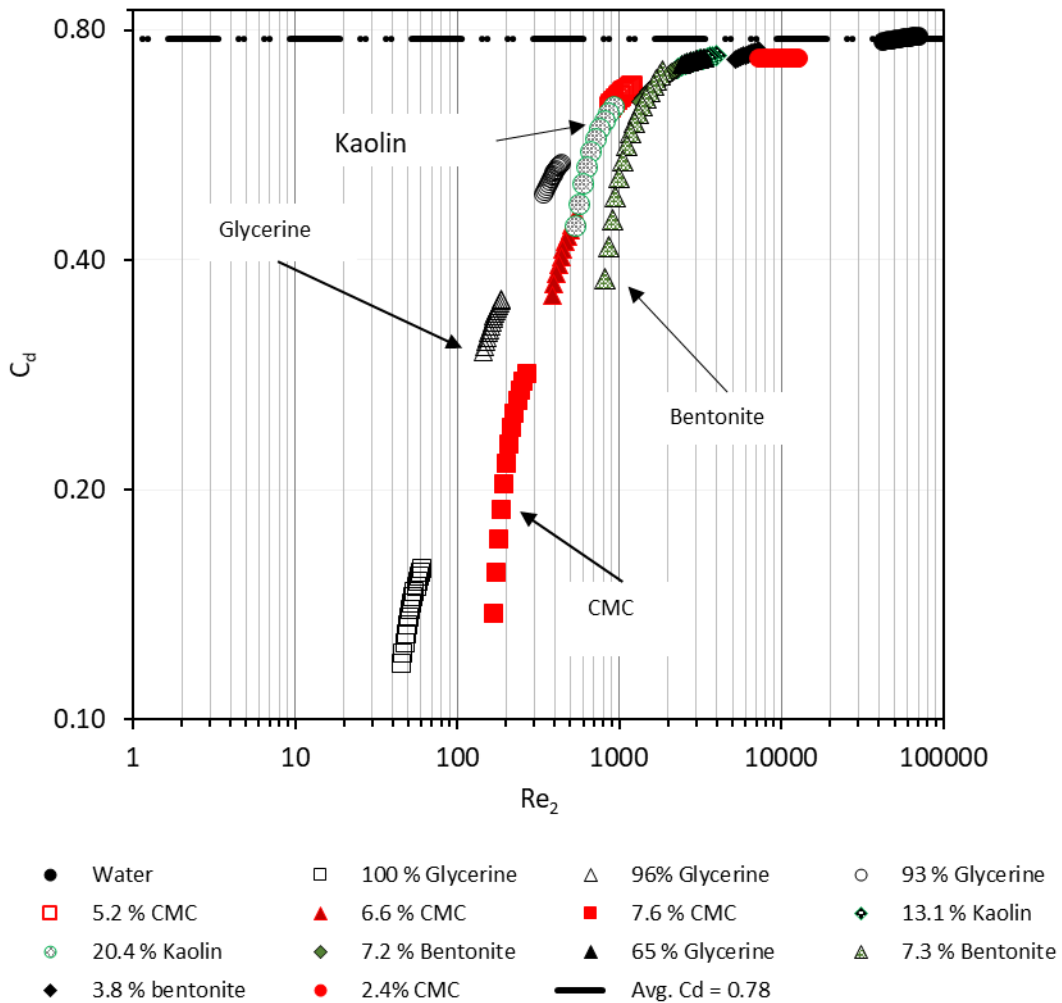


Figure 4.8 Coefficient of discharge versus Reynolds number for L/d of 5

Figure 4.9 and 4.10 display the coefficient of discharge versus Reynolds number data of Newtonian and non-Newtonian liquids respectively for aspect ratio of 0.05, 1, 3 and 5. For both graphs, the laminar flow regions show that each L/d ratio has its own flow trend. In the turbulent region, the L/d ratios of 0.05 and 1 have average C_d values in close proximity. For L/d ratios of 3 and 5 the average C_d values are also in close proximity.

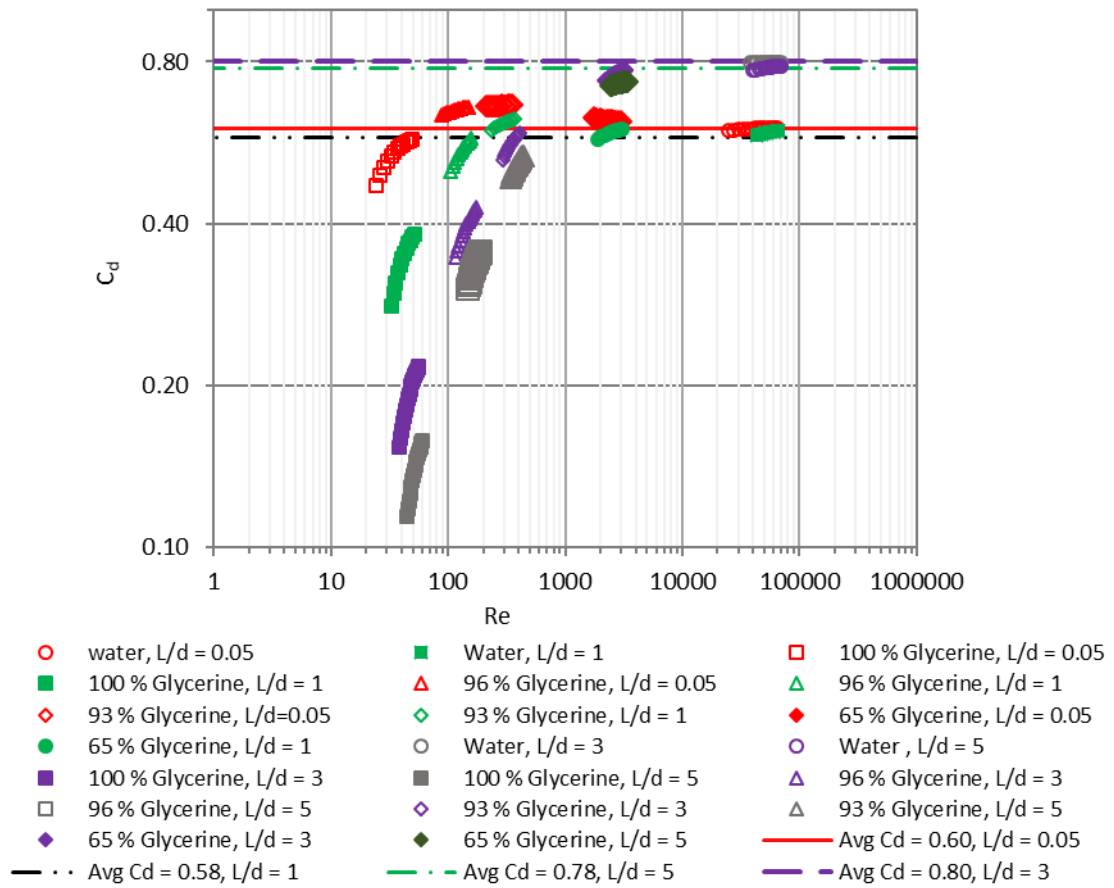


Figure 4.9 Coefficient of discharge versus Reynolds number of Newtonian liquids for L/d ratios of 0.05, 1, 3 and 5

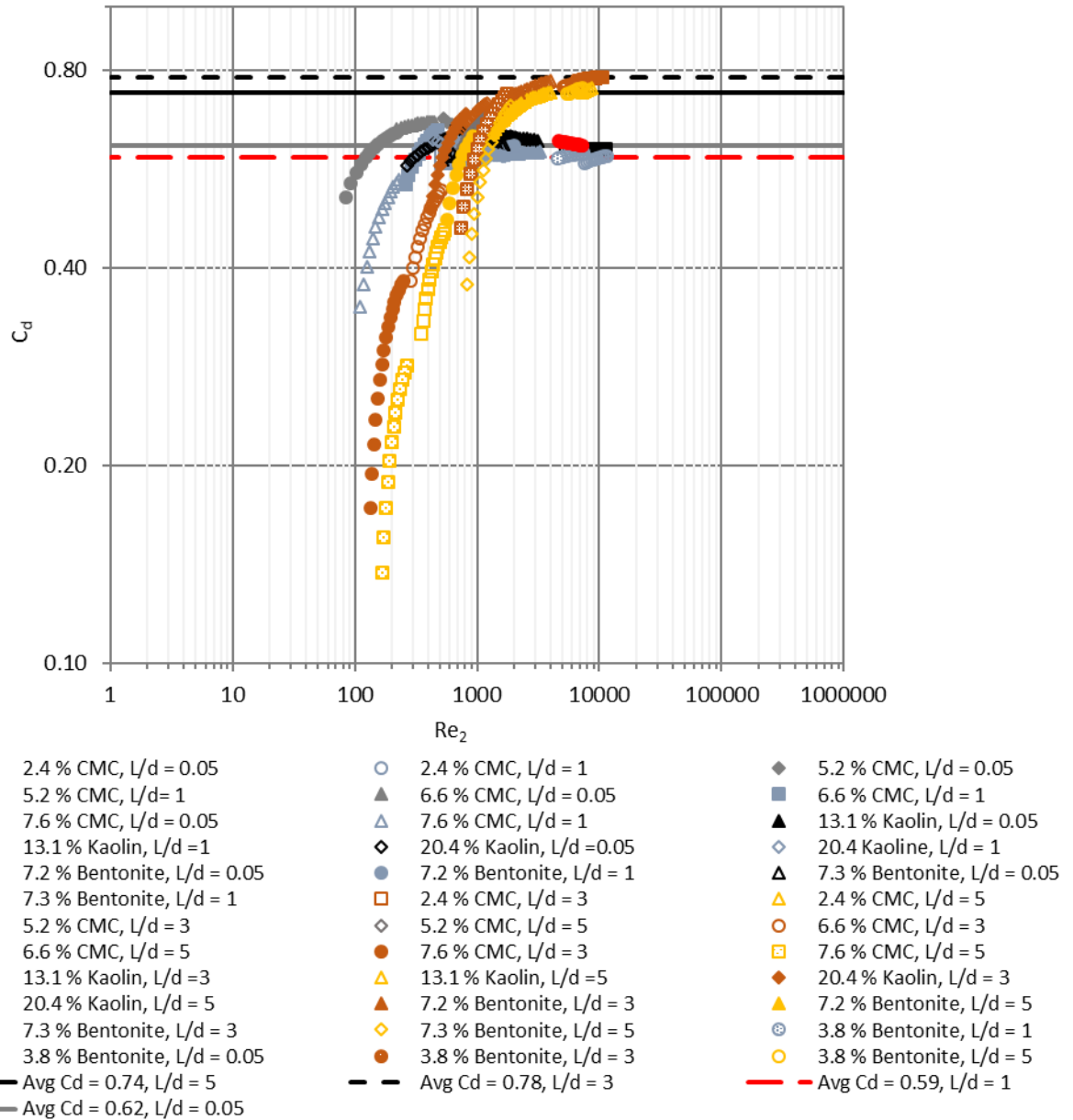


Figure 4.10 Coefficient of discharge versus Reynolds number of non-Newtonian liquids for L/d ratios of 0.05, 1, 3 and 5

Figure 4.11 displays all the coefficient of discharge versus Reynolds number of Newtonian and non-Newtonian liquids for L/d ratios of 0.05, 1, 3 and 5. The graphs suggest that for all aspect ratios, one flow trend is formed in the turbulent region, while in the laminar region there are separate flow trends.

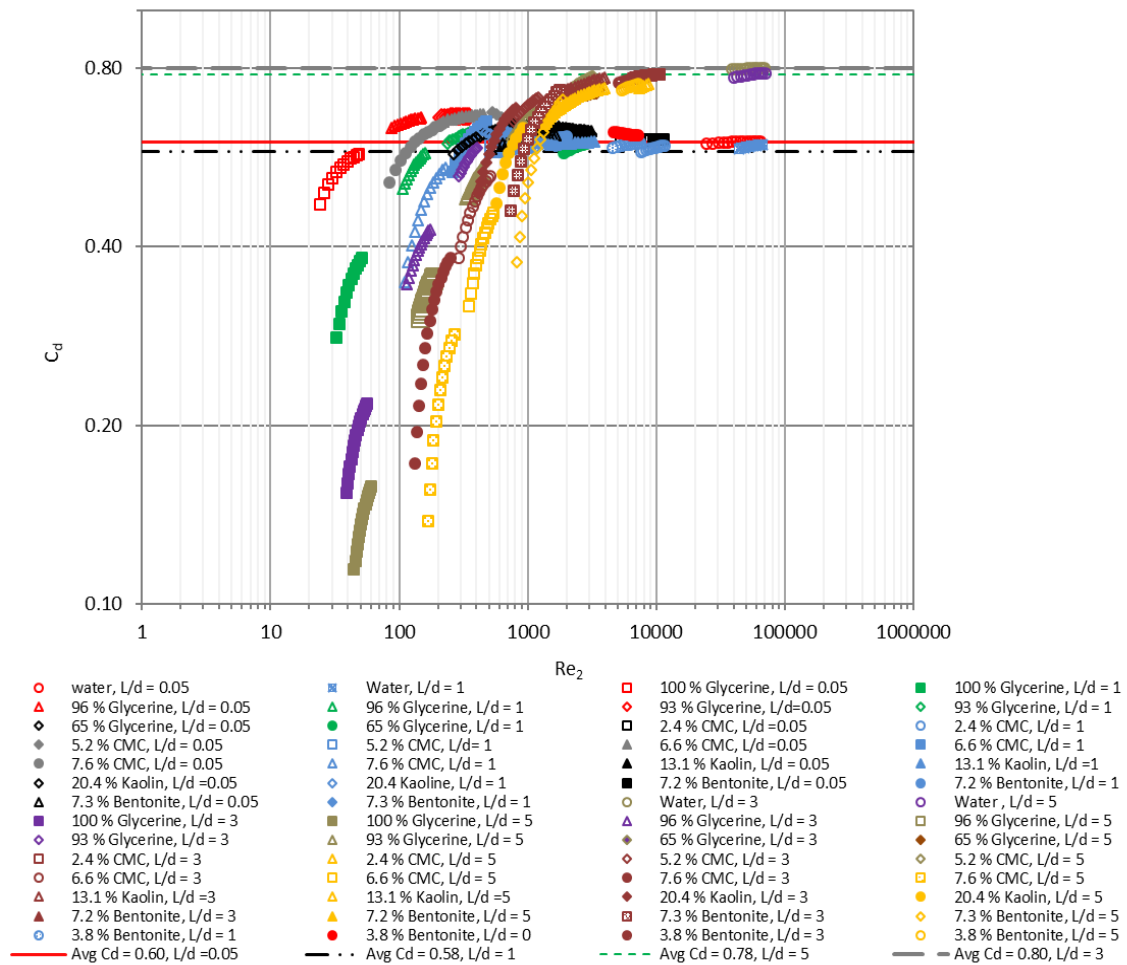


Figure 4.11 C_d versus Re_2 of Newtonian and non-Newtonian liquids for L/d ratios of 0.05, 1, 3 and 5

4.1 Relationship between C_d and Re versus L/d ratios

Figure 4.12 shows the lowest Re values for Newtonian and non-Newtonian liquids versus the respective L/d ratios in the laminar region. The Re values for CMC solutions increase with the increase in L/d ratio. For kaolin and bentonite suspensions, the Re_2 values change in a non-linear manner and shift toward higher values of Re from L/d ratio of 1 to 5. The Re values for Newtonian liquids are in the same range with the Re values of 24, 33, 39 and 49 for aspect ratios of 0.05, 1, 3 and 5, respectively.

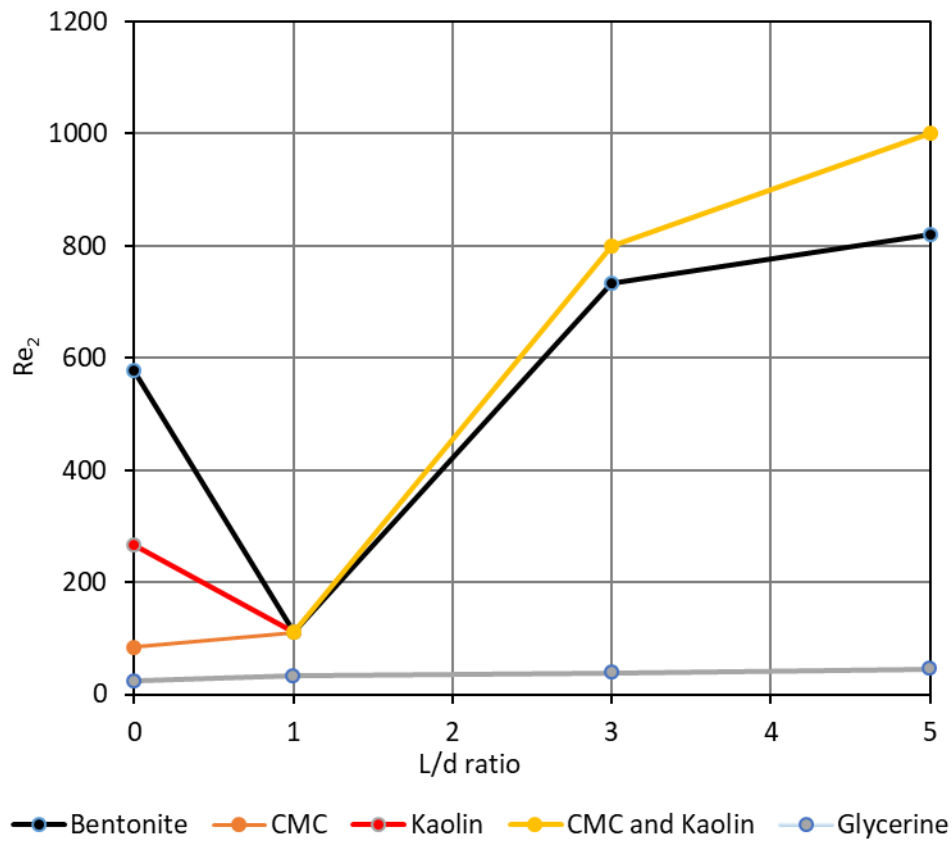


Figure 4.12 Effect of L/d ratio on the laminar region for Newtonian and non-Newtonian liquids (lowest Re vs L/d ratio)

Figure 4.13 shows average C_d values plotted against the respective aspect ratios for Newtonian and non-Newtonian liquids in the turbulent region. For an L/d ratio of 0.05, Newtonian liquids have an average C_d value of 0.60, while non-Newtonian liquids have a slightly higher average C_d value of 0.62. For an L/d ratio of 1, both liquids have the same average C_d value of 0.59, and for an L/d ratio of 3, Newtonian liquids have an average C_d value of 0.80. Non-Newtonian liquids have a slightly lower average C_d value of 0.78. For an L/d ratio of 5, Newtonian liquids have an average C_d value of 0.78 while non-Newtonian liquids have a lower average C_d value of 0.74.

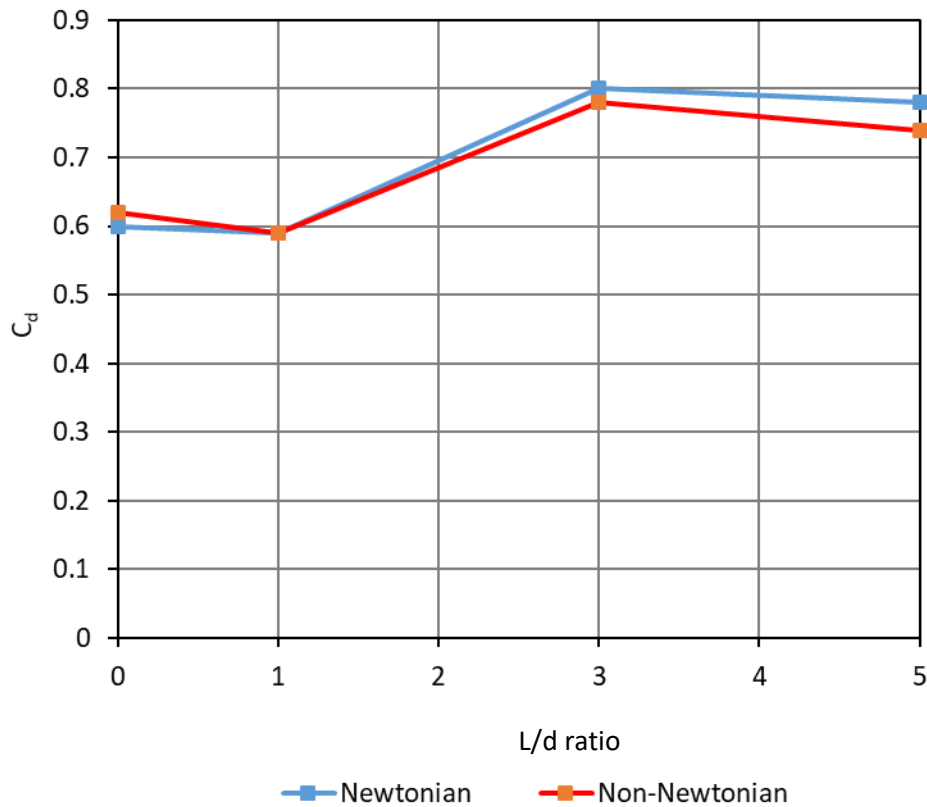


Figure 4.13 Effect of L/d on the turbulent region for Newtonian and non-Newtonian liquids (average C_d vs aspect ratio)

4.2 Conclusion

Rheological parameters of the tested liquids obtained from the rheometer have been presented in this chapter and were used to determine the C_d and Reynolds numbers relationship. The results showed that in the laminar flow region C_d values are dependent on Reynolds number, increasing as Re increases. This behaviour is valid for all the L/d ratios. In the laminar region for an L/d ratio of 0.05 all the non-Newtonian liquids formed separate flow trends. As the L/d ratio increased from 0.05 to 1, all the non-Newtonian liquids merged to form one flow trend. For an L/d ratio of 3, CMC and kaolin combined to form one flow trend and bentonite formed its own flow trend. This behaviour is also observed for an L/d ratio of 5.

For an L/d ratio of 0.05 and 1 the turbulent flow region for Newtonian liquids was defined by average C_d values of 0.60 to 0.59 respectively. For an L/d ratio of 3 and 5, the average C_d values were 0.8 and 0.78 respectively. For an L/d ratio of 0.05, the turbulent region of non-Newtonian liquids is observed at $Re_2 > 7000$ with an average C_d value of 0.62. For an L/d ratio of 1, the turbulent region of non-Newtonian liquids is observed at $Re_2 > 2000$, the liquids having combined to form one flow trend with an average C_d value of 0.59 for both Newtonian and non-Newtonian liquids. For an L/d of 3, the turbulent flow of non-Newtonian liquids, is observed at $Re_2 > 7000$ with an average C_d value of 0.78. For an L/d of 5 for non-Newtonian liquids, the turbulent flow, is observed at $Re_2 > 7300$ with an average C_d value of 0.74. The flow trend patterns differ from one L/d ratio to another.

Chapter 5 MODEL PREDICTION FOR C_d

5.1 Introduction

This chapter presents the prediction of a single composite equation applied only to Newtonian liquids for circular orifices of varying aspect ratios. This is done by fitting data with a logistic dose response curve to a set of data for each aspect ratio. Laminar and turbulent data obtained from the Newtonian liquid flow experiments from the bottom of a tank through orifices for each L/d ratios are compiled and analysed to obtain C_d composite factor correlations. As far as can be ascertained it is the first composite correlation to be made for Newtonian gravitational flow measurements out of tanks through orifices of varying L/d ratios.

5.1.1 Single composite equation

A single composite equation (Equation 5.1) was applied to all Newtonian data points to predict the Newtonian C_d values that describe the data from the laminar to turbulent region for each L/d ratio of 0.05, 1, 3 and 5 (Patankar *et al.*, 2002).

$$C_d = f_2 + \frac{(f_1 - f_2)}{\left(1 + \left(\frac{Re}{t^*}\right)^{c^*}\right)^{d^*}} \quad \text{Equation (5.1)}$$

The coefficient f_1 (Equation 5.2) denotes the slope in the laminar region and f_2 the turbulent region (Equation 5.3)

$$f_1 = A_1^* Re^{B_1} \quad \text{Equation (5.2)}$$

$$f_2 = A_2^* Re^{B_2} \quad \text{Equation (5.3)}$$

t^* , c^* and d^* are parameters obtained by fitting Equation 5.1 to the data points using the non-linear optimisation method of Microsoft® Excel Solver minimising the residual mean square error. The parameters A_1^* , A_2^* , B_1 and B_2 are obtained from fitting the data with power law correlations in the laminar and turbulent flow regions. Equation 5.1 implies that the correlation over the entire range can be represented by power laws connected to the transition regions. The parameters t^* , c^* , d^* , A_2^* , B_1 and B_2 for each correlation are presented in table 5.1. The composite correlation for the C_d values of Newtonian liquids used in this study are then given by equations shown on each graph.

Table 5.1 Optimised composite equation factor values

L/d	f ₁	f ₂	t*	c*	d*
0.05	0.04 Re ^{0.66}	0.60 Re ⁰	300	0.66	4.37
1	0.03 Re ^{0.59}	0.59 Re ⁰	350	1.37	4.15
3	0.02 Re ^{0.41}	0.80 Re ⁰	300	1.14	0.99
5	0.03 Re ^{0.26}	0.76 Re ⁰	350	1.40	1.29

Figures 5.1, 5.2, 5.3 and 5.4 show the fitting of Equation 5.1 for L/d ratios of 0.05, 1, 3 and 5, respectively. The laminar region occurred at Re < 100 for an L/d ratio of 0.05 and at Re < 160 for an L/d ratio of 1. For an L/d ratio of 3 and 5 the laminar region occurred at Re < 200. In this region, the C_d is dependent on the Re value increasing as the Re increases. For an L/d = 0.05 the turbulent flow occurred at Re > 4000 and for an L/d ratio of 1 the turbulent flow occurred by Re > 3000. For an L/d = 3 and 5 the turbulent flow region is defined by Re > 5000.

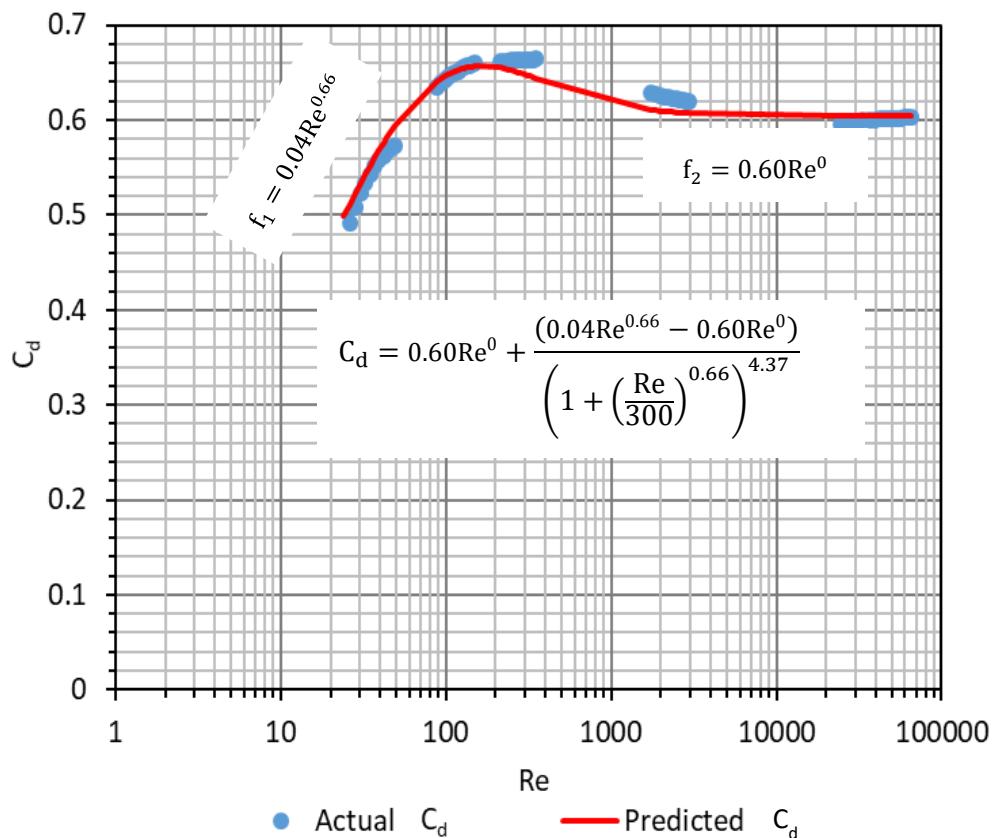


Figure 5.1 Logistic dose response curve for L/d ratio of 0.05

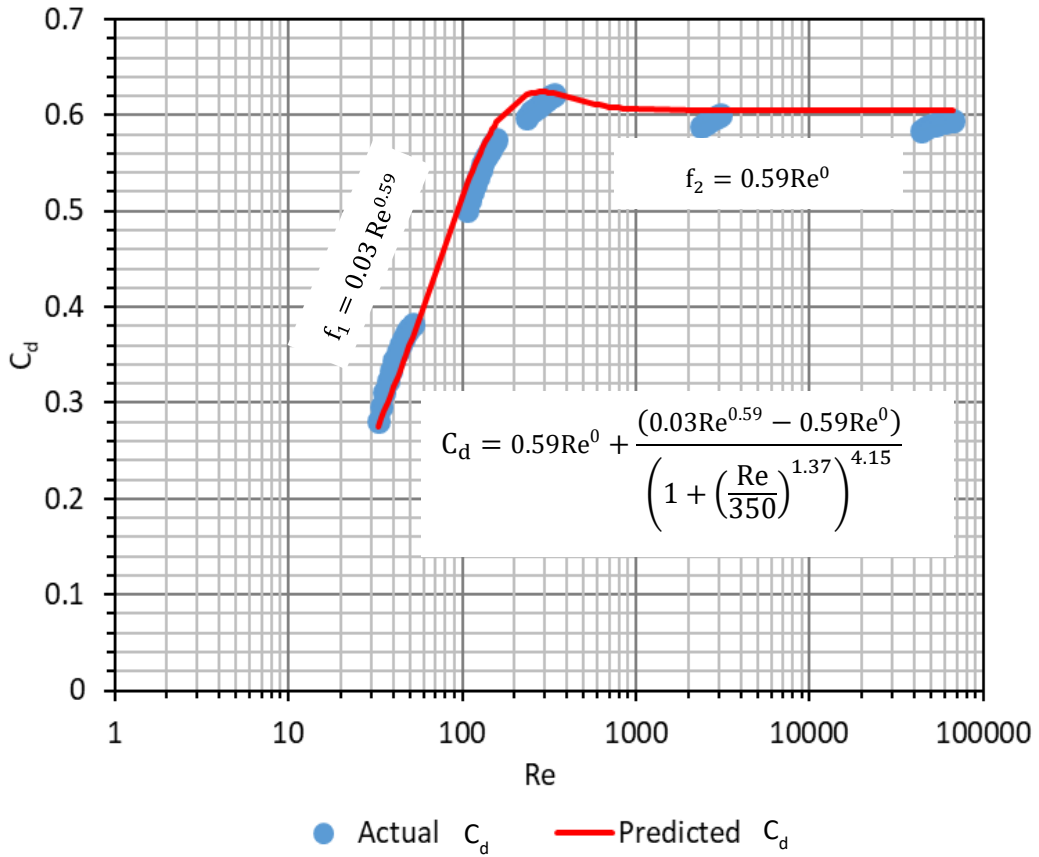


Figure 5.2 Logistic dose response curve for L/d ratio of 1

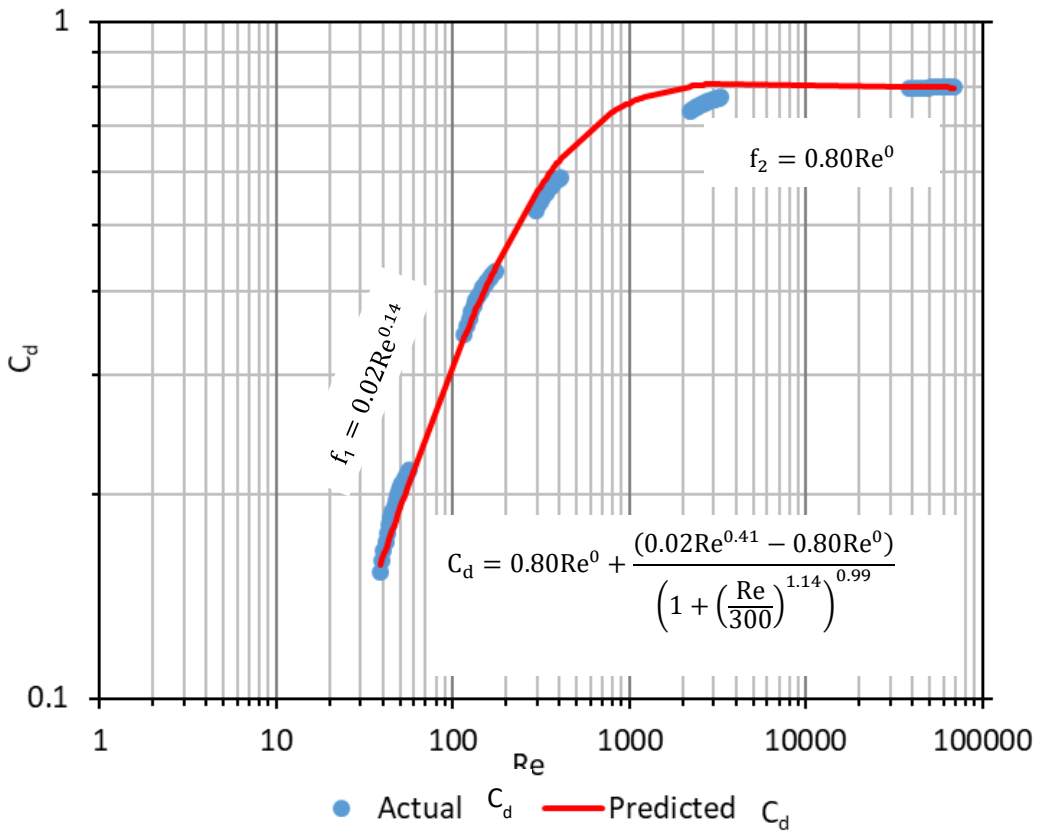


Figure 5.3 Logistic dose response curve for L/d ratio of 3

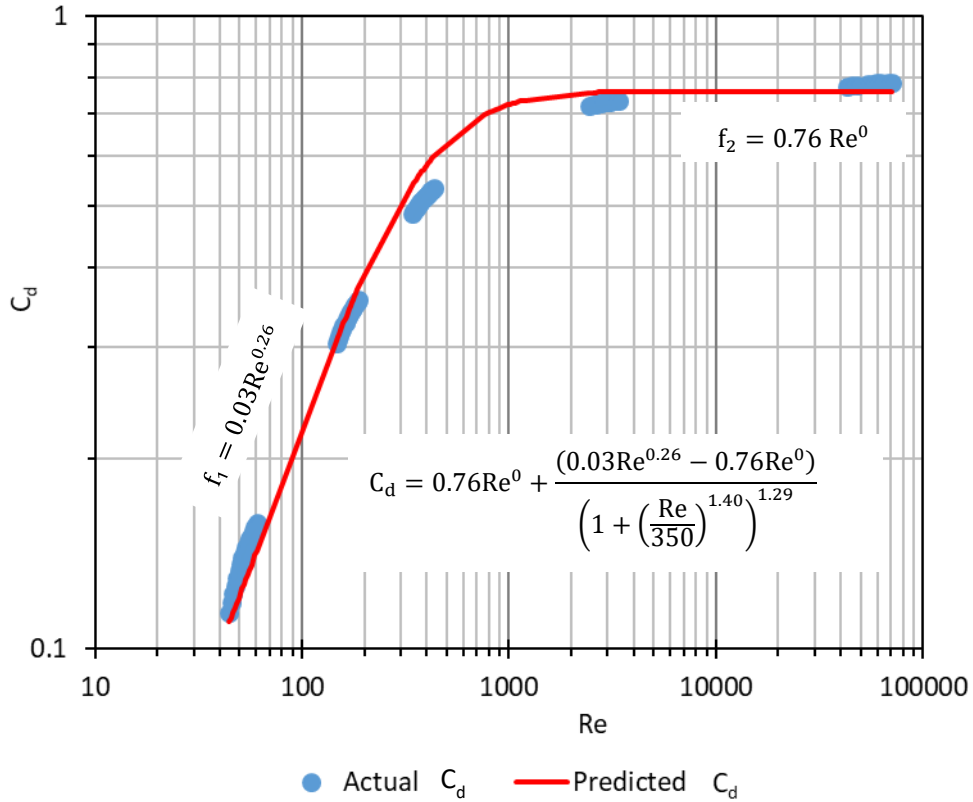


Figure 5.4 Logistic dose response curve for L/d ratio of 5

From the predictions of C_d the predicted flow rates for all the Newtonian data was then calculated using Equation 5.4 for each L/d ratio.

$$Q_{\text{actual}} = A_0 \times C_{d\text{predicted}} \times \sqrt{2gh} \tag{Equation (5.4)}$$

The plots of $Q_{(\text{predicted})}$ against $Q_{(\text{actual})}$ are as presented in Figures 5.5, 5.6, 5.7 and 5.8. For L/d ratios of 0, 1, 3 and 5, all the data points are within $\pm 3\%$ error margins.

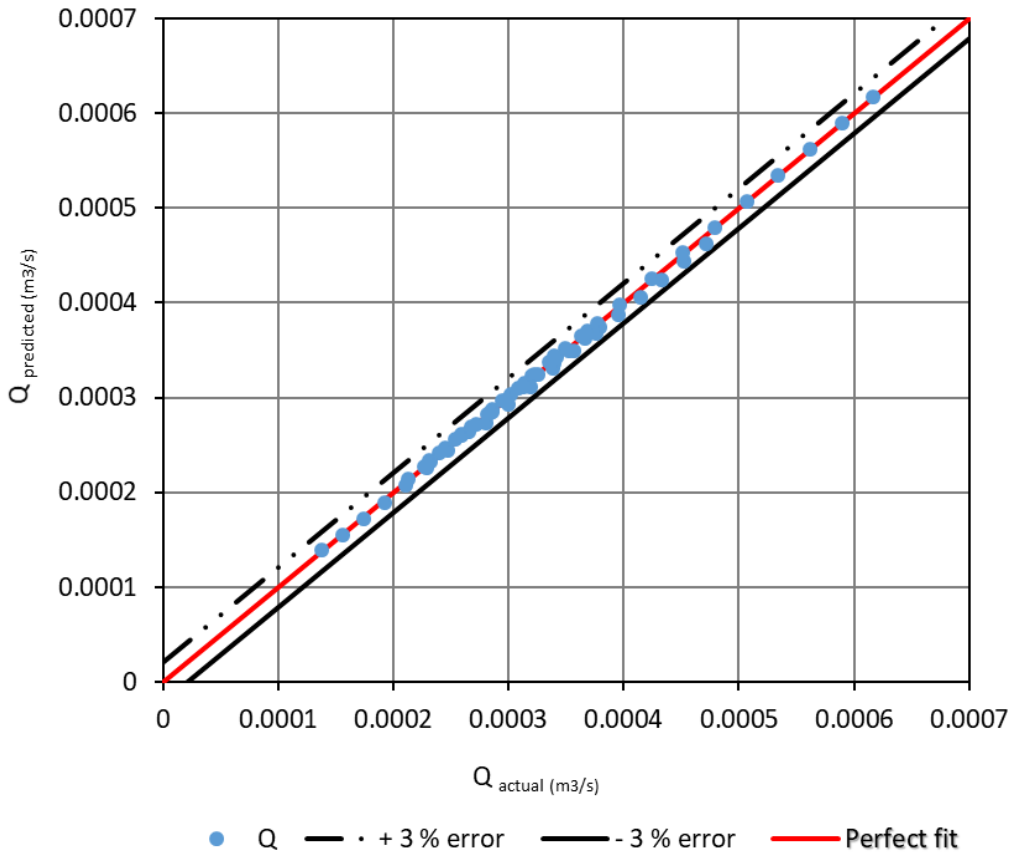


Figure 5.5 Comparison between the actual and predicted flow rates through L/d ratio of 0.05

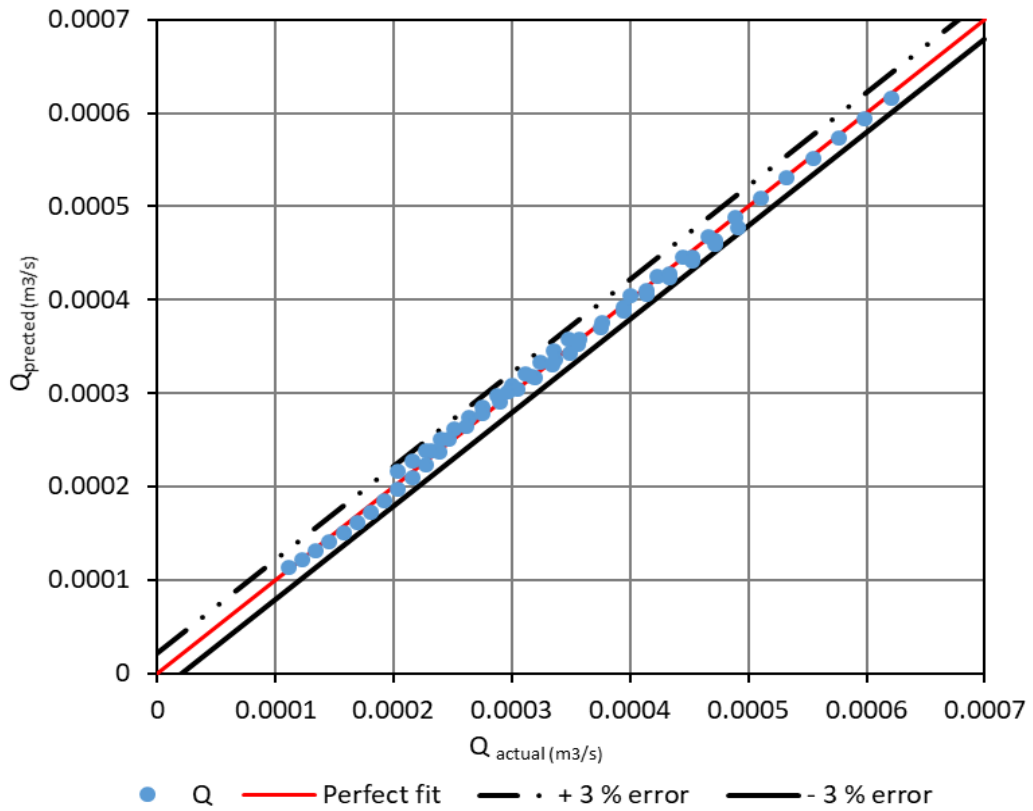


Figure 5.6 Comparison between the actual and predicted flow rates through L/d ratio of 1

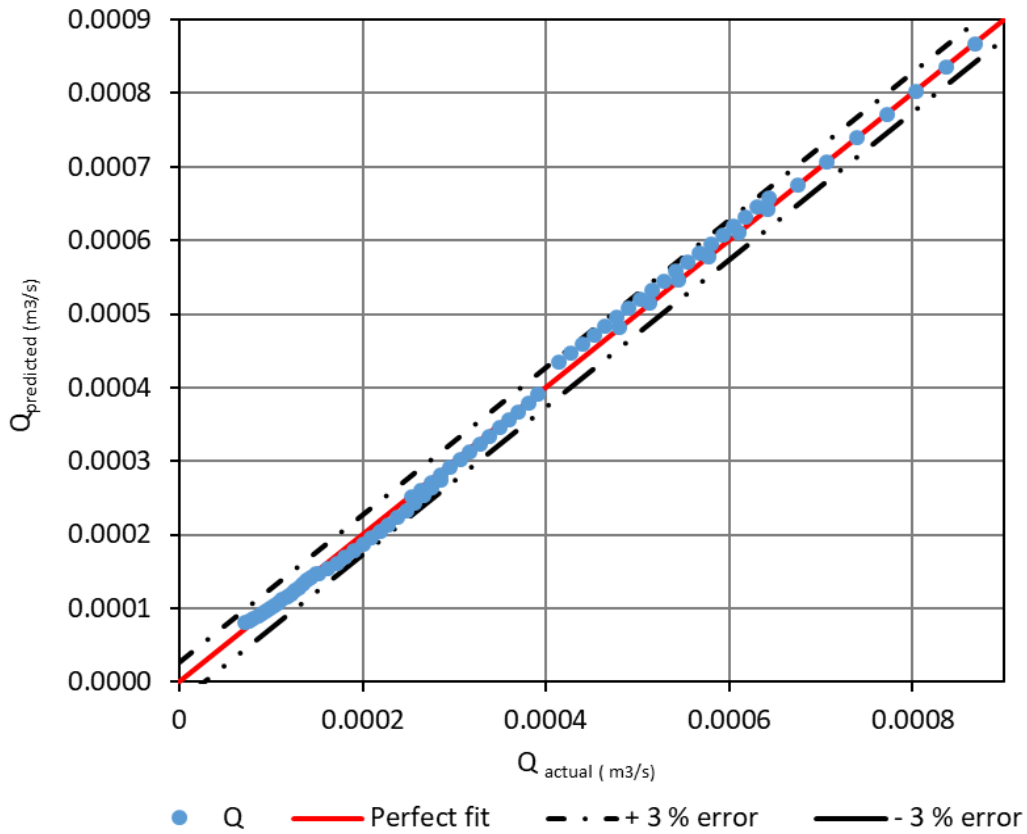


Figure 5.7 Comparison between the actual and predicted flow rates through L/d ratio of 3

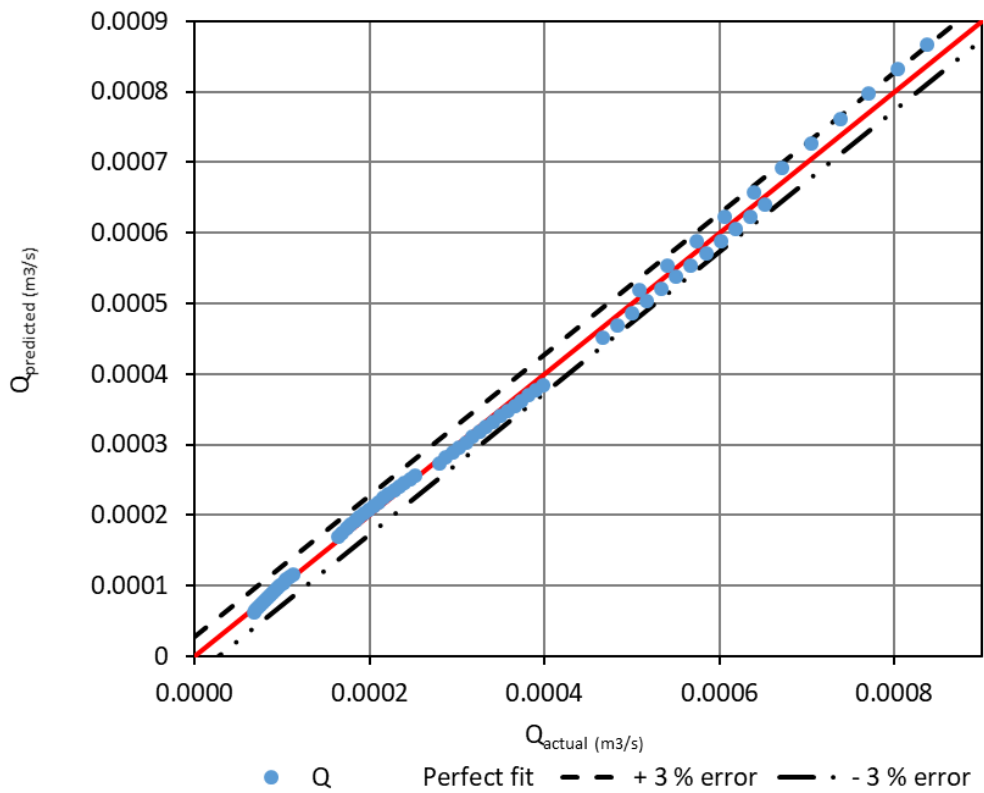


Figure 5.8 Comparison between the actual and predicted flow rates through L/d ratio of 5

5.2 Conclusion

A single composite power law equation was applied to all Newtonian data obtained for each aspect ratio, and predicted C_d values were plotted against Re . In the laminar flow, the C_d values were dependent on the Re , and in the turbulent, the C_d values were independent of Reynolds number with average constant C_d value of 0.60 and 0.59 for an L/d of 0.05 and 1 respectively; L/d ratios of 3 and 5 had a constant C_d value of 0.80 and 0.78, accordingly. The error margins for the actual flow rates and the predicted flow rates were within $\pm 3\%$ for all L/d ratios.

Chapter 6 COMPARISON OF CURRENT RESULTS WITH LITERATURE

6.1 Introduction

This section evaluates and discusses the results presented in Chapter 4, comparing them to the data published in the literature. For flow rate measurement of non-Newtonian liquids from tanks through orifices, only the work by Dziubiński and Marcinkowski (2006) was identified. The discussion is supported by the literature on the gravitational flow rate measurement of Newtonian liquids through orifices. The effect of the aspect ratio on gravitational discharge of Newtonian and non-Newtonian liquids flow from tanks is discussed.

6.2 Calibration

For an L/d ratio of 0.05, the coefficient of discharge of 0.60 obtained from calibration was determined as within $\pm 2\%$ deviation compared to the standard C_d value of 0.61 for sharp-crested orifices. This is in line with work by previous researchers such as Lea (1938); Lienhard and Lienhard (1984) and Swamee and Swamee (2010) as found in textbooks. The average C_d value obtained by Dziubiński and Marcinkowski (2006) for an L/d ratio of 0 was 0.62. For an L/d ratio of 1, the average C_d value obtained was 0.59; this is within $\pm 5.5\%$ deviation compared to the standard C_d value for sharp-crested orifices. For an L/d ratio of 3, the average C_d value obtained was 0.80 which is equal to an average C_d value obtained by Fox and Stalk (1989). For an L/d ratio of 5, the average C_d value obtained was 0.78 it is within $\pm 2\%$ deviation from the average C_d value of 0.79 obtained by Çobanoğlu (2008).

6.3 C_d -Re relationship

6.3.1 Newtonian liquids

Figure 6.1 shows C_d versus the Re graphs for Newtonian liquids for an orifice with L/d ratio of 0 obtained for this study and the available data from Lea (1938) and Medaugh and Johnson (1940). The C_d values obtained in this study only drop as low as 0.47 as compared to the C_d value obtained by Lea (1938). This is due to the fact that they used more viscous liquids and smaller orifice diameter sizes. There is a good agreement in the turbulent flow between the data from the current study and those of Lea, 1938 and Medaugh and Johnson (1940). The average C_d value obtained for this study is 0.60 which is comparable to 0.61 obtained by Lea (1938) and Medaugh and Johnson (1940). Turbulent flow data is observed when $Re > 1000$ where the data combines and form one flow trend. Both graphs have peak values in the transition zone with Lea's peak C_d value at 0.8 and the peak of the current study at 0.67, perhaps due to the orifice diameter size and geometry of the tank used. Medaugh and Johnson's (1940) data only covers the turbulent region, while Lea's data covers laminar, turbulent and transition regions.

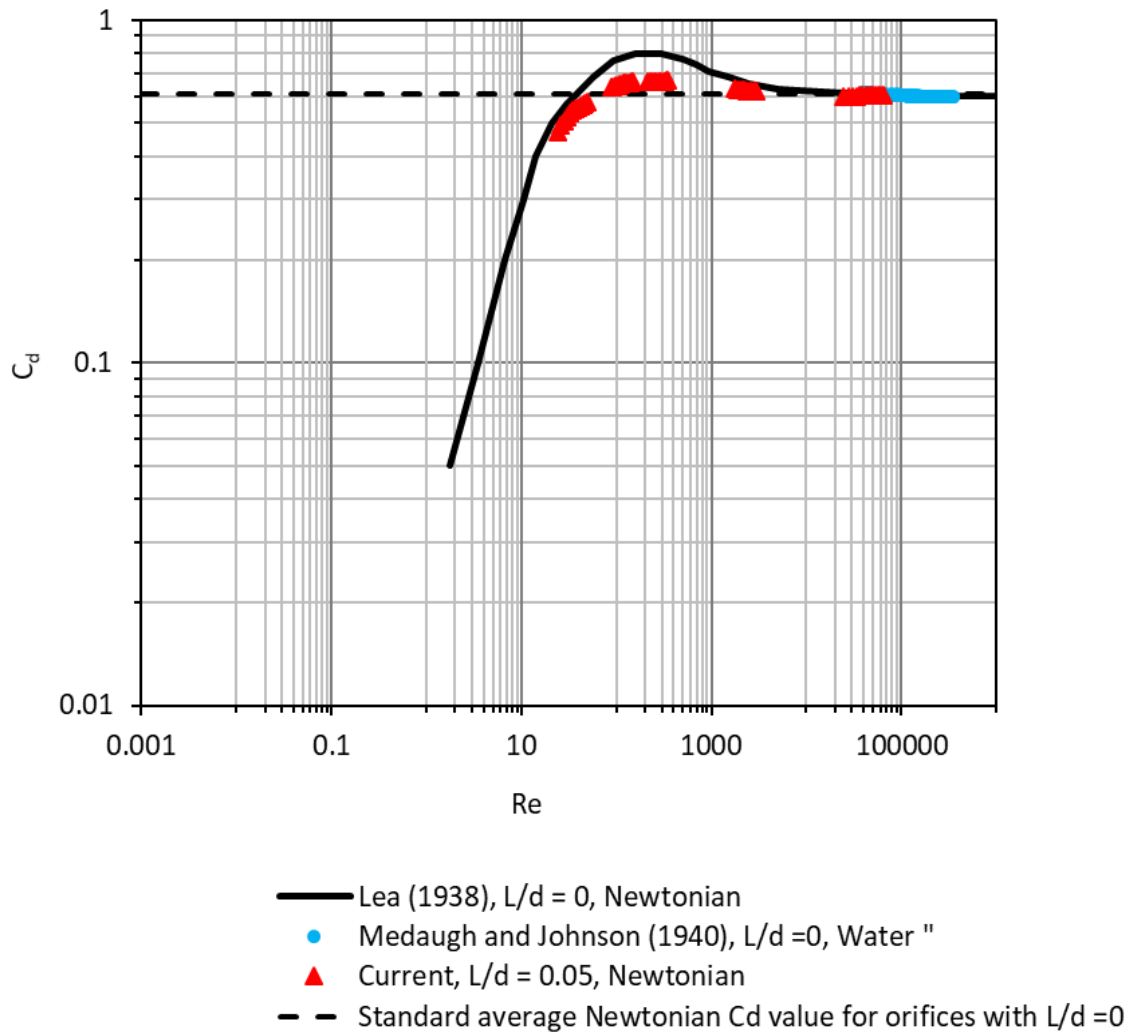


Figure 6.1 C_d versus the Re graphs for Newtonian liquids for Lea, 1938; Medaugh & Johnson, 1940; and the current study

Figure 6.2 shows C_d versus the Re graphs for Newtonian liquids for an orifice with L/d ratio of 1 for this study and the available data from Dziubiński and Marcinkowski (2006) and Kiljański (1993). The figure clarifies that each study has its own flow trend, a result of the different orifice and tank geometries used when conducting the study. However, there is good agreement in the turbulent flow region: Dziubiński and Marcinkowski's (2006) average C_d value is 0.62 while that of this study is 0.59. A peak C_d value of 0.64 was obtained for an L/d ratio of 1 and a peak C_d value of 0.73 was obtained by Dziubiński and Marcinkowski (2006) for L/d ratio of 1. Kiljański's (1993) data only covers the laminar region and Dziubiński and Marcinkowski's (2006) data covers laminar, transition and turbulent regions. Dziubiński and Marcinkowski's (2006) turbulent data goes up to 10000 while the turbulent data of this current study escalates to 67000.

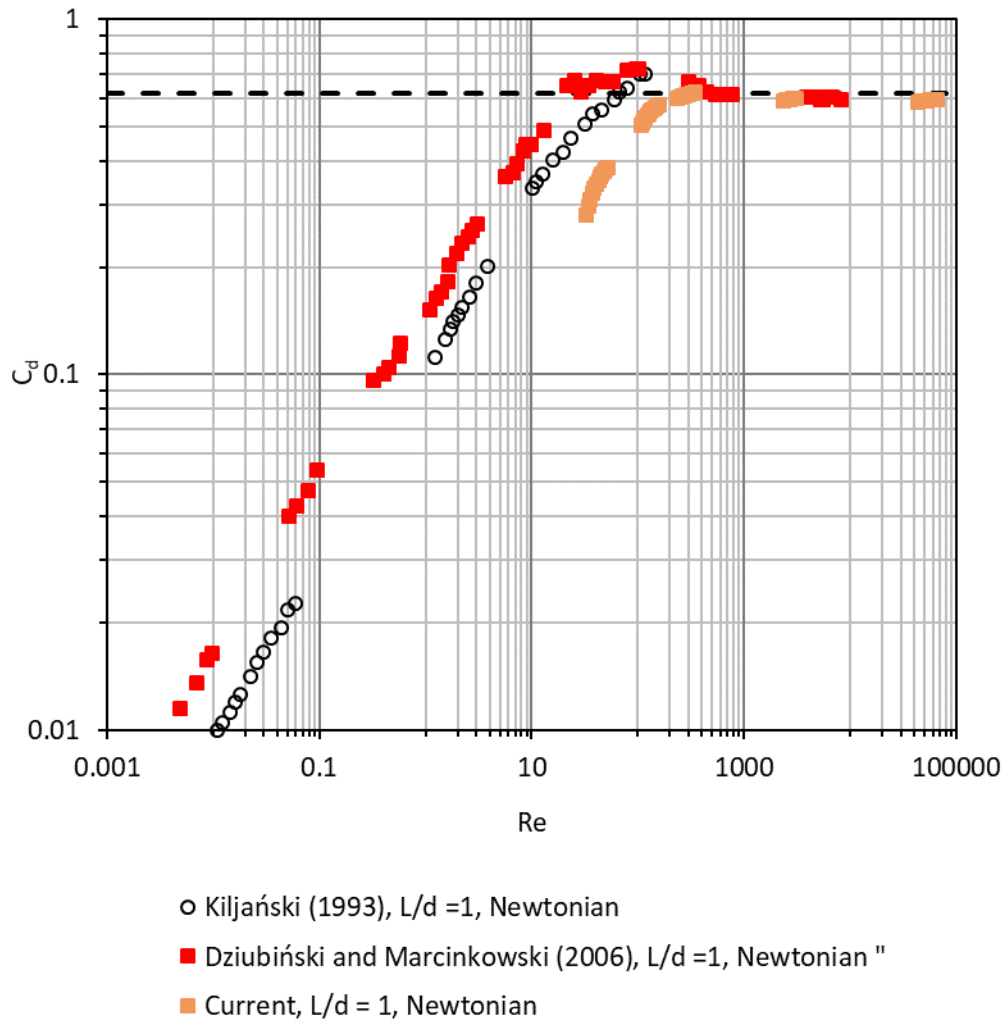


Figure 6.2 C_d versus the Re graphs for Newtonian liquids for an orifice with L/d ratio of 1 (Dziubiński & Marcinkowski, 2006; Kiljański, 1993; and the current study)

Figure 6.3 shows C_d versus the Re graphs for Newtonian liquids for an orifice with L/d ratio of 3 for this study and the available data from Fox and Stark (1989) and Dziubiński and Marcinkowski (2006). Dziubiński and Marcinkowski's (2006) data only covers the laminar region, while Fox and Stark's (1989) covers part of the turbulent and part of the laminar region. Fox and Stark's (1989) data and the current data form one flow trend at $Re > 1000$. There is good agreement between Fox and Stark's (1989) turbulent data and the current study's turbulent data with an average C_d value of 0.8 for both studies. In the laminar region, the liquids have separate flow trends.

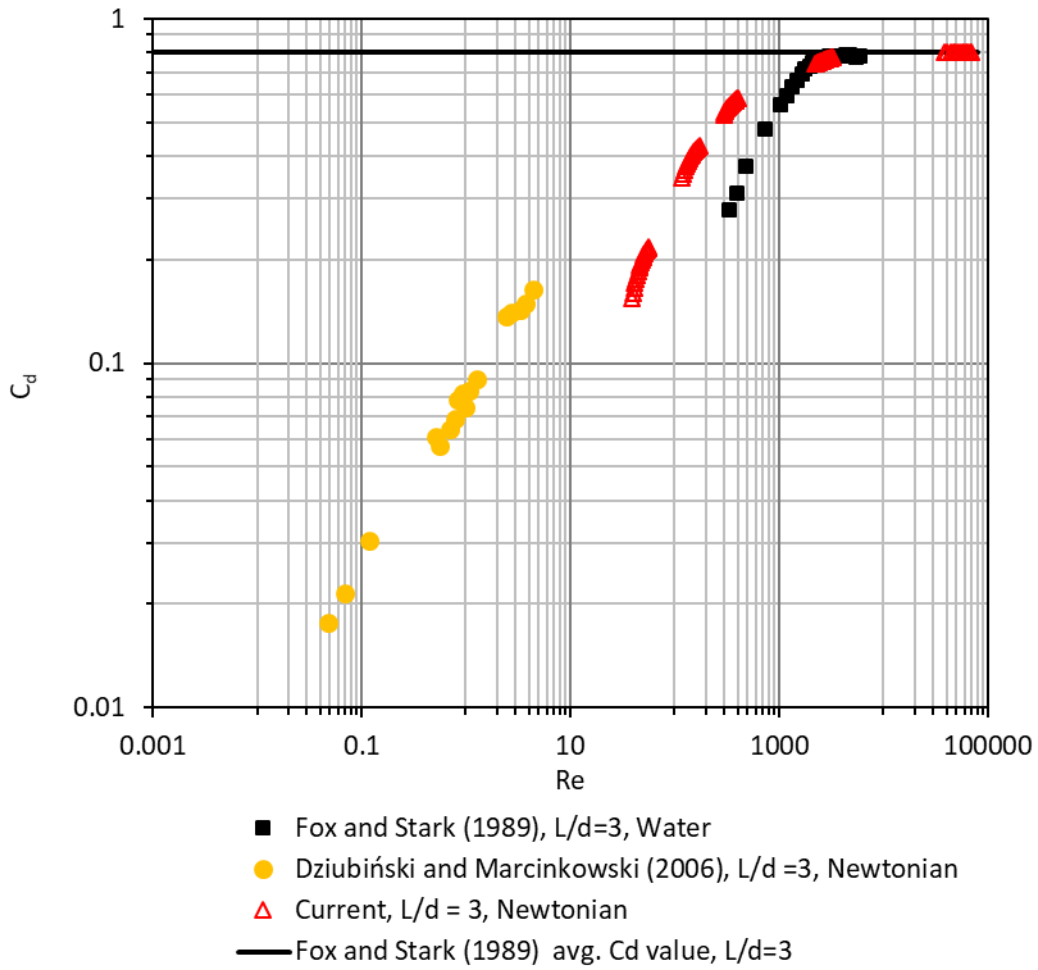


Figure 6.3 Comparison of C_d versus the Re graphs for Newtonian liquids for an orifice with L/d ratio of 3 between Dziubiński & Marcinkowski (2006); Fox & Stark (1989); and the current study

Figure 6.4 shows C_d versus the Re graphs for Newtonian liquids for an orifice with aspect ratio of 5 obtained in this study and the available data from Çobanoğlu (2008). Although Çobanoğlu's data (2008) covers part of the turbulent flow region, there is good agreement between the current study and Çobanoğlu (2008), with an average C_d value of 0.79 for Çobanoğlu's (2008) study and an average C_d value of 0.78 for this current study.

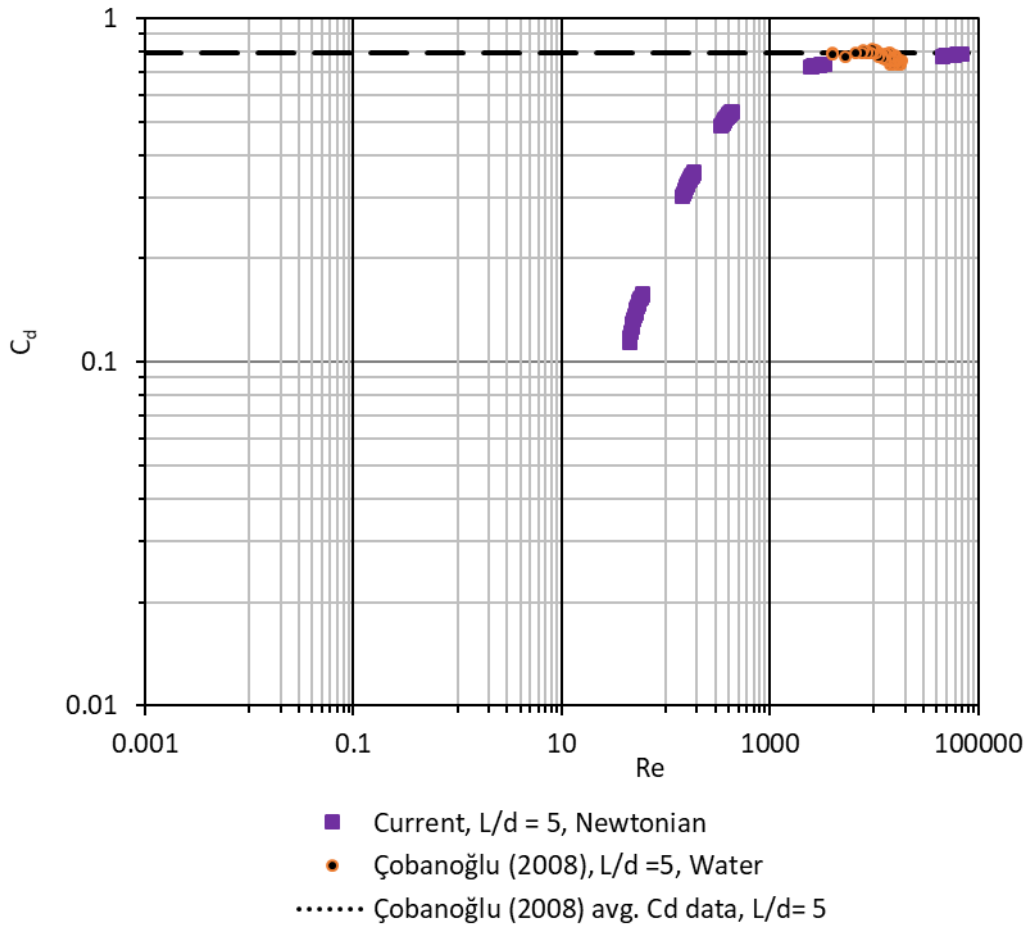


Figure 6.4 Comparison of C_d versus the Re graphs for Newtonian liquids for an orifice with L/d ratio of 3 between Çobanoğlu (2008) and the current study

Figure 6.5 shows the average coefficient of discharge against the aspect ratios of 0, 1 and 3 in the turbulent region for Newtonian liquids as per the current study and Dziubiński and Marcinkowski (2006). Dziubiński and Marcinkowski's (2006) results show that as the aspect ratios increase, the average C_d value remains as 0.62 for all aspect ratios used, while the current study shows that for aspect ratios of 0, 1 and 3, the average C_d values were 0.60, 0.59 and 0.80, respectively, demonstrating a non-linear increase in the average C_d values as the aspect ratios increase.

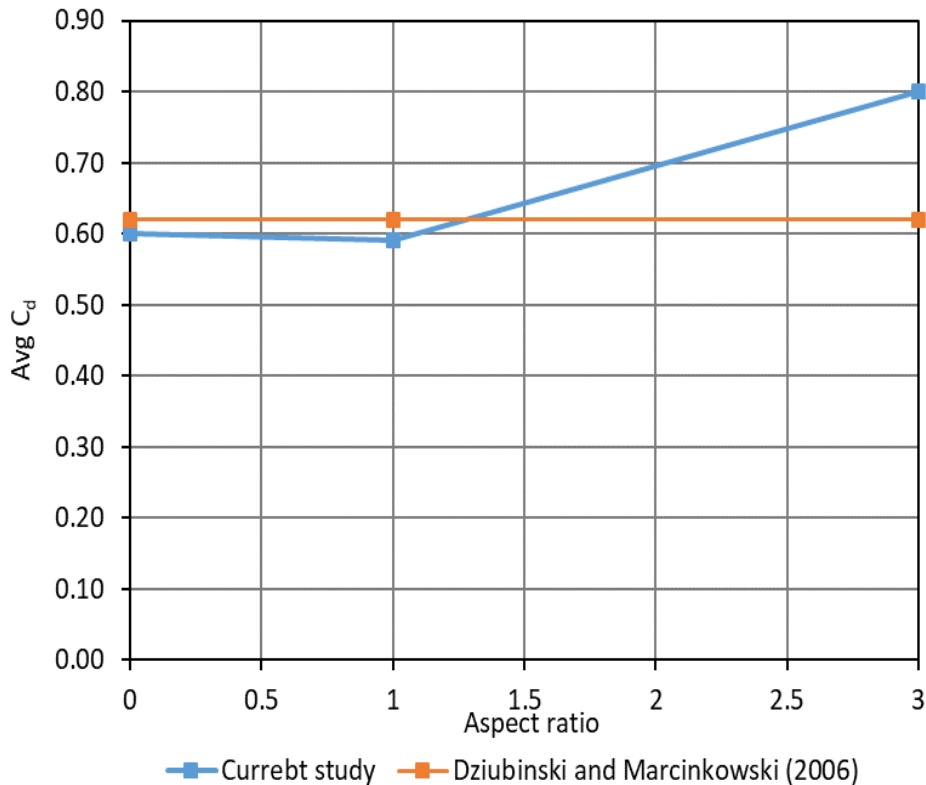


Figure 6.5 Effect of the L/d ratio in the turbulent region for Newtonian liquids as per the current study and that of Dziubiński and Marcinkowski (2006)

6.3.2 Non-Newtonian liquids

Figure 6.6 shows C_d versus the Re graphs for non-Newtonian liquids for an orifice with L/d of 0.05 obtained in this study and data from Dziubiński and Marcinkowski (2006). Dziubiński and Marcinkowski's (2006) data covers the laminar region and part of the transition region. The peak C_d value obtained by Dziubiński and Marcinkowski (2006) was 0.76 while the peak C_d value for the current data is 0.67. Both flow curves intersect at $Re=200$. In the laminar flow region, data of the current study reveals different flow trends for the different liquids. Dziubiński and Marcinkowski (2006) tested CMC solutions only, finding that in the turbulent flow the average C_d value was 0.67, but the data retrieved only covered the laminar and transition region. For the current study, the turbulent flow occurred at $Re > 4000$ with an average C_d value of 0.59.

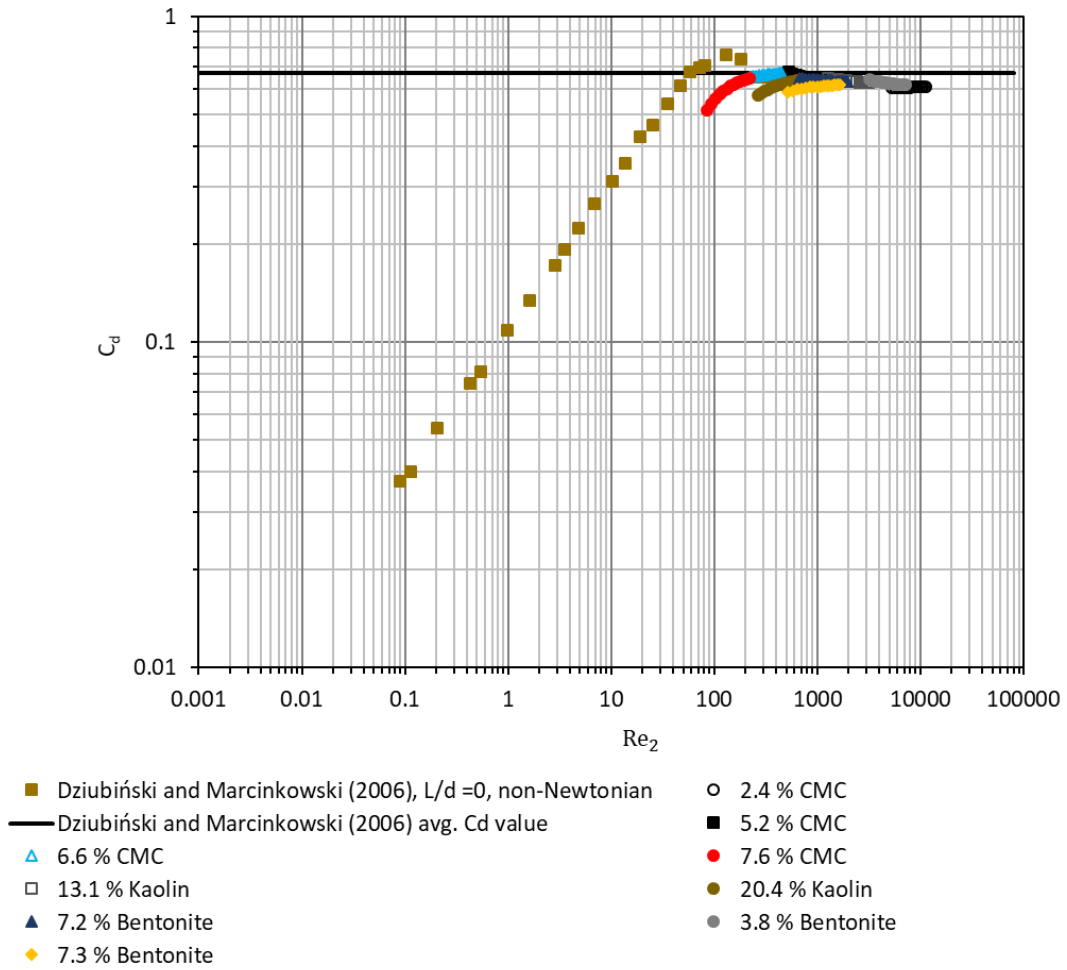


Figure 6.6 Comparison of C_d versus the Re graphs for non-Newtonian liquids between Dziubiński and Marcinkowski (2006) and the current study

Figure 6.7 shows a comparison of experimental data for the gravitational flow of non-Newtonian liquids from a tank between the current study and Dziubiński and Marcinkowski’s (2006) study for an aspect ratio of 1. Dziubiński and Marcinkowski’s (2006) data covers the laminar region and part of the transition region. The flow curves intersect at $Re=400$ in the transition zone. The peak C_d values of 0.71 and 0.64 are obtained for Dziubiński and Marcinkowski’s (2006) data and the current data, respectively. The current study shows that in the laminar region, the different liquid have combined to form one flow trend, likely because of the increase in the aspect ratio from 0.05 to 1. The turbulent region occurs at $Re > 1000$ where an average C_d value of 0.59 was obtained. Dziubiński and Marcinkowski (2006) attained an average C_d value of 0.67 for 5.2% CMC.

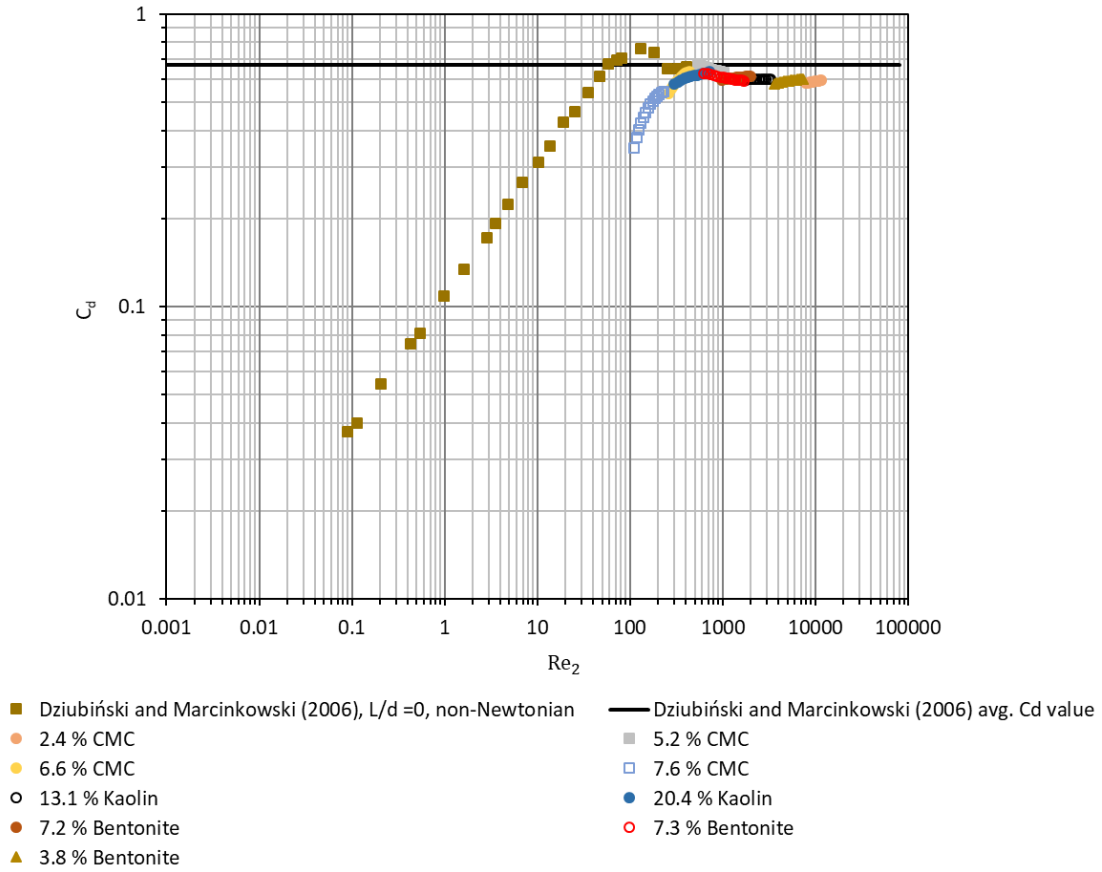


Figure 6.7 Comparison of C_d versus the Re graphs for non-Newtonian liquids for an orifice with L/d ratio of 1 between Dziubiński and Marcinkowski (2006) and the current study

Figure 6.8 presents C_d versus the Re graphs for non-Newtonian liquids for an orifice with L/d ratio of 3 obtained in this study compared to the available data from Dziubiński and Marcinkowski (2006). In the laminar region of the current study, the liquids form separate flow trends (CMC solutions and kaolin suspensions combine to form one flow trend and the other flow trend is formed by bentonite suspensions). Even through the turbulent region is not well defined, an average C_d value of 0.78 was obtained while Dziubiński and Marcinkowski (2006) achieved an average C_d value of 0.67.

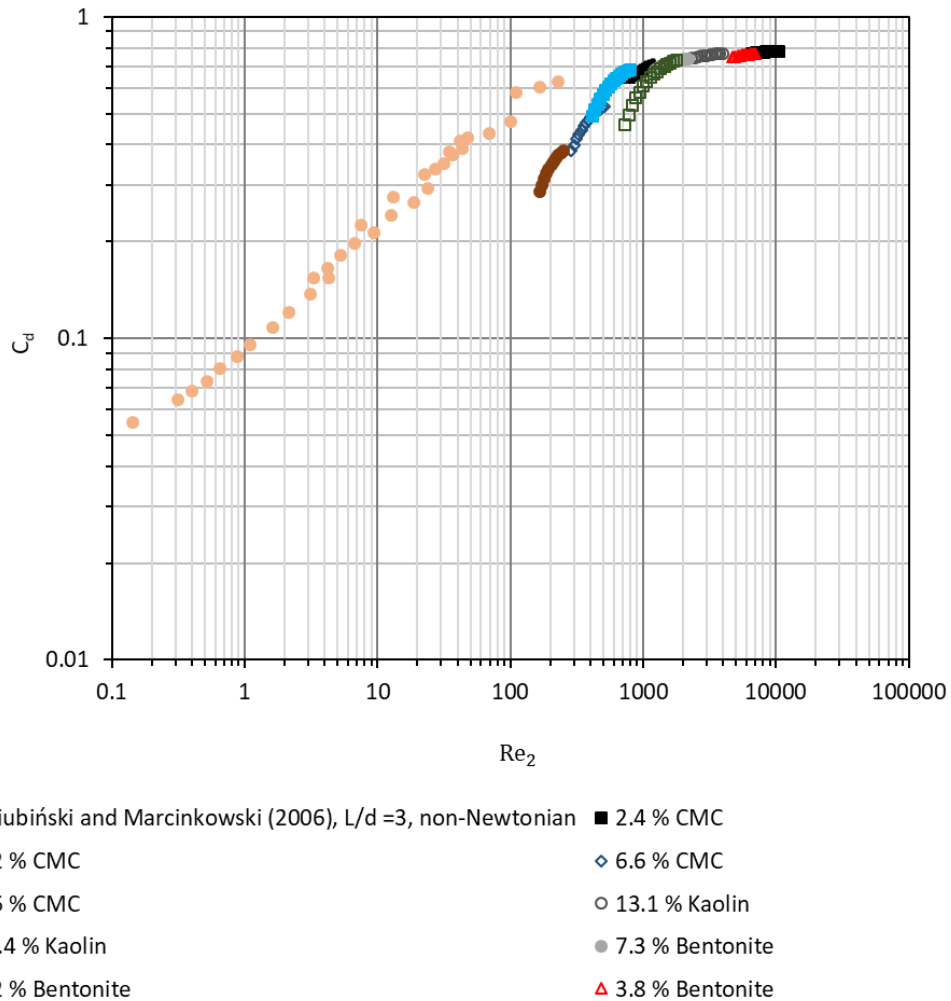


Figure 6.8 Comparison of C_d versus the Re graphs for non-Newtonian liquids for an orifice with L/d ratio of 3 between Dziubiński and Marcinkowski (2006) and the current study

Figure 6.9 illustrates combined plots of coefficient of discharge values against Re for non-Newtonian liquids for an L/d ratio of 0.05, 1 and 3 for the current study and data from Dziubiński and Marcinkowski (2006). For the current study, the average C_d value in the turbulent region was determined to be different for each aspect ratio, with L/d ratio of 0 and 1 having average C_d values of 0.60 and 0.59, respectively, and L/d ratio of 3 having an average C_d value of 0.78.

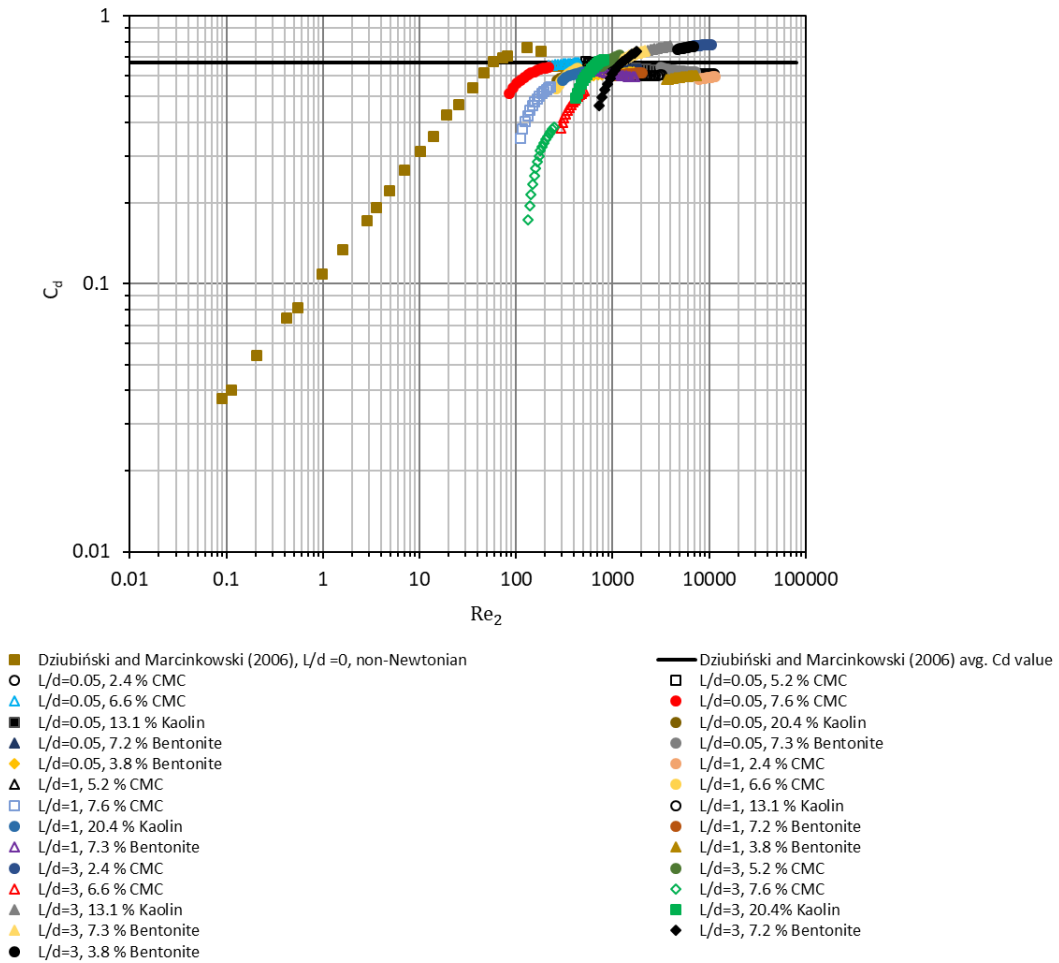


Figure 6.9 Comparison of C_d versus the Re graphs for non-Newtonian liquids between Dziubiński and Marcinkowski (2006) and the current study

Figure 6.10 shows the average coefficient of discharge against the L/d ratios of 0.05, 1 and 3 in the turbulent region for non-Newtonian liquids as per the current study and Dziubiński and Marcinkowski (2006). Dziubiński and Marcinkowski's (2006) results show that as the L/d ratios increase, the average C_d value remains as 0.67 for all L/d ratios used, while the current study shows that for L/d ratios of 0.05, 1 and 3, the average C_d values were 0.62, 0.59 and 0.78 respectively, presenting a non-linear increase in the average C_d values as the aspect ratios increased.

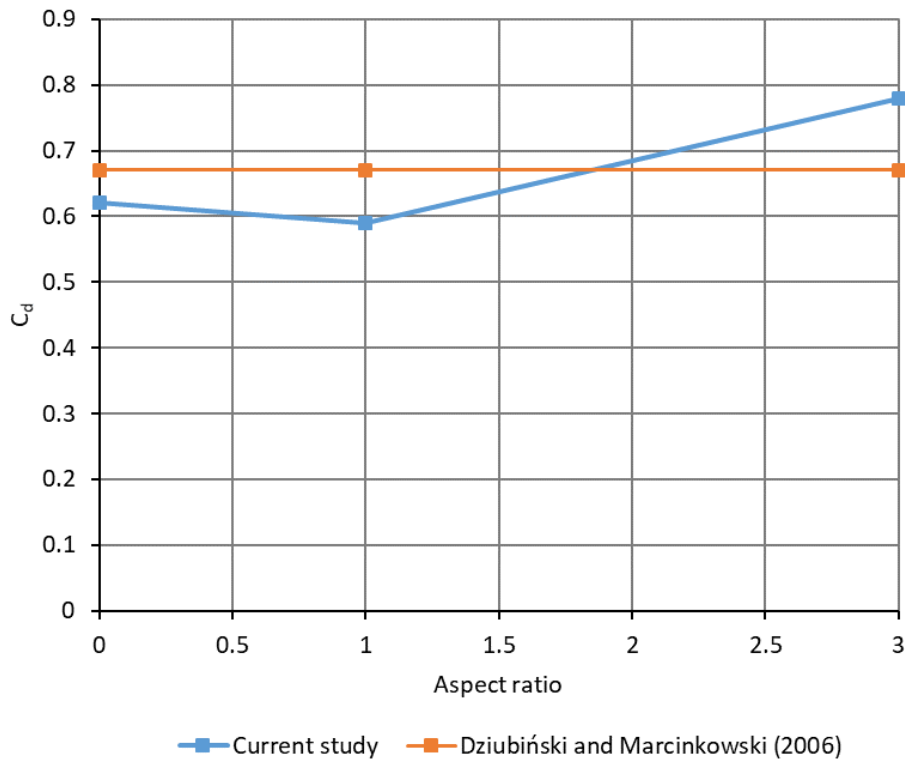


Figure 6.10 Effect of the L/d ratio in the turbulent region of non-Newtonian liquids as per the current study and that of Dziubiński and Marcinkowski (2006)

6.4 Conclusion

The aim of this work was to establish the effect of round orifice L/d ratios on the gravitational discharge of non-Newtonian liquids from a tank, as a function of liquid properties. Table 6.1 summarises the current study data and that of the literature. For the current study, it is observed that in the turbulent flow region of Newtonian and non-Newtonian liquids, there is an inconsistent increase in average C_d values. Dziubiński & Marcinkowski, 2006 found an average C_d value of 0.62 in the turbulent flow region of Newtonian liquids for all the L/d ratios. For non-Newtonian liquids, Dziubiński & Marcinkowski, 2006 stated an average C_d value of 0.67 in the turbulent flow, however, the retrieved data only covered the laminar and transition regions.

In the laminar region of the current study it is observed that as the aspect ratio increases, lower Re values are obtained. The literature has obtained lower Re values in the laminar region ($Re < 12$) whilst the lowest obtained for the current study is $Re < 100$. Also, in the laminar region of the current study, non-Newtonian liquids show that for each L/d ratio there are separate flow trends, this is in agreement with the literature (Kiljański, 1993 & Dziubiński & Marcinkowski, 2006).

Table 6.1 Summary of the effect of aspect ratio on flow regions

Current study					Literature					
Newtonian					Newtonian					
L/d	Laminar region	Turbulent region	Peak C_d	Average C_d	L/d	Authors	Laminar region	Turbulent region	Peak C_d	Average C_d
0.05	Re < 100	Re > 40000	0.67	0.60	0	Lea (1938)	Re < 12	Re > 10000	0.8	0.61
					0	Medaugh and Johnson (1940)	(-)	Re > 40000	-	0.61
					0	Kiljański (1993)	Re < 10	-	0.84	-
					0	Dziubiński and Marcinkowski (2006)	Re < 10	Re > 1000	0.64	0.62
1	Re < 200	Re > 40000	0.64	0.59	1	Kiljański (1993)	Re < 10	-	0.70	-
					1	Dziubiński and Marcinkowski (2006)	Re < 10	Re > 1000	0.73	0.62
3	Re < 405	Re > 2000	-	0.80	3	Fox and Stark (1989)	Re < 1000	Re > 4000	-	0.80
					3	Dziubiński and Marcinkowski (2006)	Re < 10	Re > 1000	0.63	0.62
5	Re < 440	Re > 2000	-	0.78	5	Çobanoğlu (2008)	-	Re > 4000	-	0.79
Non- Newtonian					Non-Newtonian					

COMPARISON OF CURRENT RESULTS WITH LITERATURE

L/d	Liquid	Laminar region	Turbulent region	Peak C_d	Average C_d	L/d	Authors	Laminar region	Turbulent region	Peak C_d	Average C_d
0.05	CMC	$80 < Re_2 < 200$	$7000 < Re_2$	0.67	0.62	0	Dziubiński and Marcinkowski (2006)	Re < 10	-	0.74	0.67
	Bentonite	$500 < Re_2 < 1000$	$4200 < Re_2$	0.62							
	Kaolin	$200 < Re_2 < 700$	$2300 < Re_2$	0.64							
1	CMC	$Re_2 < 230$	$Re_2 > 2000$	0.62	0.59	1	Dziubiński and Marcinkowski (2006)	Re < 10	-	0.72	0.67
	Bentonite	$Re_2 < 230$	$Re_2 > 2000$	0.62							
	Kaolin	$Re_2 < 230$	$Re_2 > 2000$	0.62							
3	CMC	$Re_2 < 510$	$Re_2 > 6900$	-	0.78	3	Dziubiński and Marcinkowski (2006)	Re < 10	-	-	0.67
	Bentonite	$Re_2 < 1000$	$Re_2 > 3900$	-							
	Kaolin	$Re_2 < 510$	$Re_2 > 6900$	-							
5	CMC	$Re_2 < 930$	$Re_2 > 4000$	-	0.74	5	So far, no L/d ratio of 5 has been used for flow rate measurement of non-Newtonian liquids				
	Bentonite	$Re_2 < 1400$	$Re_2 > 4000$	-							
	Kaolin	$Re_2 < 930$	$Re_2 > 4000$	-							

Chapter 7 CONCLUSION AND RECOMMENDATIONS

7.1 Introduction

Orifice plates have been used for many years and will continue to be used as they are inexpensive and easy to use, underscoring their use in so many industries. This work adds to the scarce research on Newtonian and non-Newtonian liquid gravitational flow rate measurements from tanks using orifices of varying aspect ratios. This study used a logistic response curve formulated by (Patankar *et al.*, 2002) to predict the coefficient of discharge from the laminar to turbulent region for Newtonian liquids. It reiterates the objective and outlines the literature explored and applied. It also contains recommendations for further work.

7.2 Summary

Non-Newtonian liquids behave differently from water; they have complicated rheological characteristics. When gravitationally discharging these liquids from the bottom of a tank, there are volumes of material remaining in the tank, resulting in product wastage and a subsequent loss of money. Even though there is a study conducted on the gravitational discharge of non-Newtonian liquids using orifices of varying aspect ratios (Dziubiński & Marcinkowski, 2006), only CMC was used. Numerous other studies have been conducted from tanks using Newtonian liquids and where the orifice was placed on the side of the tank (Lea, 1938; Medaugh & Johnson, 1940; Lienhard & Lienhard, 1984; Fox & Stark, 1989; Kiljański, 1993; Çobanoğlu, 2008). However, there is insufficient work relating to the discharge of non-Newtonian liquids from the bottom of tanks using orifices of varying L/d ratios. As such, it is evident that additional experimental data is needed for a more comprehensive comparison.

This research uses additional types of non-Newtonian liquids exhibiting different non-Newtonian liquid behaviour. The models used to characterise non-Newtonian liquids for this study are Bingham plastic, pseudoplastic and yield-pseudoplastic or Herschel-Bulkley. The aim of this research was to determine the effect of round orifice L/d ratios on the gravitational discharge of non-Newtonian liquids from a tank, as a function of liquid properties. This was achieved by determining the flow rates through circular orifice plates of varying L/d ratios using water and various concentrations of glycerine and CMC solutions, and bentonite and kaolin suspensions.

Experiments were done in the slurry laboratory at the Cape Peninsula University of Technology. A tank rig was used for conducting all the experiments. Four circular orifices, all of 20 mm in diameter and varying L/d ratios of 0.05, 1, 3 and 5, were fitted at the bottom of the tank flush with the inside surface. A Paar-Physica MCR 300 rheometer measured the rheological parameters of the liquids. Newtonian, power-law and Herschel-Bulkley were used to determine the rheological parameters of the test liquids. Data was derived by correlating the coefficient of discharge (C_d) and an appropriate Reynolds number value for all the liquids. For Newtonian liquids, flow measurements are highly dependent on the density and temperature of the liquid. Non-Newtonian liquid flow measurement is dependent on the aforementioned parameters rheological characteristics as well as orifice geometry.

Calibration results indicated that the aspect ratios have an effect on the flow rate measurements of non-Newtonian liquids as the effect was evident in the laminar region as well as the turbulent region. The

calibration results reveal a non-constant increase in C_d values as the aspect ratio increases; the average C_d values were 0.60, 0.59, 0.80 and 0.78 with standard deviations of 0.002, 0.006, 0.001 and 0.004 for aspect ratios of 0, 1, 3 and 5, respectively. The average C_d value for L/d ratio of 0.05 was within $\pm 2\%$ error of the standard C_d value for sharp-crested orifices of 0.61, and the average C_d value for L/d ratio of 1 is within $\pm 5.5\%$ error. For an L/d of 3, the average C_d value is comparable to the average C_d value obtained by Stark and Fox (1989) of 0.80. Lastly, an L/d ratio of 5 is within $\pm 2\%$ error of Çobanoğlu's (2008) average C_d value of 0.79. For an L/d ratio = 0.05 and 1, the turbulent flow occurred at $Re > 4000$, and for an L/d ratio = 3 and 5, the turbulent flow occurred at $Re > 10000$. The transition region for L/d ratio of 0.05 and 1 is defined by $100 < Re < 4000$ and that of L/d ratios of 3 and 5 is defined by $200 < Re < 10000$.

In the laminar region, there are separate flow trends for each L/d ratio. For an L/d ratio of 0.05, each liquid type has its own flow trend. As the L/d ratio increased from 0.05 to 1, all non-Newtonian liquids formed one flow trend. For an L/d of 3, CMC solutions and kaolin suspensions formed one flow trend and bentonite suspensions formed their own flow trend. This behaviour is also observed for an L/d ratio of 5. For an L/d ratio of 0, the turbulent region of non-Newtonian liquids is observed at $Re > 7000$ with an average C_d value of 0.62. For an L/d ratio of 1, the turbulent region for non-Newtonian liquids is observed at $Re_2 > 2000$; all liquids have combined forming one flow trend with an average C_d value of 0.59 for both Newtonian and non-Newtonian liquids. For an L/d ratio of 3, the turbulent flow of non-Newtonian liquids is observed at $Re > 7000$ with an average C_d value of 0.78. For an L/d ratio of 5 for non-Newtonian liquids, the turbulent region is observed at $Re_2 > 7300$ with an average C_d value of 0.74.

The outcomes of this study are supported by the literature on the gravitational discharge of Newtonian and non-Newtonian liquids from tanks through orifice. Comparable behaviour of gravitational discharge of Newtonian liquids was attained by Lea (1938) for an L/d ratio of 0.05. He obtained lower Re values in the laminar region ($Re < 12$) whilst the lowest obtained for the current study is $Re < 100$. In the laminar region, Dziubiński and Marcinkowski (2006) and Kiljański (1993) attained separate flow trends for each aspect ratio as was established in the current study; however, their laminar region was defined by $Re < 10$ and that of the current study was defined by $Re < 100$. Dziubiński and Marcinkowski (2006) determined the turbulent region of non-Newtonian liquids to have an average C_d value of 0.67 irrespective of the aspect ratio used. The retrieved data only covered the laminar and transition regions. For the current study, the average C_d values of non-Newtonian liquids in turbulent flow were found to increase non-linearly as the aspect ratios increased.

The average C_d values attained for non-Newtonian liquids were 0.62, 0.59, 0.78 and 0.74 for L/d ratios of 0.05, 1, 3 and 5, respectively. For Newtonian liquids the average C_d values attained were 0.60, 0.59, 0.80 and 0.78 for L/d ratios of 0.05, 1, 3 and 5, demonstrating a non-linear increase as the L/d ratios increased.

Dziubiński and Marcinkowski (2006) reported an average C_d value of 0.62 and 0.67 in turbulent flow of Newtonian and non-Newtonian liquids respectively for all aspect ratios. The difference in the limit values for the laminar regime is mainly due to the difference in the diameter sizes used. The smallest diameter size used in literature is 2 mm and with that diameter size the lowest Re value of less than 12 was attained. The diameter size used in this study was 20 mm and the lowest Re values attained was 100. Also, the difference in the average C_d values obtained in the turbulent flow for both Newtonian and non-Newtonian liquids was mainly due to the L/d ratio difference. However, there are many other factors such as the

temperature, the orifice entry shape, orifice diameter, the head and the inner surface roughness of the orifice affect the value of the C_d . Brater and King (1982) suggested that C_d values for lower heads are higher compared to C_d values for higher heads. As far as could be ascertained, there is no data available on the flow of non-Newtonian liquids through an aspect ratio of 5.

A single composite equation formulated by (Patankar *et al.*, 2002) was applied to all the Newtonian data obtained for each L/d ratio and the predicted C_d values were plotted against Re. The error margins, when comparing the actual flow rate and the predicted flow rates, were $\pm 3\%$.

7.3 Recommendations

The database on flow rate measurement of non-Newtonian liquids using orifices of varying aspect ratios can be extended by using orifices with varying aspect ratio sizes and small diameter sizes can be used to obtain Reynolds numbers less than 10. It can further be extended by using CFD modeling which can be calibrated using the experimental database. The effect of the aspect ratio on non-Newtonian and Newtonian liquids can further be explored by using other orifice shapes. It is recommended that various edged shaped orifices be used. When conducting the experiments, the focal area was the one before the vortex. It is therefore recommended that the flow phenomenon that occurs at the vortex area be investigated as this will extend an opportunity to develop more predictions for C_d in terms of an appropriate Reynolds number.

References

- Abou El-Azem Aly, A., Chong, A., Nicolleau, F & Beck, S. 2010. Experimental study of the pressure drop after fractal-shaped orifices in turbulent pipe flows. *Experimental Thermal and Fluid Science*, 34(1): 104-111.
- Ali, A., Underwood, A., Lee, Y. R & Wilson, D.I. 2016. Self-drainage of viscous liquids in vertical and inclined pipes. *Food and Bioproducts Processing*, 99(7): 38-50.
- ASME, 1990. *Measurement of Fluid Flow in Pipes Using Orifice, Nozzle, and Venturi*, American Society of Mechanical Engineers Standard.
- Barnes, H.A., Hutton, J.F. & Walters, K. 1989. *An introduction to rheology*. Amsterdam: Elsevier.
- Barr, G. 1931. *A Monograph of Viscometry*. Oxford University Press, London.
- Beaupré, D., Chapdelaine, F., Domone, P., Koehler, E., Shen, L., Sonebi, M., Struble, L., Tepke, D., Wallevik, J.E. & Wallevik, O. 2004. *Comparison of concrete rheometers: International tests at MBT*. Cleveland OH, USA.
- Benzinger, J.B. & Aksay, I.A. 1999. Notes on data analysis: Chemical Engineering 346 Spring Term. Princeton, New Jersey: Department of chemical engineering, Princeton University.
- Bingham, E.C. 1916. *An investigation of the laws of plastic flow*. Bureau standards. Bulletin. US.
- Bird, R.B. 2002. *Transport Phenomena*. New York: John Wiley and Sons.
- Bistafa, S.R. 2018. *Theoretical reconstruction of Galileo's two-bucket experiment*. University of São Paulo, São Paulo, Brazil.
- Borutzky, W., Barnard, B. & Thomas, J. 2002. An orifice flow model for laminar and turbulent conditions. *Simulation Modelling Practice and Theory*, 10(3-4): 141-152.
- Bohra, L.K. 2004. Flow and pressure drop of highly viscous fluids in small aperture orifices. Unpublished MS thesis, School of Mechanical Engineering, Georgia Institute of Technology.
- Bos, M.G. 1989. *Discharge measurement structures*. International Institute for Land Reclamation and Improvement, Wageningen, The Netherlands.
- Brater, E.F. & King, H.W. 1982. *Handbook of Hydraulics for the Solution of Hydraulic Engineering Problems*. New York, McGraw-Hill.
- Brinkworth, B.J. 1968. *An introduction to experimentation*. London: English Universities Press.
- Brookfield Engineering Labs Inc. 2010a. *More Solutions to Sticky Problems: A Guide to Getting More From Your Brookfield Viscometer*. Bull. Brookfield Eng. Labs.

- Chhabra, R.P. & Richardson, J.F. 1999. *Non-Newtonian fluids in the process industries: fundamentals and engineering applications*. Oxford: Butterworth-Heinemann.
- Chhabra, R. & Richardson, J.F. 2008. *Non-Newtonian flow and applied rheology*. Oxford: Butterworth-Heinemann.
- Chowdhury, M. R. 2010. Determination of Pressure Loss and Discharge Coefficients for Non-Newtonian Fluids in Long Square-Edged Orifices. Unpublished MTech thesis, Cape Peninsula University of Technology, Cape Town, South Africa.
- Coulson, J.M. & Richardson, J.F. 2008. *Chemical Engineering*. Oxford: Pergamon Press.
- Crabtree, M.A. 2009. Industrial flow measurement. Unpublished Master of Science thesis, University of Huddersfield. West Yorkshire, England.
- Çobanoğlu, Ğ. 2008. Experimental study of single and multiple outlets behaviour under constant head, M.S. Thesis, Department of Civil Engineering, Middle East Technical University, Ankara.
- Dally, J.W., Riley, W.F. & McConnell, K.G. 1993. *Instrumentation for engineering measurements*, USA: John Wiley and Sons.
- Davis, C.V. 1952. *Handbook of applied hydraulics*. McGraw-Hill Book Company, Inc.
- de Almeida Medeiros., A. K, de Lima., J. F. de Medeiros., G. G. da Silva Junior., N.F. Felipe., R.N.B & dos Santos Felipe., R. C. T. 2006. *Parameters for Dimensional Inspection of Orifice Plates and Roughness of the Straight Stretches of the Tubing*. Brazilian Archives of Biology and Technology.
- Delmée, G. J. 2003. *Manual de medição de vazão*. 3^o ed. São Paulo: Edgard Blücher.
- de Nevers, N. 1991. *Fluid Mechanics for Chemical Engineers*, 2nd ed., McGraw-Hill, New York.
- Dziubiński, M. & Marcinkowski, A. 2006. Discharge of Newtonian and non-Newtonian liquids from tanks. Institution of Chemical Engineering. *Chemical Engineering for Research and Design*, 84(A12): 1191-1198.
- ESDU, 2007. *Incompressible flow through orifice plates – a review of the data in the literature*. Engineering Science data unit.
- Fan, M., Phinney, D.M. & Heldman, D.R. 2015. Effectiveness of rinsewater during in-place cleaning of stainless steel pipe lines. *Journal of Food Science*, 80(7): 1490-1499.
- Fester, V., Mbiya, B. & Slatter, P. 2008. Energy losses of non-Newtonian fluids in sudden pipe contractions. *Chemical Engineering Journal*, 145(1): 57-63.

- Fox, A. T & Stark, J. 1989. Characteristics of miniature short-tube orifice. *Journal of Mechanical Engineering Science*, 203(C5): 351-358.
- Haldenwang, R, Slatter, P. & Chhabra, P.R .2010. An experimental study of non-Newtonian fluid flow in rectangular flumes in laminar, transition and turbulent flow regimes, *Journal of the South African Institution of Civil Engineering*, 52(2): 11-19.
- Haldenwang, R. 2003. Flow on non-Newtonian fluids in open channels. Unpublished DTech thesis, Cape Technikon, Cape Town, South Africa.
- Hall, G. W. 1963. Analytical determination of the discharge characteristics of cylindrical tube orifices. *Journal of Mechanical Engineering Science*, 5(1): 91-97.
- Hartnett, J. P. & Hu, R. Y. Z. 1989. Technical note: The yield stress – An Engineering reality. *Journal of Rheology*, 33(1): 671-675.
- ISO 5167-1. 1991. *Measurement of fluid flow by means of pressure differential devices – Part 1: Orifice plates, nozzles and venturi tubes inserted in circular cross-section conduits running full*. International Organization for Standardization, Switzerland.
- ISO 5167-1. 2003. *Measurement of fluid flow by means of pressure differential devices inserted in circular-cross section conduits running full*. International Organization for Standardization, Switzerland.
- James, A. J. 1961. Flow through a long orifice. B.Sc. thesis, Nottingham University.
- Johansen, F.C. 1930. Flow through pipe orifices at low Reynolds number. *The royal society*, 126(801): 231-245.
- Kazemian, S., Prasad, A. & Huat B. B. K. 2012. *Rheological Behaviour of Grout in Context of Newtonian and non-Newtonian Fluids*. Taylor and Francis Group, London.
- Kiljański, T. 1993. Investigation of the discharge and coefficients of small circular orifices. *Journal of Fluid Engineering*, 115(4): 778-781.
- Lea, F. C. 1938. *Hydraulics for engineers and engineering students*. Arnold, London.
- Lichtarowicz, A., Duggins, R. K. & Markland, E. 1965. Discharge Coefficients for Incompressible, Non-Cavitating Flow through Long Orifices, *Journal of Mechanical Engineering Science*, 7(2): 210-219.
- Lienhard, J. H. & Lienhard, J. H. 1984. Velocity Coefficients for Free Jets from Sharp-Edged Orifices. *Journal of Fluids Engineering*, 106(1): 13-17.
- Liu, H. 2003. *Pipeline Engineering*. Boca Raton, FL: Lewis Publishers.

Martins, N. 1998. Manual de medição de vazão: através de placas de orifício, bocais e venturis. Rio de Janeiro: Interciência/Petrobras.

Medaugh, F.W. & Johnson, G.D. 1940. Investigation of the discharge coefficients of small circular orifices. *Civil Engineering Journal*, 7(7): 422- 424.

Metzner, A. B. & Reed, J. C. 1955. Flow of non-Newtonian fluids—correlation of the laminar, transition, and turbulent flow regions. *AIChE Journal*, 1(1): 434-440.

Mickaily, E.S. & Middleman, S., 1993. Hydrodynamic cleaning of a viscous film from the inside of a long tube. *AIChE Journal*, 39(): 885-893.

Mincks, L.M. 2002. Pressure drop characteristics of viscous fluid flow across orifices. Unpublished MS thesis, Mechanical Engineering, Iowa State University.

Morrison, G.L., Deotte, R. E., Moen, M., Hall, K. R. & Holste, J. C. 1990. Beta ratio, swirl and Reynolds number dependence of wall pressure in orifice flow meters. *Flow Measurement and Instrumentation*, 1(5): 269-277.

Morgan, J.G.D. 1963. Flow through long orifice at low Reynolds number. B.Sc. thesis, Nottingham University.

Nally, B.M. 2010. *Pump, Centrifugal pumps, PD pumps, seals and mechanical seals data*. From: [Http://www. Mcnallyinstitute.com/13-html/13-12.html](http://www.Mcnallyinstitute.com/13-html/13-12.html).

Ntamba Ntamba, B.M. 2011. Non-Newtonian Pressure Loss and Discharge Coefficients for Short Square-Edged Orifice. Unpublished MTech thesis. Cape Peninsula University of Technology, Cape Town, South Africa.

Palabiyik, I., Olunloyo, B., Fryer, P.J. & Robbins, P.T. 2014. Flow regimes in the emptying of pipes filled with a Herschel-Bulkley fluid. *Chemical Engineering Research and Design Journal*, 92(11): 2201-2212.

Patankar, N.A., Joseph, D.D., Wang, J., Barree, R.D., Conway, M. & Asadi, M. 2002. Power law correlations for sediment transport in pressure driven channel flows. *International Journal Multiphase Flows*, 28(8): 1269-1292.

Paterson, A. & Cooke, R. 1999. *The design of slurry pipeline systems*. Short course presented at the Cape Technikon, Cape Town.

Ramamurthi, K. & Nandakumar, K. 1999. Characteristics of Flow through Small Sharp-Edge Cylindrical Orifices. *Flow Measurement and Instrumentation*, 10(3): 133-143.

Rituraj, F. & Vacca, A. 2018. External gear pumps operating with non-Newtonian fluids: Modelling and experimental validation. *Mechanical Systems and Signal Processing*, 106(1): 284-302.

- Sahin, B. & Ceyhan, H. 1996. Numerical and experimental analysis of laminar flow through square-edged orifice with variable thickness. *Transactions of the Institute of Measurement and Control*, 18(4): 166-174.
- Salas-Valerio, W. F. & Steffe, J. F. 1990. Orifice Discharge Coefficient for Power Law fluids. *Journal of Food Processing Engineering*, 12(2): 89-98.
- Sandersoen, W. 1962. Flow through long orifices, B.Sc. thesis, Nottingham University.
- Sakri, F.M., Ali.M.S.M., Salim. S.Z.A.S. & Muhamad, S. 2017. Numerical simulation of liquids draining from a tank using Open FOAM. *Material Science and Engineering*, 81(1): 101–109.
- Slatter, P.T., 1994. Transitional and turbulent flow of non-Newtonian slurries in pipes; PhD Thesis; University of Cape Town. South Africa.
- Slatter, P T & Lazarus, J H 1993. Critical flow in slurry pipelines. Proceedings, Hydrotransport-12: *12th International Conference on Slurry Handling and Pipeline Transport*, Brugge, Belgium, pp. 639–654.
- Sochi.T. 2010. Flow of non-Newtonian fluids in porous media. *Journal of Polymer Science*, 51(22): 5007–5023.
- Spencer, R. 2013. Investigation of Discharge Behaviour from a Sharp-Edged Circular Orifice in Both Weir and Orifice Flow Regimes Using an Unsteady Experimental Procedure, Electronic Thesis and Dissertation University of Western Ontario. London.
- Swamee, P.K. & Swamee, N. 2010. Discharge equation of a circular sharp-crested orifice. *Journal of Hydraulic Research*, 48(1): 106–107.
- Tanner, R.I. 2002. *Engineering Rheology*. 2nd edition. Oxford University Press.
- Torrance, B. McK. 1963. Friction factors for turbulent non-Newtonian flow in circular pipes, *S. A. Mechanical Engineer*, 13 (4): 89-92.
- Torricelli, E. 1643. De motu gravium naturaliter accelerator. Firenze.
- Tunay, T. Sahin, B. & Akilli, H. 2004. Investigation of laminar and turbulent flow through an orifice plate inserted in a pipe. *Transactions of the Canadian Society for Mechanical Engineering*, 28(2B): 403-414.
- Tuğçe, Y. 2010. Scrutinization of flow characteristics through orifices. A Thesis submitted to the graduate school of applied sciences, Middle East Technical University.
- Upadhyay, A.K. 2012. *Fluid mechanics and Hydraulics*. S.K Kataria and Sons.
- White, D.E., Moggridge, G.D. & Wilson, D.I.

2008. Solid–liquid transitions in the rheology of a structured yeast extract paste, Marmite TM. *Journal of Food Engineering*, 88(3): 353-363.

Wilkes, J.O. 1999. *Fluid Mechanics for Chemical Engineers*. Prentice-Hall PTR, Upper Saddle River.

Woodford, C. 2018. *Forces and motion*. Cambridge University Press.

Appendices

Appendix A. Calibration certificate



**Revere
Transducers**

Calibration Certificate

We certify that the product described below conforms to all applicable published specifications. All calibration is traceable to the National Institute of Standards and Technology.

General Data

Model: 9363-D3-100KG-20P1-R
Serial Number: 62063259
Material: ALLOY STEEL

Capacity: 100KG
Excitation: 10 Vdc Nominal, 15 Vdc Max
Insulation Resistance : > 5G Ohm @ 50Vdc

Calibration Data

Full Scale Output: 3.249 m V/V
Zero Balance: $\pm 1\%$ FS
Input Resistance: $390 \pm 15 \Omega$
Output Resistance: $350 \pm 3.5 \Omega$

Combined Error: $\pm 0.02\%$ FS
Hysteresis: $\pm 0.02\%$ FS
Non-Repeatability: $\pm 0.01\%$ FS
Non linearity $\pm 0.02\%$ FS

Temp Effect on Zero: $<0.0008\%$ FS/ °F
Temp Effect on Span: $<0.001\%$ Load/ °F

Compensated Temp Range: 14°F to 104 °
Operating Temp: -65°F to 200 °F

Safe Overload: 150% of Rated Capacity
Ultimate Overload: 300% of Rated Capacity

Cable Length: 20ft

Class : D3

Electrical Connections

RED ——— + EXC
GRN ——— + SIGNAL
WHT ——— - SIGNAL
BLK ——— - EXC
BARE ——— SHIELD



CAUTION: Cutting cable will affect the Full Scale Output calibration.

Quality: A.Sakthivel
Specifications are subject to change without notice.
Date: 22/Jun/14



Vishay Precision Transducers India Private Limited
OZ-22, Sipcot Hi-Tech SEZ, Oragadam, Sriperumbudur – 602 105 Tamil Nadu India
Phone +91-44-3999 4000 Fax +91-44-3999 4002 www.vishaypg.com
Vishay Precision Groups Brands BLH • Celtron • Nobel • Revere • Sensortronics • TedeA-Huntleigh
Vishay is One of the World's Largest Manufacturer's of Discrete Semiconductors and Passive Components

Figure A.1 100 kg load cell calibration certificate



Calibration Certificate

We certify that the product described below conforms to all applicable published specifications. All calibration is traceable to the National Institute of Standards and Technology.

General Data

Model: 00363-250K-D3-00F
Serial Number: 79143755
Material: ALLOY STEEL

Capacity: 250KG
Excitation: 10 Vdc Nominal, 15 Vdc Max
Insulation Resistance :>2G Ohm @ 50Vdc

Calibration Data

Full Scale Output: 3.248 mV/V
Zero Balance: ± 1 % FS
Input Resistance: 390± 15 Ω
Output Resistance: 350± 3.5 Ω

Combined Error: ±0.03 % FS
Hysteresis : ±0.02 % FS
Non Repeatability: ±0.01 % FS
Non Linearity: ±0.03 % FS

Temp Effect on Zero: <0.0025% FS/ °F
Temp Effect on Span: <0.001% Load/ °F

Compensated Temp Range: 14°F to 104 °F
Operating Temp: -65°F to 200 °F

Safe Overload: 150% of Rated Capacity
Ultimate Overload: 300% of Rated Capacity

Cable Length : 20 FT

Class : D3

Electrical Connections

- RED ----- + INPUT
- GRN ----- + OUTPUT
- WHT ----- - OUTPUT
- BLK ----- - INPUT
- BARE ----- + SHIELD



CAUTION : Cutting cable will affect the full Scale Output calibration

Quality : A.Sakthivel
Specifications are subject to change without notice.
Date: 10.03.2017



Vishay Precision Transducers India Private Limited
OZ-22, Sipcot Hi-Tech SEZ, Oragadam, Sriperumbudur - 602 105, Tamilnadu, India
Phone : +91-44-3999 4000 Fax : +91-44-3999 4005 www.vishaypg.com

Vishay Precision Groups Brands BLH • Celtron • Nobel • Revere • Sensortronics • Tedea-Huntleigh
Vishay is One of the World's Largest Manufacturer's of Discrete Semiconductors and Passive Components

Figure A.2 250 kg load cell calibration certificate

Appendix B. Load cell specifications

Table B.7.1 Load cell specifications

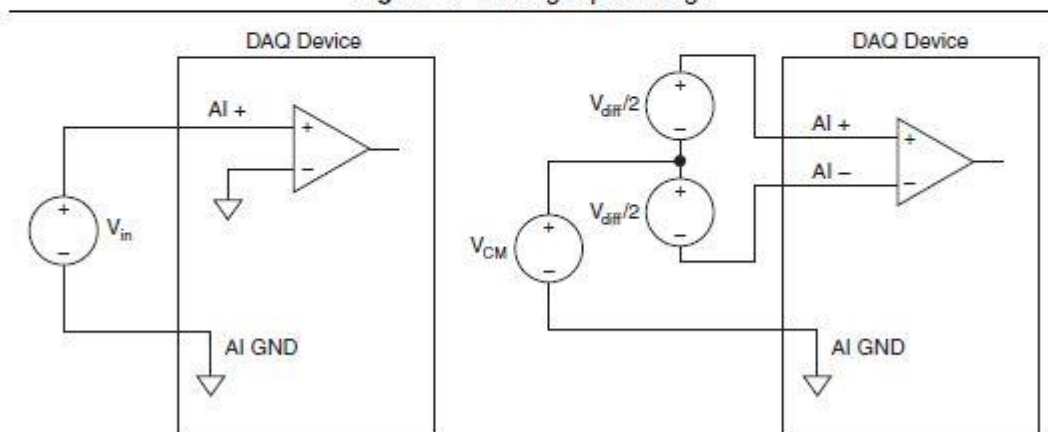
SPECIFICATIONS				
PARAMETER	VALUE			UNIT
Standard capacities (E_{max})	50, 100, 250, 500, 1000, 2500, 5000, 7500, 10000*			kg
Standard capacities (E_{max})	50, 75, 100, 150, 200, 250, 300, 500, 750, 1k, 1.5k, 2k, 3k, 5k, 10k, 15k, 20k			lbs
Accuracy class per OIML R-60 / NTEP	NTEP III L	Non-Approved	OIML C3	
Maximum no. of verification intervals (n)	10000	D3	3000	
Minimum verification intervals (V_{min})			$E_{max}/9000$	
Rated output (=FS)	3.0			mV/V
Rated output tolerance	0.0075			±mV/V
Zero balance	1.0			±% FSO
Combined error	0.0200	0.0300	0.0200	±% FSO
Non-repeatability	0.0100	0.0100	0.0100	±% FSO
Minimum dead load output return		0.0300	0.0165	±% applied load
Temp. effect on min. dead load output	(0.001)	(0.0015)	0.0140	±% FSO/5°C (°F)
Temperature effect on sensitivity	(0.0008)	(0.0008)	0.0055	±% applied load/5°C (°F)
Maximum safe overload	150			% E_{max}
Ultimate overload	250			% E_{max}
Excitation voltage	5 to 12			V
Maximum excitation voltage	15			V
Input resistance	390±15			Ω
Output resistance	350±3.5			Ω
Insulation resistance	≥5000			MΩ
Compensated temperature range	14 to +104°F	-10 to +40		°C
Operating temperature range	-65 to +200°F	-40 to +80		°C
Element material (DIN)	Stainless steel			
Sealing (DIN 40.050)	IP67			

Appendix C. Data acquisition voltage input range

Input Range

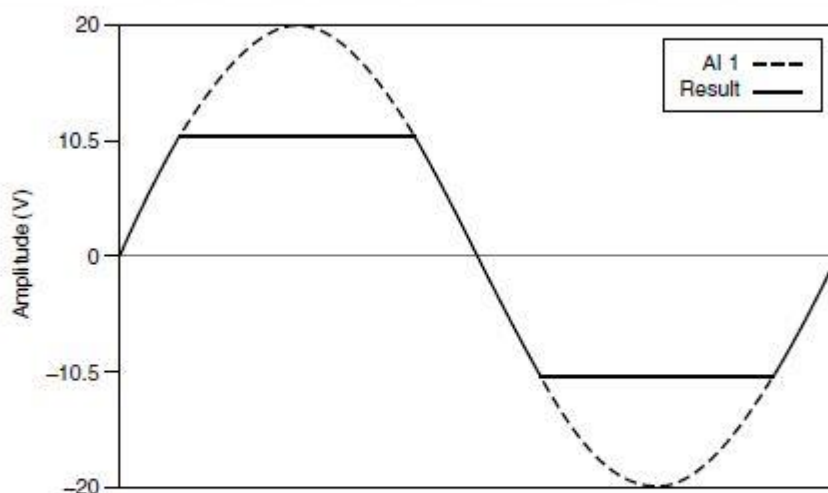
The NI DAQ device has an input range of ± 10 V. For differential mode, each AI should stay within ± 10 V with respect to AI GND, and the voltage between positive and negative inputs should be lower or equal to ± 10 V. For RSE mode, signals of ± 10 V at any analog input terminal with respect to AI GND are accurately measured.

Figure 9. Analog Input Range



Beyond ± 10 V, the input signal begins clipping as shown in Figure 10. Typically, this clipping begins at ± 10.5 V.

Figure 10. Exceeding ± 10 V on AI Returns Clipped Results



When no signals are connected to the analog input terminal, the input could be anywhere between $+10.5$ V and -10.5 V or may rail to ± 10.5 V. This behavior is normal and does not affect the measurement when a signal is connected. For more information about field and wiring noise considerations for analog signals, go to ni.com/info and enter Info Code `rdfwn3`.

Figure C.7.1 Voltage input range

Appendix D. NI USB 6001

1. Screw terminator connector plugs
2. Hi-Speed Micro USB Cable

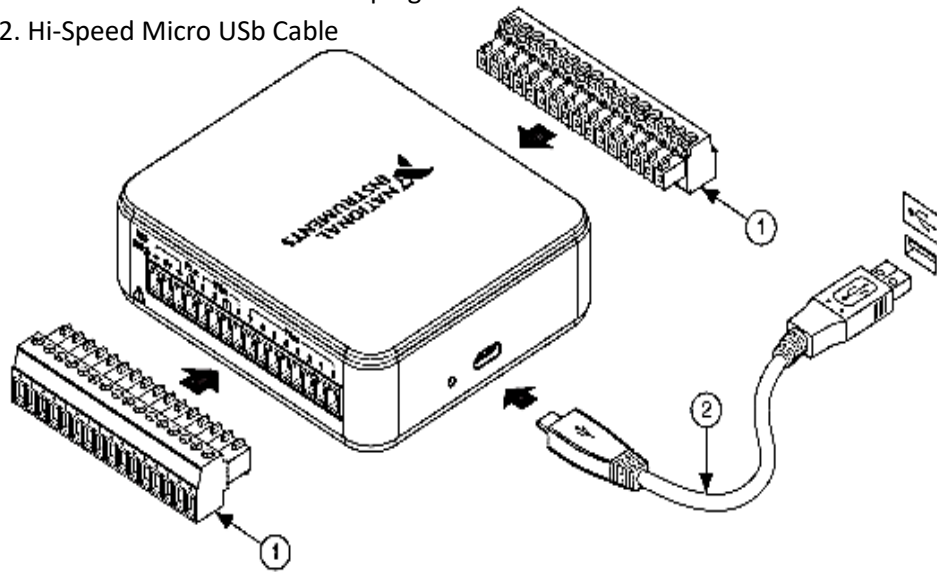


Figure 7.2 Data acquisition

Appendix E. Signal Description

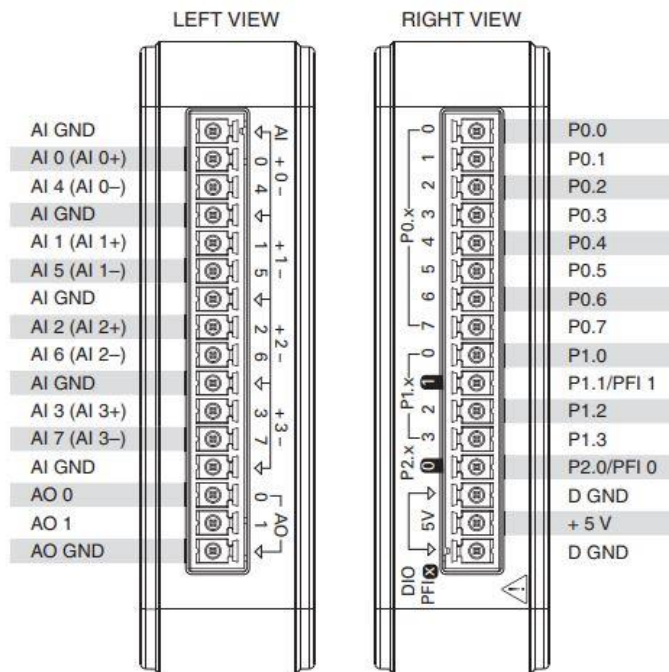


Figure E.1 Signal description

Appendix F. Orifice calibration results

Table F.1 Orifice calibration results for L/d of 0.05

Water	
Orifice d (m)	0.02
Orifice A (m ²)	3.142E-04
Tank A (m ²)	0.16
μ (Pa.s)	0.001
Density (kg/m ³)	1000
Gravity (m/s ²)	9.81

Time	Time difference	Mass of water in tank	Volume of water in tank	Height of water in tank	Height difference	Velocity in tank	Flow in tank	Velocity in orifice	C _d	Re
s	s	kg	m ³	m	m	m/s	m ³ /s	m/s		
2.075	0.000	86.570	8.657E-02	5.411E-01	0.000E+00	3.856E-03	6.170E-04	3.258	0.60	65163
14.575	12.500	79.030	7.903E-02	4.939E-01	4.712E-02	3.684E-03	5.894E-04	3.113	0.60	62261
27.075	25.000	71.852	7.185E-02	4.491E-01	9.199E-02	3.511E-03	5.618E-04	2.968	0.60	59366
39.575	37.500	65.010	6.501E-02	4.063E-01	1.347E-01	3.339E-03	5.342E-04	2.823	0.60	56469
52.075	50.000	58.490	5.849E-02	3.656E-01	1.755E-01	3.167E-03	5.067E-04	2.678	0.60	53562
64.575	62.500	52.320	5.232E-02	3.270E-01	2.141E-01	2.994E-03	4.791E-04	2.533	0.60	50659
77.075	75.000	46.509	4.651E-02	2.907E-01	2.504E-01	2.822E-03	4.515E-04	2.388	0.60	47763
89.575	87.500	41.032	4.103E-02	2.564E-01	2.846E-01	2.650E-03	4.239E-04	2.243	0.60	44862
102.075	100.000	35.895	3.589E-02	2.243E-01	3.167E-01	2.477E-03	3.964E-04	2.098	0.60	41960
114.575	112.500	31.142	3.114E-02	1.946E-01	3.464E-01	2.305E-03	3.688E-04	1.954	0.60	39083
127.075	125.000	26.679	2.668E-02	1.667E-01	3.743E-01	2.132E-03	3.412E-04	1.809	0.60	36175
139.575	137.500	22.606	2.261E-02	1.413E-01	3.998E-01	1.960E-03	3.136E-04	1.665	0.60	33299
152.075	150.000	18.836	1.884E-02	1.177E-01	4.233E-01	1.788E-03	2.860E-04	1.520	0.60	30395
164.575	162.500	15.444	1.544E-02	9.652E-02	4.445E-01	1.615E-03	2.585E-04	1.376	0.60	27523
177.075	175.000	12.393	1.239E-02	7.746E-02	4.636E-01	1.443E-03	2.309E-04	1.233	0.60	24655

Average C_d 0.60

Table F.2 Orifice calibration results for L/d of 1

Water	
Orifice d (m)	0.02
Orifice A (m ²)	3.142E-04
Tank A (m ²)	0.16
μ (Pa.s)	0.001
Density (kg/m ³)	1000
Gravity (m/s ²)	9.81

Time	Time difference	Mass of water in tank	Volume of water in tank	Height of water in tank	Height difference	Velocity in tank	Flow in tank	Velocity in orifice	C _d	Re
s	s	kg	m ³	m	m	m/s	m ³ /s	m/s		
0.825	0.000	86.682	8.67E-02	5.62E-01	0.00E+00	3.88E-03	6.21E-04	3.320	0.60	66398
10.825	10.000	80.579	8.06E-02	5.24E-01	3.81E-02	3.74E-03	5.99E-04	3.205	0.59	64104
20.825	20.000	74.709	7.47E-02	4.87E-01	7.48E-02	3.60E-03	5.77E-04	3.091	0.59	61818
30.825	30.000	69.069	6.91E-02	4.52E-01	1.10E-01	3.47E-03	5.55E-04	2.977	0.59	59538
40.825	40.000	63.623	6.36E-02	4.18E-01	1.44E-01	3.33E-03	5.33E-04	2.863	0.59	57251
50.825	50.000	58.405	5.84E-02	3.85E-01	1.77E-01	3.19E-03	5.11E-04	2.749	0.59	54970
60.825	60.000	53.403	5.34E-02	3.54E-01	2.08E-01	3.05E-03	4.89E-04	2.635	0.59	52691
70.825	70.000	48.622	4.86E-02	3.24E-01	2.38E-01	2.92E-03	4.67E-04	2.521	0.59	50417
80.825	80.000	44.083	4.41E-02	2.96E-01	2.66E-01	2.78E-03	4.45E-04	2.408	0.59	48159
90.825	90.000	39.740	3.97E-02	2.68E-01	2.93E-01	2.64E-03	4.23E-04	2.295	0.59	45893
100.825	100.000	35.626	3.56E-02	2.43E-01	3.19E-01	2.50E-03	4.01E-04	2.182	0.58	43640
110.825	110.000	31.715	3.17E-02	2.18E-01	3.44E-01	2.37E-03	3.79E-04	2.069	0.58	41383
120.825	120.000	28.030	2.80E-02	1.95E-01	3.67E-01	2.23E-03	3.57E-04	1.957	0.58	39138
130.825	130.000	24.586	2.46E-02	1.74E-01	3.88E-01	2.09E-03	3.35E-04	1.846	0.58	36918

Average C_d 0.59

Table F.3 Orifice calibration results for L/d of 3

Water	
Orifice d (m)	0.02
Orifice A (m ²)	3.142E-04
Tank A (m ²)	0.16
μ (Pa.s)	0.001
Density (kg/m ³)	1000
Gravity (m/s ²)	9.81

Time	Time difference	Mass of water in tank	Volume of water in tank	Height of water in tank	Height difference	Velocity in tank	Flow in tank	Velocity in orifice	C _d	Re
s	s	kg	m ³	m	m	m/s	m ³ /s	m/s		
0.825	0.000	87.900	8.790E-02	6.094E-01	0.000E+00	5.430E-03	8.688E-04	3.458	0.80	69155
9.158	8.333	80.808	8.081E-02	5.650E-01	4.432E-02	5.228E-03	8.364E-04	3.330	0.80	66592
17.492	16.667	73.983	7.398E-02	5.224E-01	8.698E-02	5.025E-03	8.041E-04	3.201	0.80	64029
25.825	25.000	67.398	6.740E-02	4.812E-01	1.281E-01	4.823E-03	7.717E-04	3.073	0.80	61455
34.158	33.333	61.111	6.111E-02	4.419E-01	1.674E-01	4.621E-03	7.393E-04	2.945	0.80	58893
42.492	41.667	55.081	5.508E-02	4.043E-01	2.051E-01	4.418E-03	7.069E-04	2.816	0.80	56326
50.825	50.000	49.328	4.933E-02	3.683E-01	2.411E-01	4.216E-03	6.746E-04	2.688	0.80	53762
59.158	58.333	43.834	4.383E-02	3.340E-01	2.754E-01	4.014E-03	6.422E-04	2.560	0.80	51195
67.492	66.667	38.621	3.862E-02	3.014E-01	3.080E-01	3.811E-03	6.098E-04	2.432	0.80	48634
75.825	75.000	33.667	3.367E-02	2.704E-01	3.390E-01	3.609E-03	5.774E-04	2.303	0.80	46068
84.159	83.334	29.011	2.901E-02	2.413E-01	3.681E-01	3.407E-03	5.451E-04	2.176	0.80	43519
92.492	91.667	24.613	2.461E-02	2.138E-01	3.955E-01	3.204E-03	5.127E-04	2.048	0.80	40965
100.825	100.000	20.446	2.045E-02	1.878E-01	4.216E-01	3.002E-03	4.803E-04	1.919	0.80	38390

Average C_d 0.80

Table F.4 Orifice calibration results for L/d of 5

Water	
Orifice d (m)	0.02
Orifice A (m ²)	3.142E-04
Tank A (m ²)	0.16
μ (Pa.s)	0.001
Density (kg/m ³)	1000
Gravity (m/s ²)	9.81

Time	Time difference	Mass of water in tank	Volume of water in tank	Height of water in tank	Height difference	Velocity in tank	Flow in tank	Velocity in orifice	C _d	Re
s	s	kg	m ³	m	m	m/s	m ³ /s	m/s		
0.825	0.000	84.561	8.456E-02	6.285E-01	0.000E+00	5.415E-03	8.665E-04	3.512	0.79	70232
9.992	9.167	76.749	7.675E-02	5.797E-01	4.882E-02	5.198E-03	8.316E-04	3.372	0.78	67449
19.158	18.333	69.281	6.928E-02	5.330E-01	9.550E-02	4.980E-03	7.968E-04	3.234	0.78	64676
28.325	27.500	62.135	6.213E-02	4.883E-01	1.402E-01	4.763E-03	7.620E-04	3.095	0.78	61907
37.492	36.667	55.304	5.530E-02	4.456E-01	1.829E-01	4.545E-03	7.272E-04	2.957	0.78	59139
46.658	45.833	48.792	4.879E-02	4.050E-01	2.236E-01	4.327E-03	6.924E-04	2.819	0.78	56374
55.825	55.000	42.636	4.264E-02	3.665E-01	2.620E-01	4.110E-03	6.576E-04	2.681	0.78	53629
64.992	64.167	36.781	3.678E-02	3.299E-01	2.986E-01	3.892E-03	6.227E-04	2.544	0.78	50882
74.158	73.333	31.252	3.125E-02	2.953E-01	3.332E-01	3.674E-03	5.879E-04	2.407	0.78	48143
83.325	82.500	25.987	2.599E-02	2.624E-01	3.661E-01	3.457E-03	5.531E-04	2.269	0.78	45381
92.492	91.667	21.065	2.107E-02	2.317E-01	3.968E-01	3.239E-03	5.183E-04	2.132	0.77	42639
101.659	100.834	16.465	1.646E-02	2.029E-01	4.256E-01	3.022E-03	4.835E-04	1.995	0.77	39905

Average C_d 0.78

Appendix G. Compatibility between load cell and camera

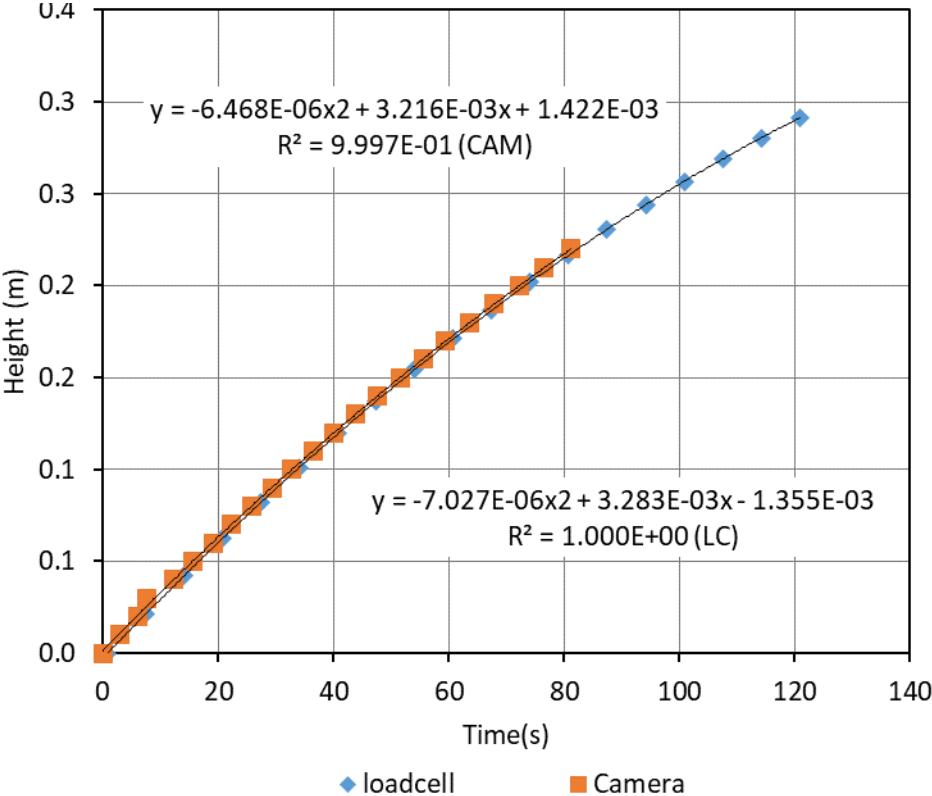


Figure G.1 Compatibility between load cell and camera for L/d=0

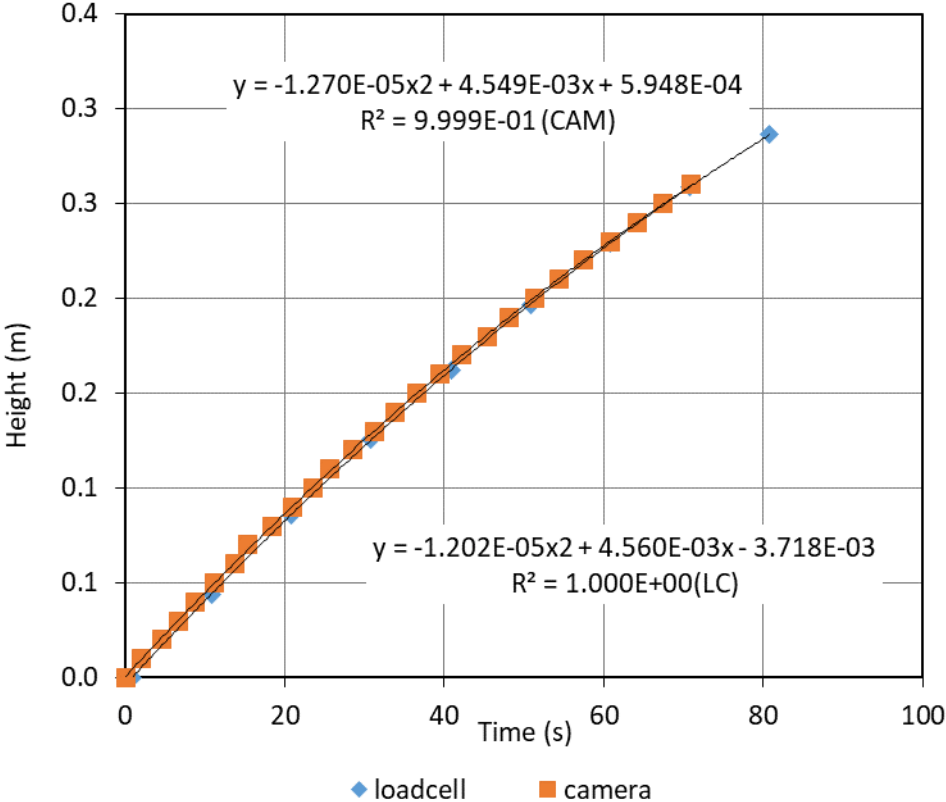


Figure G.2 Compatibility between load cell and camera for L/d=3

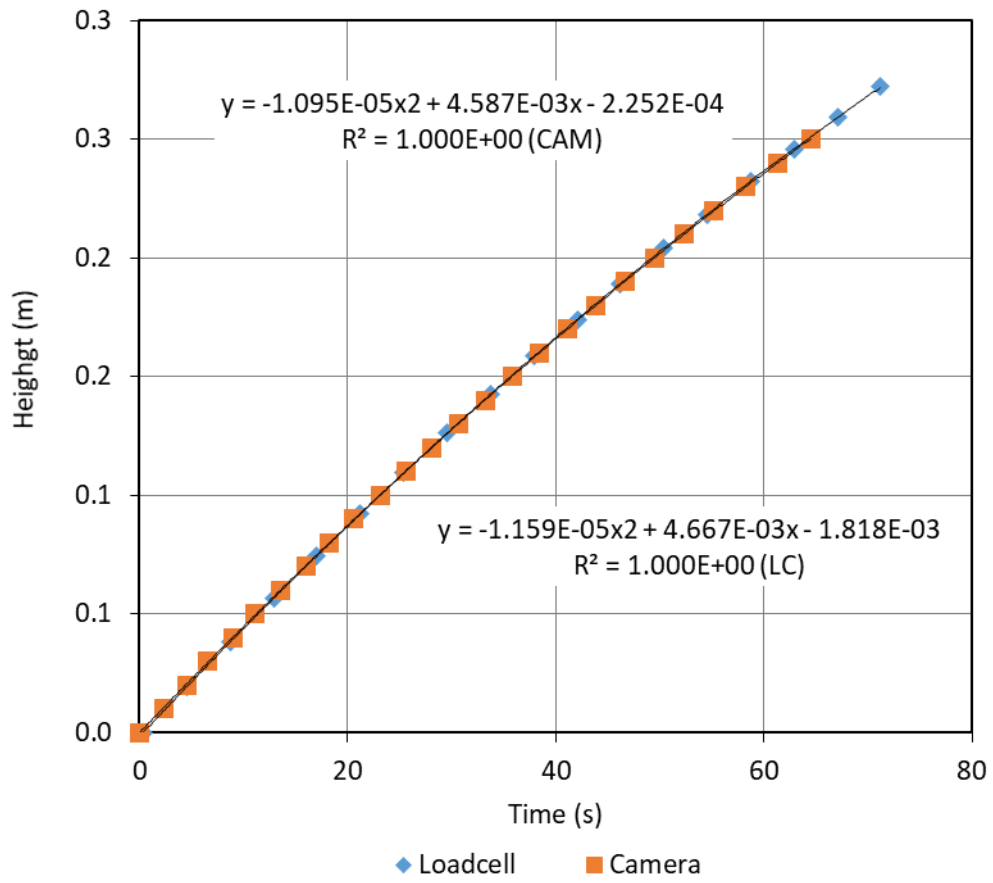


Figure G.3 Compatibility between load cell and camera for L/d=5

Appendix H. Rheometer measuring system data sheet

Measuring System Data Sheet Messsystem-Datenblatt

CC 27

Description

CC 27 with $\delta = 1,0847$ is a coaxial standard measuring system according to the ISO 3219 standard.

$$\gamma = \frac{1}{10} \cdot \frac{1 + \delta^2}{\delta^2 - 1} \cdot \varphi ; \quad \delta = \frac{r_e}{r_i} = 1.0847$$

$$\dot{\gamma}_{rep} = \frac{\pi \cdot n}{30} \cdot \frac{1 + \delta^2}{\delta^2 - 1} ; \quad \omega = \frac{2\pi}{60} \cdot n$$

Variable

τ ...shear stress
 M ...torque
 γ ...strain
 φ ...deflection angle
 $\dot{\gamma}$...shear rate
 n ...speed
 δ ...radius ratio
 r_i / r_e ...internal/external cylinder radius
 ω ...angular velocity
 C_L ...end effect correction factor

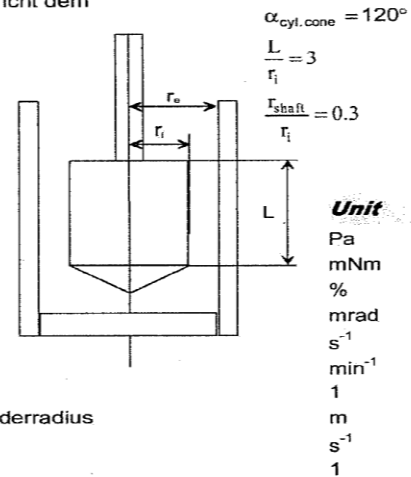
Beschreibung

Das koaxiale Standard-Zylindermesssystem CC 27 mit $\delta = 1,0847$ entspricht dem ISO 3219 Standard.

$$\tau_{rep} = \frac{1 + \delta^2}{2000 \cdot \delta^2} \cdot \frac{M}{2\pi L \cdot r_i^2 \cdot C_L}$$

Variable

τ ...Schubspannung
 M ...Moment
 γ ...Deformation
 φ ...Auslenkwinkel
 $\dot{\gamma}$...Scherrate
 n ...Geschwindigkeit
 δ ...Radienverhältnis
 r_i / r_e ...innerer/äußerer Zylinderradius
 ω ...Winkelgeschwindigkeit
 C_L ...Stirnflächen-Faktor



Dimensions

Dimensions	Abmessungen	
Measuring Bob Radius r_i	Radius Messkörper r_i	13.33 mm
Measuring Cup Radius r_e	Radius Messbecher r_e	14.46 mm
Ratio of Radii ⁽²⁾ δ	Radienverhältnis ⁽²⁾ δ	1.0847
Gap Length L	Länge Messspalt L	40.00 mm
Cone Angle	Kegelwinkel	120 °
Measuring Gap ⁽²⁾	Messspalt ⁽²⁾	1.13 mm
End Effect Correction Factor ⁽⁴⁾ C_L	Stirnflächen-Faktor ⁽⁴⁾ C_L	1.10

Geometry Data

Geometry Data	Geometriedaten	
Active Length	Aktive Länge	119.2 mm
Check Length	Prüflänge	119.2 mm
Length for ISO Position	Länge für ISO-Position	71.5 mm
Sample Volume ⁽²⁾	Probenmenge ⁽²⁾	19.35 ml

Conversion Factors

Conversion Factors	Umrechnungsfaktoren	
Conversion Factor C_{SS} ⁽¹⁾⁽²⁾	Umrechnungsfaktor C_{SS} ⁽¹⁾⁽²⁾	18.8297 Pa / mNm
Conversion Factor C_{SR} ⁽²⁾	Umrechnungsfaktor C_{SR} ⁽²⁾	1.2910 s^{-1} / min^{-1}

(1) Conversion Factor C_{SS} for US200>V2.00

(2) Calculated Values

(1) Umrechnungsfaktor C_{SS} für US200>V2.00

(2) berechnete Werte

PHYSICA Messtechnik GmbH
 Vor dem Lauch 6 - D 70567 STUTTGART
 GERMANY - EUROPE

<http://www.physica.de>
<mailto:info@physica.anton-paar.com>
 Phone +49 711 72091-0
 Fax +49 711 72091-30

File:
 CC27.xls
 Revision: 13.11.2000

Figure H.1 CC27 measuring data sheet

Appendix I. Flow rate measurements using aspect ratio of 0.05

Table I.1 100% glycerine flow measurement results

100% Glycerine	
Orifice d (m)	0.02
Orifice A (m ²)	3.142E-04
Tank A (m ²)	0.16
μ (Pa.s)	0.970
Density (kg/m ³)	1258
Gravity (m/s ²)	9.81

Time	Time difference	Mass of glycerine in tank	Volume of glycerine in tank	Height of glycerine in tank	Height difference	Velocity in tank	Flow in tank	Velocity in orifice	C _d	Re
s	s	kg	m ³	m	m	m/s	m ³ /s	m/s		
0.825	0.000	36.318	2.887E-02	1.804E-01	0.000E+00	2.119E-03	3.390E-04	1.882	0.57	49
9.158	8.333	32.831	2.610E-02	1.631E-01	1.732E-02	2.004E-03	3.207E-04	1.789	0.57	46
17.492	16.667	29.544	2.349E-02	1.468E-01	3.365E-02	1.889E-03	3.023E-04	1.697	0.57	44
25.825	25.000	26.475	2.105E-02	1.315E-01	4.890E-02	1.775E-03	2.840E-04	1.606	0.56	42
34.158	33.333	23.591	1.875E-02	1.172E-01	6.323E-02	1.660E-03	2.656E-04	1.516	0.56	39
42.492	41.667	20.917	1.663E-02	1.039E-01	7.652E-02	1.545E-03	2.472E-04	1.428	0.55	37
50.825	50.000	18.431	1.465E-02	9.157E-02	8.887E-02	1.430E-03	2.289E-04	1.340	0.54	35
59.158	58.333	16.141	1.283E-02	8.019E-02	1.002E-01	1.316E-03	2.105E-04	1.254	0.53	33
67.492	66.667	14.044	1.116E-02	6.977E-02	1.107E-01	1.201E-03	1.922E-04	1.170	0.52	30
75.825	75.000	12.124	9.638E-03	6.024E-02	1.202E-01	1.086E-03	1.738E-04	1.087	0.51	28
84.159	83.334	10.371	8.244E-03	5.152E-02	1.289E-01	9.715E-04	1.554E-04	1.005	0.49	26
92.492	91.667	8.805	7.000E-03	4.375E-02	1.367E-01	8.567E-04	1.371E-04	0.926	0.47	24

Table I.2 96% glycerine flow measurement results

96 % Glycerine	
Orifice d (m)	0.02
Orifice A (m ²)	3.142E-04
Tank A (m ²)	0.16
μ (Pa.s)	0.304
Density (kg/m ³)	1248
Gravity (m/s ²)	9.81

Time	Time difference	Mass of glycerine in tank	Volume of glycerine in tank	Height of glycerine in tank	Height difference	Velocity in tank	Flow in tank	Velocity in orifice	C _d	Re
s	s	kg	m ³	m	m	m/s	m ³ /s	m/s		
0.825	0.000	33.621	2.694E-02	1.684E-01	0.000E+00	2.354E-03	3.766E-04	1.818	0.66	149
5.825	5.000	31.332	2.511E-02	1.569E-01	1.146E-02	2.269E-03	3.630E-04	1.755	0.66	144
10.825	10.000	29.087	2.331E-02	1.457E-01	2.271E-02	2.183E-03	3.493E-04	1.691	0.66	139
15.825	15.000	26.944	2.159E-02	1.349E-01	3.344E-02	2.098E-03	3.357E-04	1.627	0.66	134
20.825	20.000	24.913	1.996E-02	1.248E-01	4.361E-02	2.012E-03	3.220E-04	1.565	0.66	128
25.825	25.000	22.922	1.837E-02	1.148E-01	5.358E-02	1.927E-03	3.083E-04	1.501	0.65	123
30.825	30.000	21.066	1.688E-02	1.055E-01	6.288E-02	1.842E-03	2.947E-04	1.439	0.65	118
35.825	35.000	19.259	1.543E-02	9.645E-02	7.192E-02	1.756E-03	2.810E-04	1.376	0.65	113
40.825	40.000	17.538	1.405E-02	8.783E-02	8.055E-02	1.671E-03	2.673E-04	1.313	0.65	108
45.825	45.000	15.947	1.278E-02	7.986E-02	8.851E-02	1.585E-03	2.537E-04	1.252	0.65	103
50.825	50.000	14.382	1.152E-02	7.203E-02	9.635E-02	1.500E-03	2.400E-04	1.189	0.64	98
55.825	55.000	12.919	1.035E-02	6.470E-02	1.037E-01	1.415E-03	2.264E-04	1.127	0.64	93
60.825	60.000	11.557	9.260E-03	5.788E-02	1.105E-01	1.329E-03	2.127E-04	1.066	0.64	87

Table I.3 93% glycerine flow measurement results

93 % glycerine	
Orifice d (m)	0.02
Orifice A (m ²)	3.142E-04
Tank A (m ²)	0.16
μ (Pa.s)	0.130
Density (kg/m ³)	1242
Gravity (m/s ²)	9.81

Time	Time difference	Mass of glycerine in tank	Volume of glycerine in tank	Height of glycerine in tank	Height difference	Velocity in tank	Flow in tank	Velocity in orifice	C _d	Re
s		kg	m ³	m	m	m/s	m ³ /s			
0.408	0.000	33.472	2.695E-02	1.684E-01	0.000E+00	2.371E-03	3.794E-04	1.818	0.66	347
5.408	5.000	31.173	2.510E-02	1.569E-01	1.157E-02	2.287E-03	3.659E-04	1.754	0.66	335
10.408	10.000	28.932	2.329E-02	1.456E-01	2.285E-02	2.203E-03	3.525E-04	1.690	0.66	323
15.408	15.000	26.804	2.158E-02	1.349E-01	3.356E-02	2.119E-03	3.391E-04	1.627	0.66	311
20.408	20.000	24.724	1.991E-02	1.244E-01	4.402E-02	2.036E-03	3.257E-04	1.562	0.66	299
25.408	25.000	22.723	1.830E-02	1.143E-01	5.409E-02	1.952E-03	3.123E-04	1.498	0.66	286
30.408	30.000	20.833	1.677E-02	1.048E-01	6.360E-02	1.868E-03	2.988E-04	1.434	0.66	274
35.408	35.000	19.003	1.530E-02	9.563E-02	7.281E-02	1.784E-03	2.854E-04	1.370	0.66	262
40.408	40.000	17.296	1.393E-02	8.704E-02	8.140E-02	1.700E-03	2.720E-04	1.307	0.66	250
45.408	45.000	15.684	1.263E-02	7.893E-02	8.951E-02	1.616E-03	2.586E-04	1.244	0.66	238
50.408	50.000	14.092	1.135E-02	7.091E-02	9.753E-02	1.532E-03	2.452E-04	1.180	0.66	225
55.408	55.000	12.580	1.013E-02	6.331E-02	1.051E-01	1.448E-03	2.317E-04	1.114	0.66	213

Table I.4 65% glycerine flow measurement results

65 % glycerine	
Orifice d (m)	0.02
Orifice A (m ²)	3.142E-04
Tank A (m ²)	0.16
μ (Pa.s)	0.019
Density (kg/m ³)	1179
Gravity (m/s ²)	9.81

Time	Time difference	Mass of glycerine in tank	Volume of glycerine in tank	Height of glycerine in tank	Height difference	Velocity in tank	Flow in tank	Velocity in orifice	C _d	Re
s	s	kg	m ³	m	m	m/s	m ³ /s	m/s		
0.825	0.000	56.355	4.780E-02	2.987E-01	0.000E+00	2.947E-03	4.715E-04	2.421	0.62	3005
9.158	8.333	51.820	4.395E-02	2.747E-01	2.404E-02	2.828E-03	4.524E-04	2.322	0.62	2881
17.492	16.667	47.477	4.027E-02	2.517E-01	4.706E-02	2.708E-03	4.334E-04	2.222	0.62	2758
25.825	25.000	43.313	3.674E-02	2.296E-01	6.914E-02	2.589E-03	4.143E-04	2.122	0.62	2634
34.158	33.333	39.325	3.335E-02	2.085E-01	9.028E-02	2.470E-03	3.952E-04	2.022	0.62	2510
42.492	41.667	35.539	3.014E-02	1.884E-01	1.103E-01	2.351E-03	3.761E-04	1.923	0.62	2386
50.825	50.000	31.940	2.709E-02	1.693E-01	1.294E-01	2.231E-03	3.570E-04	1.823	0.62	2262
59.158	58.333	28.531	2.420E-02	1.512E-01	1.475E-01	2.112E-03	3.380E-04	1.723	0.62	2138
67.492	66.667	25.303	2.146E-02	1.341E-01	1.646E-01	1.993E-03	3.189E-04	1.622	0.63	2013
75.825	75.000	22.270	1.889E-02	1.181E-01	1.807E-01	1.874E-03	2.998E-04	1.522	0.63	1889
84.159	83.334	19.410	1.646E-02	1.029E-01	1.958E-01	1.754E-03	2.807E-04	1.421	0.63	1763

Table I.5 2.4% CMC flow measurement results

2.4 % CMC	
Orifice d (m)	0.02
Orifice A (m ²)	3.142E-04
Tank A (m ²)	0.16
Density (kg/m ³)	1014
Gravity (m/s ²)	9.81
k (Pa.s ⁿ)	0.010
n (-)	1

Time	Time difference	Mass of CMC in tank	Volume of CMC in tank	Height of CMC in tank	Height difference	Velocity in tank	Flow in tank	Velocity in orifice	C _d	Re
s	s	kg	m ³	m	m	m/s	m ³ /s	m/s		
0.825	0.000	85.523	8.434E-02	5.271E-01	0.000E+00	3.833E-03	0.000E+00	3.216	0.61	6522
9.992	9.167	79.928	7.882E-02	4.927E-01	3.449E-02	3.705E-03	5.927E-04	3.109	0.61	6305
19.158	18.333	74.522	7.349E-02	4.593E-01	6.781E-02	3.576E-03	5.722E-04	3.002	0.61	6088
28.325	27.500	69.292	6.834E-02	4.271E-01	1.000E-01	3.448E-03	5.516E-04	2.895	0.61	5871
37.492	36.667	64.249	6.336E-02	3.960E-01	1.311E-01	3.319E-03	5.311E-04	2.787	0.61	5653
46.658	45.833	59.426	5.861E-02	3.663E-01	1.609E-01	3.191E-03	5.105E-04	2.681	0.61	5437
55.825	55.000	54.766	5.401E-02	3.376E-01	1.896E-01	3.062E-03	4.900E-04	2.574	0.61	5219
64.992	64.167	50.300	4.961E-02	3.100E-01	2.171E-01	2.934E-03	4.694E-04	2.466	0.61	5002
74.158	73.333	46.047	4.541E-02	2.838E-01	2.433E-01	2.806E-03	4.489E-04	2.360	0.61	4786
83.325	82.500	41.960	4.138E-02	2.586E-01	2.685E-01	2.677E-03	4.283E-04	2.253	0.61	4568
92.492	91.667	38.068	3.754E-02	2.346E-01	2.925E-01	2.549E-03	4.078E-04	2.146	0.60	4351
101.659	100.834	34.366	3.389E-02	2.118E-01	3.153E-01	2.420E-03	3.873E-04	2.039	0.60	4134
110.825	110.000	30.846	3.042E-02	1.901E-01	3.370E-01	2.292E-03	3.667E-04	1.931	0.60	3917
119.992	119.167	27.531	2.715E-02	1.697E-01	3.574E-01	2.163E-03	3.462E-04	1.825	0.60	3700
129.159	128.334	24.459	2.412E-02	1.508E-01	3.764E-01	2.035E-03	3.256E-04	1.720	0.60	3488
138.325	137.500	21.524	2.123E-02	1.327E-01	3.945E-01	1.907E-03	3.051E-04	1.613	0.60	3272
147.492	146.667	18.752	1.849E-02	1.156E-01	4.116E-01	1.778E-03	2.845E-04	1.506	0.60	3054

Table I.6 5.2% CMC flow measurement results

5.2 % CMC	
Orifice d (m)	0.02
Orifice A (m ²)	3.142E-04
Tank A (m ²)	0.16
Density (kg/m ³)	1029
Gravity (m/s ²)	9.81
k (Pa.s ⁿ)	0.210
n (-)	0.790

Time	Time difference	Mass of CMC in tank	Volume of CMC in tank	Height of CMC in tank	Height difference	Velocity in tank	Flow in tank	Velocity in orifice	C _d	Re
s	s	kg	m ³	m	m	m/s	m ³ /s	m/s		
0.408	0.000	57.509	5.589E-02	3.493E-01	0.000E+00	3.246E-03	5.194E-04	2.618	0.63	1050
8.742	8.333	53.124	5.163E-02	3.227E-01	2.664E-02	3.129E-03	5.006E-04	2.516	0.63	1001
17.075	16.667	48.908	4.753E-02	2.971E-01	5.224E-02	3.011E-03	4.818E-04	2.414	0.64	952
25.408	25.000	44.832	4.357E-02	2.723E-01	7.700E-02	2.894E-03	4.630E-04	2.311	0.64	903
33.742	33.333	40.978	3.982E-02	2.489E-01	1.004E-01	2.777E-03	4.443E-04	2.210	0.64	856
42.075	41.667	37.244	3.619E-02	2.262E-01	1.231E-01	2.659E-03	4.255E-04	2.107	0.64	808
50.408	50.000	33.679	3.273E-02	2.046E-01	1.447E-01	2.542E-03	4.067E-04	2.003	0.65	760
58.742	58.333	30.246	2.939E-02	1.837E-01	1.656E-01	2.425E-03	3.879E-04	1.899	0.65	712
67.075	66.667	27.027	2.627E-02	1.642E-01	1.851E-01	2.307E-03	3.692E-04	1.795	0.65	665
75.408	75.000	23.925	2.325E-02	1.453E-01	2.040E-01	2.190E-03	3.504E-04	1.689	0.66	618
83.742	83.334	20.991	2.040E-02	1.275E-01	2.218E-01	2.073E-03	3.316E-04	1.582	0.67	571
92.075	91.667	18.238	1.772E-02	1.108E-01	2.385E-01	1.955E-03	3.129E-04	1.474	0.68	524

Table I.7 6.6% CMC flow measurement results

6.6 % CMC	
Orifice d (m)	0.02
Orifice A (m ²)	3.142E-04
Tank A (m ²)	0.16
Density (kg/m ³)	1037
Gravity (m/s ²)	9.81
k (Pa.s ⁿ)	0.880
n (-)	0.700

Time	Time difference	Mass of CMC in tank	Volume of CMC in tank	Height of CMC in tank	Height difference	Velocity in tank	Flow in tank	Velocity in orifice	C _d	Re
s	s	kg	m ³	m	m	m/s	m ³ /s	m/s		
0.825	0.000	49.196	4.744E-02	2.965E-01	0.000E+00	3.167E-03	5.067E-04	2.412	0.67	416
7.492	6.667	45.745	4.411E-02	2.757E-01	2.080E-02	3.051E-03	4.882E-04	2.326	0.67	397
14.158	13.333	42.443	4.093E-02	2.558E-01	4.070E-02	2.936E-03	4.697E-04	2.240	0.67	378
20.825	20.000	39.299	3.790E-02	2.369E-01	5.965E-02	2.820E-03	4.512E-04	2.156	0.67	359
27.492	26.667	36.218	3.493E-02	2.183E-01	7.822E-02	2.704E-03	4.327E-04	2.069	0.67	341
34.158	33.333	33.272	3.208E-02	2.005E-01	9.598E-02	2.588E-03	4.142E-04	1.984	0.66	323
40.825	40.000	30.461	2.937E-02	1.836E-01	1.129E-01	2.473E-03	3.956E-04	1.898	0.66	305
47.492	46.667	27.792	2.680E-02	1.675E-01	1.290E-01	2.357E-03	3.771E-04	1.813	0.66	287
54.158	53.333	25.265	2.436E-02	1.523E-01	1.442E-01	2.241E-03	3.586E-04	1.728	0.66	270
60.825	60.000	22.858	2.204E-02	1.378E-01	1.587E-01	2.126E-03	3.401E-04	1.644	0.66	253
67.492	66.667	20.582	1.985E-02	1.240E-01	1.725E-01	2.010E-03	3.216E-04	1.560	0.66	236
74.158	73.333	18.396	1.774E-02	1.109E-01	1.856E-01	1.894E-03	3.031E-04	1.475	0.65	219
80.825	80.000	16.367	1.578E-02	9.865E-02	1.979E-01	1.779E-03	2.846E-04	1.391	0.65	203

Table I.8 7.6% CMC flow measurements result

7.6 % CMC	
Orifice d (m)	0.02
Orifice A (m ²)	3.142E-04
Tank A (m ²)	0.16
Density (kg/m ³)	1043
Gravity (m/s ²)	9.81
k (Pa.s ⁿ)	2.390
n (-)	0.640

Time	Time difference	Mass of CMC in tank	Volume of CMC in tank	Height of CMC in tank	Height difference	Velocity in tank	Flow in tank	Velocity in orifice	C _d	Re
s	s	kg	m ³	m	m	m/s	m ³ /s	m/s		
0.825	0.000	45.339	4.347E-02	2.717E-01	0.000E+00	2.918E-03	4.669E-04	2.309	0.64	216
9.158	8.333	41.378	3.967E-02	2.479E-01	2.374E-02	2.772E-03	4.435E-04	2.206	0.64	203
17.492	16.667	37.623	3.607E-02	2.254E-01	4.624E-02	2.625E-03	4.201E-04	2.103	0.64	191
25.825	25.000	34.109	3.270E-02	2.044E-01	6.729E-02	2.479E-03	3.967E-04	2.003	0.63	178
34.158	33.333	30.743	2.948E-02	1.842E-01	8.746E-02	2.333E-03	3.733E-04	1.901	0.62	166
42.492	41.667	27.594	2.646E-02	1.654E-01	1.063E-01	2.187E-03	3.499E-04	1.801	0.62	154
50.825	50.000	24.667	2.365E-02	1.478E-01	1.239E-01	2.040E-03	3.265E-04	1.703	0.61	143
59.158	58.333	21.938	2.103E-02	1.315E-01	1.402E-01	1.894E-03	3.031E-04	1.606	0.60	132
67.492	66.667	19.420	1.862E-02	1.164E-01	1.553E-01	1.748E-03	2.797E-04	1.511	0.59	122
75.825	75.000	17.085	1.638E-02	1.024E-01	1.693E-01	1.602E-03	2.563E-04	1.417	0.58	111
84.159	83.334	14.963	1.435E-02	8.966E-02	1.820E-01	1.455E-03	2.329E-04	1.326	0.56	102
92.492	91.667	13.048	1.251E-02	7.819E-02	1.935E-01	1.309E-03	2.095E-04	1.239	0.54	93
100.825	100.000	11.313	1.085E-02	6.779E-02	2.039E-01	1.163E-03	1.860E-04	1.153	0.51	84

Table I.9 13.1% kaolin flow measurement results

13.1 % Kaolin	
Orifice d (m)	0.02
Orifice A (m ²)	3.142E-04
Tank A (m ²)	0.16
Density (kg/m ³)	1217
Gravity (m/s ²)	9.81
τ (Pa)	8.900
k(Pa.s ⁿ)	0.070
n (-)	0.720

Time	Time difference	Mass of Kaolin in tank	Volume of Kaolin in tank	Height of Kaolin in tank	Height difference	Velocity in tank	Flow in tank	Velocity in orifice	C _d	Re
s	s	kg	m ³	m	m	m/s	m ³ /s	m/s		
0.408	0.000	57.621	4.735E-02	2.959E-01	0.000E+00	2.952E-03	4.723E-04	2.410	0.62	3014
7.908	7.500	53.406	4.388E-02	2.743E-01	2.164E-02	2.845E-03	4.552E-04	2.320	0.62	2834
15.408	15.000	49.313	4.052E-02	2.532E-01	4.267E-02	2.738E-03	4.382E-04	2.229	0.63	2656
22.908	22.500	45.381	3.729E-02	2.331E-01	6.286E-02	2.632E-03	4.211E-04	2.138	0.63	2481
30.408	30.000	41.639	3.421E-02	2.138E-01	8.208E-02	2.525E-03	4.040E-04	2.048	0.63	2312
37.908	37.500	38.065	3.128E-02	1.955E-01	1.004E-01	2.418E-03	3.869E-04	1.958	0.63	2148
45.408	45.000	34.539	2.838E-02	1.774E-01	1.185E-01	2.311E-03	3.698E-04	1.866	0.63	1982
52.908	52.500	31.254	2.568E-02	1.605E-01	1.354E-01	2.205E-03	3.527E-04	1.775	0.63	1824
60.408	60.000	28.138	2.312E-02	1.445E-01	1.514E-01	2.098E-03	3.357E-04	1.684	0.63	1672
67.908	67.500	25.133	2.065E-02	1.291E-01	1.668E-01	1.991E-03	3.186E-04	1.591	0.64	1521
75.408	75.000	22.322	1.834E-02	1.146E-01	1.813E-01	1.884E-03	3.015E-04	1.500	0.64	1377
82.908	82.500	19.640	1.614E-02	1.009E-01	1.951E-01	1.778E-03	2.844E-04	1.407	0.64	1236

Table I.10 20.4% kaolin flow measurement results

20.4 % Kaolin	
Orifice d (m)	0.02
Orifice A (m ²)	3.142E-04
Tank A (m ²)	0.16
Density (Kg/m ³)	1336
Gravity (m/s ²)	9.81
τ (Pa)	39.42
k(Pa.s ⁿ)	3.960
n (-)	0.360

Time	Time difference	Mass of Kaolin in tank	Volume of Kaolin in Tank	Height of Kaolin in tank	Height difference	Velocity in tank	Flow in tank	Velocity in orifice	C _d	Re
s	s	kg	m ³	m	m	m/s	m ³ /s	m/s		
5.825	0.000	59.443	4.449E-02	2.781E-01	0.000E+00	2.930E-03	4.688E-04	2.336	0.64	679
10.825	5.000	56.409	4.222E-02	2.639E-01	1.419E-02	2.845E-03	4.552E-04	2.275	0.64	648
15.825	10.000	53.432	3.999E-02	2.500E-01	2.812E-02	2.760E-03	4.416E-04	2.215	0.63	617
20.825	15.000	50.515	3.781E-02	2.363E-01	4.176E-02	2.675E-03	4.279E-04	2.153	0.63	586
25.825	20.000	47.717	3.572E-02	2.232E-01	5.485E-02	2.589E-03	4.143E-04	2.093	0.63	557
30.825	25.000	44.984	3.367E-02	2.104E-01	6.764E-02	2.504E-03	4.007E-04	2.032	0.63	528
35.825	30.000	42.359	3.171E-02	1.982E-01	7.992E-02	2.419E-03	3.871E-04	1.972	0.62	500
40.825	35.000	39.812	2.980E-02	1.862E-01	9.184E-02	2.334E-03	3.735E-04	1.912	0.62	473
45.825	40.000	37.346	2.795E-02	1.747E-01	1.034E-01	2.249E-03	3.598E-04	1.851	0.62	446
50.825	45.000	34.998	2.620E-02	1.637E-01	1.144E-01	2.164E-03	3.462E-04	1.792	0.61	420
55.825	50.000	32.733	2.450E-02	1.531E-01	1.250E-01	2.079E-03	3.326E-04	1.733	0.61	396
60.825	55.000	30.538	2.286E-02	1.429E-01	1.352E-01	1.994E-03	3.190E-04	1.674	0.61	372
65.825	60.000	28.466	2.131E-02	1.332E-01	1.449E-01	1.908E-03	3.054E-04	1.616	0.60	349
70.825	65.000	26.458	1.980E-02	1.238E-01	1.543E-01	1.823E-03	2.917E-04	1.558	0.60	326
75.825	70.000	24.574	1.839E-02	1.150E-01	1.631E-01	1.738E-03	2.781E-04	1.502	0.59	305
80.825	75.000	22.780	1.705E-02	1.066E-01	1.715E-01	1.653E-03	2.645E-04	1.446	0.58	285
85.825	80.000	21.078	1.578E-02	9.861E-02	1.795E-01	1.568E-03	2.509E-04	1.391	0.57	265

Table I.11 7.2% bentonite flow measurement results

7.2 % Bentonite	
Orifice d (m)	0.02
Orifice A (m ²)	3.142E-04
Tank A (m ²)	0.16
Density (kg/m ³)	1044
Gravity (m/s ²)	9.81
τ (Pa)	15.738
k(Pa.s ⁿ)	0.014
n (-)	1

Time	Time difference	Mass of Bentonite in tank	Volume of Bentonite in Tank	Height of bentonite in tank	Height difference	Velocity in Tank	Flow in Tank	Velocity in orifice	C _d	Re
s	s	kg	m ³	m	m	m/s	m ³ /s	m/s		
0.408	0.000	59.874	5.735E-02	3.584E-01	0.000E+00	3.286E-03	5.258E-04	2.652	0.63	1936
5.408	5.000	57.224	5.481E-02	3.426E-01	1.587E-02	3.212E-03	5.140E-04	2.593	0.63	1871
10.408	10.000	54.604	5.230E-02	3.269E-01	3.155E-02	3.138E-03	5.022E-04	2.533	0.63	1805
15.408	15.000	52.034	4.984E-02	3.115E-01	4.694E-02	3.065E-03	4.904E-04	2.472	0.63	1739
20.408	20.000	49.495	4.741E-02	2.963E-01	6.214E-02	2.991E-03	4.786E-04	2.411	0.63	1674
25.408	25.000	47.056	4.507E-02	2.817E-01	7.674E-02	2.917E-03	4.668E-04	2.351	0.63	1610
30.408	30.000	44.665	4.278E-02	2.674E-01	9.106E-02	2.843E-03	4.549E-04	2.290	0.63	1546
35.408	35.000	42.303	4.052E-02	2.533E-01	1.052E-01	2.770E-03	4.431E-04	2.229	0.63	1482
40.408	40.000	40.028	3.834E-02	2.396E-01	1.188E-01	2.696E-03	4.313E-04	2.168	0.63	1419
45.408	45.000	37.778	3.619E-02	2.262E-01	1.323E-01	2.622E-03	4.195E-04	2.106	0.63	1356
50.408	50.000	35.607	3.411E-02	2.132E-01	1.453E-01	2.548E-03	4.077E-04	2.045	0.63	1294
55.408	55.000	33.504	3.209E-02	2.006E-01	1.579E-01	2.475E-03	3.959E-04	1.984	0.64	1233
60.408	60.000	31.478	3.015E-02	1.884E-01	1.700E-01	2.401E-03	3.841E-04	1.923	0.64	1173
65.408	65.000	29.491	2.825E-02	1.765E-01	1.819E-01	2.327E-03	3.723E-04	1.861	0.64	1113
70.408	70.000	27.560	2.640E-02	1.650E-01	1.935E-01	2.253E-03	3.605E-04	1.799	0.64	1054
75.408	75.000	25.717	2.463E-02	1.540E-01	2.045E-01	2.180E-03	3.487E-04	1.738	0.64	997
80.408	80.000	23.936	2.293E-02	1.433E-01	2.151E-01	2.106E-03	3.369E-04	1.677	0.64	940
85.409	85.001	22.208	2.127E-02	1.330E-01	2.255E-01	2.032E-03	3.251E-04	1.615	0.64	885
90.409	90.001	20.552	1.969E-02	1.230E-01	2.354E-01	1.958E-03	3.133E-04	1.554	0.64	830
95.409	95.001	18.986	1.819E-02	1.137E-01	2.448E-01	1.885E-03	3.015E-04	1.493	0.64	777
100.409	100.001	17.459	1.672E-02	1.045E-01	2.539E-01	1.811E-03	2.897E-04	1.432	0.64	725
105.409	105.001	16.032	1.536E-02	9.598E-02	2.625E-01	1.737E-03	2.779E-04	1.372	0.64	675

Table I.12 3.8% bentonite flow measurement results

3.8 % Bentonite	
Orifice d (m)	0.02
Orifice A (m ²)	3.142E-04
Tank A (m ²)	0.16
Density (kg/m ³)	1023
Gravity (m/s ²)	9.81
τ (Pa)	1.009
k(Pa.s ⁿ)	0.007
n (-)	1

Time	Time difference	Mass of bentonite in tank	bentonite inTank	Height	Height difference	Velocity in Tank	Flow in Tank	Velocity in orifice	C _d	Re
s	s	kg	m ³	m	m	m/s	m ³ /s	m/s		
0.408	0.000	58.662	5.735E-02	3.584E-01	0.000E+00	3.204E-03	5.126E-04	2.652	0.62	7214
6.242	5.833	55.715	5.447E-02	3.404E-01	1.801E-02	3.123E-03	4.996E-04	2.584	0.62	7007
12.075	11.667	52.742	5.156E-02	3.223E-01	3.617E-02	3.042E-03	4.867E-04	2.514	0.62	6793
17.908	17.500	49.927	4.881E-02	3.051E-01	5.337E-02	2.960E-03	4.737E-04	2.446	0.62	6585
23.742	23.333	47.127	4.607E-02	2.880E-01	7.048E-02	2.879E-03	4.607E-04	2.377	0.62	6373
29.575	29.167	44.336	4.334E-02	2.709E-01	8.753E-02	2.798E-03	4.477E-04	2.305	0.62	6155
35.408	35.000	41.749	4.081E-02	2.551E-01	1.033E-01	2.717E-03	4.347E-04	2.237	0.62	5946
41.242	40.833	39.204	3.833E-02	2.395E-01	1.189E-01	2.636E-03	4.217E-04	2.168	0.62	5735
47.075	46.667	36.684	3.586E-02	2.241E-01	1.343E-01	2.554E-03	4.087E-04	2.097	0.62	5520
52.908	52.500	34.277	3.351E-02	2.094E-01	1.490E-01	2.473E-03	3.957E-04	2.027	0.62	5307
58.742	58.333	31.994	3.128E-02	1.955E-01	1.629E-01	2.392E-03	3.827E-04	1.958	0.62	5099
64.575	64.167	29.776	2.911E-02	1.819E-01	1.765E-01	2.311E-03	3.697E-04	1.889	0.62	4890
70.408	70.000	27.606	2.699E-02	1.687E-01	1.898E-01	2.230E-03	3.567E-04	1.819	0.62	4678
76.242	75.833	25.513	2.494E-02	1.559E-01	2.025E-01	2.148E-03	3.437E-04	1.749	0.63	4466
82.075	81.667	23.485	2.296E-02	1.435E-01	2.149E-01	2.067E-03	3.308E-04	1.678	0.63	4252
87.909	87.500	21.528	2.105E-02	1.315E-01	2.269E-01	1.986E-03	3.178E-04	1.606	0.63	4038
93.742	93.334	19.685	1.924E-02	1.203E-01	2.382E-01	1.905E-03	3.048E-04	1.536	0.63	3827
99.575	99.167	17.952	1.755E-02	1.097E-01	2.487E-01	1.824E-03	2.918E-04	1.467	0.63	3621
105.409	105.000	16.227	1.586E-02	9.915E-02	2.593E-01	1.742E-03	2.788E-04	1.395	0.64	3406
111.242	110.834	14.559	1.423E-02	8.895E-02	2.695E-01	1.661E-03	2.658E-04	1.321	0.64	3188

Table I.12 7.3% bentonite flow measurement results

7.3 % Bentonite	
Orifice diameter	0.02
Orifice Area	0.00031
Area of Tank	0.16
Density	1046
Gravity	9.81
τ (Pa)	30.493
$k(\text{Pa}\cdot\text{s}^n)$	0.021
n (-)	1

Time	Time difference	Mass of bentonite in tank	Volume of bentonite in Tank	Height	Heigh difference	Velocity in Tank	Flow in Tank	Velocity in orifice	C_d	Re
s	s	kg	m ³	m	m	m/s	m ³ /s	m/s		
0.825	0.000	98.383	9.406E-02	5.879E-01	0.000E+00	4.116E-03	6.586E-04	3.396	0.62	1649
10.825	10.000	91.747	8.771E-02	5.482E-01	3.965E-02	3.968E-03	6.349E-04	3.280	0.62	1563
20.825	20.000	85.338	8.159E-02	5.099E-01	7.794E-02	3.821E-03	6.113E-04	3.163	0.62	1479
30.825	30.000	79.146	7.566E-02	4.729E-01	1.149E-01	3.673E-03	5.877E-04	3.046	0.61	1395
40.825	40.000	73.175	6.996E-02	4.372E-01	1.506E-01	3.525E-03	5.641E-04	2.929	0.61	1313
50.825	50.000	67.416	6.445E-02	4.028E-01	1.850E-01	3.378E-03	5.404E-04	2.811	0.61	1231
60.825	60.000	61.874	5.915E-02	3.697E-01	2.181E-01	3.230E-03	5.168E-04	2.693	0.61	1151
70.825	70.000	56.511	5.403E-02	3.377E-01	2.502E-01	3.083E-03	4.932E-04	2.574	0.61	1071
80.825	80.000	51.433	4.917E-02	3.073E-01	2.805E-01	2.935E-03	4.696E-04	2.456	0.61	994
90.825	90.000	46.581	4.453E-02	2.783E-01	3.095E-01	2.787E-03	4.460E-04	2.337	0.61	918
100.825	100.000	41.996	4.015E-02	2.509E-01	3.369E-01	2.640E-03	4.223E-04	2.219	0.61	844
110.825	110.000	37.688	3.603E-02	2.252E-01	3.627E-01	2.492E-03	3.987E-04	2.102	0.60	773
120.825	120.000	33.672	3.219E-02	2.012E-01	3.867E-01	2.344E-03	3.751E-04	1.987	0.60	704
130.825	130.000	29.948	2.863E-02	1.789E-01	4.089E-01	2.197E-03	3.515E-04	1.874	0.60	639
140.825	140.000	26.529	2.536E-02	1.585E-01	4.293E-01	2.049E-03	3.278E-04	1.764	0.59	578
150.825	150.000	23.394	2.237E-02	1.398E-01	4.481E-01	1.901E-03	3.042E-04	1.656	0.58	520

Appendix J. Flow rate measurements using aspect ratio of 1

Table J.1 100% glycerine flow rate measurement results

100% Glycerine	
Orifice d (m)	0.02
Orifice A (m ²)	3.142E-04
Tank A (m ²)	0.16
μ (Pa.s)	0.968
Density (kg/m ³)	1257.8
Gravity (m/s ²)	9.81

Time	Time difference	Mass of glycerine in tank	Volume of glycerine in tank	Height of glycerine in tank	Height difference	Velocity in tank	Flow in tank	Velocity in orifice	C _d	Re
s	s	kg	m ³	m	m	m/s	m ³ /s	m/s		
0.825	0.000	36.548	2.906E-02	2.016E-01	0.000E+00	1.493E-03	2.389E-04	1.989	0.38	52
10.825	10.000	33.570	2.669E-02	1.868E-01	1.480E-02	1.420E-03	2.273E-04	1.914	0.38	50
20.825	20.000	30.761	2.446E-02	1.729E-01	2.875E-02	1.348E-03	2.157E-04	1.842	0.37	48
30.825	30.000	28.112	2.235E-02	1.597E-01	4.192E-02	1.275E-03	2.041E-04	1.770	0.37	46
40.825	40.000	25.625	2.037E-02	1.473E-01	5.428E-02	1.203E-03	1.925E-04	1.700	0.36	44
50.825	50.000	23.288	1.851E-02	1.357E-01	6.589E-02	1.130E-03	1.808E-04	1.632	0.35	42
60.825	60.000	21.109	1.678E-02	1.249E-01	7.672E-02	1.058E-03	1.692E-04	1.565	0.34	41
70.825	70.000	19.070	1.516E-02	1.148E-01	8.685E-02	9.852E-04	1.576E-04	1.501	0.33	39
80.825	80.000	17.164	1.365E-02	1.053E-01	9.632E-02	9.127E-04	1.460E-04	1.437	0.32	37
90.825	90.000	15.396	1.224E-02	9.650E-02	1.051E-01	8.401E-04	1.344E-04	1.376	0.31	36
100.825	100.000	13.760	1.094E-02	8.837E-02	1.132E-01	7.676E-04	1.228E-04	1.317	0.30	34
110.825	110.000	12.227	9.721E-03	8.075E-02	1.209E-01	6.951E-04	1.112E-04	1.259	0.28	33

Table J.2 96% glycerine flow rate measurement results

96 % Glycerine	
Orifice d (m)	0.02
Orifice A (m ²)	3.142E-04
Tank A (m ²)	0.16
μ (Pa.s)	0.304
Density (kg/m ³)	1248
Gravity (m/s ²)	9.81

Time	Time difference	Mass of glycerine in tank	Volume of glycerine in tank	Height of glycerine in tank	Height difference	Velocity in tank	Flow in tank	Velocity in orifice	C _d	Re
s	s	kg	m ³	m	m	m/s	m ³ /s	m/s		
0.825	0.000	33.685	2.70E-02	1.89E-01	0.00E+00	2.17E-03	3.48E-04	1.924	0.58	158
5.825	5.000	31.559	2.53E-02	1.78E-01	1.06E-02	2.10E-03	3.36E-04	1.869	0.57	153
10.825	10.000	29.479	2.36E-02	1.68E-01	2.11E-02	2.02E-03	3.24E-04	1.813	0.57	149
15.825	15.000	27.507	2.20E-02	1.58E-01	3.09E-02	1.95E-03	3.12E-04	1.759	0.56	144
20.825	20.000	25.591	2.05E-02	1.48E-01	4.05E-02	1.87E-03	3.00E-04	1.705	0.56	140
25.825	25.000	23.744	1.90E-02	1.39E-01	4.98E-02	1.80E-03	2.88E-04	1.651	0.55	136
30.825	30.000	21.982	1.76E-02	1.30E-01	5.86E-02	1.72E-03	2.76E-04	1.597	0.55	131
35.825	35.000	20.352	1.63E-02	1.22E-01	6.68E-02	1.65E-03	2.64E-04	1.546	0.54	127
40.825	40.000	18.721	1.50E-02	1.14E-01	7.49E-02	1.57E-03	2.52E-04	1.494	0.54	123
45.825	45.000	17.190	1.38E-02	1.06E-01	8.26E-02	1.50E-03	2.40E-04	1.443	0.53	118
50.825	50.000	15.741	1.26E-02	9.88E-02	8.98E-02	1.42E-03	2.28E-04	1.392	0.52	114
55.825	55.000	14.334	1.15E-02	9.18E-02	9.69E-02	1.35E-03	2.16E-04	1.342	0.51	110
60.825	60.000	13.015	1.04E-02	8.52E-02	1.03E-01	1.27E-03	2.04E-04	1.293	0.50	106

Table J.3 93% glycerine flow rate measurement results

93 % glycerine	
Orifice d (m)	0.02
Orifice A (m ²)	0.0003
Tank A (m ²)	0.16
μ (Pa.s)	0.13
Density (Kg/m ³)	1242
Gravity (m/s ²)	9.81

Time	Time difference	Mass of glycerine in tank	Volume of glycerine in tank	Height of glycerine in tank	Height difference	Velocity in tank	Flow in tank	Velocity in orifice	C _d	Re
s	s	kg	m ³	m	m	m/s	m ³ /s	m/s		
12.075	11.667	28.321	2.28E-02	1.62E-01	2.65E-02	2.18E-03	3.49E-04	1.785	0.62	341
17.908	17.500	25.853	2.08E-02	1.50E-01	3.89E-02	2.09E-03	3.34E-04	1.716	0.62	328
23.742	23.333	23.471	1.89E-02	1.38E-01	5.09E-02	2.00E-03	3.20E-04	1.646	0.62	315
29.575	29.167	21.224	1.71E-02	1.27E-01	6.22E-02	1.91E-03	3.05E-04	1.577	0.62	301
35.408	35.000	19.046	1.53E-02	1.16E-01	7.32E-02	1.81E-03	2.90E-04	1.507	0.61	288
41.242	40.833	17.014	1.37E-02	1.06E-01	8.34E-02	1.72E-03	2.76E-04	1.439	0.61	275
47.075	46.667	15.041	1.21E-02	9.57E-02	9.33E-02	1.63E-03	2.61E-04	1.370	0.61	262
52.908	52.500	13.175	1.06E-02	8.63E-02	1.03E-01	1.54E-03	2.47E-04	1.301	0.60	249
58.742	58.333	11.494	9.25E-03	7.78E-02	1.11E-01	1.45E-03	2.32E-04	1.236	0.60	236

Table J.4 65% glycerine flow rate measurement results

65 % glycerine	
Orifice d (m)	0.02
Orifice A (m ²)	3.142E-04
Tank A (m ²)	0.16
μ (Pa.s)	0.019
Density (kg/m ³)	1179
Gravity (m/s ²)	9.81

Time	Time difference	Mass of glycerine in tank	Volume of glycerine in tank	Height of glycerine in tank	Height difference	Velocity in tank	Flow in tank	Velocity in orifice	C _d	Re
s	s	kg	m ³	m	m	m/s	m ³ /s	m/s		
0.825	0.000	56.411	4.79E-02	3.19E-01	0.00E+00	2.95E-03	4.72E-04	2.502	0.60	3072
9.158	8.333	51.876	4.40E-02	2.95E-01	2.40E-02	2.83E-03	4.52E-04	2.406	0.60	2954
17.492	16.667	47.533	4.03E-02	2.72E-01	4.71E-02	2.71E-03	4.33E-04	2.310	0.60	2837
25.825	25.000	43.369	3.68E-02	2.50E-01	6.92E-02	2.59E-03	4.14E-04	2.215	0.60	2719
34.158	33.333	39.382	3.34E-02	2.29E-01	9.03E-02	2.47E-03	3.95E-04	2.119	0.59	2602
42.492	41.667	35.595	3.02E-02	2.09E-01	1.10E-01	2.35E-03	3.76E-04	2.024	0.59	2485
50.825	50.000	31.996	2.71E-02	1.90E-01	1.29E-01	2.23E-03	3.57E-04	1.929	0.59	2368

Table J.5 2.4% CMC flow rate measurement results

2.4 % CMC	
Orifice d (m)	0.02
Orifice A (m ²)	3.142E-04
Tank A (m ²)	0.16
Density (kg/m ³)	1014
Gravity (m/s ²)	9.81
k (Pa.s ⁿ)	0.006
n (-)	1

Time	Time difference	Mass of CMC in tank	Volume of CMC in tank	Height of CMC in tank	Height difference	Velocity in tank	Flow in tank	Velocity in orifice	C _d	Re
s	s	kg	m ³	m	m	m/s	m ³ /s	m/s		
0.825	0.000	87.108	8.588E-02	5.567E-01	0.000E+00	3.846E-03	6.154E-04	3.305	0.59	11618.97
9.992	9.167	81.450	8.030E-02	5.219E-01	3.486E-02	3.720E-03	5.952E-04	3.200	0.59	11249.352
19.158	18.333	76.024	7.495E-02	4.884E-01	6.830E-02	3.594E-03	5.750E-04	3.096	0.59	10882.999
28.325	27.500	70.799	6.980E-02	4.563E-01	1.005E-01	3.467E-03	5.548E-04	2.992	0.59	10518.267
37.492	36.667	65.727	6.480E-02	4.250E-01	1.317E-01	3.341E-03	5.346E-04	2.888	0.59	10151.622
46.658	45.833	60.863	6.000E-02	3.950E-01	1.617E-01	3.215E-03	5.144E-04	2.784	0.59	9787.0802
55.825	55.000	56.156	5.536E-02	3.660E-01	1.907E-01	3.089E-03	4.942E-04	2.680	0.59	9420.9966
64.992	64.167	51.655	5.093E-02	3.383E-01	2.185E-01	2.962E-03	4.740E-04	2.576	0.59	9057.0182
74.158	73.333	47.353	4.669E-02	3.118E-01	2.450E-01	2.836E-03	4.538E-04	2.473	0.58	8694.9484
83.325	82.500	43.218	4.261E-02	2.863E-01	2.704E-01	2.710E-03	4.336E-04	2.370	0.58	8332.0982
92.492	91.667	39.271	3.872E-02	2.620E-01	2.948E-01	2.584E-03	4.134E-04	2.267	0.58	7970.3443

Table J.6 5.2% CMC flow rate measurement results

5.2 % CMC	
Orifice d (m)	0.02
Orifice A (m ²)	3.142E-04
Tank A (m ²)	0.16
Density (kg/m ³)	1029
Gravity (m/s ²)	9.81
k (Pa.s ⁿ)	0.210
n (-)	0.791

Time	Time difference	Mass of CMC in tank	Volume of CMC in tank	Height of CMC in tank	Height difference	Velocity in tank	Flow in tank	Velocity in orifice	C _d	Re
s	s	kg	m ³	m	m	m/s	m ³ /s	m/s		
0.825	0.000	52.129	5.064E-02	3.365E-01	0.000E+00	3.072E-03	4.915E-04	2.569	0.61	1028
9.158	8.333	47.978	4.661E-02	3.113E-01	2.520E-02	2.951E-03	4.721E-04	2.471	0.61	981
17.492	16.667	44.037	4.278E-02	2.874E-01	4.913E-02	2.829E-03	4.527E-04	2.374	0.61	935
25.825	25.000	40.243	3.909E-02	2.643E-01	7.217E-02	2.708E-03	4.333E-04	2.277	0.61	889
34.158	33.333	36.574	3.553E-02	2.421E-01	9.444E-02	2.587E-03	4.139E-04	2.179	0.60	843
42.492	41.667	33.116	3.217E-02	2.211E-01	1.154E-01	2.465E-03	3.945E-04	2.083	0.60	798
50.825	50.000	29.829	2.898E-02	2.011E-01	1.354E-01	2.344E-03	3.750E-04	1.986	0.60	754
59.158	58.333	26.692	2.593E-02	1.821E-01	1.544E-01	2.223E-03	3.556E-04	1.890	0.60	710
67.492	66.667	23.728	2.305E-02	1.641E-01	1.724E-01	2.101E-03	3.362E-04	1.794	0.60	667
75.825	75.000	20.932	2.033E-02	1.471E-01	1.894E-01	1.980E-03	3.168E-04	1.699	0.59	625
84.159	83.334	18.304	1.778E-02	1.311E-01	2.054E-01	1.859E-03	2.974E-04	1.604	0.59	583
92.492	91.667	15.810	1.536E-02	1.160E-01	2.205E-01	1.737E-03	2.780E-04	1.509	0.59	541

Table J.7 6.6% CMC flow rate measurement results

6.6 % CMC	
Orifice d (m)	0.02
Orifice A (m ²)	3.14E-04
Tank A (m ²)	0.16
Density (kg/m ³)	1037
Gravity (m/s ²)	9.81
k (Pa.s ⁿ)	0.880
n (-)	0.700

Time	Time difference	Mass of CMC in tank	Volume of CMC in tank	Height of CMC in tank	Height difference	Velocity in tank	Flow in tank	Velocity in orifice	C _d	Re
s	s	kg	m ³	m	m	m/s	m ³ /s	m/s		
15.825	15.000	43.759	4.220E-02	2.837E-01	4.653E-02	2.956E-03	4.729E-04	2.359	0.64	404
23.325	22.500	40.130	3.870E-02	2.619E-01	6.840E-02	2.812E-03	4.499E-04	2.267	0.63	384
30.825	30.000	36.734	3.542E-02	2.414E-01	8.887E-02	2.668E-03	4.270E-04	2.176	0.62	364
38.325	37.500	33.501	3.231E-02	2.219E-01	1.084E-01	2.525E-03	4.040E-04	2.087	0.62	344
45.825	45.000	30.462	2.937E-02	2.036E-01	1.267E-01	2.381E-03	3.810E-04	1.999	0.61	326
53.325	52.500	27.606	2.662E-02	1.864E-01	1.439E-01	2.238E-03	3.580E-04	1.912	0.60	307
60.825	60.000	24.911	2.402E-02	1.701E-01	1.601E-01	2.094E-03	3.350E-04	1.827	0.58	290
68.325	67.500	22.396	2.160E-02	1.550E-01	1.753E-01	1.950E-03	3.120E-04	1.744	0.57	273
75.825	75.000	20.049	1.933E-02	1.408E-01	1.894E-01	1.807E-03	2.891E-04	1.662	0.55	256
83.325	82.500	17.847	1.721E-02	1.276E-01	2.027E-01	1.663E-03	2.661E-04	1.582	0.54	240

Table J.8 7.6% CMC flow rate measurement results

7.6 % CMC	
Orifice d (m)	0.02
Orifice A (m ²)	3.142E-04
Tank A (m ²)	0.16
Density (kg/m ³)	1042
Gravity (m/s ²)	9.81
k (Pa.s ⁿ)	2.394
n (-)	0.636

Time	Time difference	Mass of CMC in tank	Volume of CMC in tank	Height of CMC in tank	Height difference	Velocity in tank	Flow in tank	Velocity in orifice	C _d	Re
s	s	kg	m ³	m	m	m/s	m ³ /s	m/s		
0.825	0.000	45.544	4.373E-02	2.933E-01	0.000E+00	2.564E-03	4.102E-04	2.399	0.54	234
9.158	8.333	42.018	4.034E-02	2.721E-01	2.115E-02	2.441E-03	3.906E-04	2.311	0.54	222
17.492	16.667	38.665	3.712E-02	2.520E-01	4.128E-02	2.318E-03	3.709E-04	2.224	0.53	211
25.825	25.000	35.509	3.409E-02	2.331E-01	6.021E-02	2.195E-03	3.512E-04	2.138	0.52	200
34.158	33.333	32.545	3.124E-02	2.153E-01	7.800E-02	2.072E-03	3.316E-04	2.055	0.51	190
42.492	41.667	29.763	2.857E-02	1.986E-01	9.469E-02	1.949E-03	3.119E-04	1.974	0.50	179
50.825	50.000	27.169	2.608E-02	1.830E-01	1.103E-01	1.826E-03	2.922E-04	1.895	0.49	170
59.158	58.333	24.751	2.376E-02	1.685E-01	1.248E-01	1.703E-03	2.725E-04	1.818	0.48	160
67.492	66.667	22.491	2.159E-02	1.550E-01	1.383E-01	1.580E-03	2.529E-04	1.744	0.46	151
75.825	75.000	20.391	1.958E-02	1.424E-01	1.509E-01	1.457E-03	2.332E-04	1.671	0.44	143
84.159	83.334	18.450	1.771E-02	1.307E-01	1.626E-01	1.334E-03	2.135E-04	1.601	0.42	135
92.492	91.667	16.670	1.600E-02	1.200E-01	1.733E-01	1.212E-03	1.938E-04	1.535	0.40	127
100.825	100.000	15.033	1.443E-02	1.102E-01	1.831E-01	1.089E-03	1.742E-04	1.470	0.38	120
109.159	108.334	13.534	1.299E-02	1.012E-01	1.921E-01	9.656E-04	1.545E-04	1.409	0.35	113

Table J.9 13.1% kaolin flow rate measurement results

13.1 % Kaolin	
Orifice d (m)	0.02
Orifice A (m ²)	3.142E-04
Tank A (m ²)	0.16
Density (kg/m ³)	1217
Gravity (m/s ²)	9.81
τ (Pa)	8.901
k(Pa.s ⁿ)	0.067
n (-)	0.716

Time	Time difference	Mass of Kaolin in tank	Volume of Kaolin in tank	Height of Kaolin in tank	Height difference	Velocity in tank	Flow in tank	Velocity in orifice	C _d	Re
s	s	kg	m ³	m	m	m/s	m ³ /s	m/s		
0.825	0.000	56.864	4.672E-02	3.120E-01	0.000E+00	2.911E-03	4.658E-04	2.474	0.60	3262
7.492	6.667	53.161	4.368E-02	2.930E-01	1.902E-02	2.819E-03	4.511E-04	2.398	0.60	3099
14.158	13.333	49.571	4.073E-02	2.746E-01	3.745E-02	2.728E-03	4.364E-04	2.321	0.60	2938
20.825	20.000	46.067	3.785E-02	2.566E-01	5.545E-02	2.636E-03	4.217E-04	2.244	0.60	2779
27.492	26.667	42.731	3.511E-02	2.394E-01	7.258E-02	2.544E-03	4.070E-04	2.167	0.60	2625
34.158	33.333	39.479	3.244E-02	2.227E-01	8.928E-02	2.452E-03	3.924E-04	2.091	0.60	2473
40.825	40.000	36.341	2.986E-02	2.066E-01	1.054E-01	2.361E-03	3.777E-04	2.013	0.60	2324
47.492	46.667	33.359	2.741E-02	1.913E-01	1.207E-01	2.269E-03	3.630E-04	1.937	0.60	2180
54.158	53.333	30.437	2.501E-02	1.763E-01	1.357E-01	2.177E-03	3.483E-04	1.860	0.60	2036
60.825	60.000	27.695	2.276E-02	1.622E-01	1.498E-01	2.085E-03	3.336E-04	1.784	0.60	1900
67.492	66.667	25.042	2.058E-02	1.486E-01	1.634E-01	1.994E-03	3.190E-04	1.708	0.59	1765
74.158	73.333	22.522	1.851E-02	1.357E-01	1.764E-01	1.902E-03	3.043E-04	1.631	0.59	1635
80.825	80.000	20.120	1.653E-02	1.233E-01	1.887E-01	1.810E-03	2.896E-04	1.556	0.59	1508

Table J.10 20.4% kaolin flow rate measurement results

20.4 % Kaolin	
Orifice d (m)	0.02
Orifice A (m ²)	3.142E-04
Tank A (m ²)	0.16
Density (Kg/m ³)	1336
Gravity (m/s ²)	9.81
τ (Pa)	39.420
k(Pa.s ⁿ)	3.962
n (-)	0.365

Time	Time difference	Mass of Kaolin in tank	Volume of Kaolin in Tank	Height	Height difference	Velocity in Tank	Flow in Tank	Velocity in orifice	C _d	Re
s	s	kg	m ³	m	m	m/s	m ³ /s	m/s		
0.825	0.000	59.481	4.454E-02	2.984E-01	0.000E+00	3.011E-03	4.818E-04	2.419	0.63	711
7.492	6.667	55.446	4.152E-02	2.795E-01	1.888E-02	2.900E-03	4.640E-04	2.342	0.63	670
14.158	13.333	51.538	3.859E-02	2.612E-01	3.717E-02	2.790E-03	4.463E-04	2.264	0.63	631
20.825	20.000	47.755	3.576E-02	2.435E-01	5.487E-02	2.679E-03	4.286E-04	2.186	0.62	592
27.492	26.667	44.019	3.296E-02	2.260E-01	7.235E-02	2.568E-03	4.109E-04	2.106	0.62	554
34.158	33.333	40.370	3.023E-02	2.089E-01	8.943E-02	2.457E-03	3.932E-04	2.025	0.62	516
40.825	40.000	36.787	2.754E-02	1.922E-01	1.062E-01	2.347E-03	3.755E-04	1.942	0.62	478
47.492	46.667	33.404	2.501E-02	1.763E-01	1.220E-01	2.236E-03	3.578E-04	1.860	0.61	442
54.158	53.333	30.248	2.265E-02	1.616E-01	1.368E-01	2.125E-03	3.401E-04	1.780	0.61	409
60.825	60.000	27.298	2.044E-02	1.477E-01	1.506E-01	2.015E-03	3.223E-04	1.703	0.60	377
67.492	66.667	24.592	1.841E-02	1.351E-01	1.633E-01	1.904E-03	3.046E-04	1.628	0.60	348
74.158	73.333	22.100	1.655E-02	1.234E-01	1.749E-01	1.793E-03	2.869E-04	1.556	0.59	320
80.825	80.000	19.824	1.484E-02	1.128E-01	1.856E-01	1.683E-03	2.692E-04	1.487	0.58	295

Table J.11 7.2% bentonite flow rate measurement results

7.2 % Bentonite	
Orifice d (m)	0.02
Orifice A (m ²)	3.142E-04
Tank A (m ²)	0.16
Density (kg/m ³)	1044
Gravity (m/s ²)	9.81
τ (Pa)	15.738
k(Pa.s ⁿ)	0.014
n (-)	1

Time	Time difference	Mass of bentonite in tank	Volume of bentonite in Tank	Height of bentonite in tank	Height difference	Velocity in Tank	Flow in Tank	Velocity in orifice	C _d	Re
s	s	kg	m ³	m	m	m/s	m ³ /s	m/s		
0.408	0.000	59.874	5.735E-02	3.784E-01	0.000E+00	3.280E-03	5.248E-04	2.725	0.61	2018
5.408	5.000	57.224	5.481E-02	3.626E-01	1.587E-02	3.206E-03	5.130E-04	2.667	0.61	1953
10.408	10.000	54.604	5.230E-02	3.469E-01	3.155E-02	3.132E-03	5.012E-04	2.609	0.61	1889
15.408	15.000	52.034	4.984E-02	3.315E-01	4.694E-02	3.059E-03	4.894E-04	2.550	0.61	1824
20.408	20.000	49.495	4.741E-02	3.163E-01	6.214E-02	2.985E-03	4.776E-04	2.491	0.61	1760
25.408	25.000	47.056	4.507E-02	3.017E-01	7.674E-02	2.911E-03	4.658E-04	2.433	0.61	1697
30.408	30.000	44.665	4.278E-02	2.874E-01	9.106E-02	2.837E-03	4.540E-04	2.375	0.61	1635
35.408	35.000	42.303	4.052E-02	2.733E-01	1.052E-01	2.764E-03	4.422E-04	2.315	0.61	1572
40.408	40.000	40.028	3.834E-02	2.596E-01	1.188E-01	2.690E-03	4.304E-04	2.257	0.61	1511
45.408	45.000	37.778	3.619E-02	2.462E-01	1.323E-01	2.616E-03	4.186E-04	2.198	0.61	1449
50.408	50.000	35.607	3.411E-02	2.332E-01	1.453E-01	2.542E-03	4.068E-04	2.139	0.61	1389
55.408	55.000	33.504	3.209E-02	2.206E-01	1.579E-01	2.469E-03	3.950E-04	2.080	0.60	1329
60.408	60.000	31.478	3.015E-02	2.084E-01	1.700E-01	2.395E-03	3.832E-04	2.022	0.60	1271
65.408	65.000	29.491	2.825E-02	1.965E-01	1.819E-01	2.321E-03	3.714E-04	1.964	0.60	1213
70.408	70.000	27.560	2.640E-02	1.850E-01	1.935E-01	2.247E-03	3.596E-04	1.905	0.60	1156
75.408	75.000	25.717	2.463E-02	1.740E-01	2.045E-01	2.174E-03	3.478E-04	1.847	0.60	1100
80.408	80.000	23.936	2.293E-02	1.633E-01	2.151E-01	2.100E-03	3.360E-04	1.790	0.60	1046
85.409	85.000	22.208	2.127E-02	1.530E-01	2.255E-01	2.026E-03	3.242E-04	1.732	0.60	992

Table J.12 3.8% bentonite flow rate measurement results

3.8 % Bentonite	
Orifice d (m)	0.02
Orifice A (m ²)	3.142E-04
Tank A (m ²)	0.16
Density (kg/m ³)	1023
Gravity (m/s ²)	9.81
τ (Pa)	1.009
k(Pa.s ⁿ)	0.007
n (-)	1

Time	Time difference	Mass of bentonite in tank	Volume of bentonite in Tank	Height of bentonite in tank	Height difference	Velocity in Tank	Flow in Tank	Velocity in orifice	C _d	Re
s	s	kg	m ³	m	m	m/s	m ³ /s	m/s		
0.408	0.000	58.662	5.735E-02	3.784E-01	0.000E+00	3.204E-03	5.126E-04	2.725	0.60	7438
6.242	5.833	55.715	5.447E-02	3.604E-01	1.801E-02	3.123E-03	4.996E-04	2.659	0.60	7237
12.075	11.667	52.742	5.156E-02	3.423E-01	3.617E-02	3.042E-03	4.867E-04	2.591	0.60	7029
17.908	17.500	49.927	4.881E-02	3.251E-01	5.337E-02	2.960E-03	4.737E-04	2.525	0.60	6827
23.742	23.333	47.127	4.607E-02	3.080E-01	7.048E-02	2.879E-03	4.607E-04	2.458	0.60	6621
29.575	29.167	44.336	4.334E-02	2.909E-01	8.753E-02	2.798E-03	4.477E-04	2.389	0.60	6410
35.408	35.000	41.749	4.081E-02	2.751E-01	1.033E-01	2.717E-03	4.347E-04	2.323	0.60	6209
41.242	40.833	39.204	3.833E-02	2.595E-01	1.189E-01	2.636E-03	4.217E-04	2.257	0.59	6006
47.075	46.667	36.684	3.586E-02	2.441E-01	1.343E-01	2.554E-03	4.087E-04	2.189	0.59	5799
52.908	52.500	34.277	3.351E-02	2.294E-01	1.490E-01	2.473E-03	3.957E-04	2.122	0.59	5595
58.742	58.333	31.994	3.128E-02	2.155E-01	1.629E-01	2.392E-03	3.827E-04	2.056	0.59	5396
64.575	64.167	29.776	2.911E-02	2.019E-01	1.765E-01	2.311E-03	3.697E-04	1.990	0.59	5196
70.408	70.000	27.606	2.699E-02	1.887E-01	1.898E-01	2.230E-03	3.567E-04	1.924	0.59	4995
76.242	75.833	25.513	2.494E-02	1.759E-01	2.025E-01	2.148E-03	3.437E-04	1.858	0.59	4794
82.075	81.667	23.485	2.296E-02	1.635E-01	2.149E-01	2.067E-03	3.308E-04	1.791	0.59	4593
87.909	87.500	21.528	2.105E-02	1.515E-01	2.269E-01	1.986E-03	3.178E-04	1.724	0.59	4392
93.742	93.334	19.685	1.924E-02	1.403E-01	2.382E-01	1.905E-03	3.048E-04	1.659	0.58	4195
99.575	99.167	17.952	1.755E-02	1.297E-01	2.487E-01	1.824E-03	2.918E-04	1.595	0.58	4004

Table J.13 7.3% bentonite flow rate measurement results

7.3 % Bentonite	
Orifice d (m)	0.02
Orifice A (m ²)	0.0003
Tank A (m ²)	0.16
Density (kg/m ³)	1046
Gravity (m/s ²)	9.81
τ (Pa)	30.49
k(Pa.s ⁿ)	0.02
n (-)	1

Time	Time difference	Mass of bentonite in tank	Volume of bentonite in Tank	Height of bentonite in tank	Height difference	Velocity in Tank	Flow in Tank	Velocity in orifice	C _d	Re
s	s	kg	m ³	m	m	m/s	m ³ /s	m/s		
0.825	0.000	97.574	9.328E-02	6.030E-01	0.000E+00	3.996E-03	6.394E-04	3.440	0.59	1681
9.992	9.167	91.550	8.752E-02	5.670E-01	3.599E-02	3.881E-03	6.210E-04	3.335	0.59	1604
19.158	18.333	85.711	8.194E-02	5.321E-01	7.088E-02	3.767E-03	6.027E-04	3.231	0.59	1528
28.325	27.500	80.054	7.653E-02	4.983E-01	1.047E-01	3.652E-03	5.844E-04	3.127	0.59	1453
37.492	36.667	74.559	7.128E-02	4.655E-01	1.375E-01	3.538E-03	5.661E-04	3.022	0.60	1378
46.658	45.833	69.233	6.619E-02	4.337E-01	1.693E-01	3.423E-03	5.478E-04	2.917	0.60	1305
55.825	55.000	64.123	6.130E-02	4.031E-01	1.999E-01	3.309E-03	5.294E-04	2.812	0.60	1232
64.992	64.167	59.147	5.655E-02	3.734E-01	2.296E-01	3.194E-03	5.111E-04	2.707	0.60	1160
74.158	73.333	54.331	5.194E-02	3.446E-01	2.584E-01	3.080E-03	4.928E-04	2.600	0.60	1089
83.325	82.500	49.648	4.746E-02	3.167E-01	2.864E-01	2.965E-03	4.745E-04	2.493	0.61	1018
92.492	91.667	45.069	4.309E-02	2.893E-01	3.137E-01	2.851E-03	4.561E-04	2.382	0.61	947
101.659	100.834	40.669	3.888E-02	2.630E-01	3.400E-01	2.736E-03	4.378E-04	2.272	0.61	877
110.825	110.000	36.473	3.487E-02	2.379E-01	3.651E-01	2.622E-03	4.195E-04	2.161	0.62	808
119.992	119.167	32.567	3.114E-02	2.146E-01	3.884E-01	2.507E-03	4.012E-04	2.052	0.62	743
129.159	128.334	29.010	2.773E-02	1.933E-01	4.097E-01	2.393E-03	3.829E-04	1.948	0.63	682
138.325	137.500	25.805	2.467E-02	1.742E-01	4.288E-01	2.278E-03	3.645E-04	1.849	0.63	625

Appendix K. Flow rate measurements using aspect ratio of 3

Table K.1 100 % glycerine flow rate measurement results

100 % Glycerine	
Orifice d (m)	0.02
Orifice A (m ²)	3.142E-04
Tank A (m ²)	0.16
μ (Pa.s)	0.968
Density (kg/m ³)	1258
Gravity (m/s ²)	9.81

Time	Time difference	Mass of glycerine in tank	Volume of glycerine in tank	Height of glycerine in tank	Height difference	Velocity in tank	Flow in tank	Velocity in orifice	C _d	Re
s	s	kg	m ³	m	m	m/s	m ³ /s	m/s		
0.825	0.000	36.426	2.896E-02	2.410E-01	0.000E+00	9.289E-04	1.486E-04	2.174	0.22	57
11.658	10.833	34.376	2.733E-02	2.308E-01	1.018E-02	9.007E-04	1.441E-04	2.128	0.22	55
22.492	21.667	32.415	2.577E-02	2.211E-01	1.993E-02	8.726E-04	1.396E-04	2.083	0.21	54
33.325	32.500	30.513	2.426E-02	2.116E-01	2.938E-02	8.444E-04	1.351E-04	2.038	0.21	53
44.158	43.333	28.710	2.283E-02	2.027E-01	3.834E-02	8.162E-04	1.306E-04	1.994	0.21	52
54.992	54.167	26.952	2.143E-02	1.939E-01	4.708E-02	7.881E-04	1.261E-04	1.951	0.21	51
65.825	65.000	25.284	2.010E-02	1.856E-01	5.536E-02	7.599E-04	1.216E-04	1.908	0.20	50
76.658	75.833	23.654	1.881E-02	1.775E-01	6.346E-02	7.317E-04	1.171E-04	1.866	0.20	49
87.492	86.667	22.111	1.758E-02	1.699E-01	7.113E-02	7.036E-04	1.126E-04	1.826	0.20	47
98.325	97.500	20.619	1.639E-02	1.625E-01	7.854E-02	6.754E-04	1.081E-04	1.785	0.19	46
109.159	108.334	19.186	1.525E-02	1.553E-01	8.566E-02	6.472E-04	1.036E-04	1.746	0.19	45
119.992	119.167	17.832	1.418E-02	1.486E-01	9.239E-02	6.191E-04	9.905E-05	1.708	0.18	44
130.825	130.000	16.528	1.314E-02	1.421E-01	9.887E-02	5.909E-04	9.454E-05	1.670	0.18	43
141.659	140.834	15.257	1.213E-02	1.358E-01	1.052E-01	5.627E-04	9.004E-05	1.632	0.18	42
152.492	151.667	14.048	1.117E-02	1.298E-01	1.112E-01	5.346E-04	8.553E-05	1.596	0.17	41
163.325	162.500	12.893	1.025E-02	1.241E-01	1.169E-01	5.064E-04	8.102E-05	1.560	0.17	41
174.159	173.334	11.796	9.378E-03	1.186E-01	1.224E-01	4.782E-04	7.652E-05	1.526	0.16	40
184.992	184.167	10.731	8.531E-03	1.133E-01	1.277E-01	4.501E-04	7.201E-05	1.491	0.15	39

Table K.2 96% glycerine flow rate measurement results

96 % Glycerine	
Orifice d (m)	0.02
Orifice A (m ²)	3.142E-04
Tank A (m ²)	0.16
μ (Pa.s)	0.304
Density (kg/m ³)	1248
Gravity (m/s ²)	9.81

Time	Time difference	Mass of glycerine in tank	Volume of glycerine in tank	Height of glycerine in tank	Height difference	Velocity in tank	Flow in tank	Velocity in orifice	C _d	Re
s	s	kg	m ³	m	m	m/s	m ³ /s	m/s		
0.825	0.000	33.760	2.704E-02	2.290E-01	0.000E+00	1.782E-03	2.851E-04	2.120	0.43	174
7.492	6.667	31.404	2.516E-02	2.172E-01	1.179E-02	1.723E-03	2.757E-04	2.064	0.43	170
14.158	13.333	29.135	2.334E-02	2.059E-01	2.315E-02	1.664E-03	2.662E-04	2.010	0.42	165
20.825	20.000	26.933	2.157E-02	1.948E-01	3.418E-02	1.605E-03	2.567E-04	1.955	0.42	161
27.492	26.667	24.850	1.991E-02	1.844E-01	4.461E-02	1.546E-03	2.473E-04	1.902	0.41	156
34.158	33.333	22.837	1.829E-02	1.743E-01	5.468E-02	1.486E-03	2.378E-04	1.849	0.41	152
40.825	40.000	20.907	1.675E-02	1.647E-01	6.434E-02	1.427E-03	2.284E-04	1.797	0.40	148
47.492	46.667	19.035	1.525E-02	1.553E-01	7.372E-02	1.368E-03	2.189E-04	1.746	0.40	143
54.158	53.333	17.268	1.383E-02	1.465E-01	8.256E-02	1.309E-03	2.094E-04	1.695	0.39	139
60.825	60.000	15.573	1.247E-02	1.380E-01	9.105E-02	1.250E-03	2.000E-04	1.645	0.39	135
67.492	66.667	13.966	1.119E-02	1.299E-01	9.910E-02	1.191E-03	1.905E-04	1.597	0.38	131
74.158	73.333	12.407	9.938E-03	1.221E-01	1.069E-01	1.132E-03	1.811E-04	1.548	0.37	127
80.825	80.000	10.902	8.733E-03	1.146E-01	1.144E-01	1.073E-03	1.716E-04	1.499	0.36	123
87.492	86.667	9.545	7.646E-03	1.078E-01	1.212E-01	1.013E-03	1.622E-04	1.454	0.35	119
94.159	93.334	8.183	6.555E-03	1.010E-01	1.280E-01	9.543E-04	1.527E-04	1.407	0.35	116

Table K.3 93% glycerine flow rate measurement results

93 % Glycerine	
Orifice d (m)	0.02
Orifice A (m ²)	3.142E-04
Tank A (m ²)	0.16
μ (Pa.s)	0.130
Density (kg/m ³)	1242
Gravity (m/s ²)	9.81

Time	Time difference	Mass of glycerine in tank	Volume of glycerine in tank	Height of glycerine in tank	Height difference	Velocity in tank	Flow in tank	Velocity in orifice	C _d	Re
s	s	kg	m ³	m	m	m/s	m ³ /s	m/s		
0.825	0.000	33.575	2.702E-02	2.289E-01	0.000E+00	2.448E-03	3.917E-04	2.119	0.59	405
4.992	4.167	31.569	2.541E-02	2.188E-01	1.009E-02	2.381E-03	3.810E-04	2.072	0.59	396
9.158	8.333	29.627	2.385E-02	2.090E-01	1.986E-02	2.315E-03	3.704E-04	2.025	0.58	387
13.325	12.500	27.707	2.230E-02	1.994E-01	2.952E-02	2.248E-03	3.597E-04	1.978	0.58	378
17.492	16.667	25.868	2.082E-02	1.901E-01	3.877E-02	2.182E-03	3.491E-04	1.931	0.58	369
21.658	20.833	24.086	1.939E-02	1.812E-01	4.774E-02	2.115E-03	3.384E-04	1.885	0.57	360
25.825	25.000	22.395	1.803E-02	1.727E-01	5.625E-02	2.048E-03	3.278E-04	1.841	0.57	352
29.992	29.167	20.716	1.667E-02	1.642E-01	6.469E-02	1.982E-03	3.171E-04	1.795	0.56	343
34.158	33.333	19.136	1.540E-02	1.563E-01	7.264E-02	1.915E-03	3.065E-04	1.751	0.56	335
38.325	37.500	17.567	1.414E-02	1.484E-01	8.053E-02	1.849E-03	2.958E-04	1.706	0.55	326
42.492	41.667	16.060	1.293E-02	1.408E-01	8.811E-02	1.782E-03	2.851E-04	1.662	0.55	318
46.658	45.833	14.592	1.174E-02	1.334E-01	9.550E-02	1.716E-03	2.745E-04	1.618	0.54	309
50.825	50.000	13.208	1.063E-02	1.264E-01	1.025E-01	1.649E-03	2.638E-04	1.575	0.53	301
54.992	54.167	11.841	9.531E-03	1.196E-01	1.093E-01	1.582E-03	2.532E-04	1.532	0.53	293

Table K.4 65% glycerine flow rate measurement results

65 % Glycerine	
Orifice d (m)	0.02
Orifice A (m ²)	3.142E-04
Tank A (m ²)	0.16
μ (Pa.s)	0.019
Density (kg/m ³)	1179
Gravity (m/s ²)	9.81

Time	Time difference	Mass of glycerine in tank	Volume of glycerine in tank	Height of glycerine in tank	Height difference	Velocity in tank	Flow in tank	Velocity in orifice	C _d	Re
s	s	kg	m ³	m	m	m/s	m ³ /s	m/s		
0.825	0.000	56.353	4.781E-02	3.588E-01	0.000E+00	4.022E-03	6.435E-04	2.653	0.77	3258
4.158	3.333	53.867	4.570E-02	3.456E-01	1.319E-02	3.942E-03	6.308E-04	2.604	0.77	3197
7.492	6.667	51.440	4.364E-02	3.328E-01	2.605E-02	3.863E-03	6.180E-04	2.555	0.77	3137
10.825	10.000	49.060	4.162E-02	3.201E-01	3.867E-02	3.783E-03	6.052E-04	2.506	0.77	3077
14.158	13.333	46.735	3.965E-02	3.078E-01	5.100E-02	3.703E-03	5.925E-04	2.457	0.77	3017
17.492	16.667	44.427	3.769E-02	2.956E-01	6.324E-02	3.623E-03	5.797E-04	2.408	0.77	2957
20.825	20.000	42.204	3.581E-02	2.838E-01	7.503E-02	3.544E-03	5.670E-04	2.360	0.76	2897
24.158	23.333	40.035	3.397E-02	2.723E-01	8.653E-02	3.464E-03	5.542E-04	2.311	0.76	2838
27.492	26.667	37.928	3.218E-02	2.611E-01	9.770E-02	3.384E-03	5.415E-04	2.263	0.76	2779
30.825	30.000	35.825	3.039E-02	2.500E-01	1.088E-01	3.304E-03	5.287E-04	2.215	0.76	2719
34.158	33.333	33.810	2.868E-02	2.393E-01	1.195E-01	3.225E-03	5.159E-04	2.167	0.76	2660
37.492	36.667	31.840	2.701E-02	2.288E-01	1.300E-01	3.145E-03	5.032E-04	2.119	0.76	2602
40.825	40.000	29.910	2.538E-02	2.186E-01	1.402E-01	3.065E-03	4.904E-04	2.071	0.75	2543

Table K.5 2.4% CMC flow rate measurement results

2.4 % CMC	
Orifice d (m)	0.02
Orifice A (m ²)	3.142E-04
Tank A (m ²)	0.16
Density (kg/m ³)	1014
Gravity (m/s ²)	9.81
k (Pa.s ⁿ)	0.006
n (-)	1

Time	Time difference	Mass of CMC in tank	Volume of CMC in tank	Height of CMC in tank	Height difference	Velocity in tank	Flow in tank	Velocity in orifice	C _d	Re
s	s	kg	m ³	m	m	m/s	m ³ /s	m/s		
0.825	0.000	64.534	6.362E-02	4.577E-01	0.000E+00	4.597E-03	7.355E-04	2.997	0.78	10534
5.825	5.000	60.833	5.998E-02	4.348E-01	2.281E-02	4.479E-03	7.167E-04	2.921	0.78	10268
10.825	10.000	57.255	5.645E-02	4.128E-01	4.486E-02	4.361E-03	6.978E-04	2.846	0.78	10005
15.825	15.000	53.757	5.300E-02	3.912E-01	6.641E-02	4.244E-03	6.790E-04	2.771	0.78	9740
20.825	20.000	50.389	4.968E-02	3.705E-01	8.716E-02	4.126E-03	6.601E-04	2.696	0.78	9478
25.825	25.000	47.095	4.643E-02	3.502E-01	1.075E-01	4.008E-03	6.413E-04	2.621	0.78	9215
30.825	30.000	43.862	4.324E-02	3.303E-01	1.274E-01	3.890E-03	6.224E-04	2.546	0.78	8949
35.825	35.000	40.777	4.020E-02	3.113E-01	1.464E-01	3.772E-03	6.036E-04	2.471	0.78	8688
40.825	40.000	37.744	3.721E-02	2.926E-01	1.651E-01	3.655E-03	5.847E-04	2.396	0.78	8423
45.825	45.000	34.824	3.433E-02	2.746E-01	1.831E-01	3.537E-03	5.659E-04	2.321	0.78	8160
50.825	50.000	31.988	3.154E-02	2.571E-01	2.005E-01	3.419E-03	5.470E-04	2.246	0.78	7896
55.825	55.000	29.275	2.886E-02	2.404E-01	2.173E-01	3.301E-03	5.282E-04	2.172	0.77	7635
60.825	60.000	26.658	2.628E-02	2.243E-01	2.334E-01	3.183E-03	5.093E-04	2.098	0.77	7374
65.825	65.000	24.126	2.379E-02	2.087E-01	2.490E-01	3.066E-03	4.905E-04	2.023	0.77	7113
70.825	70.000	21.672	2.137E-02	1.935E-01	2.641E-01	2.948E-03	4.716E-04	1.949	0.77	6850
75.825	75.000	19.343	1.907E-02	1.792E-01	2.785E-01	2.830E-03	4.528E-04	1.875	0.77	6592

Table K.6 5.2% CMC flow rate measurement results

5.21 % CMC	
Orifice d (m)	0.02
Orifice A (m ²)	3.142E-04
Tank A (m ²)	0.16
Density (kg/m ³)	1029
Gravity (m/s ²)	9.81
k (Pa.s ⁿ)	0.210
n (-)	0.791

Time	Time difference	Mass of CMC in tank	Volume of CMC in tank	Height of CMC in tank	Height difference	Velocity in tank	Flow in tank	Velocity in orifice	C _d	Re
s	s	kg	m ³	m	m	m/s	m ³ /s	m/s		
0.825	0.000	54.961	5.339E-02	4.337E-01	0.000E+00	3.852E-03	6.163E-04	2.917	0.71	1192
5.825	5.000	51.837	5.036E-02	4.147E-01	1.897E-02	3.752E-03	6.003E-04	2.853	0.71	1160
10.825	10.000	48.783	4.739E-02	3.962E-01	3.751E-02	3.652E-03	5.843E-04	2.788	0.71	1128
15.825	15.000	45.826	4.452E-02	3.782E-01	5.546E-02	3.551E-03	5.682E-04	2.724	0.70	1097
20.825	20.000	42.945	4.172E-02	3.607E-01	7.296E-02	3.451E-03	5.522E-04	2.660	0.70	1066
25.825	25.000	40.090	3.895E-02	3.434E-01	9.029E-02	3.351E-03	5.362E-04	2.596	0.70	1035
30.825	30.000	37.427	3.636E-02	3.272E-01	1.065E-01	3.251E-03	5.201E-04	2.534	0.69	1005
35.825	35.000	34.779	3.379E-02	3.112E-01	1.225E-01	3.151E-03	5.041E-04	2.471	0.69	975
40.825	40.000	32.228	3.131E-02	2.957E-01	1.380E-01	3.050E-03	4.881E-04	2.409	0.69	945
45.825	45.000	29.760	2.891E-02	2.807E-01	1.530E-01	2.950E-03	4.720E-04	2.347	0.68	916
50.825	50.000	27.388	2.661E-02	2.663E-01	1.674E-01	2.850E-03	4.560E-04	2.286	0.68	887
55.825	55.000	25.058	2.434E-02	2.521E-01	1.816E-01	2.750E-03	4.400E-04	2.224	0.67	859
60.825	60.000	22.835	2.218E-02	2.386E-01	1.951E-01	2.650E-03	4.239E-04	2.164	0.66	831
65.825	65.000	20.669	2.008E-02	2.255E-01	2.082E-01	2.549E-03	4.079E-04	2.103	0.66	803
70.825	70.000	18.653	1.812E-02	2.133E-01	2.204E-01	2.449E-03	3.919E-04	2.045	0.65	776

Table K.7 6.6% CMC flow rate measurement results

6.6 % CMC	
Orifice d (m)	0.02
Orifice A (m ²)	3.142E-04
Tank A (m ²)	0.16
Density (kg/m ³)	1037
Gravity (m/s ²)	9.81
k (Pa.s ⁿ)	0.881
n (-)	0.701

Time	Time difference	Mass of CMC in tank	Volume of CMC in tank	Height of CMC in tank	Height difference	Velocity in tank	Flow in tank	Velocity in orifice	C _d	Re
s	s	kg	m ³	m	m	m/s	m ³ /s	m/s		
0.825	0.000	50.421	4.862E-02	3.639E-01	0.000E+00	2.758E-03	4.413E-04	2.672	0.53	472
8.325	7.500	46.973	4.530E-02	3.431E-01	2.078E-02	2.653E-03	4.245E-04	2.595	0.52	454
15.825	15.000	43.711	4.215E-02	3.234E-01	4.044E-02	2.548E-03	4.077E-04	2.519	0.52	437
23.325	22.500	40.560	3.911E-02	3.045E-01	5.944E-02	2.443E-03	3.910E-04	2.444	0.51	420
30.825	30.000	37.604	3.626E-02	2.866E-01	7.725E-02	2.339E-03	3.742E-04	2.371	0.50	404
38.325	37.500	34.738	3.350E-02	2.694E-01	9.452E-02	2.234E-03	3.574E-04	2.299	0.49	388
45.825	45.000	32.086	3.094E-02	2.534E-01	1.105E-01	2.129E-03	3.406E-04	2.230	0.49	373
53.325	52.500	29.534	2.848E-02	2.380E-01	1.259E-01	2.024E-03	3.238E-04	2.161	0.48	358
60.825	60.000	27.088	2.612E-02	2.233E-01	1.406E-01	1.919E-03	3.071E-04	2.093	0.47	343
68.325	67.500	24.758	2.387E-02	2.092E-01	1.547E-01	1.814E-03	2.903E-04	2.026	0.46	329
75.825	75.000	22.600	2.179E-02	1.962E-01	1.677E-01	1.709E-03	2.735E-04	1.962	0.44	316
83.325	82.500	20.520	1.979E-02	1.837E-01	1.802E-01	1.605E-03	2.567E-04	1.898	0.43	303
90.825	90.000	18.563	1.790E-02	1.719E-01	1.920E-01	1.500E-03	2.400E-04	1.836	0.42	290
98.325	97.500	16.738	1.614E-02	1.609E-01	2.030E-01	1.395E-03	2.232E-04	1.777	0.40	278
105.825	105.000	15.005	1.447E-02	1.504E-01	2.135E-01	1.290E-03	2.064E-04	1.718	0.38	266

Table K.8 7.6% CMC flow rate measurement results

7.6 % CMC	
Orifice d (m)	0.02
Orifice A (m ²)	3.142E-04
Tank A (m ²)	0.16
Density (kg/m ³)	1042
Gravity (m/s ²)	9.81
k (Pa.s ⁿ)	2.394
n (-)	0.636

Time	Time difference	Mass of CMC in tank	Volume of CMC in tank	Height of CMC in tank	Height difference	Velocity in tank	Flow in tank	Velocity in orifice	C _d	Re
s	s	kg	m ³	m	m	m/s	m ³ /s	m/s		
0.825	0.000	45.478	4.366E-02	3.329E-01	0.000E+00	1.921E-03	3.074E-04	2.556	0.38	255
10.825	10.000	42.212	4.053E-02	3.133E-01	1.960E-02	1.835E-03	2.936E-04	2.479	0.38	245
20.825	20.000	39.123	3.756E-02	2.948E-01	3.813E-02	1.749E-03	2.799E-04	2.405	0.37	235
30.825	30.000	36.211	3.477E-02	2.773E-01	5.561E-02	1.663E-03	2.662E-04	2.332	0.36	225
40.825	40.000	33.484	3.215E-02	2.609E-01	7.197E-02	1.578E-03	2.524E-04	2.263	0.36	216
50.825	50.000	30.936	2.970E-02	2.456E-01	8.726E-02	1.492E-03	2.387E-04	2.195	0.35	207
60.825	60.000	28.544	2.740E-02	2.313E-01	1.016E-01	1.406E-03	2.250E-04	2.130	0.34	199
70.825	70.000	26.321	2.527E-02	2.179E-01	1.150E-01	1.320E-03	2.112E-04	2.068	0.33	191
80.825	80.000	24.250	2.328E-02	2.055E-01	1.274E-01	1.234E-03	1.975E-04	2.008	0.31	184
90.825	90.000	22.315	2.142E-02	1.939E-01	1.390E-01	1.148E-03	1.838E-04	1.950	0.30	176
100.825	100.000	20.518	1.970E-02	1.831E-01	1.498E-01	1.063E-03	1.700E-04	1.895	0.29	170
110.825	110.000	18.856	1.810E-02	1.731E-01	1.597E-01	9.768E-04	1.563E-04	1.843	0.27	163
120.825	120.000	17.302	1.661E-02	1.638E-01	1.691E-01	8.909E-04	1.425E-04	1.793	0.25	157
130.825	130.000	15.870	1.524E-02	1.552E-01	1.777E-01	8.051E-04	1.288E-04	1.745	0.23	152
140.825	140.000	14.540	1.396E-02	1.472E-01	1.856E-01	7.192E-04	1.151E-04	1.700	0.22	146
150.825	150.000	13.311	1.278E-02	1.399E-01	1.930E-01	6.334E-04	1.013E-04	1.657	0.19	141
160.825	160.000	12.156	1.167E-02	1.329E-01	1.999E-01	5.476E-04	8.761E-05	1.615	0.17	136

Table K.9 13.1% kaolin flow rate measurement results

13.1 % Kaolin	
Orifice d (m)	0.02
Orifice A (m ²)	3.142E-04
Tank A (m ²)	0.16
Density (kg/m ³)	1217
Gravity (m/s ²)	9.81
τ (Pa)	8.901
k(Pa.sn)	0.067
n (-)	0.716

Time	Time difference	Mass of Kaolin in tank	Volume of Kaolin in tank	Height of Kaolin in tank	Height difference	Velocity in tank	Flow in tank	Velocity in orifice	C_d	Re
s	s	kg	m ³	m	m	m/s	m ³ /s	m/s		
0.825	0.000	57.397	4.716E-02	3.948E-01	0.000E+00	4.037E-03	6.459E-04	2.783	0.77	3949
5.825	5.000	53.496	4.396E-02	3.747E-01	2.004E-02	3.925E-03	6.280E-04	2.711	0.77	3786
10.825	10.000	49.694	4.083E-02	3.552E-01	3.956E-02	3.813E-03	6.101E-04	2.640	0.77	3625
15.825	15.000	45.983	3.778E-02	3.361E-01	5.862E-02	3.702E-03	5.923E-04	2.568	0.76	3466
20.825	20.000	42.438	3.487E-02	3.179E-01	7.683E-02	3.590E-03	5.744E-04	2.498	0.76	3312
25.825	25.000	38.983	3.203E-02	3.002E-01	9.457E-02	3.478E-03	5.565E-04	2.427	0.76	3161
30.825	30.000	35.632	2.928E-02	2.830E-01	1.118E-01	3.366E-03	5.386E-04	2.356	0.76	3012
35.825	35.000	32.398	2.662E-02	2.664E-01	1.284E-01	3.254E-03	5.207E-04	2.286	0.76	2866
40.825	40.000	29.285	2.406E-02	2.504E-01	1.444E-01	3.143E-03	5.028E-04	2.216	0.75	2724
45.825	45.000	26.228	2.155E-02	2.347E-01	1.601E-01	3.031E-03	4.849E-04	2.146	0.75	2582
50.825	50.000	23.321	1.916E-02	2.198E-01	1.750E-01	2.919E-03	4.670E-04	2.076	0.75	2446
55.825	55.000	20.499	1.684E-02	2.053E-01	1.895E-01	2.807E-03	4.492E-04	2.007	0.74	2311

Table K.10 20.4% kaolin flow rate measurement results

20.4 % Kaolin	
Orifice d (m)	0.02
Orifice A (m ²)	3.142E-04
Tank A (m ²)	0.16
Density (kg/m ³)	1336
Gravity (m/s ²)	9.81
τ (Pa)	39.420
k(Pa.s ⁿ)	3.964
n (-)	0.365

Time	Time difference	Mass of Kaolin in tank	Volume of Kaolin in Tank	Height of kaolin in tank	Height difference	Velocity in Tank	Flow in Tank	Velocity in orifice	C _d	Re
s	s	kg	m ³	m	m	m/s	m ³ /s	m/s		
0.825	0.000	58.647	4.391E-02	3.345E-01	0.000E+00	3.452E-03	5.523E-04	2.562	0.69	787
5.825	5.000	54.913	4.112E-02	3.170E-01	1.747E-02	3.328E-03	5.324E-04	2.494	0.68	750
10.825	10.000	51.280	3.840E-02	3.000E-01	3.448E-02	3.203E-03	5.125E-04	2.426	0.67	714
15.825	15.000	47.756	3.576E-02	2.835E-01	5.097E-02	3.079E-03	4.926E-04	2.358	0.66	679
20.825	20.000	44.630	3.342E-02	2.689E-01	6.560E-02	2.954E-03	4.727E-04	2.297	0.66	647
25.825	25.000	41.797	3.130E-02	2.556E-01	7.885E-02	2.830E-03	4.528E-04	2.239	0.64	618
30.825	30.000	38.993	2.920E-02	2.425E-01	9.198E-02	2.706E-03	4.329E-04	2.181	0.63	590
35.825	35.000	36.335	2.721E-02	2.300E-01	1.044E-01	2.581E-03	4.130E-04	2.124	0.62	562
40.825	40.000	33.821	2.532E-02	2.183E-01	1.162E-01	2.457E-03	3.931E-04	2.069	0.60	536
45.825	45.000	31.424	2.353E-02	2.071E-01	1.274E-01	2.332E-03	3.732E-04	2.016	0.59	511
50.825	50.000	29.152	2.183E-02	1.964E-01	1.380E-01	2.208E-03	3.533E-04	1.963	0.57	488
55.825	55.000	27.007	2.022E-02	1.864E-01	1.481E-01	2.084E-03	3.334E-04	1.912	0.55	465
60.825	60.000	24.961	1.869E-02	1.768E-01	1.576E-01	1.959E-03	3.135E-04	1.863	0.54	443
65.825	65.000	23.082	1.728E-02	1.680E-01	1.664E-01	1.835E-03	2.936E-04	1.816	0.51	423
70.825	70.000	21.262	1.592E-02	1.595E-01	1.749E-01	1.710E-03	2.737E-04	1.769	0.49	404

Table K.11 7.2% bentonite flow rate measurement results

7.2 % Bentonite	
Orifice d (m)	0.02
Orifice A (m ²)	3.142E-04
Tank A (m ²)	0.16
Density (kg/m ³)	1044
Gravity (m/s ²)	9.81
τ (Pa)	15.738
k(Pa.s ⁿ)	0.014
n (-)	1

Time	Time difference	Mass of Bentonite in tank	Volume of Bentonite in Tank	Height of bentonite in tank	Height difference	Velocity in Tank	Flow in Tank	Velocity in orifice	C _d	Re
s	s	kg	m ³	m	m	m/s	m ³ /s	m/s		
0.825	0.000	60.049	5.752E-02	4.195E-01	0.000E+00	4.166E-03	6.666E-04	2.869	0.74	2180
4.992	4.167	57.230	5.482E-02	4.026E-01	1.688E-02	4.072E-03	6.515E-04	2.811	0.74	2114
9.158	8.333	54.484	5.219E-02	3.862E-01	3.331E-02	3.978E-03	6.365E-04	2.753	0.74	2049
13.325	12.500	51.794	4.961E-02	3.701E-01	4.942E-02	3.884E-03	6.214E-04	2.695	0.73	1984
17.492	16.667	49.210	4.714E-02	3.546E-01	6.489E-02	3.790E-03	6.064E-04	2.638	0.73	1920
21.658	20.833	46.668	4.470E-02	3.394E-01	8.011E-02	3.696E-03	5.914E-04	2.580	0.73	1857
25.825	25.000	44.124	4.226E-02	3.242E-01	9.534E-02	3.602E-03	5.763E-04	2.522	0.73	1793
29.992	29.167	41.717	3.996E-02	3.097E-01	1.097E-01	3.508E-03	5.613E-04	2.465	0.72	1732
34.158	33.333	39.362	3.770E-02	2.956E-01	1.238E-01	3.414E-03	5.462E-04	2.408	0.72	1671
38.325	37.500	37.064	3.550E-02	2.819E-01	1.376E-01	3.320E-03	5.312E-04	2.352	0.72	1610
42.492	41.667	34.838	3.337E-02	2.686E-01	1.509E-01	3.226E-03	5.162E-04	2.295	0.72	1551
46.658	45.833	32.669	3.129E-02	2.556E-01	1.639E-01	3.132E-03	5.011E-04	2.239	0.71	1492
50.825	50.000	30.599	2.931E-02	2.432E-01	1.763E-01	3.038E-03	4.861E-04	2.184	0.71	1435
54.992	54.167	28.610	2.740E-02	2.313E-01	1.882E-01	2.944E-03	4.710E-04	2.130	0.70	1380
59.158	58.333	26.713	2.559E-02	2.199E-01	1.996E-01	2.850E-03	4.560E-04	2.077	0.70	1326
63.325	62.500	25.123	2.406E-02	2.104E-01	2.091E-01	2.756E-03	4.410E-04	2.032	0.69	1281
67.492	66.667	23.349	2.236E-02	1.998E-01	2.197E-01	2.662E-03	4.259E-04	1.980	0.68	1229

Table K.12 3.8% bentonite flow rate measurement results

3.8 % Bentonite	
Orifice d (m)	0.02
Orifice A (m ²)	3.142E-04
Tank A (m ²)	0.16
Density (kg/m ³)	1023
Gravity (m/s ²)	9.81
τ (Pa)	1.009
k(Pa.s ⁰)	0.007
n (-)	1

Time	Time difference	Mass of Bentonite in tank	Volume of Bentonite in Tank	Height of bentonite in tank	Height difference	Velocity in Tank	Flow in Tank	Velocity in orifice	C _d	Re
s	s	kg	m ³	m	m	m/s	m ³ /s	m/s		
0.825	0.000	44.813	4.381E-02	3.338E-01	0.000E+00	3.861E-03	6.178E-04	2.559	0.77	6930
5.825	5.000	41.717	4.078E-02	3.149E-01	1.892E-02	3.744E-03	5.990E-04	2.486	0.77	6705
10.825	10.000	38.679	3.781E-02	2.963E-01	3.748E-02	3.627E-03	5.803E-04	2.411	0.77	6478
15.825	15.000	35.765	3.496E-02	2.785E-01	5.529E-02	3.510E-03	5.616E-04	2.338	0.76	6253
20.825	20.000	32.961	3.222E-02	2.614E-01	7.242E-02	3.393E-03	5.429E-04	2.265	0.76	6030
25.825	25.000	30.218	2.954E-02	2.446E-01	8.918E-02	3.276E-03	5.242E-04	2.191	0.76	5805
30.825	30.000	27.577	2.696E-02	2.285E-01	1.053E-01	3.159E-03	5.054E-04	2.117	0.76	5582
35.825	35.000	25.050	2.449E-02	2.131E-01	1.208E-01	3.042E-03	4.867E-04	2.045	0.76	5360
40.825	40.000	22.605	2.210E-02	1.981E-01	1.357E-01	2.925E-03	4.680E-04	1.972	0.76	5139
45.825	45.000	20.259	1.981E-02	1.838E-01	1.500E-01	2.808E-03	4.493E-04	1.899	0.75	4919
50.825	50.000	18.014	1.761E-02	1.701E-01	1.637E-01	2.691E-03	4.306E-04	1.827	0.75	4700

Table K.13 7.3% bentonite flow rate measurement results

7.3 % Bentonite	
Orifice d (m)	0.02
Orifice A (m ²)	3.142E-04
Tank A (m ²)	0.16
Density (kg/m ³)	1046
Gravity (m/s ²)	9.81
τ (Pa)	30.493
k(Pa.s ⁿ)	0.021
n (-)	1

Time	Time difference	Mass of bentonite in tank	Volume of bentonite in Tank	Height of bentonite in tank	Height difference	Velocity in Tank	Flow in Tank	Velocity in orifice	C _d	Re
s	s	kg	m ³	m	m	m/s	m ³ /s	m/s		
0.825	0.000	97.988	9.368E-02	6.455E-01	0.000E+00	5.141E-03	8.226E-04	3.559	0.74	1770
9.158	8.333	91.284	8.727E-02	6.054E-01	4.006E-02	4.921E-03	7.874E-04	3.447	0.73	1686
17.492	16.667	84.773	8.105E-02	5.665E-01	7.896E-02	4.701E-03	7.522E-04	3.334	0.72	1603
25.825	25.000	78.426	7.498E-02	5.286E-01	1.169E-01	4.481E-03	7.170E-04	3.220	0.71	1520
34.158	33.333	72.363	6.918E-02	4.924E-01	1.531E-01	4.261E-03	6.818E-04	3.108	0.70	1440
42.492	41.667	66.497	6.357E-02	4.573E-01	1.882E-01	4.041E-03	6.466E-04	2.995	0.69	1360
50.825	50.000	60.909	5.823E-02	4.239E-01	2.216E-01	3.821E-03	6.114E-04	2.884	0.67	1282
59.158	58.333	55.596	5.315E-02	3.922E-01	2.533E-01	3.601E-03	5.762E-04	2.774	0.66	1206
67.492	66.667	50.455	4.824E-02	3.615E-01	2.840E-01	3.381E-03	5.410E-04	2.663	0.65	1131
75.825	75.000	45.918	4.390E-02	3.344E-01	3.111E-01	3.161E-03	5.058E-04	2.561	0.63	1063
84.159	83.334	41.882	4.004E-02	3.102E-01	3.352E-01	2.941E-03	4.706E-04	2.467	0.61	1001
92.492	91.667	38.029	3.636E-02	2.872E-01	3.583E-01	2.721E-03	4.354E-04	2.374	0.58	941
100.825	100.000	34.478	3.296E-02	2.660E-01	3.795E-01	2.501E-03	4.002E-04	2.285	0.56	885
109.159	108.334	31.151	2.978E-02	2.461E-01	3.994E-01	2.281E-03	3.650E-04	2.198	0.53	831
117.492	116.667	28.094	2.686E-02	2.279E-01	4.176E-01	2.061E-03	3.298E-04	2.114	0.50	780
125.825	125.000	25.302	2.419E-02	2.112E-01	4.343E-01	1.841E-03	2.946E-04	2.036	0.46	733

Appendix L. Flow rate measurements using aspect ratio of 5

Table L.1 100% glycerine flow rate measurement results

100% Glycerine	
Orifice d (m)	0.02
Orifice A (m ²)	3.142E-04
Tank A (m ²)	0.16
μ (Pa.s)	0.968
Density (Kg/m ³)	1258
Gravity (m/s ²)	9.81

Time	Time difference	Mass of glycerine in tank	Volume of glycerine in tank	Height of glycerine in tank	Height difference	Velocity in tank	Flow in tank	Velocity in orifice	C _d	Re
s	s	kg	m ³	m	m	m/s	m ³ /s	m/s		
3.325	0.000	35.412	2.815E-02	2.760E-01	0.000E+00	7.213E-04	1.154E-04	2.327	0.16	60
18.325	15.000	33.293	2.647E-02	2.654E-01	1.053E-02	6.989E-04	1.118E-04	2.282	0.16	59
33.325	30.000	31.195	2.480E-02	2.550E-01	2.096E-02	6.764E-04	1.082E-04	2.237	0.15	58
48.325	45.000	29.175	2.320E-02	2.450E-01	3.099E-02	6.540E-04	1.046E-04	2.192	0.15	57
63.325	60.000	27.236	2.165E-02	2.353E-01	4.062E-02	6.316E-04	1.011E-04	2.149	0.15	56
78.325	75.000	25.364	2.017E-02	2.260E-01	4.993E-02	6.092E-04	9.747E-05	2.106	0.15	55
93.325	90.000	23.571	1.874E-02	2.171E-01	5.884E-02	5.867E-04	9.388E-05	2.064	0.14	54
108.325	105.000	21.839	1.736E-02	2.085E-01	6.744E-02	5.643E-04	9.029E-05	2.023	0.14	53
123.325	120.000	20.173	1.604E-02	2.002E-01	7.572E-02	5.419E-04	8.670E-05	1.982	0.14	52
138.325	135.000	18.573	1.477E-02	1.923E-01	8.367E-02	5.195E-04	8.312E-05	1.942	0.14	50
153.325	150.000	17.026	1.354E-02	1.846E-01	9.136E-02	4.970E-04	7.953E-05	1.903	0.13	49
168.325	165.000	15.544	1.236E-02	1.772E-01	9.872E-02	4.746E-04	7.594E-05	1.865	0.13	48
183.325	180.000	14.106	1.121E-02	1.701E-01	1.059E-01	4.522E-04	7.235E-05	1.827	0.13	47
198.325	195.000	12.740	1.013E-02	1.633E-01	1.127E-01	4.298E-04	6.876E-05	1.790	0.12	47
213.325	210.000	11.422	9.081E-03	1.568E-01	1.192E-01	4.073E-04	6.518E-05	1.754	0.12	46
228.325	225.000	10.157	8.075E-03	1.505E-01	1.255E-01	3.849E-04	6.159E-05	1.718	0.11	45

Table L.2 96% glycerine flow rate measurement results

93 % Glycerine	
Orifice d (m)	0.02
Orifice A (m ²)	3.142E-04
Tank A (m ²)	0.16
μ (Pa.s)	0.130
Density (Kg/m ³)	1242
Gravity (m/s ²)	9.81

Time	Time difference	Mass of glycerine in tank	Volume of glycerine in tank	Height of glycerine in tank	Height difference	Velocity in tank	Flow in tank	Velocity in orifice	C _d	Re
s	s	kg	m ³	m	m	m/s	m ³ /s	m/s		
0.825	0.000	33.008	2.657E-02	2.660E-01	0.000E+00	2.403E-03	3.845E-04	2.285	0.54	437
4.158	3.333	31.439	2.531E-02	2.582E-01	7.890E-03	2.357E-03	3.771E-04	2.251	0.53	430
7.492	6.667	29.883	2.405E-02	2.503E-01	1.572E-02	2.311E-03	3.697E-04	2.216	0.53	424
10.825	10.000	28.357	2.282E-02	2.427E-01	2.339E-02	2.265E-03	3.624E-04	2.182	0.53	417
14.158	13.333	26.894	2.165E-02	2.353E-01	3.075E-02	2.219E-03	3.550E-04	2.149	0.53	411
17.492	16.667	25.415	2.046E-02	2.279E-01	3.820E-02	2.173E-03	3.476E-04	2.114	0.52	404
20.825	20.000	24.013	1.933E-02	2.208E-01	4.525E-02	2.127E-03	3.403E-04	2.081	0.52	398
24.158	23.333	22.623	1.821E-02	2.138E-01	5.224E-02	2.081E-03	3.329E-04	2.048	0.52	391
27.492	26.667	21.226	1.708E-02	2.068E-01	5.927E-02	2.035E-03	3.255E-04	2.014	0.51	385
30.825	30.000	19.917	1.603E-02	2.002E-01	6.585E-02	1.989E-03	3.182E-04	1.982	0.51	379
34.158	33.333	18.624	1.499E-02	1.937E-01	7.236E-02	1.943E-03	3.108E-04	1.949	0.51	373
37.492	36.667	17.352	1.397E-02	1.873E-01	7.876E-02	1.896E-03	3.034E-04	1.917	0.50	366
40.825	40.000	16.090	1.295E-02	1.809E-01	8.510E-02	1.850E-03	2.961E-04	1.884	0.50	360
44.158	43.333	14.884	1.198E-02	1.749E-01	9.117E-02	1.804E-03	2.887E-04	1.852	0.50	354
47.492	46.667	13.722	1.104E-02	1.690E-01	9.702E-02	1.758E-03	2.813E-04	1.821	0.49	348
50.825	50.000	12.552	1.010E-02	1.631E-01	1.029E-01	1.712E-03	2.740E-04	1.789	0.49	342

Table L.3 93% glycerine flow rate measurement results

93 % Glycerine	
Orifice d (m)	0.02
Orifice A (m ²)	3.142E-04
Tank A (m ²)	0.16
μ (Pa.s)	0.130
Density (Kg/m ³)	1242
Gravity (m/s ²)	9.81

Time	Time difference	Mass of glycerine in tank	Volume of glycerine in tank	Height of glycerine in tank	Height difference	Velocity in tank	Flow in tank	Velocity in orifice	C _d	Re
s	s	kg	m ³	m	m	m/s	m ³ /s	m/s		
0.825	0.000	33.008	2.657E-02	2.660E-01	0.000E+00	2.403E-03	3.845E-04	2.285	0.54	437
4.158	3.333	31.439	2.531E-02	2.582E-01	7.890E-03	2.357E-03	3.771E-04	2.251	0.53	430
7.492	6.667	29.883	2.405E-02	2.503E-01	1.572E-02	2.311E-03	3.697E-04	2.216	0.53	424
10.825	10.000	28.357	2.282E-02	2.427E-01	2.339E-02	2.265E-03	3.624E-04	2.182	0.53	417
14.158	13.333	26.894	2.165E-02	2.353E-01	3.075E-02	2.219E-03	3.550E-04	2.149	0.53	411
17.492	16.667	25.415	2.046E-02	2.279E-01	3.820E-02	2.173E-03	3.476E-04	2.114	0.52	404
20.825	20.000	24.013	1.933E-02	2.208E-01	4.525E-02	2.127E-03	3.403E-04	2.081	0.52	398
24.158	23.333	22.623	1.821E-02	2.138E-01	5.224E-02	2.081E-03	3.329E-04	2.048	0.52	391
27.492	26.667	21.226	1.708E-02	2.068E-01	5.927E-02	2.035E-03	3.255E-04	2.014	0.51	385
30.825	30.000	19.917	1.603E-02	2.002E-01	6.585E-02	1.989E-03	3.182E-04	1.982	0.51	379
34.158	33.333	18.624	1.499E-02	1.937E-01	7.236E-02	1.943E-03	3.108E-04	1.949	0.51	373
37.492	36.667	17.352	1.397E-02	1.873E-01	7.876E-02	1.896E-03	3.034E-04	1.917	0.50	366
40.825	40.000	16.090	1.295E-02	1.809E-01	8.510E-02	1.850E-03	2.961E-04	1.884	0.50	360
44.158	43.333	14.884	1.198E-02	1.749E-01	9.117E-02	1.804E-03	2.887E-04	1.852	0.50	354
47.492	46.667	13.722	1.104E-02	1.690E-01	9.702E-02	1.758E-03	2.813E-04	1.821	0.49	348
50.825	50.000	12.552	1.010E-02	1.631E-01	1.029E-01	1.712E-03	2.740E-04	1.789	0.49	342

Table L.4 65% glycerine flow rate measurement results

65 % glycerine	
Orifice d (m)	0.02
Orifice A (m ²)	3.142E-04
Tank A (m ²)	0.16
μ (Pa.s)	0.019
Density (Kg/m ³)	1179
Gravity (m/s ²)	9.81

Time	Time difference	Mass of glycerine in tank	Volume of glycerine in tank	Height of glycerine in tank	Height difference	Velocity in tank	Flow in tank	Velocity in orifice	C _d	Re
s	s	kg	m ³	m	m	m/s	m ³ /s	m/s		
0.825	0.000	54.744	4.644E-02	3.903E-01	0.000E+00	3.998E-03	6.397E-04	2.767	0.74	3398
5.825	5.000	51.021	4.329E-02	3.705E-01	1.974E-02	3.891E-03	6.226E-04	2.696	0.74	3311
10.825	10.000	47.412	4.022E-02	3.514E-01	3.888E-02	3.785E-03	6.056E-04	2.626	0.73	3224
15.825	15.000	43.891	3.724E-02	3.327E-01	5.755E-02	3.678E-03	5.886E-04	2.555	0.73	3137
20.825	20.000	40.469	3.433E-02	3.146E-01	7.569E-02	3.572E-03	5.715E-04	2.484	0.73	3050
25.825	25.000	37.153	3.152E-02	2.970E-01	9.327E-02	3.465E-03	5.545E-04	2.414	0.73	2964
30.825	30.000	33.934	2.879E-02	2.799E-01	1.103E-01	3.359E-03	5.374E-04	2.344	0.73	2877
35.825	35.000	30.804	2.613E-02	2.633E-01	1.269E-01	3.252E-03	5.204E-04	2.273	0.73	2791
40.825	40.000	27.820	2.360E-02	2.475E-01	1.428E-01	3.146E-03	5.034E-04	2.204	0.73	2706
45.825	45.000	24.879	2.111E-02	2.319E-01	1.584E-01	3.039E-03	4.863E-04	2.133	0.73	2619
50.825	50.000	22.058	1.871E-02	2.170E-01	1.733E-01	2.933E-03	4.693E-04	2.063	0.72	2533
55.825	55.000	19.363	1.643E-02	2.027E-01	1.876E-01	2.826E-03	4.522E-04	1.994	0.72	2448

Table L.5 2.4% CMC flow rate measurement results

2.4 % CMC	
Orifice d (m)	0.02
Orifice A (m ²)	0.0003
Tank A (m ²)	0.16
Density (Kg/m ³)	1014
Gravity (m/s ²)	9.81
k (Pa.s ⁿ)	0.01
n (-)	1

Time	Time difference	Mass of CMC in tank	Volume of CMC in tank	Height of CMC in tank	Height difference	Velocity in tank	Flow in tank	Velocity in orifice	C _d	Re
s	s	kg	m ³	m	m	m/s	m ³ /s	m/s		
0.825	0.000	92.793	9.148E-02	6.718E-01	0.000E+00	5.467E-03	8.747E-04	3.630	0.74	3398
7.492	6.667	86.965	8.574E-02	6.359E-01	3.591E-02	5.314E-03	8.502E-04	3.532	0.74	3311
14.158	13.333	81.308	8.016E-02	6.010E-01	7.077E-02	5.160E-03	8.257E-04	3.434	0.74	3224
20.825	20.000	75.793	7.472E-02	5.670E-01	1.047E-01	5.007E-03	8.011E-04	3.335	0.74	3137
27.492	26.667	70.455	6.946E-02	5.341E-01	1.376E-01	4.854E-03	7.766E-04	3.237	0.74	3050
34.158	33.333	65.291	6.437E-02	5.023E-01	1.695E-01	4.700E-03	7.521E-04	3.139	0.74	2964
40.825	40.000	60.298	5.945E-02	4.715E-01	2.002E-01	4.547E-03	7.275E-04	3.042	0.74	2877
47.492	46.667	55.460	5.468E-02	4.417E-01	2.300E-01	4.394E-03	7.030E-04	2.944	0.74	2791
54.158	53.333	50.790	5.007E-02	4.130E-01	2.588E-01	4.240E-03	6.785E-04	2.846	0.74	2706
60.825	60.000	46.266	4.561E-02	3.851E-01	2.867E-01	4.087E-03	6.539E-04	2.749	0.74	2619
67.492	66.667	41.957	4.137E-02	3.585E-01	3.132E-01	3.934E-03	6.294E-04	2.652	0.74	2533
74.158	73.333	37.776	3.724E-02	3.328E-01	3.390E-01	3.780E-03	6.049E-04	2.555	0.74	2448
80.825	80.000	33.758	3.328E-02	3.080E-01	3.638E-01	3.627E-03	5.803E-04	2.458	0.74	8642
87.492	86.667	29.948	2.953E-02	2.845E-01	3.872E-01	3.474E-03	5.558E-04	2.363	0.74	8306
94.159	93.334	26.242	2.587E-02	2.617E-01	4.101E-01	3.320E-03	5.313E-04	2.266	0.74	7966
100.825	100.000	22.727	2.241E-02	2.400E-01	4.317E-01	3.167E-03	5.067E-04	2.170	0.74	7629
107.492	106.667	19.403	1.913E-02	2.196E-01	4.522E-01	3.014E-03	4.822E-04	2.076	0.74	7297

Table L.6 5.2% CMC flow rate measurement results

5.2 % CMC	
Orifice d (m)	0.02
Orifice A (m ²)	3.142E-04
Tank A (m ²)	0.16
Density (Kg/m ³)	1029
Gravity (m/s ²)	9.81
k (Pa.s ⁿ)	0.210
n (-)	0.795

Time	Time difference	Mass of CMC in tank	Volume of CMC in tank	Height of CMC in tank	Height difference	Velocity in tank	Flow in tank	Velocity in orifice	C _d	Re
s	s	kg	m ³	m	m	m/s	m ³ /s	m/s		
0.825	0.000	54.961	5.339E-02	4.337E-01	0.000E+00	3.882E-03	6.211E-04	2.917	0.68	1160
5.825	5.000	51.837	5.036E-02	4.147E-01	1.897E-02	3.781E-03	6.050E-04	2.853	0.68	1129
10.825	10.000	48.783	4.739E-02	3.962E-01	3.751E-02	3.680E-03	5.889E-04	2.788	0.67	1098
15.825	15.000	45.826	4.452E-02	3.782E-01	5.546E-02	3.580E-03	5.727E-04	2.724	0.67	1068
20.825	20.000	42.945	4.172E-02	3.607E-01	7.296E-02	3.479E-03	5.566E-04	2.660	0.67	1038
25.825	25.000	40.090	3.895E-02	3.434E-01	9.029E-02	3.378E-03	5.405E-04	2.596	0.66	1008
30.825	30.000	37.427	3.636E-02	3.272E-01	1.065E-01	3.277E-03	5.244E-04	2.534	0.66	979
35.825	35.000	34.779	3.379E-02	3.112E-01	1.225E-01	3.176E-03	5.082E-04	2.471	0.65	949
40.825	40.000	32.228	3.131E-02	2.957E-01	1.380E-01	3.076E-03	4.921E-04	2.409	0.65	921
45.825	45.000	29.760	2.891E-02	2.807E-01	1.530E-01	2.975E-03	4.760E-04	2.347	0.65	892
50.825	50.000	27.388	2.661E-02	2.663E-01	1.674E-01	2.874E-03	4.598E-04	2.286	0.64	864
55.825	55.000	25.058	2.434E-02	2.521E-01	1.816E-01	2.773E-03	4.437E-04	2.224	0.64	836
60.825	60.000	22.835	2.218E-02	2.386E-01	1.951E-01	2.672E-03	4.276E-04	2.164	0.63	809
65.825	65.000	20.669	2.008E-02	2.255E-01	2.082E-01	2.572E-03	4.115E-04	2.103	0.62	782
70.825	70.000	18.653	1.812E-02	2.133E-01	2.204E-01	2.471E-03	3.953E-04	2.045	0.62	756
75.825	75.000	16.645	1.617E-02	2.011E-01	2.326E-01	2.370E-03	3.792E-04	1.986	0.61	730

Table L.7 6.6% CMC flow rate measurement results

6.6 % CMC	
Orifice d (m)	0.02
Orifice A (m ²)	3.142E-04
Tank A (m ²)	0.16
Density (Kg/m ³)	1037
Gravity (m/s ²)	9.81
k (Pa.s ⁿ)	0.881
n (-)	0.701

Time	Time difference	Mass of CMC in tank	Volume of CMC in tank	Height of CMC in tank	Height difference	Velocity in tank	Flow in tank	Velocity in orifice	C _d	Re
s	s	kg	m ³	m	m	m/s	m ³ /s	m/s		
0.825	0.000	50.203	4.841E-02	4.026E-01	0.000E+00	2.521E-03	4.034E-04	2.810	0.46	504
8.325	7.500	47.115	4.543E-02	3.840E-01	1.861E-02	2.430E-03	3.888E-04	2.745	0.45	488
15.825	15.000	44.112	4.254E-02	3.659E-01	3.671E-02	2.339E-03	3.742E-04	2.679	0.44	473
23.325	22.500	41.249	3.978E-02	3.486E-01	5.397E-02	2.248E-03	3.597E-04	2.615	0.44	459
30.825	30.000	38.526	3.715E-02	3.322E-01	7.037E-02	2.157E-03	3.451E-04	2.553	0.43	444
38.325	37.500	35.938	3.466E-02	3.166E-01	8.597E-02	2.066E-03	3.305E-04	2.492	0.42	431
45.825	45.000	33.397	3.221E-02	3.013E-01	1.013E-01	1.975E-03	3.160E-04	2.431	0.41	417
53.325	52.500	31.003	2.990E-02	2.869E-01	1.157E-01	1.884E-03	3.014E-04	2.372	0.40	404
60.825	60.000	28.714	2.769E-02	2.731E-01	1.295E-01	1.793E-03	2.868E-04	2.315	0.39	391
68.325	67.500	26.553	2.561E-02	2.600E-01	1.425E-01	1.702E-03	2.722E-04	2.259	0.38	379
75.825	75.000	24.473	2.360E-02	2.475E-01	1.551E-01	1.610E-03	2.577E-04	2.204	0.37	367
83.325	82.500	22.505	2.170E-02	2.356E-01	1.669E-01	1.519E-03	2.431E-04	2.150	0.36	356

Table L.8 7.6% CMC flow rate measurement results

7.6 % CMC	
Orifice d (m)	0.02
Orifice A (m ²)	3.142E-04
Tank A (m ²)	0.16
Density (Kg/m ³)	1043
Gravity (m/s ²)	9.81
k (Pa.s ⁿ)	2.390
n (-)	0.636

Time	Time difference	Mass of CMC in tank	Volume of CMC in tank	Height of CMC in tank	Height difference	Velocity in tank	Flow in tank	Velocity in orifice	C _d	Re
s	s	kg	m ³	m	m	m/s	m ³ /s	m/s		
3.325	0.000	44.759	4.293E-02	3.683E-01	0.000E+00	1.501E-03	2.402E-04	2.688	0.28	274
18.325	15.000	40.926	3.925E-02	3.453E-01	2.298E-02	1.419E-03	2.270E-04	2.603	0.28	262
33.325	30.000	37.374	3.585E-02	3.240E-01	4.427E-02	1.337E-03	2.139E-04	2.521	0.27	251
48.325	45.000	34.104	3.271E-02	3.044E-01	6.388E-02	1.254E-03	2.007E-04	2.444	0.26	241
63.325	60.000	31.092	2.982E-02	2.864E-01	8.193E-02	1.172E-03	1.876E-04	2.370	0.25	231
78.325	75.000	28.318	2.716E-02	2.698E-01	9.856E-02	1.090E-03	1.744E-04	2.301	0.24	222
93.325	90.000	25.760	2.471E-02	2.544E-01	1.139E-01	1.008E-03	1.612E-04	2.234	0.23	213
108.325	105.000	23.414	2.246E-02	2.404E-01	1.280E-01	9.256E-04	1.481E-04	2.172	0.22	205
123.325	120.000	21.248	2.038E-02	2.274E-01	1.409E-01	8.434E-04	1.349E-04	2.112	0.20	197
138.325	135.000	19.263	1.848E-02	2.155E-01	1.528E-01	7.612E-04	1.218E-04	2.056	0.19	190
153.325	150.000	17.425	1.671E-02	2.045E-01	1.639E-01	6.790E-04	1.086E-04	2.003	0.17	183
168.325	165.000	15.726	1.508E-02	1.943E-01	1.740E-01	5.968E-04	9.549E-05	1.952	0.16	177
183.325	180.000	14.165	1.359E-02	1.849E-01	1.834E-01	5.146E-04	8.234E-05	1.905	0.14	171

Table L.9 13.1% Kaolin flow rate measurement results

13.1 % Kaolin	
Orifice d (m)	0.02
Orifice A (m ²)	3.142E-04
Tank A (m ²)	0.16
Density (Kg/m ³)	1224.4
Gravity (m/s ²)	9.81
τ (Pa)	8.901
k(Pa.sn)	0.067
n (-)	0.716

Time	Time difference	Mass of Kaolin in tank	Volume of Kaolin in tank	Height of Kaolin in tank	Height difference	Velocity in tank	Flow in tank	Velocity in orifice	C_d	Re
s	s	kg	m ³	m	m	m/s	m ³ /s	m/s		
0.825	0.000	57.397	4.688E-02	3.930E-01	0.000E+00	4.037E-03	6.459E-04	2.777	0.74	3959
5.825	5.000	53.496	4.369E-02	3.731E-01	1.992E-02	3.925E-03	6.280E-04	2.705	0.74	3795
10.825	10.000	49.694	4.059E-02	3.537E-01	3.932E-02	3.813E-03	6.101E-04	2.634	0.74	3634
15.825	15.000	45.983	3.756E-02	3.347E-01	5.826E-02	3.702E-03	5.923E-04	2.563	0.74	3475
20.825	20.000	42.438	3.466E-02	3.166E-01	7.636E-02	3.590E-03	5.744E-04	2.492	0.73	3321
25.825	25.000	38.983	3.184E-02	2.990E-01	9.400E-02	3.478E-03	5.565E-04	2.422	0.73	3169
30.825	30.000	35.632	2.910E-02	2.819E-01	1.111E-01	3.366E-03	5.386E-04	2.352	0.73	3020
35.825	35.000	32.398	2.646E-02	2.654E-01	1.276E-01	3.254E-03	5.207E-04	2.282	0.73	2874
40.825	40.000	29.285	2.392E-02	2.495E-01	1.435E-01	3.143E-03	5.028E-04	2.212	0.72	2732
45.825	45.000	26.228	2.142E-02	2.339E-01	1.591E-01	3.031E-03	4.849E-04	2.142	0.72	2590
50.825	50.000	23.321	1.905E-02	2.190E-01	1.739E-01	2.919E-03	4.670E-04	2.073	0.72	2454
55.825	55.000	20.499	1.674E-02	2.046E-01	1.883E-01	2.807E-03	4.492E-04	2.004	0.71	2319

Table L.10 20.4% Kaolin flow rate measurement results

20.4 % Kaolin	
Orifice d (m)	0.02
Orifice A (m ²)	3.142E-04
Tank A (m ²)	0.16
Density (Kg/m ³)	1336
Gravity (m/s ²)	9.81
τ (Pa)	41.484
k(Pa.sn)	3.164
n (-)	0.385

Time	Time difference	Mass of Kaolin in tank	Volume of Kaolin in Tank	Height of Kaolin in tank	Height difference	Velocity in Tank	Flow in Tank	Velocity in orifice	C _d	Re
s	s	kg	m ³	m	m	m/s	m ³ /s	m/s		
0.825	0.000	61.964	4.640E-02	3.900E-01	0.000E+00	3.452E-03	5.523E-04	2.766	0.64	925
8.325	7.500	56.299	4.215E-02	3.635E-01	2.651E-02	3.265E-03	5.225E-04	2.670	0.62	869
15.825	15.000	50.788	3.803E-02	3.377E-01	5.230E-02	3.079E-03	4.926E-04	2.574	0.61	813
23.325	22.500	45.630	3.417E-02	3.135E-01	7.644E-02	2.892E-03	4.628E-04	2.480	0.59	761
30.825	30.000	41.098	3.077E-02	2.923E-01	9.764E-02	2.706E-03	4.329E-04	2.395	0.58	714
38.325	37.500	37.131	2.780E-02	2.738E-01	1.162E-01	2.519E-03	4.030E-04	2.318	0.55	673
45.825	45.000	33.470	2.506E-02	2.566E-01	1.333E-01	2.332E-03	3.732E-04	2.244	0.53	635
53.325	52.500	30.084	2.253E-02	2.408E-01	1.492E-01	2.146E-03	3.433E-04	2.174	0.50	599
60.825	60.000	26.935	2.017E-02	2.260E-01	1.639E-01	1.959E-03	3.135E-04	2.106	0.47	566
68.325	67.500	24.030	1.799E-02	2.125E-01	1.775E-01	1.773E-03	2.836E-04	2.042	0.44	535
75.825	75.000	21.371	1.600E-02	2.000E-01	1.900E-01	1.586E-03	2.538E-04	1.981	0.41	507
83.325	82.500	18.949	1.419E-02	1.887E-01	2.013E-01	1.399E-03	2.239E-04	1.924	0.37	481
90.825	90.000	16.801	1.258E-02	1.786E-01	2.113E-01	1.213E-03	1.940E-04	1.872	0.33	458
98.325	97.500	14.810	1.109E-02	1.693E-01	2.207E-01	1.026E-03	1.642E-04	1.823	0.29	436
105.825	105.000	13.114	9.819E-03	1.614E-01	2.286E-01	8.396E-04	1.343E-04	1.779	0.24	417
113.325	112.500	11.655	8.727E-03	1.545E-01	2.354E-01	6.530E-04	1.045E-04	1.741	0.19	401

Table L.11 7.2% bentonite flow rate measurement results

7.2 % Bentonite	
Orifice d (m)	0.02
Orifice A (m ²)	3.142E-04
Tank A (m ²)	0.16
Density (Kg/m ³)	1045
Gravity (m/s ²)	9.81
τ (Pa)	15.738
k(Pa.sn)	0.014
n (-)	1

Time	Time difference	Mass of Bentonite in tank	Volume of Bentonite in Tank	Height of bentonite in tank	Height difference	Velocity in Tank	Flow in Tank	Velocity in orifice	C _d	Re
s	s	kg	m ³	m	m	m/s	m ³ /s	m/s		
0.825	0.000	58.987	5.644E-02	4.527E-01	0.000E+00	4.166E-03	6.666E-04	2.980	0.71	2311
4.992	4.167	56.132	5.370E-02	4.357E-01	1.707E-02	4.072E-03	6.515E-04	2.924	0.71	2245
9.158	8.333	53.348	5.104E-02	4.190E-01	3.372E-02	3.978E-03	6.365E-04	2.867	0.71	2181
13.325	12.500	50.616	4.843E-02	4.027E-01	5.006E-02	3.884E-03	6.214E-04	2.811	0.70	2117
17.492	16.667	47.935	4.586E-02	3.866E-01	6.609E-02	3.790E-03	6.064E-04	2.754	0.70	2053
21.658	20.833	45.350	4.339E-02	3.712E-01	8.155E-02	3.696E-03	5.914E-04	2.699	0.70	1990
25.825	25.000	42.811	4.096E-02	3.560E-01	9.673E-02	3.602E-03	5.763E-04	2.643	0.69	1928
29.992	29.167	40.338	3.859E-02	3.412E-01	1.115E-01	3.508E-03	5.613E-04	2.587	0.69	1867
34.158	33.333	37.912	3.627E-02	3.267E-01	1.260E-01	3.414E-03	5.462E-04	2.532	0.69	1806
38.325	37.500	35.553	3.402E-02	3.126E-01	1.401E-01	3.320E-03	5.312E-04	2.477	0.68	1746
42.492	41.667	33.254	3.182E-02	2.988E-01	1.539E-01	3.226E-03	5.162E-04	2.421	0.68	1687
46.658	45.833	31.035	2.969E-02	2.856E-01	1.671E-01	3.132E-03	5.011E-04	2.367	0.67	1629
50.825	50.000	28.845	2.760E-02	2.725E-01	1.802E-01	3.038E-03	4.861E-04	2.312	0.67	1570
54.992	54.167	26.747	2.559E-02	2.599E-01	1.928E-01	2.944E-03	4.710E-04	2.258	0.66	1514
59.158	58.333	24.770	2.370E-02	2.481E-01	2.046E-01	2.850E-03	4.560E-04	2.206	0.66	1460
63.325	62.500	22.868	2.188E-02	2.367E-01	2.160E-01	2.756E-03	4.410E-04	2.155	0.65	1407
67.492	66.667	21.030	2.012E-02	2.258E-01	2.270E-01	2.662E-03	4.259E-04	2.105	0.64	1355

Table L.12 3.8% bentonite flow rate measurement results

3.8 % Bentonite	
Orifice d (m)	0.02
Orifice A (m ²)	3.142E-04
Tank A (m ²)	0.16
Density (Kg/m ³)	1023
Gravity (m/s ²)	9.81
τ (Pa)	1.009
k(Pa.sn)	0.007
n (-)	1

Time	Time difference	Mass of bentonite in tank	Volume of bentonite in Tank	Height of bentonite in tank	Height difference	Velocity in Tank	Flow in Tank	Velocity in orifice	C_d	Re
s	s	kg	m ³	m	m	m/s	m ³ /s	m/s		
0.825	0.000	43.175	4.221E-02	3.638E-01	0.000E+00	3.943E-03	6.309E-04	2.672	0.75	7275
5.492	4.667	40.193	3.929E-02	3.456E-01	1.822E-02	3.837E-03	6.139E-04	2.604	0.75	7067
10.158	9.333	37.308	3.647E-02	3.280E-01	3.585E-02	3.731E-03	5.970E-04	2.537	0.75	6861
14.825	14.000	34.492	3.372E-02	3.108E-01	5.305E-02	3.625E-03	5.800E-04	2.469	0.75	6655
19.492	18.667	31.786	3.107E-02	2.942E-01	6.959E-02	3.519E-03	5.630E-04	2.403	0.75	6451
24.158	23.333	29.134	2.848E-02	2.780E-01	8.579E-02	3.413E-03	5.461E-04	2.336	0.74	6246
28.825	28.000	26.568	2.597E-02	2.623E-01	1.015E-01	3.307E-03	5.291E-04	2.269	0.74	6043
33.492	32.667	24.057	2.352E-02	2.470E-01	1.168E-01	3.201E-03	5.121E-04	2.201	0.74	5837
38.158	37.333	21.670	2.118E-02	2.324E-01	1.314E-01	3.095E-03	4.952E-04	2.135	0.74	5636
42.825	42.000	19.354	1.892E-02	2.183E-01	1.455E-01	2.989E-03	4.782E-04	2.069	0.74	5436
47.492	46.667	17.111	1.673E-02	2.045E-01	1.593E-01	2.883E-03	4.612E-04	2.003	0.73	5235

Table L.13 7.3% bentonite flow rate measurement results

7.3 % Bentonite	
Orifice diameter	0.02
Orifice Area	3.142E-04
Area of Tank	0.16
Density	1046
Gravity	9.81
T	30.493
k	0.021
n	1

Time	Time difference	Mass of bentonite in tank	Volume of bentonite in Tank	Height of bentonite in tank	Height difference	Velocity in Tank	Flow in Tank	Velocity in orifice	C _d	Re
s	s	kg	m ³	m	m	m/s	m ³ /s	m/s		
0.825	0.000	98.609	9.427E-02	6.892E-01	0.000E+00	5.113E-03	8.181E-04	3.677	0.71	1859
9.158	8.333	91.965	8.792E-02	6.495E-01	3.970E-02	4.894E-03	7.831E-04	3.570	0.70	1778
17.492	16.667	85.544	8.178E-02	6.111E-01	7.806E-02	4.676E-03	7.482E-04	3.463	0.69	1698
25.825	25.000	79.291	7.580E-02	5.738E-01	1.154E-01	4.457E-03	7.132E-04	3.355	0.68	1619
34.158	33.333	73.172	6.995E-02	5.372E-01	1.520E-01	4.239E-03	6.782E-04	3.247	0.66	1539
42.492	41.667	67.311	6.435E-02	5.022E-01	1.870E-01	4.020E-03	6.433E-04	3.139	0.65	1462
50.825	50.000	61.731	5.902E-02	4.689E-01	2.203E-01	3.802E-03	6.083E-04	3.033	0.64	1386
59.158	58.333	56.397	5.392E-02	4.370E-01	2.522E-01	3.583E-03	5.734E-04	2.928	0.62	1312
67.492	66.667	51.376	4.912E-02	4.070E-01	2.822E-01	3.365E-03	5.384E-04	2.826	0.61	1241
75.825	75.000	46.899	4.484E-02	3.802E-01	3.090E-01	3.146E-03	5.034E-04	2.731	0.59	1177
84.159	83.334	42.823	4.094E-02	3.559E-01	3.333E-01	2.928E-03	4.685E-04	2.642	0.56	1117
92.492	91.667	38.997	3.728E-02	3.330E-01	3.562E-01	2.709E-03	4.335E-04	2.556	0.54	1060
100.825	100.000	35.437	3.388E-02	3.117E-01	3.775E-01	2.491E-03	3.986E-04	2.473	0.51	1005
109.159	108.334	32.127	3.071E-02	2.920E-01	3.972E-01	2.272E-03	3.636E-04	2.393	0.48	954
117.492	116.667	29.123	2.784E-02	2.740E-01	4.152E-01	2.054E-03	3.286E-04	2.319	0.45	906
125.825	125.000	26.359	2.520E-02	2.575E-01	4.317E-01	1.835E-03	2.937E-04	2.248	0.42	862
134.159	133.334	23.869	2.282E-02	2.426E-01	4.466E-01	1.617E-03	2.587E-04	2.182	0.38	821

